Analysis of dental pathologies in the Pliocene herbivores of Langebaanweg and their palaeoenvironmental implications

TAMARA FRANZ-ODENDAAL

This thesis describes original research undertaken towards the degree of

DOCTOR OF PHILOSOPHY

at the University of Cape Town, which has not been submitted in any form towards a degree at another university. I submit it as my own work and acknowledge all assistance received.

Supervised by

Anusuya Chinsamy-Turan and Julia Lee-Thorp

November 2002

ABSTRACT

The fossil fauna of Langebaanweg, which is situated on the west coast of South Africa and dating to around 5 Myr, is well-suited to document the global climate and environmental changes that were taking place during the Late Miocene-Early Pliocene transition. Earlier studies of this fauna revealed the presence of pathologies, which are useful indicators of health-status, in some animals. This study evaluates the extent of dental pathologies in several ungulate species from the Pelletal Phosphate Member (PPM) at Langebaanweg, and uses this analysis, along with stable isotope analyses, to obtain fresh insight into the local palaeoenvironment during the Early Pliocene.

Stable carbon isotope ratios from enamel carbonate indicate that the area was C_3-dominated. The presence of cool growing C_3 grasses suggests that the current winter-wet/summer-dry climate regime was established early in the Pliocene epoch. Even though the environment was C_3-dominated, $^{13}C/^{12}C$ and $^{18}O/^{16}O$ ratios in combination showed predictable patterning amongst the fauna. The diet of *Sivatherium hendeyi*, the most abundant herbivore in the PPM, was investigated by means of three techniques – hypsodonty index, microwear and mesowear analyses. Although dietary assessment was not absolutely conclusive, *S. hendeyi* appears to have been a seasonal mixed feeder.

A morphological examination of over 3000 teeth showed that several species have a high prevalence of enamel hypoplasia, a developmental tooth defect that typically manifests as a result of systemic stress. A detailed investigation of the location and nature of enamel hypoplasia in *S. hendeyi* mandibular teeth indicated that the deciduous teeth and the upper portion of the first molar do not have enamel defects. This suggests a stress-free *in utero* period. Enamel hypoplasias were also found in the continually erupting hippopotamus tusks indicating that systemic stress was experienced during adult years as well as during the growing years of life. Many teeth have more than one defect per tooth crown suggesting that stress events were episodic. Irregular tooth wear was also observed in some animals. Defects in the second and third mandibular molars of *S. hendeyi* were evaluated using high-resolution $\delta^{18}O$ sequences from across extant giraffe and sivathere tooth crowns. Results indicate that i) the weaning behaviour of the extinct sivathere occurs at a similar ontogenetic age to that in extant giraffes and that defects at the base of the second mandibular molar are not related to weaning. These defects together with those in the later erupting permanent dentition are therefore most likely associated with changing environmental conditions during the Early Pliocene, and ii) the presence of enamel hypoplasia on a tooth crown appears to correlate with periods of drought and increased aridity.

ACKNOWLEDGEMENTS

I would like to express my sincere gratitude to several members of staff from both the University of Cape Town (UCT) and Iziko Museums of Cape Town, South African Museum (Iziko-SAM). In particular I would like to thank my supervisors, Anusuya Chinsamy-Turan (Iziko-SAM and UCT) and Julia Lee-Thorp (UCT), for their invaluable advice and guidance throughout this research project. I am especially grateful to Dr. Sanghamitra Ray, postdoctoral fellow (UCT) and friend, for valued discussions about various aspects of this study, as well as for moral support.

In addition I am grateful to Dr. Margaret Avery, Mr. Derek Ohland and Ms. Pippa Haarhoff (all of Iziko-SAM) who provided access to the Langebaanweg material and permission to sample specimens. I would also like to thank the following persons from Iziko-SAM; Mr. Kerwin van Willingh for assistance with photography, Mrs. Sheena Kaal for accessioning specimens from the Langebaanweg collection, Dr. Rachel Alexander for producing X-ray micrographs, and Dr. Graham Avery for support. I am grateful to Mr. John Lanham (Stable Light Isotope Facility, UCT) and Dr. Andreas Spath (ICP-MS facility in the Department of Geological Sciences, UCT) for technical assistance with stable light isotope mass spectrometry and strontium isotope analyses, respectively. Fourier Transform Infrared Analyses were conducted in the Chemistry Department at UCT. Dr. Colleen Maloney (Zoology Department, UCT) is thanked for statistical assistance. Ms. Andrea Plos (UCT) solved many computer and printer interface problems, which was much appreciated. I would also like to thank Dr. Gerard Steenkamp (veterinarian) for his interest in this study. I am especially grateful to Prof. Nikos Solounias (New York College of Osteopathic Medicine) for his assistance and advice regarding his tooth wear techniques (mesowear and light microscope microwear analyses).

A special thank you goes to my husband, Francois Odendaal, for his encouragement, patience and understanding throughout the duration of this research project, and to my parents, Siegmar and Dorothy Franz, for their tremendous support and financial assistance throughout my academic career.

Financial support for this study was received from the National Research Foundation and from the University of Cape Town.

PREFACE

Prof. Nikos Solounias (New York College of Osteopathic Medicine) produced high-resolution casts of *S. hendeyi* tooth moulds that I made and sent to him in New York. These casts were independently analysed by Solounias and me, and our results are compared in Chapter 7. Dr. Rachel Alexander (Iziko-SAM) produced X-ray micrographs of selected *S. hendeyi* metapodials on request.

The following parts of this thesis are published or have been submitted for publication:

Franz-Odendaal, T.A., J.A. Lee-Thorp, and A. Chinsamy. 2002. New evidence for the lack of C_4 grassland expansions during the Early Pliocene at Langebaanweg, South Africa. Paleobiology 28(3): 378-388.

Franz-Odendaal, T.A., A. Chinsamy, and J. A. Lee-Thorp. Submitted. High prevalence of enamel hypoplasia in an Early Pliocene giraffid (*Sivatherium hendeyi*) assemblage. Journal of Vertebrate Paleontology.

Franz-Odendaal, T.A., J. A. Lee-Thorp, and A. Chinsamy. Submitted. Post-weaning enamel hypoplasia in fossil mammals. Journal of Vertebrate Paleontology.

TABLE OF CONTENTS

List of Figures

List of Tables

"I won't say the pieces were beginning to fall into place: but at least they were getting to look like parts of the same puzzle"

Raymond Chandler : The Little Sister

Chapter 1

INTRODUCTION

This thesis evaluates dental pathologies in several medium to large bodied herbivores from a single deposit at the Langebaanweg (LBW) locality (18° 9'E, 32°58'S). Together with stable isotope analyses, this study provides a reassessment of the palaeoenvironment during the Early Pliocene. Langebaanweg contains one of the largest assemblages of Late Tertiary fossils in Africa. The fossiliferous deposits have an inferred age of ~ 5 Myr (million years) (Hendey, 1981a) and correspond to a time when major changes in climate and vegetation were taking place. This chapter provides a background to the key global environmental changes that were taking place during the Late Miocene-Early Pliocene as well as outlines the rationale and scope of this study. The thesis layout is also described in this chapter.

1.1 Global perspectives

The tropical and subtropical mesic environments characteristic of the Miocene (6 to 22 Myr) were gradually being replaced by more temperate conditions as global cooling took place during the Late Miocene (Janis, 1989; DeMonecal, 1995). Coincident with this cooling, vegetation opened up with tropical grasslands, composed of plant species using the C_4 photosynthetic pathway, dominating most ecosystems by ~6 Myr (Quade et al., 1989; Cerling et al., 1997b). According to the C_4 global expansion model, this expansion of C_4 grasses was gradual compared to climate changes, beginning first at low latitudes and later spreading outwards to mid and high latitudes (Cerling et al., 1997b). The cause of this sudden expansion of C_4 grasses is however unresolved. Researchers first proposed that the C_3 to C_4 shift was triggered by a decrease in atmospheric CO_2, to levels below 500 parts per million by volume (p.p.m.v.). Low levels of CO_2 would have conveyed advantages to the C_4 photosynthetic pathway (Ehleringer et al., 1991, 1997; Cerling, 1993; Cerling et al., 1997b), since C_4 grasses are more efficient at fixing CO_2 than C_3 grasses. However, Pagani et al. (1999a, 1999b) suggested, on the basis of alkenone analyses, that atmospheric CO_2 levels were consistently low during the Miocene and were similar to levels recorded for the Pleistocene glacial and interglacial intervals.

These climate and vegetation changes had a major effect on faunal communities (Janis, 1989, 1993; Janis et al., 2000). Janis et al. (2000) show that there was a gradual loss of browsers throughout the C_3 to C_4 grassland transition in North America, with browser numbers reaching an absolute low around 2 Myr. Consequently, grazers begin to dominate faunal assemblages (Janis, 1989, 1993; Janis et al., 2000).

1.2 Rationale and scope of this study

Brett Hendey conducted all the early excavations and faunal collections at LBW and therefore many of the ideas and opinions regarding this locality stem directly from his research (Hendey, 1970, 1974, 1976, 1980, 1981a, 1981b, 1983a, 1983b, 1984). Hendey (1970, 1984) identified many of the fossils to species level and concluded that grazers were more abundant than browsers. He assumed this to indicate that grasslands were extensive compared to forest habitat and suggested that trees were confined to the local riverbank. This assumption is consistent with global trends, which indicate that forest habitat was on the decline. On careful examination of the fossils during sorting, Hendey (1981b) observed that a dental defect (known as enamel hypoplasia) is common in the teeth belonging to the extinct short-necked giraffid (*Sivatherium hendeyi*) and that irregular tooth wear is present in some reduncine (*Kobus* sp.) teeth. He suggested that these pathologies were the direct result of the changing environmental conditions, which were taking place globally during the Miocene-Pliocene transition (Hendey, 1981b). Enamel hypoplasia is most commonly caused by nutritional stress in humans (Goodman and Rose, 1990; Neiburger, 1990) and Hendey (1981b) therefore proposed that the sivatheres (which he assumed to be browsers) were nutritionally stressed as a consequence of habitat reduction.

Research since this early work by Hendey, suggests that there are some potential problems with his initial assumptions. For one, Hendey assumed that large bodied grazers from LBW were eating savanna grasses, which are known in South Africa to follow the C_4 photosynthetic pathway (Vogel et al., 1978). Western European and eastern Mediterranean data at mid to high northern latitudes (>36°N) however do not show any evidence for a C_4-dominated environment in the last

20 Myr (Quade et al., 1995; Cerling et al., 1997b), in spite of the presence of such grasses at other sites of similar latitudes during this time. The only data available for the Southern Hemisphere *at this critical time* and at similar mid-latitudes to LBW is in Argentina, where a clear C_3 to C_4 shift at ~ 8 Myr was found (MacFadden et al., 1996). Recently, the isotopic ecology of some South African Late Pliocene and Pleistocene localities has been evaluated. The closest site to Langebaanweg is Elandsfontein (20 km to the south), which was found to be C_3-dominated during the Pleistocene (Luyt et al., 2000). Other South African localities, Makapansgat Limeworks and Sterkfontein, situated in the summer-rainfall area, further north and inland of Langebaanweg, provide evidence for C_4 grasses during the Late Pliocene and Early Pleistocene (Luyt, 2001; Sponheimer et al., 2001). It is thus not known whether C_4 grasslands were present at LBW during the Early Pliocene. According to the C_4 global expansion model (Cerling et al., 1997b), C_4 grasses could have extended to mid latitudes of South Africa by the end of the Miocene. The presence of C_4 tropical grasslands (which favour warm growing seasons) would suggest that the current winter-wet/summer-dry climate regime had been established early on in the Pliocene epoch.

Furthermore, Hendey (1981b, 1984) and Klein (1981, 1982) have assumed the browsing and grazing habits for fossil animals from LBW on the basis of analogy with modern relatives (where these exist). For example, they assumed that the extinct giraffid (*S. hendeyi*) was a browser similar to extant members of the Giraffidae family. The only exception to these analogies were the reduncines (*Kobus* sp.), which were thought to be browsers despite extant reduncines being grazers. The reason is that the teeth of these reduncines more closely resemble those of the browsing tragelaphines (*Tragelaphus* sp.) from LBW, than extant reduncines (Gentry, 1980; Hendey, 1983a). More recently however, several authors have shown that Reduncini were mixed feeders to grazers from 6 to 3 Myr in other parts of Africa (Sponheimer et al., 1999; Zazzo et al., 2000). These assumptions regarding the dietary preferences of the LBW fauna, led Hendey and Klein to believe that the local environment consisted of extensive grasslands and limited forest habitats (Hendey, 1970, 1976, 1981b; Klein, 1981, 1982; Hendey, 1983a, 1984). It is now recognised that the diets of extant animals cannot be used to predict the diets of fossil animals accurately (Brink and Lee-Thorp, 1992; Bocherens et al., 1996; Zazzo et al., 2000).

Solounias and co-workers (Solounias et al., 1988; Solounias and Moelleken, 1993b; Solounias et al., 2000) have shown that there is much variability in the dietary habits of extinct giraffids. Both grazing and mixed feeding Sivatheriinae have been reported in Miocene-Pliocene localities in East Africa (Tanzania, at 1.8 Myr) (van der Merwe, personal communication, 2000), North Africa (Chad, at 3-3.5 Myr) (Zazzo, personal communication, 2000) as well as in Asia (Siwaliks, Miocene) (Solounias and Moelleken, 1993b).

The observed enamel hypoplasia (EH) in *S. hendeyi* was not investigated thoroughly, although it was thought by Hendey (1981b, 1984) to be linked to nutritional stress during tooth development. In addition, the extent of this pathology in other animals and the relationship between dietary preference and pathology (if any) has not been evaluated until now. Recent studies suggest that EH can be caused by a number of phenomena that disturb the enamel laying down cells (ameloblasts) during tooth development and ultimately are the result of systemic stress. For example, EH can manifest as a result of stress associated with weaning (Corruccini et al., 1985; Goodman and Rose, 1991), birth (Mead, 1999), a stressful calf-cow separation (Mead, 1999) or illness (Miles and Grigson, 1990). Some of these phenomena occur at specific ontogenetic stages and therefore by conducting a detailed investigation of the incidence and severity of EH in each tooth type, the ultimate cause of the defects can be elucidated. Few studies have reported EH in non-primate fossils (Mead, 1999; Dobney and Ervynck, 2000; Niven, 2002) and therefore the analysis of this defect in the herbivores of LBW will contribute greatly to the understanding of EH in non-primates.

In summary, the main focus of this thesis is to quantify dental pathologies, in order to explore the relationship between the observed pathologies and prevailing environmental conditions during the Early Pliocene. Stable oxygen and carbon isotopes are used for the first time on the LBW fauna to investigate the palaeoenvironment. An analysis of pathologies (first reported by Hendey, 1981b) in several ungulates is also conducted. These two approaches provide different perspectives on the prevailing environmental conditions in this region during the Early Pliocene (~ 5 Myr). In order to interpret the cause of the observed defects and the conditions under which these defects manifested, high-resolution serial isotope

sampling along tooth crowns with defects is conducted. This approach provided a unique insight into the relationship between environmental conditions and defects.

1.3 Thesis layout

This thesis is divided into eleven chapters. The first is this introductory chapter, which outlines the rationale of this study. Chapter 2 provides an overview of the LBW locality, the present climate, geological succession, taphonomy of the site, and fossil fauna and flora. A review of the published literature on the palaeoenvironment of LBW is also presented as well as a brief look at other nearby fossiliferous deposits of Late Tertiary age. In Chapter 3 an overview of tooth development and structure is given, with particular focus on enamel. A literature review of enamel defects in fossil and extant animals is provided, as well as an assessment of the current methodologies used to analyse enamel defects. Chapters 4, 5, 6, 7 and 8 form the bulk of this thesis. Each of these chapters consists of an introduction, material and methods, results, discussion and conclusion section. Chapter 4 investigates the palaeoenvironment and niche preferences of several herbivores from a single deposit, the Pelletal Phosphate Member (PPM), at LBW by means of stable carbon and oxygen isotopes from tooth enamel. The rest of this thesis focuses on palaeopathologies in the medium to large herbivores from the PPM and starts with an overview of the extent of pathologies in these herbivores (Chapter 5). The incidence and severity of both skeletal and enamel defects is investigated. In Chapter 6, a detailed analysis of enamel hypopolasia in the most abundant animal from this deposit, namely the short-necked giraffid, *S. hendeyi,* is conducted. In Chapter 7, the diet of this animal is assessed in order to facilitate interpretations regarding the observed dental pathologies. Finally, Chapter 8 uses stable isotope sequences across tooth crowns with defects to ascertain whether prevailing environmental conditions can be linked to the observed dental pathologies. This approach has not been applied previously to either fossil or modern animals, or to humans. In addition, the possibility of migration of some fauna is investigated by means of strontium isotopes. A summary of the research findings is presented in Chapter 9 together with a final reassessment of the palaeoenvironment at LBW during the Early Pliocene. Chapter 10 and 11 contain the references and appendices, respectively.

Chapter 2

THE LANGEBAANWEG LOCALITY

2.1 Introduction

This chapter provides a comprehensive introduction to the Langebaanweg (LBW) locality as well as introduces global environmental changes that were taking place during the Neogene. The present environment of the Langebaanweg area, stratigraphy of the locality and the fossil flora and fauna are also discussed. Finally, the literature describing the palaeoenvironment of Langebaanweg (prior to this study) is reviewed together with key localities of a similar age in South Africa.

2.2 Global environmental change during the Late Tertiary

The Late Miocene-Early Pliocene (10 to 4 Myr) was a time of substantial change over much of the Earth's surface and these changes had a profound effect on biological systems (Janis, 1989, 1993). Climates became cooler, more seasonal and drier compared to the more mesic conditions characteristic of the Miocene. It was during this time that the Mediterranean dried up and the 'Messinian salinity crisis' took place.

Expansion of the Antarctic ice sheet and its related sea-level changes (Loutit and Kennet, 1979) resulted in a land connection forming across the Straits of Gibraltar. The Mediterranean became a landlocked sea and the 'Messinian salinity crisis' followed. Glaciation of Antarctica caused temperatures to drop in southern mid-latitudes and as a result climates in southern Africa changed from tropical to temperate towards the end of the Late Miocene (~6 Myr). Based on deep-sea drilling cores, the Benguela Upwelling system (which is responsible for the current climate regime and aridity of the south-western region of South Africa) was apparently also established by this time (Tankard and Rogers, 1978; Siesser, 1980; Siesser and Dingle, 1981). As a consequence of the Mediterranean becoming a landlocked sea, faunal interchange between Africa and Eurasia took place and worldwide expansions of savannas occurred (Janis, 1993).

This period of climate change was terminated by an Early Pliocene marine transgression (between 4.2 and 5.2 Myr) that re-flooded the Mediterranean basin and resulted in a regressive ice-phase in Antarctica (Van Couvering, 1976). This sea level change was also responsible for the deposition of the terrestrial fossils at LBW (Hendey, 1981a).

The Early Pliocene LBW locality (and especially the fossiliferous Varswater Formation) is thus uniquely situated at a time when major changes in climate, vegetation and fauna were taking place globally. It is also the only site on the west coast of South Africa of this age that potentially documents some of these changes both directly and indirectly.

2.3 Present environment in the Langebaanweg area

The Langebaanweg locality (18° 9'E, 32°58'S) is situated 13 km inland on the west coast of South Africa (Figure 2.1) in an area dominated by winter rainfall and sclerophyllous fynbos[1] vegetation.

The mean annual temperature in this part of the country is between 12-16°C. Daily maximum temperatures for summer are 30°C and minimum temperatures for winter are 5°C (Schulze, 1997). Annual rainfall in the Langebaanweg area is 250-500 mm. Local climate in the south-western region of the country is controlled by latitudinal, seasonal movement of the South Atlantic high pressure system which operates in two ways. Firstly, it allows penetration of moist westerly winds during the winter months, but prevents penetration of moisture from the east in summer. Secondly, it induces strong, cold upwelling cells along the west coast, forming the Benguela Upwelling System. This upwelling contributes to the marked summer aridity of the region. In stark contrast, the more inland and eastern areas of the country have wet summers and dry winters.

Fynbos vegetation is recognised as one of the world's six Floristic Kingdoms (Ellis et al., 1980), and is unique to the winter rainfall areas of the country. Grasses are a very minor component of this species-rich biome and those present are

[1] Fynbos is an evergreen species-rich sclerophyllous macchia vegetation unique to the Western Cape, South Africa.

predominately C_3 grasses, which favour cool growing seasons (Vogel et al., 1978). Fynbos has the ability to grow in the sandy, low nutrient acidic soils found in the region and as a result, it has a very low nutritional content and supports few large mammals. Langebaanweg is situated in an area of coastal fynbos, consisting largely of unpalatable restiod reeds with a less dense shrub cover and a small succulent component. Nearby is a dense semi-succulent open shrubland known as strandveld. The area to the east (and inland) of the Cape Fold Mountains, with its summer-wet/winter-dry climate regime, is however dominated by woodlands and tropical C_4 grasslands, and is thus capable of supporting a rich mammalian fauna.

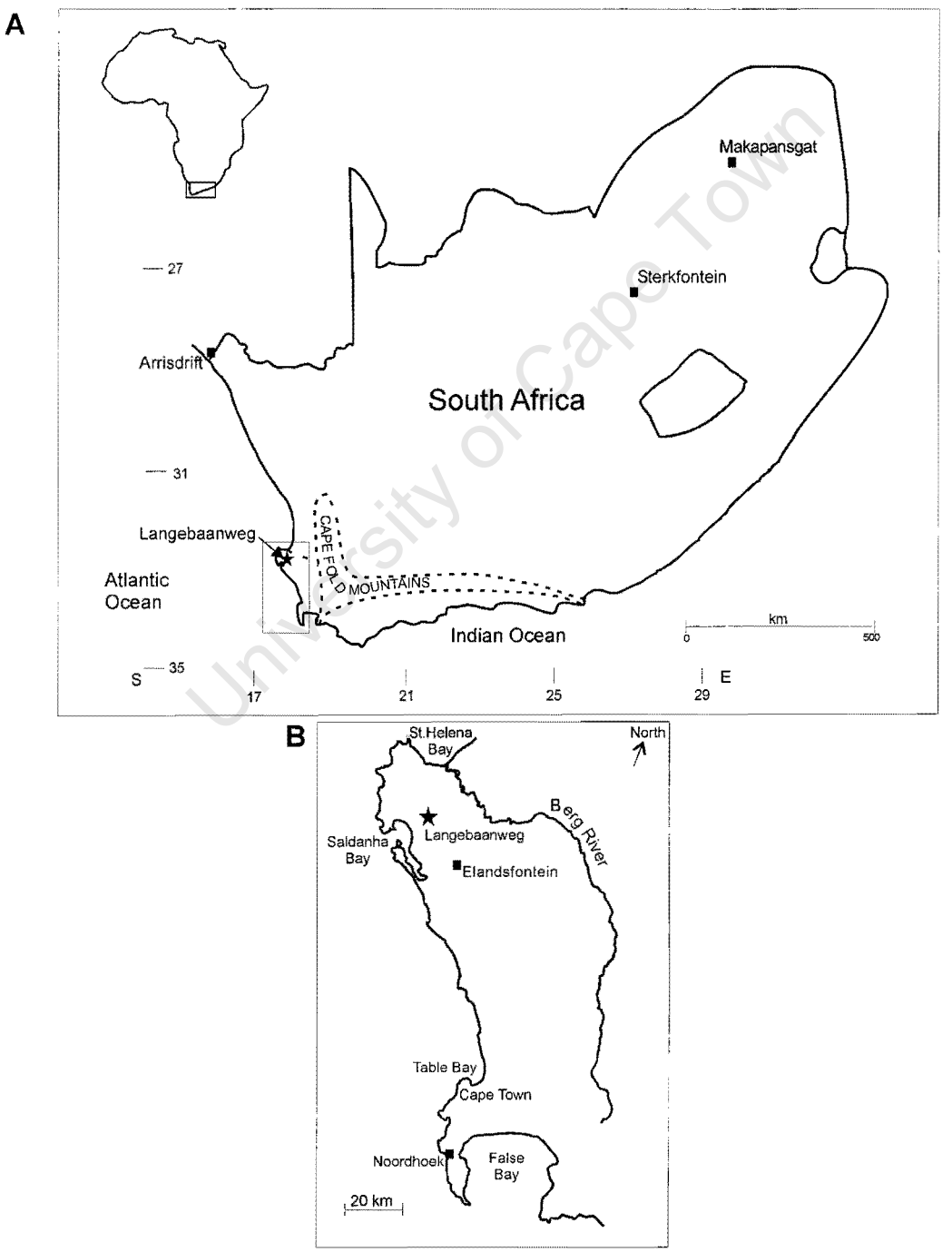

Figure 2.1. Location of Langebaanweg on the west coast of South Africa. (A) The main Late Tertiary localities in South Africa, (B) inset in (A) showing Langebaanweg in relation to the Berg River, coastline and the nearby Elandsfontein locality.

2.4 Geology of the Langebaanweg succession

The Late Cenozoic succession at LBW was first described by Hendey (1981a). It consists of up to 120 m of unconsolidated sediments (Figure 2.2), the greater part of which is made up the Elandsfontein Formation and the overlying, highly fossiliferous Varswater Formation. A narrow Saldanha Formation separates the previous two Formations. Below the Elandsfontein Formation is a bedrock Gravel Member of pre-Tertiary age. The Varswater Formation was exposed during phosphate mining operations in the late 1950s to 1960s and the exposed area of the mine is known as 'E' quarry.

Southern African coastal and continental shelf deposits have revealed that sea level changes at LBW during the Miocene and Pliocene were similar to global patterns (Dingle, 1971, 1973) (Figure 2.3). Together with similarities in the faunal assemblages of dated deposits elsewhere (especially in East Africa), the relative datings of each Formation have been assessed. The Early to Middle Miocene transgression was responsible for laying down the Elandsfontein and Saldanha Formations. The Saldanha Formation was, however, partially eroded away during the subsequent Middle to Late Miocene regression (Siesser, 1980; Siesser and Dingle, 1981) and therefore contains few terrestrial fossils. The Elandsfontein Formation has been described as a rocky and sandy marine environment (Tankard, 1975). Plant and marine elements dominate both the Elandsfontein and Saldanha Formations. A subsequent Early Pliocene transgression was responsible for laying down the fossiliferous Varswater Formation, which is discussed in detail in section 2.4.1. Overlying this Formation are two other fossiliferous deposits, Anyskop (to the south-west of 'E' quarry) and Baard's Quarry (to the east of 'E' quarry), which probably date to the Late Pliocene (Hendey, 1984). The core of Anyskop is believed to be a remnant of a coastal barrier and marine fossils dominate this deposit (Hendey, 1981a). Baard's Quarry is a complex of river channel deposits and comprises mostly fragmentary fossil material. The coastline and position of LBW during the Early Pliocene are shown in Figure 2.4.

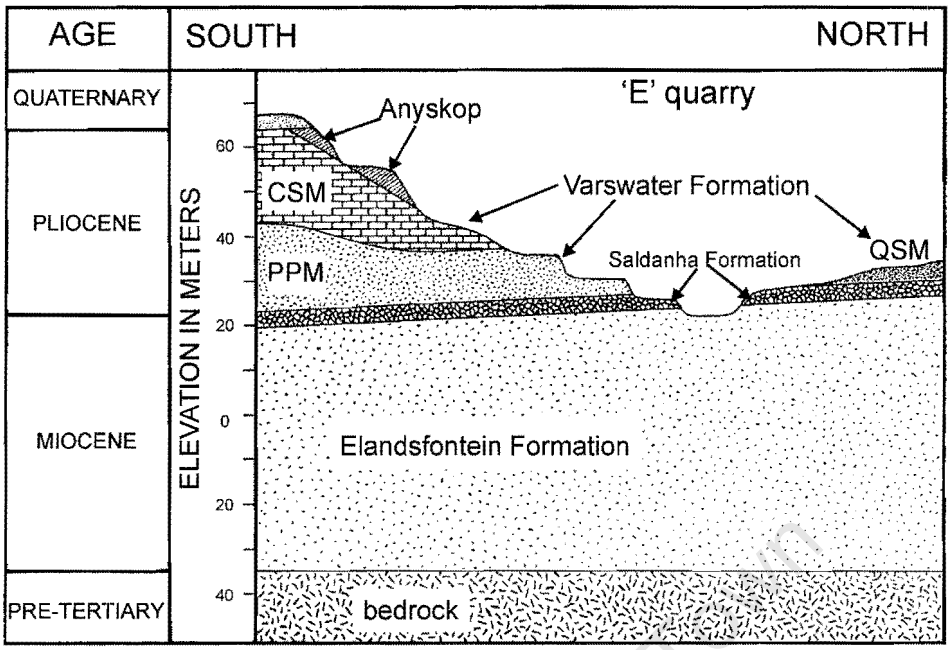

Figure 2.2. Stratigraphy of Langebaanweg, 'E' quarry (modified from Hendey, 1981a).

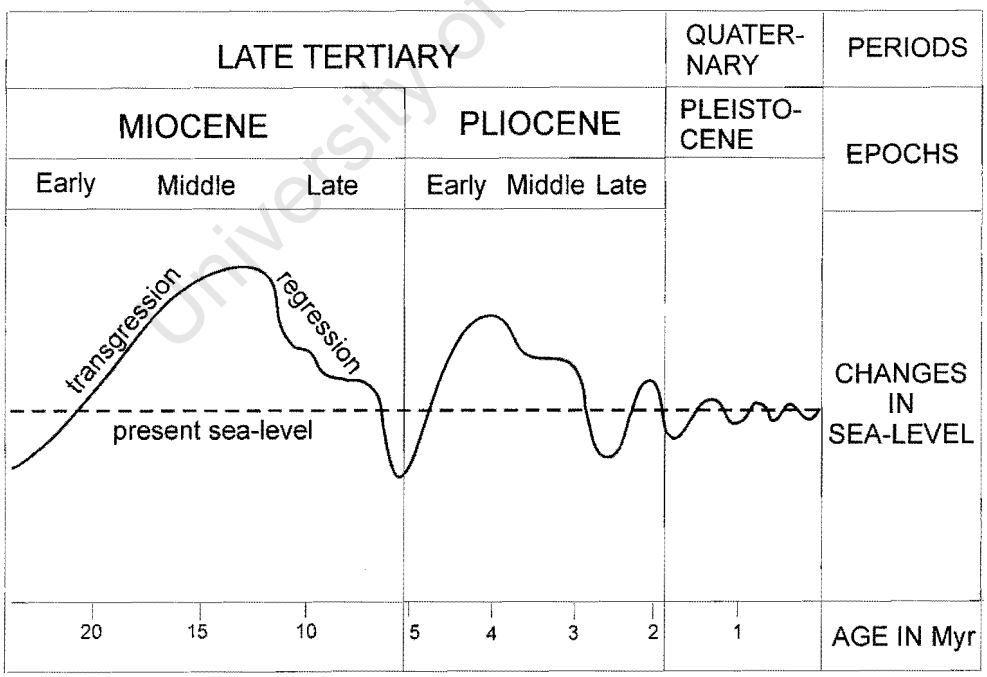

Figure 2.3. A regional curve of sea level changes during the Late Tertiary and Early Quaternary periods (modified from Hendey, 1981a).

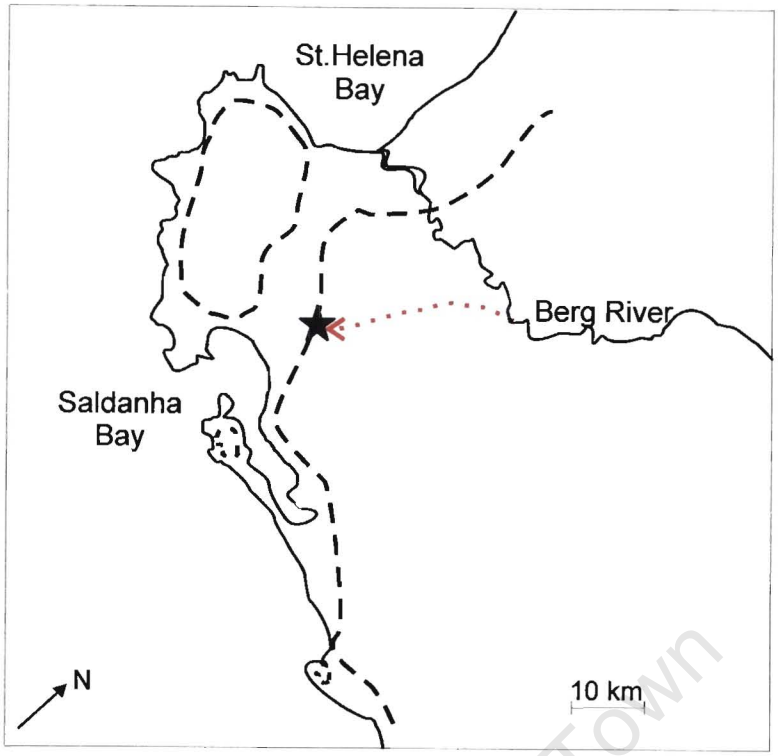

Figure 2.4. Location of Langebaanweg 'E' quarry (star) during the Early Pliocene. Dashed lines indicate the coastline during the Early Pliocene transgression and the solid line represents the present coastline. The red dashed line indicates the inferred course of the proto-Berg River ~ 5 Myr ago.

2.4.1 The Varswater Formation

The two most highly fossiliferous deposits within the Varswater Formation are the Quartzose Sand Member (QSM) and the Pelletal Phosphate Member (PPM) (Figure 2.2). The QSM is a truncated estuarine complex of deposits (including a flood-plain, salt marsh and tidal flat deposit) with a maximum development of up to 2 m. These deposits were laid down during an early stage of the Early Pliocene transgression at a time when a river (probably a precursor of the present Berg River) passed south-westwards along the southern margin of 'E' quarry. As this transgression progressed, the lower course of this river shifted northwards allowing the marine littoral environment to encroach over the QSM deposits and conditions were such that deposition of pelletal phosphate occurred. The PPM deposit comprises up to 20 m of phosphatic marine littoral and fluviatile deposits. The two river channel deposits are known as Bed 3aS and Bed 3aN. The exact stratigraphic relationship between these two Beds is not known, but the lower elevation and more southerly position of Bed 3aS suggests that it was laid down earlier during the marine

transgression than Bed 3aN (Hendey, 1976). At the time that Bed 3aS was deposited, the river flowed over unconsolidated and often highly fossiliferous QSM deposits. It has been speculated that Bed 3aS deposits may include fossils from the QSM (Hendey, 1970, 1981b; Klein, 1981). There is however no evidence to suggest this was the case with fossils from Bed 3aN. (The relative positions of these two Members are shown in Appendix A).

According to Hendey (1981b) the QSM and PPM date from a relatively short period and represent repetitive depositional phases of a single geological episode. This period was no more than 0.5 Myr and long enough for evolutionary change to occur in taxa common to more than one level (Hendey, 1981b, 1984).

During the later stages of the Early Pliocene transgression, the mouth of the river shifted northwards and the local accumulation of fossils ceased. Calcareous sediments (CSM) were subsequently laid down over the PPM and protected the underlying deposits from erosion.

2.5 Taphonomy of the Varswater Formation

The fossils from the Varswater Formation of LBW are mainly isolated well preserved elements (Figure 2.5). Only a few partially disarticulated skeletons have been recovered. Mortality profiles of some of the QSM and PPM fauna (discussed further in section 2.6.1) suggest that animals recovered from the PPM died as a result of catastrophic events (such as floods or fires), whereas those from the QSM died by natural predation (Klein, 1981, 1982). The taphonomy of the fossils from controlled excavations in Bed 3a (PPM) provide evidence that they were deposited by fast-flowing water (Hendey, 1976) (e.g. isolated teeth and bone fragments are scattered in a south-westerly direction). Most of these fossils are thought to represent remnants of animals that were washed into the area by the local (proto-Berg) river. There is however no evidence for destructive battering by, and against, cobbles and boulders in the river channel, suggesting that the skeletal remains were probably still protected by soft tissue by the time they reached the 'E' quarry estuary (Hendey, 1980). The subsequent dispersion of these fossils probably occurred locally. It is believed that the freshwater source would have attracted animals into

the immediate vicinity and that some fossils must therefore represent animals that inhabited the local area (Hendey, 1981b, 1984).

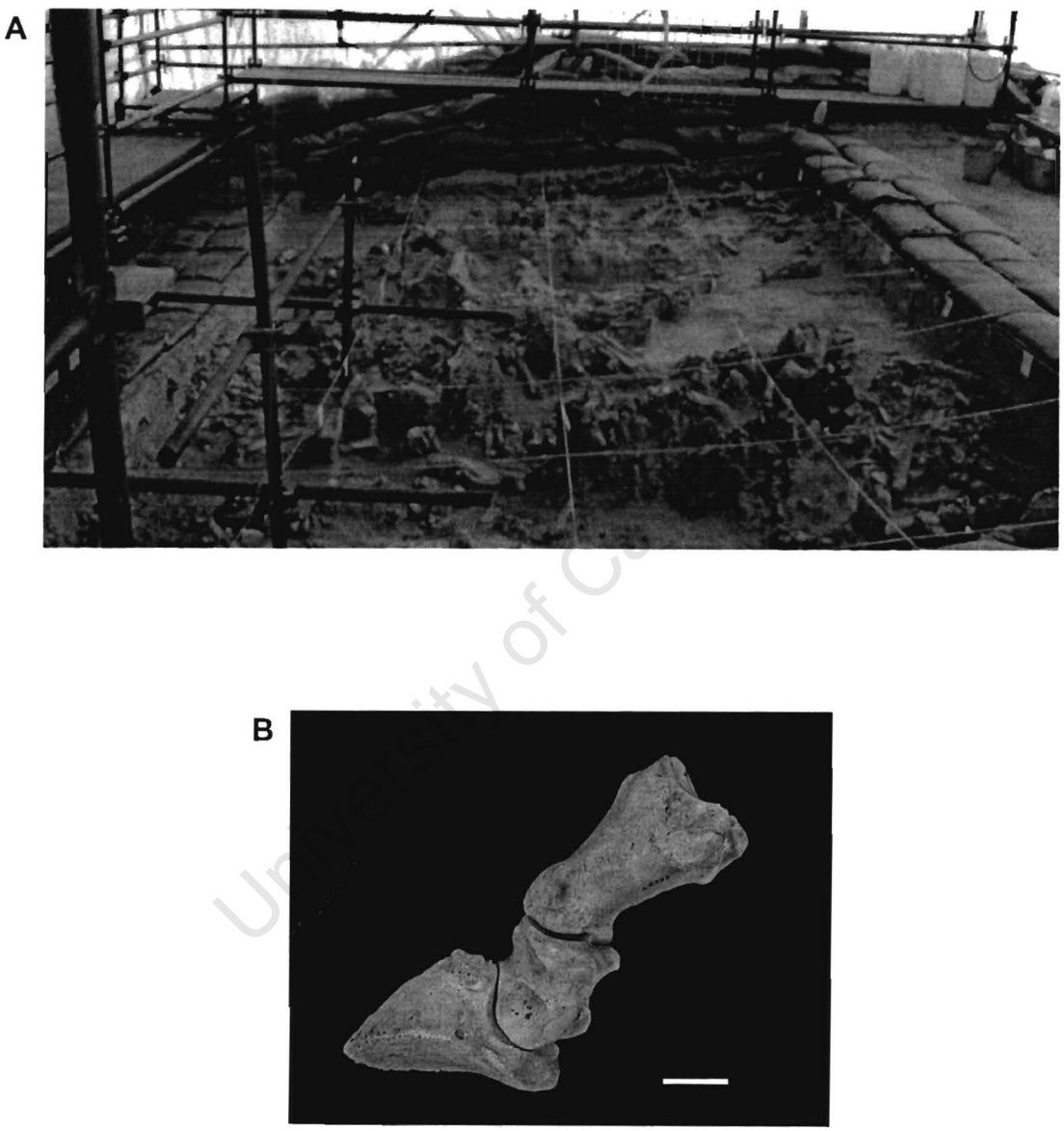

Figure 2.5. The Langebaanweg excavation and fossils. (A) The present excavation at Langebaanweg showing the disarticulated nature of the fossils. Each qaudrant is 1 m^2, and (B) lateral view of well-preserved associated phalanges (PQL 5329, PQL 5333 and PQL 5332) belonging to *S. hendeyi,* in approximate position. Scale bar represents 3 cm.

2.6 Fauna

The faunal list for LBW is impressive, both in diversity and abundance of fossils. At least 230 taxa have been recognised (Hendey, 1984). LBW is also the richest pre-Pleistocene fossil bird locality in the world (Rich, 1980). Vertebrates dominate with at least four new mammalian genera and sixteen new species represented. The full mammalian species list from the Varwater Formation, together with the deposits in which they were found, is given in Appendix B. This study focuses on the medium to large ungulates (Giraffidae, Hippopotamidae, Rhinocerotidae, Bovidae, Equidae) from the PPM, many of which were recovered during mining operations or by screening bulk sediment samples mechanically removed from the mine. Some material was also recovered from controlled excavations carried out from 1964 to 1976. (Refer to Appendix C for the excavations and dumps from which the fossils analysed in this study were recovered). All fossil material is housed at the South African Museum, Iziko Museums of Cape Town, South Africa, and all accession numbers have the prefix "SAM PQL" to denote this collection. (Throughout this thesis, only PQL is used as a prefix when referring to these fossils).

Limited studies have been conducted on the ungulates from LBW and most of these have focussed on the identifications of new species (Hendey, 1970, 1984; Bovidae (Gentry, 1974, 1980); Rhinocerotidae (Hooijer, 1976); Proboscidea (Coppens et al., 1978); Giraffidae (Harris, 1976b); Suidae (Harris and White, 1979)). Although the dietary habits of the fauna have been speculated based on analogies with extant relatives, no direct studies investigating diet (such as microwear, mesowear, premaxillary shape etc.) have been conducted. A taxonomic uniformitarian[2] approach of deducing the diet and habitat preferences of extinct fauna must be treated with caution (Brink and Lee-Thorp, 1992; Sponheimer et al., 1999; Zazzo et al., 2000). Appendix D summarises the inferred diets of the ungulates according to Hendey (1984) and compares these to other localities in Africa. Although Hendey considers certain animals as browsers and others as grazers, he does not define these terms. It is assumed therefore that he refers to the traditional definitions of Hofmann and Stewart (1972), though recent research on extant animals

[2] This approach assumes that the diet and habitat preferences of fossil animals were the same as that of their closest extant relatives.

indicates that these are quite broad terms (Janis et al., 2000). According to Hofmann and Stewart's definitions, browsers are animals that consistently consume less than 10% grass in their annual diet and grazers are species that consume more than 90% grass in their diet. Animals whose diets fall between these extremes are described as "mixed" or "intermediate" feeders. Without a detailed dietary assessment, it is impossible to determine the diets of extinct fauna more precisely than Hoffmann and Stewart's classification. The traditional definitions are therefore applied throughout this thesis (unless otherwise specified).

The medium-sized herbivores of LBW are represented by one equid (Hooijer, 1976), two suids (Harris and White, 1979) and several bovids (Gentry, 1974, 1980). The three-toed horse, *Hipparion* cf. *baardi*, is a descendent of a Late Middle Miocene immigrant to Africa and its rapid dispersal through Africa and Eurasia during the Middle Miocene is an indication that grasslands were progressively expanding at the expense of forests (Hendey, 1983a). *Hipparion* cf. *baardi* is present in both the PPM and QSM, and evidence exists that it survived into the Pleistocene (Haughton, 1932). Its ecological niche was eventually taken over by *Equus*, an immigrant from Eurasia, which entered Africa toward the end of the Pliocene. The presence of maxillary incisors in Equidae enabled them to feed on the taller, coarser grasses in the ecosystem and their appearance is believed to have opened up a niche for grazing bovids (Janis, 1982).

The two suids from LBW belong to the same genus, *Nyanzachoerus*, and were studied by Harris and White (1979). *Nyanzachoerus* cf. *pattersoni* is present in the older QSM while *N.* cf. *jaeger* is present in Bed 3aS of the PPM. It is unclear whether these two species were contemporaneous because of potential mixing between the QSM and Bed 3aS deposits (see section 2.6.1). *Notochoerus* was bushpig-like, preferring more open habitats to its ancestor *Nyanzachoerus* (a warthog-like animal) (Hendey, 1983a). The presence of *Nyanzachoerus* at LBW therefore supports evidence that at least some closed habitats were present during the Early Pliocene.

A large group of bovids are represented at LBW and include members of eight tribes (Appendix B) (Gentry, 1974, 1980). All, but one tribe (Reduncini), are

represented in the QSM. In the PPM, the most abundant bovids are the bovine (*Simatherium demissum*), the boselaphine (*Mesembriportax acrae)*, two alcelaphine species (*Damalacra* sp.*)* and the reduncines (*Kobus* sp.) (Hendey, 1981b). The other bovids in this deposit are poorly represented. According to Hendey (1983a) and Klein (1981, 1982), the boselaphine and reduncine species favoured more closed habitats, while the alcelaphines and bovine were probably open country grazers. Reduncines from other localites in Africa were mixed feeders to grazers at 3 to 5 Myr (North Africa: Chad) (Zazzo et al., 2000) or pure grazers by ~3 Myr (Makapansgat, South Africa) (Sponheimer et al., 1999). There is some uncertainty however regarding the identification of the reduncines at LBW (Gentry, 1980). Although horn-cores belonging to *Kobus* sp. are present, the associated teeth more closely resemble those of the tragelaphines than *Kobus*. This uncertainty has not been resolved though it is generally considered that these teeth belong to *Kobus* sp. despite their resemblance to the browsing tragelaphines. (A direct assessment of their diet is obviously required).

The large ungulates from the Varswater Formation are also impressive. A white rhinoceros, a hippopotamus and three giraffids are present. The hippopotamus species has not been determined. It is present in Bed 3aS and 3aN (PPM) only and probably foraged on riverside grasses similar to extant hippos (Hendey, 1984). Recent studies from North Africa (Chad) indicate the presence of a mixed feeding hippopotamus (*Hexaprotodon*) at 5-6 Myr and pure grazing hippos only by 4-5 Myr (Zazzo et al., 2000). This genus is however on a different lineage to extant hippos (Coryndon, 1970; Coryndon and Coppens, 1973) and until the genus of the LBW hippopotamus is known, no inferences regarding its diet can be made.

The rhinoceros (*Ceratotherium praecox*) is a probable ancestor of the modern white rhinoceros (*C. simum*) (Hooijer, 1976) and is believed to have inhabited a similar ecological niche to that of an open country grazer. Although the rhinoceros is abundant in the QSM, only a few rhino fossils were recovered from Bed 3aS (PPM). It has been speculated that these fossils were initially deposited on the floodplain (QSM) and later washed into the river channel during a flood event (Hendey, 1981b). *C. praecox* is also known from Early Pliocene deposits in Kenya (Hooijer and Patterson, 1972). Studies in North Africa indicate that *C. praecox* was a mixed

feeder to grazer from 4-5 Myr and a pure grazer only at 3-3.5 Myr (Zazzo et al., 2000). At Makapansgat (~3 Myr) in South Africa, *C. simum,* the extant species, appears not to have been a pure grazer, incorporating up to 30% browse in its diet (Sponheimer et al., 2001).

All three members of the Giraffidae – Sivatheriinae, Palaeotraginae and Giraffinae (Harris, 1976b) – are present at LBW. The evolution of the giraffids according to Churcher, (1978) is summarised in Figure 2.6A. However, several authors disagree with this synopsis of the Giraffidae (Hamilton, 1978; Solounias et al., 2000). The recent classification of the extinct Giraffoid species based on Hamilton (1978) and modified by Solounias et al. (2000) is given in Figure 2.6B. The sivathere (*Sivatherium hendeyi*) and the long-necked giraffe (*Giraffa* cf. *jumae*) are present in both the river-channel (PPM) and floodplain (QSM) deposits, although they are more abundant in the PPM. *Palaeotragus* cf. *germaini* on the other hand is rare and only occurs in Bed 3aS. The only other living Giraffidae is the rare okapi of the central African forests (*Okapi johnstoni*). According to Hendey (1984), the decline of forests into more open woodlands with savannas during the Early Pliocene would have reduced the habitats of the Palaeotraginae but at the same time would have created new ones to suite other giraffids (Hendey, 1984). The *Giraffa* sp. with their long necks would have been able to reach a food source, high in the canopy, unobtainable by other species and could therefore co-exist with other browsers. The sivathere, *S. hendeyi*, with its shorter neck, presumably competed neither for the closed habitats of the Palaeotraginae nor for the canopy vegetation favoured by *Giraffa* sp. These speculations are however based entirely on the assumption that all three giraffids from LBW were browsers, but no evidence for their dietary preferences exist. At other localities in Africa and Asia, the diets of the Giraffidae have been found to be highly heterogeneous (Solounias et al., 1988, 2000). Only *Giraffa* appears to have been a conservative browser through time.

A

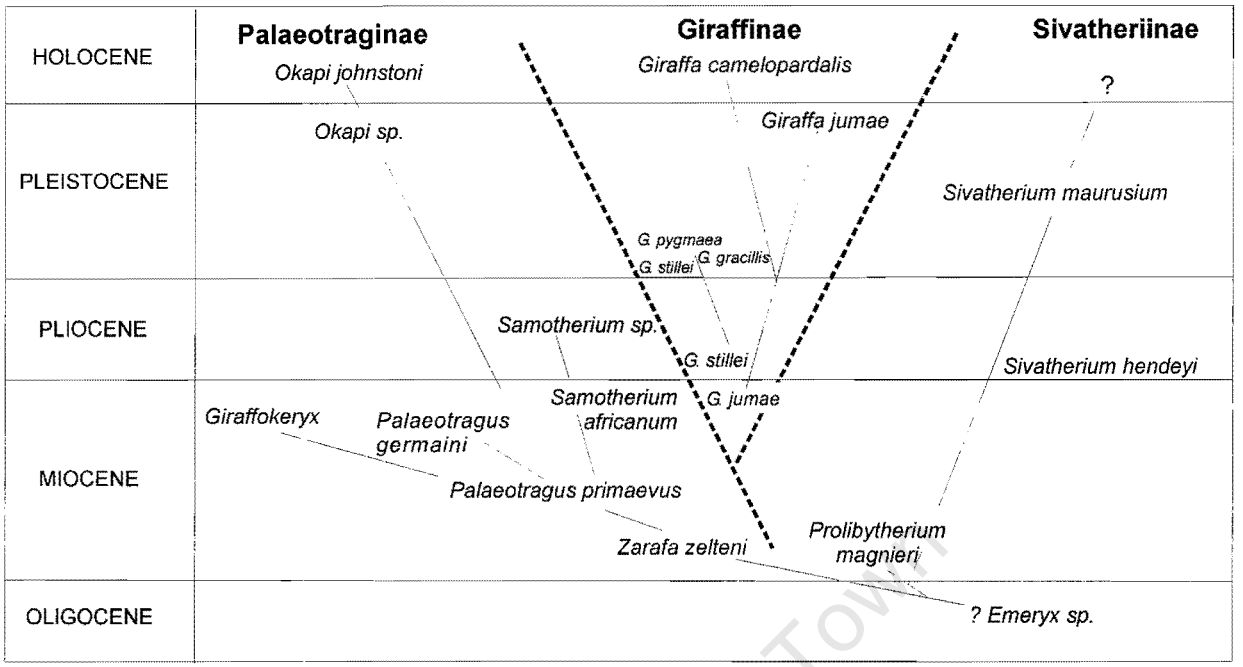

B

Superfamily: Giraffoidea
Prolibytherium magnieri
Family: Giraffidae
Subfamily: Sivatheriinae
"Palaeotragus" primaevus
Giraffokeryx punjabiensis
Bramatherium megacephalum
Sivatherium giganteum
Helladotherium duvernoyi
Subfamily: Palaeotraginae
Palaeotragus rouenii
Palaeotragus coelophrys
Palaeotragus quadricornis
Subfamily: Samotheriinae
Samotherium boissieri
Samotherium major
Samotherium neumayri
Subfamily: Giraffinae
"Palaeotragus" tungurensis
Bohlinia attica
Honanotherium schlosseri

Figure 2.6. The Giraffidae Family. (A) The evolution of the Giraffidae of Africa according to Churcher (1978), and (B) the extinct Giraffoidea modified by Solounias et al. (2000).

There is some evidence that a second species of sivathere may be present at LBW. *S. hendeyi* was described as having two pairs of conical ossicones (Harris, 1976b) – an anterior broad ossicone arising from the frontals and a slender, longer posterior one. The absence of flanges and knobs on the posterior ossicones together with the conical nature of anterior ossicones distinguishes *S. hendeyi* as a new species of sivathere. The lack of ornamentation may however be a function of age (Harris, 1976b) or sexual dimorphism (Churcher, 1978). All the conical ossicones described for *S. hendeyi* may therefore be from immature individuals or from females. Churcher (1978) suggested that *S. hendeyi* may not be a unique species but that it may be a variant of *S. maurusium,* which is present at the nearby Pleistocene Elandsfontein locality (Figure 2.1). (Anterior ossicones are greatly reduced or lost in *S. maurusium* (Harris, 1976a)). Recently however, some highly branched sivathere ossicones have been recovered from the QSM deposits of LBW (P. Haarhoff, personal communication, 2000). It is not clear whether these are anterior or posterior ossicones as the base of the ossicones are missing (personal observation). Nevertheless, these branching ossicones resemble those of *S. maurusium* and of *S. giganteum (*from the Pleistocene of North Kenya) (Harris, 1976a). The discovery of branching ossicones in the QSM and the presence of only conical ossicones in the PPM, suggests that two species of sivathere may be present at LBW. The lack of ornamentation in the ossicones from the PPM is thus unlikely to be a function of age or sex.

Although essentially the fauna in the QSM and PPM are similar, the relative abundance of fossils varies dramatically between the two units. In the QSM, no single species appears to dominate, whereas, in the PPM, the alcelaphine antelopes (*Damalacra* spp.) and giraffids (*Giraffa* sp. and *S. hendeyi*) are abundant compared to other species (Hendey, 1981b). Within the PPM, there are differences in relative abundances of taxa, with for example the alcelaphines dominating in the earlier Bed 3aS and the giraffids dominating later in Bed 3aN. The implication is that either woodlands became progressively more widespread during deposition of the Varswater Formation, or taphonomic factors were such that woodland species were incorporated in the deposits more frequently (Hendey, 1980). Since grasslands were expanding in the rest of the world at this time (Cerling et al., 1997b), it has been assumed that they were also expanding in the southern parts of Africa.

2.6.1 Mortality profiles

Klein (1981, 1982) constructed mortality profiles for several ungulates from the QSM and PPM deposits at LBW. In the QSM, attritional mortality profiles for the rhinoceros (C. *praecox*), buffalo (*S. demissum*) and the boselaphine (*M. acrae*) suggest that death occurred by natural predation, accidents, or disease, i.e. factors that disproportionately affected the young and old individuals in a population.

In the PPM, classic catastrophic (step-wise) mortality profiles for *Giraffa* (Bed 3aN), *Sivatherium* (Bed 3aN) and the alcelaphine (*Damalacra* spp.) (Bed 3aS) suggest that death probably occurred by drowning during peak or flash floods. According to Klein (1982), the giraffids were probably restricted to the closed canopy habitat lining the riverbank, while the alcelaphines were probably attracted to floodplain meadows between riverine forest and fringing grassland (Klein, 1981, 1982). Klein speculates that the alcelaphines probably died in attempts to cross the river during periods of high flow (possibly seasonally). Drowning animals trapped in the floodplain would have been carried to the river mouth and deposited. Here, the abundance of carcasses would have in turn attracted both marine and terrestrial scavengers (Hendey, 1981b). Evidence for predation in the form of tooth marks is visible on some herbivore bones (Hendey, 1974). Some mortality profiles from the PPM are however, not 'catastrophic' in shape. *M. acrae* and *S. demissum* both have profiles resembling those of the QSM (i.e. attritional) and Klein (1982) suggests that it is likely that these dentitions were either reworked from the QSM or washed off the floodplain into the adjacent river channel. The post-crania of these animals have not been examined for signs of weathering.

2.7 Flora

Faunal composition provides indirect evidence of vegetation, for example, the presence of browsing and grazing animals indicate that both trees and grasslands were present. Pollen on the other hand can provide more specific information as to the type of trees/grasses that were present and their relative abundance. The Varswater Formation deposits are not rich in pollen, but a limited number of fossil pollens have been studied from both this Formation and underlying deposits (Coetzee, 1978; Coetzee and Rogers, 1982; Scott, 1995). Together with pollens from nearby sites this has provided some insight into the vegetation of the LBW area

during the Early Pliocene. A constraint of pollen analyses, however, is that the presence of pollens in sediments does not necessarily indicate the local palaeovegetation. Pollen grains are easily transported by wind and can blow into an area from distant regions, and subsequently become incorporated into sediments. Pollen analyses must therefore be interpreted with caution.

Two initial pollen studies were conducted at LBW. The first investigated pollens from a single peat deposit in the Elandsfontein Formation and indicated that the vegetation during the Miocene included subtropical to tropical forest components as well as some marsh plants and very few fynbos taxa (Coetzee, 1978; Coetzee and Rogers, 1982). A second pollen study from the fossiliferous Varswater Formation yielded a single pollen spectrum of which 92% of the pollens were unidentified (Tankard and Rogers, 1978). Scott (1995) has recently re-analysed this pollen spectrum together with two additional pollen samples – one from the floor of the quarry (QSM) and the other from 6.4 m below the floor. The spectrum from below the quarry floor is transitional between the quarry floor (QSM) pollens and those of the Miocene Elandsfontein Formation studied by Coetzee and co-authors. In this sample Restionaceae and palm-pollens are dominant and tree pollens are a minor component. The QSM quarry floor sample indicates swampy conditions with ~20% Cyperaceae, ~10% Asteraceae and a few fynbos and tree elements. The dominant pollens from the unidentified pollen spectrum from the fossiliferous deposits (Tankard and Rogers, 1978) belong to the Ranunculaceae (buttercup) family (Scott, 1995). These plants are believed to have been aquatic or semi-aquatic and probably occurred in the swampy basin. Very few diagnostic elements indicating more open-vegetation were found in this spectrum. In summary, pollen results indicate a shift from a more tropical forest environment (below the quarry floor) to a more open swampy environment with some minor fynbos elements (in the QSM and PPM).

A pollen sequence from a drilling core off Noordhoek (Figure 2.1B) in the winter rainfall area of South Africa supports this finding and indicates that subtropical forests (including palms) were present during the Early Miocene (Coetzee, 1978).

Together with faunal evidence from LBW, it is generally agreed that during the Early Pliocene transgression the vegetation became more open – the subtropical to

tropical forests that were characteristic of the Miocene were gradually replaced by expanding grasslands. In addition, Scott (1995) has provided evidence that fynbos was beginning to establish itself at this time. The precise dating of the establishment of fynbos and succulent karoo biomes is not known but it is believed to have been coincident with the establishment of C_4 grasslands during the cooling of the Late Tertiary (Vogel et al., 1978; Coetzee and Rogers, 1982; Scott, 1995; Scott et al., 1997; Scott, 2002).

2.8 Review of the palaeoenvironment of LBW prior to this study

All the early excavations and interpretations of the palaeoenvironment at Langebaanweg during the Early Pliocene were made by Hendey (Hendey, 1981a, 1981b, 1983a, 1984) and Klein (1981, 1982) and are summarised in Table 2.1.

Insight into the prevailing environmental conditions of the time stem mostly from the nature of the deposits and incorporated fossils. Marine fauna from the Saldanha Formation (molluscs and sharks) indicate warm-water conditions (warm temperate to subtropical), whereas the marine fauna of the Varswater Formation (molluscs, seal, penguins) indicate cold-water conditions (cold temperate) (Hendey, 1981b). A shift from a warm temperate or subtropical environment to colder temperate conditions was taking place in the LBW area during the Late Miocene to Early Pliocene epochs. Terrestrial fauna (parrots, giraffids and waterbuck) also suggest subtropical to tropical palaeotemperatures and indicate that at least some remnants of the tropical biota managed to survive into the Early Pliocene. Other indicators of more tropical conditions are however absent (crocodiles) or rare (primates). The absence of crocodiles is odd since they are fairly common in African fluviatile deposits laid down in warm climatic conditions (i.e. where freezing temperatures are lacking) (e.g. Arrisdrift) (Figure 2.1). Only two primate teeth (an upper and lower deciduous fourth premolar) have been found at LBW. These teeth were found in close association to one another and are of a similar wear stage, preservation state and size, which lead to the conclusion that they probably belonged to the same individual (Grine and Hendey, 1981). The rarity of primates suggests that either forests were not tropical (i.e. trees could not provide food throughout the

year) or taphonomic factors were such that remains of primates were not preserved in these deposits.

There is no clear evidence as to whether the climate regime at LBW was winter-wet/summer-dry or winter-dry/summer-wet, but according to Hendey (1981a, 1984) extremely harsh seasons prevailed during the Early Pliocene. The presence of burnt bones, especially of slow moving animals, in the QSM and PPM suggest that the climate included a pronounced dry season during which fires were common. It is most likely that lightning started these fires as human and volcanic activity can be excluded. If lightning followed a prolonged dry season that had left vegetation and peat deposits dessicated then veld fires could have flared up. These fires would have placed the fauna under extreme stress – trapping animals attracted to the floodplain and river margins and further reducing food supplies. Electrical storms are common in the summer rainfall areas of South Africa and if Hendey's conclusion that lightning started the fires is correct, then this would imply that the present winter-wet/summer-dry climate regime was either not in place yet, or, that deposition occurred at a time when a transition in climate regime was taking place (Hendey, 1981b). Hendey (1976, 1980) concludes that the QSM fossils accumulated during a dry season and by the time deposition of the PPM occurred, the environment was strongly seasonal with Bed 3aS and 3aN representing flood-season accumulations. Overall, there appears to have been a shift from a stable, less seasonal environment to a harsher, more seasonal environment.

In summary, although there was no solid evidence of the climate regime or seasonality of the LBW area prior to this study, it is believed that an adaptation to cooler conditions with more open vegetation was progressing at the time of deposition of the fossiliferous deposits.

Table 2.1. Summary of the palaeoenvironment of LBW (modified from Hendey, 1981a).

Deposit	Age	Depositional environment	Sea-level	Pollen evidence	Faunal evidence	Climate
Bredasdrop Formation: Baard's Quarry	Late Pliocene (2.8-3.8 Myr) OR (1.7-1.9 Myr)	Fluviatile	Stillstand during regression OR transgression climax		Open country forms dominate	Becoming colder
Bredasdrop Formation: Anyskop terrestrial deposits	Late Pliocene (3.8-4.2 Myr)	Terrestrial (possibly a sand bar)	Stillstand during regression		Open country forms dominate	Warm temperate
Varswater formation: CSM	Early Pliocene (4.2-5.2 Myr)	Marine and fluviatile				Becoming warmer
Varswater Formation: PPM		Marine and fluviatile		More fynbos elements present (Scott, 1995)	Forest forms decline, some open country forms present	
Varswater Formation: QSM		Estuarine		Transition from subtropical woodland to fynbos (Scott, 1995)	Forest forms decline, some open country forms present; seals and penguins also present	Cold temperate
Saldanha Formation	Late Miocene (6.6-9.8 Myr)	Marine	stillstand during regression		Molluscs and sharks present	becoming cooler; warm temperate to subtropical conditions
Elandsfontein Formation	Early to middle Miocene (14-22 Myr)	Marine and terrestrial	Transgression	Subtropical forests with swamps (Coetzee, 1978; Scott, 1995)	Forest forms dominate (closed habitats) (Hendey, 1981b)	Tropical to subtropical

2.9 Other Late Tertiary deposits in South Africa

Further evidence of local prevailing environmental conditions during the Late Tertiary stem from fossil assemblages pre- and post-dating the LBW fauna. These are however limited.

Only marine fossils from the Early Miocene are known. The earliest evidence for terrestrial faunal communities on the west coast of Southern Africa come from the Early - Middle Miocene locality, Arrisdrift (Figure 2.1). At this time the cold Benguella Upwelling System had not been established and the vegetation, climate (and fauna) of this region was probably similar to that of the LBW area, further south (Hendey, 1984). Crocodiles are fairly well represented at Arrisdrift and indicate that relatively high temperatures occurred. The faunal composition at this locality has led to the general conclusion that during the Early-Middle Miocene, this region of the continent was made up of forest with dense undergrowth. Some grassy areas were also present (Hendey, 1984). Compared to Arrisdrift, the Langebaanweg taxa are more derived (Hendey, 1984). The small herbivores, however, are not as common as in the Miocene assemblage possibly because of a decline in the preferred habitats (i.e. dense undergrowth) of these animals (Hendey, 1981b). Alternatively this is a preservation bias.

In South Africa, the vertebrate fossil record is virtually non-existent for the entire Middle to Late Miocene (15 to 6 Myr). The fossil record elsewhere in Africa is also comparatively poor yet this was a time when Africa's mammalian faunal communities underwent dramatic changes (Hendey, 1984). LBW is therefore uniquely placed at a critical time period to document some of these changes.

The only fossil assemblages on the west coast of South Africa that date to the Late Pliocene are from Baard's quarry and Anyskop near LBW. These assemblages contain mostly fragmentary material but open-country grazers are better represented than in the Early Pliocene Varswater Formation, indicating that there was a further opening up of vegetation with grasslands being a significant component of the ecosystem. Some presumed forest dwellers are however still present, such as sivatheres (Sivatheriinae) and elephants (Proboscideae). The black rhinoceros (*Diceros diceros*), which is not present in the Varswater Formation, is a new addition

to the faunal composition (Hendey, 1984). The extant species (*Diceros bicornis*) is a browser and is well adapted to living in arid conditions (Apps, 1986).

The next closest localities to LBW in terms of age are Makapansgat Limeworks Member 3 (~3 Myr) and Sterkfontein Member 4 (~2.4 Myr) (Vrba, 1982). Both these localities are situated inland in the summer-rainfall area of South Africa (Figure 2.1A). Ungulates from these localities include a diverse collection of both artiodactyls and perrissodactyls and suggest the presence of extensive grasslands. Vrba (1985) has shown that major faunal turnover occurred at around 2.5 Myr in southern Africa when wooded environments opened up further. Recent isotopic evidence has shown that in both localities, C_4 grasslands were common during the Late Pliocene and Early Pleistocene (Luyt, 2001; Sponheimer et al., 2001).

Chapter 3

TOOTH DEVELOPMENT, STRUCTURE AND ENAMEL DEFECTS

3.1 Introduction

This chapter provides a background to mammalian tooth development and structure in order to understand the dental defects that are documented in subsequent chapters. Since defects in enamel are the main focus of these chapters, the histology and ultrastructure of enamel is described. Enamel defects, in particular enamel hypoplasia, are described together with the methods used to assess these defects. A literature review of enamel hypoplasia in fossil animals is also provided.

3.2 Tooth development

During fossilisation, three mineralised tissues – enamel, dentine and cementum – are preserved in mammalian teeth. Enamel is of ectodermal (epithelial) origin whereas dentine and cementum develop from mesenchyme. Tooth development is essentially the product of interactions between the ectoderm and mesoderm (Kollar and Lumsden, 1979) (Figure 3.1). The enamel epithelium invaginates and becomes progressively more cap-shaped as the mesenchyme adjacent to and beneath it differentiates to form a cellular mass called the dental papilla (Figure 3.1A-B). During the cap stage (Figure 3.1C), the cells of the inner epithelium differentiate to become enamel-producing cells (ameloblasts) and induce the cells beneath it to differentiate into odontoblasts (dentine-producing cells). This induction begins in the apical region of the dental papilla (star in Figure 3.1C). As ameloblasts and odontoblasts differentiate at the tip of the crown, a layer of predentine matrix is laid down between these cellular layers. The deposition of dentine induces the production of enamel by adjacent ameloblasts, which is laid down on top of the predentine mould. The basement membrane situated between these two cellular layers (Figure 3.1C) eventually becomes the enamel-dentine junction and the ameloblast and odontoblast layer become separated by newly secreted dentine and enamel. Thus both enamel and dentine develop extracellularly.

As cells further down the crown differentiate, progressively more dentine and enamel are laid down. Teeth thus essentially develop from the tip of the crown down towards its base, so that the enamel at the top of the crown is "older" than the enamel at the base of the crown. In conjunction with a downward development, enamel also increases in thickness from the enamel-dentine junction outwards.

The reason why the basement membrane of the dental papilla folds in a particular way is not well understood, but may simply be a combination of growth and shape change due to cell division (mitosis) and cell movement (Fortelius, 1985).

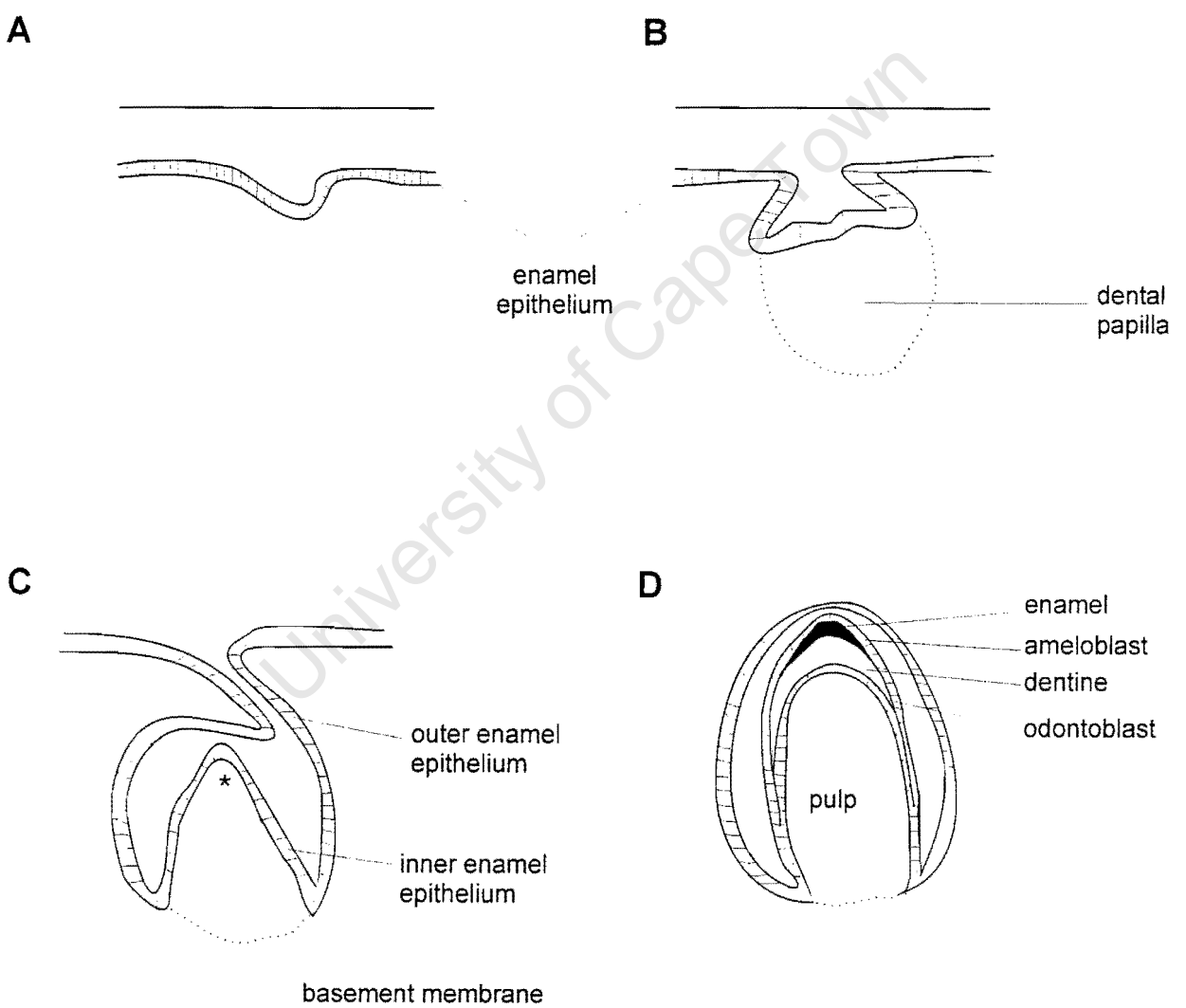

Figure 3.1. Mammalian tooth development (modified from Carlson, 1990). (A) enamel epithelium invaginates, (B) dental papilla differentiates, (C) ameloblasts from the inner epithelium induce cells beneath it to differentiate into odontoblasts (star), and (D) enamel and dentine are laid down between the ameloblast and odontoblast layers.

Once the dentine and enamel have been laid down, mineralisation commences (Scott and Symons, 1977). Dentine mineralises first, followed by enamel and then cementum. Dentine and cementum can continue to form throughout life whereas once enamel has mineralised it is no longer in contact with cellular elements and therefore cannot continue to form. The process of amelogenesis[1] is discussed in more detail in section 3.3. Root formation is not completed until some time after crown formation is complete (Weinreb, 1964, Scott and Symons, 1977). In hypsodont teeth the crown base may still be forming when the tooth erupts (Carlson, 1990).

3.3 Normal enamel development

Enamel is extremely compact and is composed of apatite crystals (~ 50 nm in diameter) that are held together by a protein, amelogenin. Mature enamel consists of ~96% inorganic component, a small organic component (~1%) and ~3% water. Once formed, enamel is not entirely inert as ion exchange can take place from the saliva into the surface layer of enamel.

Amelogenesis is a two-phase process involving the laying down of organic enamel matrix followed by its mineralisation. These two processes do not simply occur in succession but rather are integrated steps with enamel in one region mineralising soon after it is laid down and before enamel is laid down in adjacent regions.

First phase: laying down the matrix

Enamel is laid down incrementally starting at the enamel-dentine junction, at the tip of the tooth. Enamel secretion first caps the tooth and these increments are laid down on top of one another so that each successive layer obscures the previous layer (Figure 3.2). These increments of enamel then spread down the tooth as ameloblasts move, in more or less concentric zones around the tooth. Successive positions of the enamel matrix forming front are marked in the tissue by incremental lines (Striae of Retzius) visible in light microscopy (Retzius, 1836) (Figure 3.2B). Each layer is laid down slightly cervically to the previous layer so that perikymata can

[1] Enamel formation including mineralisation.

be seen on the surface of the enamel. Some authors have used counts of perikymata grooves to represent counts of the underlying Striae of Retzius (Hillson, 1992). The developing tooth is thus covered by cells at different stages of differentiation; the "oldest" at the top of the tooth and the "youngest" towards the secretory margin. All ameloblasts go through the same developmental sequence so that the resulting enamel tissue shows regular layering, which is parallel to the enamel-dentine junction and the surface of the tooth.

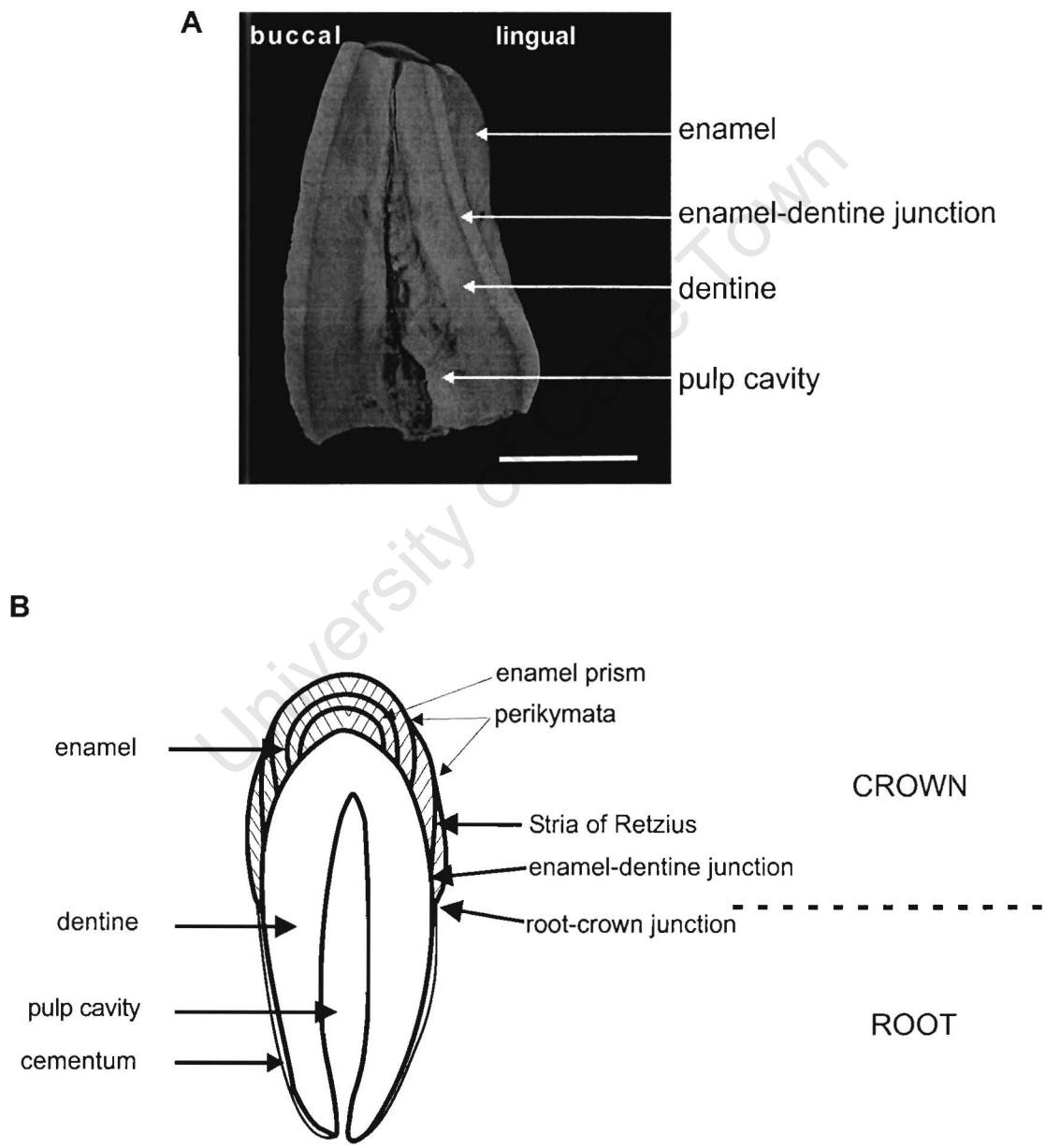

Figure 3.2. Tooth microstructure. (A) *S. hendeyi* tooth crown (PQL 58677) showing internal features. Scale bar represents 1 cm. (B) diagrammatical representation of the histological features of a tooth (modified from Goodman and Rose, 1990).

Enamel secretion takes place from only one end of the ameloblasts. These cells are columnar in shape and have reversed polarity in that they secrete a product towards the basement membrane, rather than away from it. In mammals the secretory end of these cells have a process known as a Tomes' process (Figure 3.3). As ameloblasts secrete protein matrix and move out of position, they leave a pit previously occupied by the end of their Tomes' process. The shape of this pit reflects both the shape and dynamics of the secretory surface (Boyde, 1964, 1976).

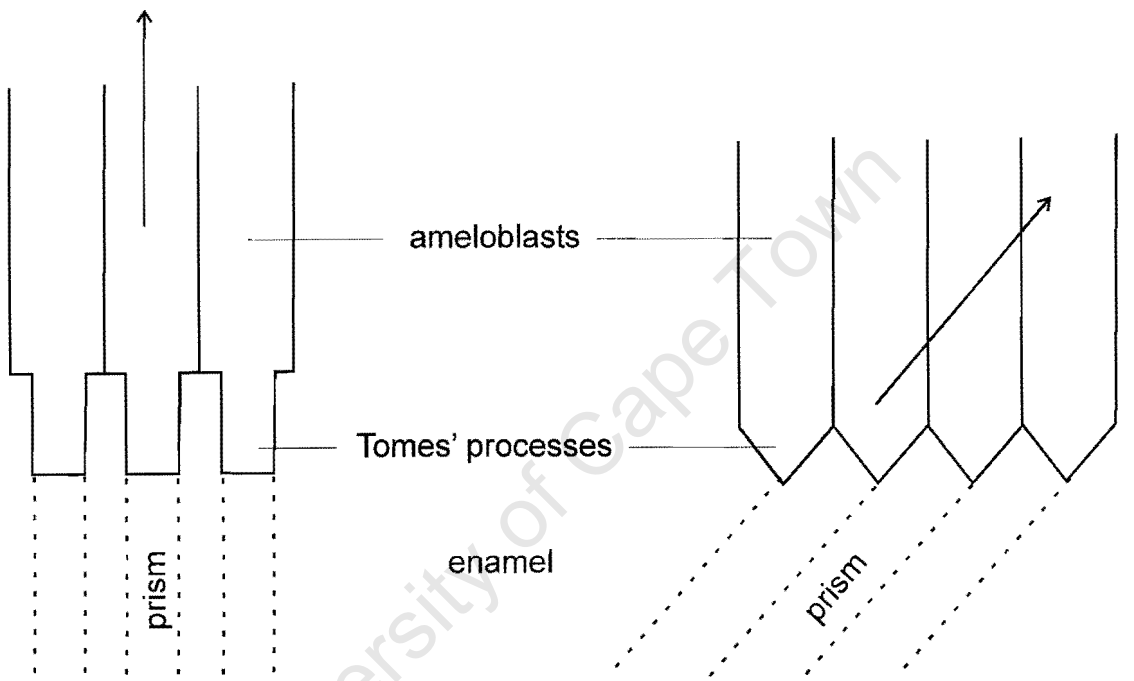

Figure 3.3. Enamel matrix production by ameloblasts (modified from Carlson, 1990). The arrows indicate the direction of ameloblast movement.

Second phase: mineralisation

As enamel matures and mineralises, the protein content of the matrix drops and the crystals grow from less than 10 nm to 40-60 nm in diameter (Boyde, 1976). This mineralisation process is not a one-step process and recent evidence has shown that it occurs in waves across the depth of the enamel in sheep and goats (Shupe et al., 1984; Suckling, 1989; Suga, 1989). Mineralisation appears to occur in three waves – the first proceeds from the surface of the tooth towards the enamel-dentine junction, the second wave moves back towards the surface of the tooth and the third wave proceeds in the original direction back to the enamel-dentine junction.

The timings of these mineralisation steps in relation to matrix formation are not known (Suckling, 1989). Enamel that has mineralised fully can easily be distinguished from unmineralised enamel based on morphology (Figure 3.4). In *S. hendeyi* molars, enamel mineralisation begins at the top of the crown before enamel has been laid down at the base of the tooth crown. Enamel development of teeth with tooth folds (such as in the molars and premolars), is complex and not fully understood (Fortelius, 1985) although it has been documented in some domestic animals (e.g. sheep: Weinreb, 1964).

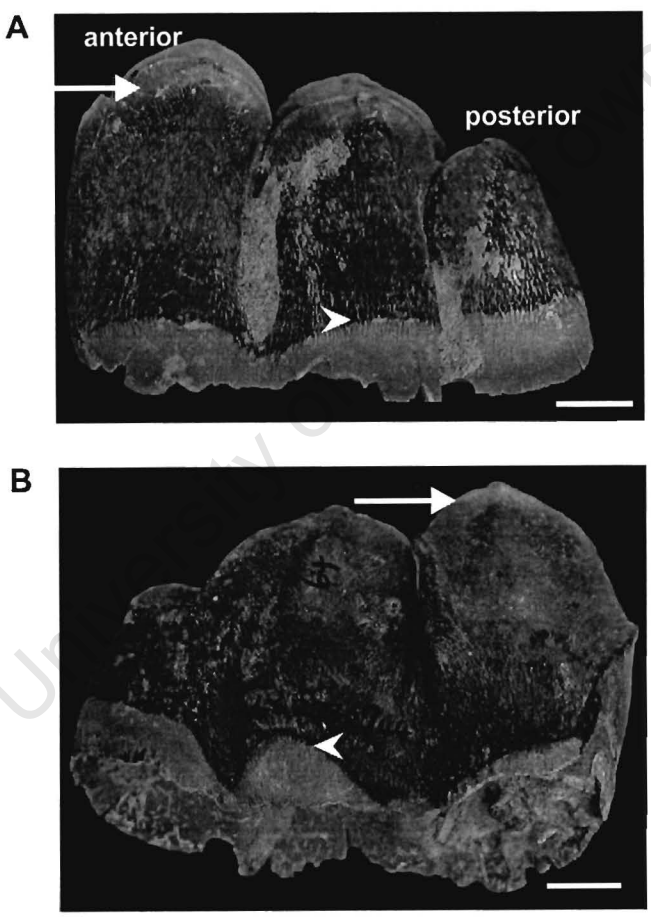

Figure 3.4. Amelogenesis in a third mandibular molar (PQL 62732/44) belonging to *S. hendeyi*. (A) buccal view, (B) lingual view. The enamel forming front (arrowheads) can be seen towards the base of the tooth in both views. In (A), mineralisation of the enamel has begun at the tips of the anterior and middle cusps (arrows), whereas in (B) only the tip of the anterior cusp has begun to mineralise.

3.3.1 Enamel histology

Incremental lines can be distinguished in all three mineralised tissues of teeth. In dentine, these incremental lines are called 'contour lines of Owen', whereas in enamel they are referred to as 'Striae of Retzius' (Figure 3.2). Incremental lines record the rhythmic nature of the cells laying down the respective tissue type and occur at regular intervals. The amount of time lapsed between these lines varies among individuals of different taxa, at different ontogenetic stages and in different environments. If the relationship of these lines to daily, monthly and yearly time periods is established, then these lines can be used to estimate the age and season of death as well as to calculate growth rates (Carlson, 1990). For example, a neonatal line (which is essentially an accentuated incremental line) resulting from nutritional and environmental disturbances at birth is visible in the dentine and enamel of teeth that are mineralising at birth. According to Hillson (1986), the brown appearance of striae is related to changes in crystallite size or orientation, or enamel porosity. Striae of Retzius are associated with a hypomineralisation of the enamel but can be (on rare occasions) associated with hypermineralisation. In general, dark incremental lines are formed at times of little or arrested growth whereas light bands form during periods of rapid growth (Stallibrass, 1982; Hillson, 1986).

Schour and co-workers (Schour and Smith, 1934; Schour and Hoffman, 1940) observed a calcification rhythm of 16 micron (μm) in a range of enamel and dentine samples from endothermic and ectothermic vertebrates. However others have shown that in primates, the rate of dentine apposition is 4 μm per day and this rate varies from 2 to 12 μm (per day) at different positions in a single tooth, and among teeth in the dentition (Schour and Smith, 1934; Schour and Hoffman, 1940). Incremental lines representing known increments of time have been described for mammalian dentine and cementum. In ungulates these layers are annual (Klevezal, 1996). The formation of these regularly spaced incremental lines have been shown to relate to seasonal variations in rainfall, temperature and hormonal/breeding cycles (Bromage and Dean, 1985). The increments of enamel are thought to be daily layers, but they have only been analysed in detail in humans (Klevezal, 1996). The regular growth rhythm of enamel is thus not fully understood in other mammals.

3.3.2 Enamel ultrastructure

The ultrastructure of enamel, first described by Boyde (1964, 1976), affects both the mechanical properties and the morphology of the worn surface (Rensberger and von Koenigswald, 1980; Fortelius, 1985; von Koenigswald and Sander, 1997).

The apatite crystals are orientated perpendicular to the secretory surface, below which they develop. Discontinuities in crystal orientation between portions secreted by different parts of the surface of the Tomes' processes are responsible for the appearance of so-called enamel prisms or rods. These prisms are long rod-like structures, which extend from the dentine substrate to just below the surface of the tooth[2]. They are composed of similarly orientated apatite crystallites and are separated from adjacent prisms by an organic "prism sheath" and interprismatic crystallites (Glimcher, 1959; LeGeros, 1981) (Figure 3.5). The crystallites between each prism change their orientation in a gradual and predictable manner, but near the prism sheaths they change orientation abruptly. The prism sheaths are typically cylindrical or U-shaped. When the pit formed by the Tomes' process has a cylindrical wall then the corresponding prisms are completely surrounded by interprismatic enamel (Figure 3.5A-B). When the pit is U-shaped the prism boundary is incomplete and the prismatic phase is continuous with the interprismatic phase (Figure 3.5C-F). The interprismatic enamel is less dense and contains more water and protein than prismatic enamel. The break in the prism boundary is situated on the side of the Tomes' process that is not buried in the matrix and which is facing away from the direction of movement (see Figure 3.3).

Boyde (1964) recognised three main types of prisms, Patterns 1-3 (described below), based on variations in size, shape, orientation and relative density of the prisms. These patterns relate to the direction of ameloblast movement, their size and rate of secretion.

[2] A thin layer of prismless (or aprismatic) enamel is present at the surface of most mammalian teeth. This enamel is denser and more resistant to wear than prismatic enamel and results from ameloblasts that have lost their Tomes' processes (Boyde, 1964, 1976; Carlson, 1990).

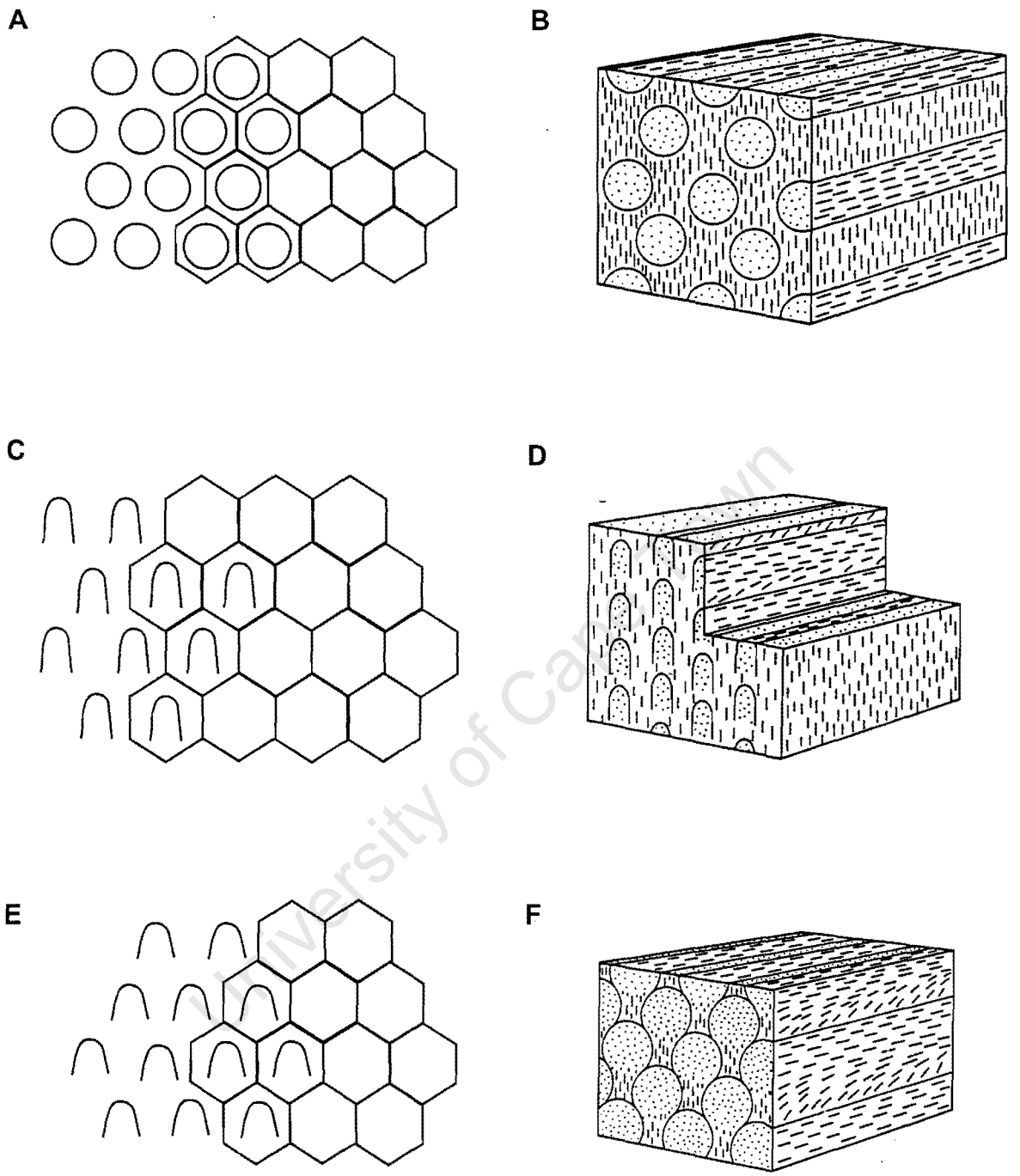

Figure 3.5. Enamel prism patterns of Boyde (1964). (A,B) Pattern 1 prisms (1.2-1.6 μm), (C, D) Pattern 2 prisms (0.7-1.2 μm), and (E, F) Pattern 3 prisms (1.6-2.0 μm). Short lines in B, D and F indicate orientation of crystallites. (Modified from Carlson, 1990).

All enamel prisms are packed hexagonally as shown in the Figure 3.5. Pattern 1 prisms are circular in cross-section and intermediate in size (1.2 - 1.6 µm). Pattern 2 prisms are the smallest (0.7 - 1.2 µm) while Pattern 3 prisms are the largest (1.6 - 2.0 µm). Both Pattern 2 and 3 prisms have incomplete boundaries. This prism arrangement results in prominent "inter-row sheets" or layers of interprismatic enamel in Pattern 2 but very little interprismatic enamel in Pattern 3. This size relationship of prisms cuts across taxonomic groups and is very consistent. There are also differences in prism packing at different depths within the enamel. For example, Pattern 1 prisms are found throughout the enamel of some animals (e.g. bats and whales) but in most mammals it only occurs near the enamel-dentine junction and near the surface of the tooth (Boyde, 1964, 1976). Although all three prism patterns can often be found somewhere in the enamel of most mammalian teeth, usually only one pattern predominates (Hillson, 1986).

During early secretion, the ameloblasts do not move relative to one another and consequently Pattern 1 enamel is formed close to the enamel-dentine junction. If enamel prisms of successive layers cross one another at an angle then a phenomenon called "decussation" can be observed. Pattern 1 prisms are thus not associated with decussation. Soon afterwards however, bands of ameloblasts begin to move relative to one another and decussating enamel is formed. Decussation may involve a single layer of prisms or several layers, with a transition that may be abrupt or gradual (Rensberger and von Koenigswald, 1980). Layers of decussating prisms are known as decussating zones or Hunter-Schreger bands[3]. Decussation of Pattern 3 enamel is usually more abrupt than in Pattern 2 enamel, which has prominent inter-row sheets. During later stages of development the tendency of ameloblasts to move relative to each other is reduced and less decussating or non-decussating enamel is formed. In the final stages of secretion, the ameloblasts lose their Tomes' processes and a layer of aprismatic (or prismless) enamel is formed. This layer is thought to increase the area of attachment of the coronal cementum. In horses, the cementum layer is attached after parts of the enamel are resorbed by osteoclasts (Jones and Boyde, 1974). In some ungulates no such layer is found.

[3] Hunter-Schreger bands are a specific type of prism decussation in which prisms decussate in layers (von Koenigswald and Sander, 1997).

The main differences between each of the prism patterns described above are summarised in Table 3.1.

Crystal orientation and packing is important in wear resistance (Rensberger and von Koenigswald, 1980; Carlson, 1990) but the relationship between decussating prisms and wear is not clear. The development and evolution of prism decussation and Hunter-Schreger bands is thought to have a functional significance and may relate to body size (Rensberger and von Koenigswald, 1980; von Koenigswald and Pfretzschner, 1987). According to von Koenigswald and Pfretzschner (1987) the evolution of Hunter-Schreger bands enhanced the diversification of mammals by allowing increased dietary diversity, because the presence of these bands makes enamel better able to withstand higher masticatory stresses. Little is known about decussating prisms in ungulates (Carlson, 1990).

Table 3.1. The main differences between enamel prism Pattern 1, 2 and 3.

	Pattern 1	**Pattern 2**	**Pattern 3**
Prism boundaries	Complete	Incomplete	Incomplete
Decussation	None	Present	Present
Inter-row sheets	None (but does have interprismatic enamel)	Prominent	Little
Prism size	1.2-1.6 µm	0.7-1.2 µm	1.6-2.0 µm

3.3.2.1 Evolutionary aspects of enamel ultrastucture

The size, shape and organisation of prisms within enamel vary amongst mammalian taxa (Gantt et al., 1980; Grine et al., 1986; von Koenigswald et al., 1987; Carlson, 1990) and have been used for taxonomy in human evolution (Vrba and Grine, 1978; Boyde and Martin, 1982). Grine et al. (1986) analysed the enamel ultrastructure of two bovid species (sheep, *Ovis aries*, and goats, *Capra hircus*), and found that these two species differ significantly in several quantitative parameters (such as prism density and size), despite having the same prism pattern (Pattern 2). Ultrastructural patterns can even vary within a single tooth (Boyde and Martin, 1984), but this seems to only occur in mammals with relatively thick enamel layers. Pattern

1 is considered to be primitive among mammals (Kozawa, 1984; Sahni, 1984) and is the normal structure for the thin enamel of the odontocete whales (Hillson, 1986). This pattern occurs in some multituberculates, some marsupials, some chiropterans, most insectivores, some cetaceans, sirenians, tapirids, some lemurs, and some hominoids (Boyde, 1976; Boyde and Martin, 1984; Kozawa, 1984). Pattern 2 is the arrangement for Artiodactyla and Perissodactyla. It can also be found in most marsupials, rodents, lagomorphs and some primates (Boyde, 1976). Inter-row sheets are particularly prominent and decussation is fairly common in the enamel of both artiodactyl and perissodactyl ungulates. Pattern 3 prisms are found in some multituberculates, some cetaceans, proboscideans, carnivores, some primates and man (Boyde, 1976).

The enamel structure in Early Mesozoic (~220 Myr) mammals appears to be more organised than in later (Tertiary to recent) mammals. Some Mesozoic mammals do not have true prismatic enamel (Poole, 1967). Hunter-Schreger bands have been traced back as far as the Early Paleocene (~65 Myr) condylarth mammals (von Koenigswald and Pfretzschner, 1987) and appear to be absent in Mesozoic mammalian enamel. Prism decussation is absent in earlier species but present in later ungulates, carnivores, and primates. It appears to have evolved several times independently within mammals.

3.4 Developmental enamel defects

Developmental enamel defects are of two types – enamel hypomineralisation or enamel hypoplasia. Hypomineralisation results from a disruption in the mineralisation (or maturation) phase of enamel formation and unlike enamel hypoplasia it is qualitative (Suckling and Purdell-Lewis, 1982). It is recognised as a discolouration of the surface enamel (Neiburger, 1990). Since, tooth colour is often altered during fossilisation by diagenesis, a distinction between true hypomineralisation and the effects of diagenesis is almost impossible to make. For this reason, mineralisation defects are typically not investigated when dealing with fossil specimens.

Enamel hypoplasia (EH) on the other hand is a developmental tooth defect that results from a disruption in ameloblasts during the laying down phase of enamel

development. This disruption results in shortened enamel rods and ultimately presents as a thinning of the enamel (Figure 2 in Goodman and Rose, 1990). These defects can be linear or non-linear depending on the arrangement of the defect on the tooth crown (see section 3.4.1). Enamel hypoplasia is a relatively sensitive (and permanent), non-specific indicator of systemic stress, although it can develop as a result of local (direct) trauma, or it can develop as the result of a genetic defect (Goodman and Rose, 1990). The morphology and distribution of enamel hypoplasia on various tooth types can indicate the cause of the defect. For example, in inherited cases all teeth will be affected (Stewart and Poole, 1982) and the animal is also likely to have other congenital abnormalities resulting in an overall low survival rate (Goodman and Rose, 1990). In humans, EH related to genetically inherited disorders is termed *amelogenesis imperfecta* (Hillson, 1992). Localised trauma on the other hand, would cause EH in single or adjacent teeth and would not affect the contralateral (uninjured) side of the mouth (Skinner, 1986; Skinner and Hung, 1986, 1989). EH as a result of a physiological stress (such as weaning, parturition, nutritional stress, illness and calf-cow separation) that occurs at a particular ontogenetic age, would affect all teeth developing at the time of the stress and would present as a linearly (or horizontally) arranged enamel hypoplasia (Neiburger, 1990; Goodman and Rose, 1990; Mead, 1999; Dobney and Ervynck, 2000; Lukacs, 2001). (These defects are discussed further in section 3.4.1.1). Both inherited cases and those as a result of local injury are rarely reported (in humans and primates) and no reports of these defects exist in non-primates.

Several fundamental issues regarding the aetiology of enamel hypoplasia are not fully understood – such as the amount of time that a stress event should be imposed before a defect manifests (Goodman and Rose, 1990). Interpretations of enamel hypoplasias are therefore complex. All enamel hypoplasia defects are however considered as indications of severe stress as they result from a cellular disruption during development (Goodman and Rose, 1990).

EH can also manifest as a result of the intake of abnormally high levels of fluoride, a condition known as fluoride toxicosis. Fluoride toxicosis can develop in modern animals living near industrial sites and has been reported in several wild deer and boar populations in Europe (Shearer et al., 1978; Kierdorf et al., 1993, 1996,

2000). It presents as dental lesions (dental fluorosis and irregular dental wear), bone structure changes (osteofluorosis[4]), as well as above normal levels of fluoride in bone, urine and blood. Bones that are more active metabolically such as those used in locomotion, chewing or breathing are more affected than bones that are primarily involved in a protective, less active function (Shupe et al., 1984). The severity of fluoride toxicosis depends on the amount of fluoride ingested, the species of animal, the age of the animal at the time of ingestion, duration of ingestion and the nutritional or health-status of the animal (Shupe et al., 1984). In the case of continual exposure to high levels of fluoride during tooth development, EH will affect all teeth in the mouth. The major lesions induced by excessive fluoride intake are found in developing permanent teeth and in developing and remodelling bones. Teeth are affected during enamel matrix formation and mineralisation only and once erupted, fluoride ingestion will have little or no effect. Bones however, may be affected throughout life and skeletal lesions (such as increased bone density) makes bones brittle and less able to resist stress. In teeth, the condition presents as mottled chalky patches of the enamel infiltrated with hypoplastic pitting and areas of hypomineralisation (Shearer et al., 1978).

3.4.1 Classification and significance of enamel hypoplasia

The FDI index (Federation Dentaire International, 1982) for EH recognises pits (single or multiple), grooves (vertical, horizontal, or oblique) and areas missing enamel. Essentially, linear defects are horizontal enamel defects – either a linear (horizontal) arrangement of small pits or a linear/horizontal groove across the tooth surface. Non-linear defects include pits (single or multiple diffuse pitting), grooves (vertical, oblique or short horizontal) and areas completely missing enamel (known as enamel aplasia).

3.4.1.1 Linear enamel hypoplasia

In humans, linear enamel hypoplasia is most commonly observed in maxillary central incisors and it appears that this tooth type is the most susceptible to ameloblast disruption (Goodman and Rose, 1990). The magnitude and response to physiological disruption, however, does not appear to be consistent regardless of

[4] These include sclerosis, porosis, periosteal hyperostosis, osteophytosis and/or malacia.

tooth type, so that tooth crowns developing at the same time may not be equally exposed and responsive to stress (Condon, 1981; Goodman and Armelagos, 1985). Whatever the pattern, there appears to be both an inter- and intra-tooth variation in susceptibility to hypoplasia in humans (Goodman and Armelagos, 1985; Goodman and Rose, 1990). In order to fully understand the conditions under which defects manifest, this difference in tooth susceptibility and tooth type incidence must be assessed for each animal.

Linear enamel hypoplasias that develop as the result of systemic stress are extremely useful as indicators of health-status. Because teeth develop from the tip to the base of the crown, the age at which a defect formed (i.e. the ontogenetic timing of the stress episode) can be estimated from its position on the tooth crown relative to the root-crown junction. In addition, the width of the linear defect relates to the duration of the stress episode and its depth is thought to relate to the severity of the stress period (Goodman and Rose, 1980; Suckling, 1989). The methods of assessing linear enamel hypoplasia are discussed in section 3.6.

3.4.1.2 Non-linear enamel hypoplasia

Few authors report non-linear enamel hypoplasia in human teeth (Blakey and Armelagos, 1985; Skinner, 1986; Skinner and Hung, 1986, 1989; Lukacs, 2001). These defects are essentially of two types, localised defects (such as single pits, short grooves or areas of enamel aplasia) and multiple non-linear pitting. The latter has been described in domestic animals as the result of a general calcium deficiency (Miles and Grigson, 1990). Since non-linear enamel hypoplasias are also the result of a disruption in ameloblasts during the laying down phase of enamel, the timing (or age) at which these defects manifest can be determined in the same manner as for linear defects. If the timing at which non-linear and linear defects manifest coincides, then this could indicate a common stress event that simply disrupted ameloblasts in a slightly different manner.

Localised enamel hypoplasias have only been reported in detail in the deciduous canine of humans (El-Najjar et al., 1978; Skinner and Hung, 1986, 1989; Skinner, 1996) and primates (Lukacs, 2001) and are the result of direct (local) trauma to the developing unerupted tooth. These defects have been attributed to the infant

attempting to put objects into its mouth, which may damage ameloblasts directly through fenestrations (i.e. openings) in the cortical bone overlying the developing tooth crypt. Skinner and Hung (1986) have shown that nutritional factors (such as deficiencies in calcium, vitamin A or vitamin D) are likely to contribute to the thinning of the facial bone that supports the tooth sockets. Poor maternal diet and premature births have also been tentatively implicated in producing these defects (Skinner, 1986). Localised EH in other deciduous teeth are however thought to relate to systemic stress. Only one report of a localised (non-linear) enamel hypoplasia on a permanent tooth crown has been made (Miles and Grigson, 1990). In this case, an abscess on the root of a deciduous tooth came in close contact with the unerupted permanent tooth crown (situated below it) and resulted in a localised defect forming on the permanent tooth.

Although numerous studies have investigated enamel hypoplasia in human and primate populations (Goodman et al., 1984; Skinner, 1986; Alaluusua et al., 1996; Skinner, 1996; Lukacs, 2001), only a few recent studies have reported enamel hypoplasia in non-primate fossils (Mead, 1999; Dobney and Ervynck, 2000; Niven, 2002) and none of these report non-linear defects.

3.5 Defect formation models (after Goodman and Rose, 1990)

Goodman and Rose (1990) constructed two models of enamel hypoplasia formation (summarised in Figure 3.6). The first, the epidemiological model, highlights a sequence of events that lead to defect manifestation (Figure 3.6A). Environmental constraints (such as poor nutrition) combine with an individual's host resistance to determine the type, duration and intensity of systemic stress. Changes in ameloblast activity, if prolonged and severe enough, may induce a permanent developmental change in the enamel structure (i.e. an enamel hypoplasia). The type of defect (e.g. a localised enamel aplasia versus a linear enamel hypoplasia) is determined by the functional state of the active ameloblast at the time of disruption. Similarly, the size of a defect may relate to the severity and intensity of disruption to the ameloblasts (Suckling, 1989).

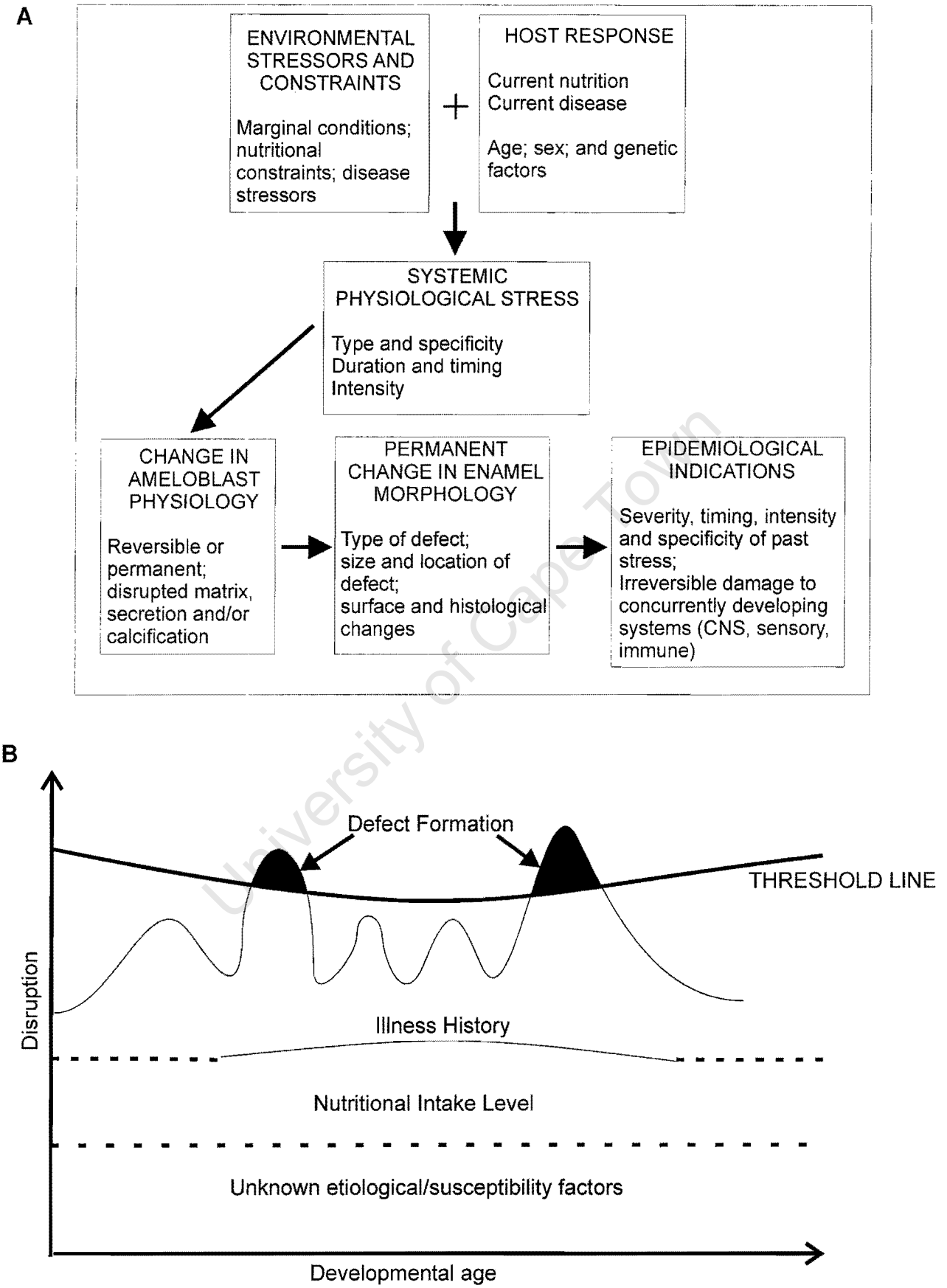

Figure 3.6. Models of enamel developmental defects (after Goodman and Rose,1990). (A) Epidemiological model and (B) Threshold model. The magnitude of ameloblast disruption is presented on the y-axis and developmental age on the x-axis.

The second or 'threshold" model highlights the aetiology of developmental defects (Figure 3.6B). Essentially, enamel developmental defects manifest when ameloblast disruption is pushed over the threshold level, due to a combination of factors. According to Goodman and Rose (1990), the first factors affecting ameloblast disruption are unknown susceptibility factors (such as genetic factors) that render the individual susceptible to stress or that weaken ameloblasts. The potential contribution of these factors to the development of enamel hypoplasia is not known, but Goodman and Rose (1990) place them hypothetically at 30% of the threshold. Nutrition is the next factor that is likely to have a significant effect on ameloblast disruption and on whether ameloblasts are pushed over the threshold level. Illness history is the final factor contributing to ameloblast disruption and is portrayed in the model as a wavy line. The amplitude of each crest is an indication of the severity of illness and the base of the line is determined by prior background genetic, nutritional and other resistance factors. According to this model, enamel defects manifest when the illness is severe enough that ameloblasts are disrupted to a greater degree than the threshold line. Goodman and Rose (1990), depict the threshold line as curved, because they found that ameloblasts are more sensitive to disruption in the middle third of teeth (as this region records the most defects in humans).

3.6 Methods of analysing enamel hypoplasia

Essentially there are three methods to analyse enamel hypoplasia. The first method determines an estimated age of the individual at the time the defect manifested; the second determines the duration of the stress period (Blakey et al., 1994), and the amount of tooth crown involved in the defect (Ensor and Irish, 1995), while the third examines enamel hypoplasia microscopically.

3.6.1 The estimation of age

In order to estimate the age at which a defect manifested, the following must be known: i) the tooth type affected, ii) the position of the defect on the tooth crown, and iii) the sequence and timing of tooth development for the animal concerned. The process of tooth development is distinct from the process of eruption. The former pertains to the development or formation of the tooth (crown and root) in the jaw, while the latter is the process of bringing the tooth into position for its function in

processing food. The first two criteria can easily be determined or can be measured directly while the third is particular to the animal under study.

3.6.2 Determining the duration of stress episodes and the amount of defective enamel

In order to determine the duration of each stress event, the width of each defect must be measured and the rate of enamel development (of each tooth type) for the animal under study must be known. A wide defect is essentially the result of a disruption in a larger number of ameloblasts than a narrower defect (if development rates are constant). The amount of tooth crown involved in a defect can be expressed as a percentage of the total crown height and is reflected by the Tooth Hypoplastic Area (THA) score (Ensor and Irish, 1995). In this method acute hypoplasias are defined arbitrarily as having a width of 0.5 mm or less and chronic hypoplasias as larger than 0.5 mm. For each chronic hypoplasia the percentage of crown disturbance is calculated by dividing the width of the defect by a two-thirds unworn crown height estimate. (This two-thirds crown height estimate is used in order to take tooth wear into account). A chronic defect covering 50% of the crown surface is given a value of 0.50. To allow compatibility with chronic values each acute hypoplasia is given a score of 0.10, even though an acute defect may not cover 10% of the crown surface (Ensor and Irish, 1995).

A constraint with this scoring method is that the different developmental rates of teeth are not considered. For most ungulates these are however unknown. Reid and Dean (2000) showed that at least in humans, no relationship exists between crown height and the total time taken to form enamel.

3.6.3 Histological features associated with enamel hypoplasia

In areas with linear enamel hypoplasia, a reduction in enamel thickness in the area with the defect, convergence of Striae of Retzius as they approach the enamel surface and an absence of the normal prism structure along the surface of the defect can be observed (Rose, 1977). The enamel within the defect is well mineralised indicating that ameloblasts do not die in the area of the defect but recover sufficiently to complete maturation. The convergence of striae suggests that matrix secretion slows down considerably after the insult and that ameloblasts do not die but rather

cease secretion after a period of reduced secretion. Typically normal enamel develops cervically to the macroscopic defect indicating that adjacent ameloblasts are not damaged. Suckling and Thurley (1984) noted that the longer ameloblasts have been secreting enamel matrix, the more vulnerable the ameloblast is to disruption. In humans, accentuated striae, also known as Wilson bands, typically lead off the defect and are frequently associated with enamel hypoplasia (Goodman and Rose, 1990). In sheep teeth that are (physically) severely traumatised accentuated lines are always associated with a linear defect (Suckling and Purdell-Lewis, 1982). Enamel hypoplasia associated with fluorosis also has grossly accentuated striae leading off or underlying the defect. The enamel forming these striae loses its normal prism structure and is aprismatic (and sometimes hypomineralised) (Kierdorf et al., 1993; Kierdorf and Kierdorf, 1997).

Defects manifesting during the early stages of amelogenesis, when the tooth tip is being capped, will not be visible as surface defects unless the ameloblasts are completely disrupted. In this case all subsequent enamel layers will be defective and a surface enamel aplasia (i.e. an area missing enamel) will be present.

All three of the above methods have been used to assess linear enamel hypoplasia (LEH) in humans and primates. However, in studies investigating LEH in non-primate fossil animals (Miocene rhinoceros: Mead, 1999; archaeological pigs: Dobney and Ervynck, 1998, 2000; archaeological bison: Niven, 2002) only the first method has been applied. Some of these authors merely report incidence of linear enamel hypoplasia, others attempt to determine the age and seasonality at which the defects manifested. Each of these studies is discussed below.

3.7 Previous studies of linear enamel hypoplasia in non-primates

In Mead's (1999) study of Miocene rhinoceroses (*Teleoceras*), the incidence of LEH in different tooth types was used to establish the age at which defects manifested, based on the tooth eruption sequence of extant black rhinoceroses (*Diceros bicornis*). They found that 87% of the recorded hypoplasia occurred in the deciduous fourth premolar (dp4). The relative constant position of the defect on the buccal side of the dp4s suggested a stress event occurring at a common ontogenetic stage. Based on the tooth development pattern in the extant species the timing of

the dp4 stress event was determined to be birth. Enamel hypoplasia was also found in 37% of the permanent fourth premolars (p4). It was speculated that this stress event (at around 3-4 years of age) was the abandonment of the calf by its mother prior to the birth of a new offspring, a phenomenon observed in extant rhinos. These authors examined only one extant rhinoceros mandible and found linear enamel hypoplasia on the p4. If their explanation for this stress episode is correct, then linear defects should be much more prevalent unless the fossil rhino was not producing calves at a mean calving interval of 3-4 years, as in their extant relatives. In order to confirm this speculation a large comparative sample of extant rhinoceros needs to be examined. The low incidence of linear enamel hypoplasia in the second and third molars (7.7% and 2.2% respectively) is explained as random, isolated occurrences of a disruption in amelogenesis and no further explanation as to what was responsible for this disruption is given.

Dobney and Ervynck (1998, 2000) examined linear enamel hypoplasia in pigs from several archaeological sites. They report the incidence of linear enamel hypoplasia in European archaeological sites of different ages and interpret the defects in terms of changing environmental conditions during the Middle Ages. A recent study (Dobney and Ervynck, 2000) attributes two discrete positions of linear defects on the first molar as a result of a birth (10% incidence) and then a weaning stress (14% incidence). A period of under-nutrition encountered during the first winter of life is thought to be the main factor responsible for linear defects observed in the second and third molar (m2: ~15% incidence; m3: 8-10% incidence). In this study the only reference to defect widths is a brief mention that, " third molar defects are broad compared to those in the second molar".

Niven (2002) investigated linear enamel hypoplasia in bison from an archaeological site about 2 500 B.P. She estimated the season and age of the animal at the time that the defect formed within a 2-3 month period, by dividing the monthly amount of enamel growth by the height of each defect from the base of the crown. These monthly increments of enamel were obtained by analysing modern bison skulls of known age. Her results indicate that enamel hypoplasia developed in three distinct periods of time when the bison was between two and 24 months of age. The only exception was a single fourth deciduous premolar, which has a linear defect

that must have developed *in utero*. The distinct age and seasonal peaks at which hypoplasia developed suggest that a combination of age-specific and season-specific factors affected the overall nutritional condition of these animals.

Chapter 4

ISOTOPIC PALAEOECOLOGY OF THE LANGEBAANWEG FAUNA

4.1 INTRODUCTION

This chapter details stable carbon and oxygen isotope analyses from tooth enamel carbonate of several members of the Langebaanweg (LBW) fossil fauna. Results of this analysis are used to reassess the palaeoenvironment of LBW during the Early Pliocene as well as elucidate the habitat preferences of several of the fossil fauna. Carbon isotopes are typically used to determine dietary preferences and floral composition, whereas oxygen isotopes can provide more subtle information on behavioural differences between taxa as well as small-scale seasonal fluctuations. The stable isotope approach for palaeodietary assessments is well established and has been applied to both extant animals (Vogel, 1978; Lee-Thorp, 1989; Koch et al., 1995; Cerling et al., 1997a; Lee-Thorp et al., 1997; Cerling and Harris, 1999; Cerling et al., 1999) and fossil fauna (Lee-Thorp and van der Merwe, 1991; Lee-Thorp et al., 1994; Quade et al., 1995; MacFadden and Cerling, 1996; Cerling et al., 1997a; MacFadden and Shockey, 1997; Cerling et al., 1999b; MacFadden et al., 1999; Zazzo et al., 2000).

4.1.1 Stable isotope preservation

The tool of stable isotope analyses relies on the integrity of the carbonate in biological apatite being preserved through time. Typically with fossils millions of years old, tooth enamel is preferred over dentine and bone, since it is denser, has a lower organic content and consists of larger apatite crystals. These characteristics make enamel more resistant to diagenetic alteration (Lee-Thorp and van der Merwe, 1987, 1991; Wang and Cerling, 1994; Sponheimer and Lee-Thorp, 1999a). Many authors have shown that carbon isotopes from tooth enamel can survive largely unaltered and that the distinction between C_3 and C_4 consumers is preserved in fossil animals over long periods of time: the present to Early Pliocene (Lee-Thorp and van der Merwe, 1987; Bocherens et al., 1996; MacFadden and Cerling, 1996; Cerling et al., 1999; MacFadden et al., 1999; Sponheimer and Lee-Thorp, 1999b); Miocene and

beyond (MacFadden and Cerling, 1994; Morgan et al., 1994; Quade et al., 1995; MacFadden and Cerling, 1996; MacFadden et al., 1996; Cerling et al., 1997a; Cerling et al., 1999; Zazzo et al., 2000).

The preservation of oxygen isotopes is, however, more difficult to assess. Several studies have shown that predictable patterns of water-related behaviours are maintained in fossil faunal assemblages (Bocherens et al., 1996; Sponheimer and Lee-Thorp, 1999b, 2001) and that seasonal patterns can be obtained from intra-tooth $\delta^{18}O$ variations[1] (Feranec and MacFadden, 2000). Bocherens et al. (1996) and Quade et al. (1995) observed that $\delta^{18}O$ values of both extant and fossil hippos are always significantly depleted compared to other fauna in the ecosystem. These authors proposed that this distinction provided a good test for the validity of the $\delta^{18}O$ signal and hence isotope preservation. The reason for this difference may be that hippos drink frequently and employ different methods from other artiodactyls to prevent body temperatures from rising during hot daytime temperatures. Many artiodactyls either pant or use evaporative cooling to maintain body temperatures below air temperatures (Pough et al., 1996). Hippos however, spend the hottest parts of the day wallowing in water pools and feed (on land) during the cooler night temperatures (Kingdon, 1982).

Although alteration of both $\delta^{13}C$ and $\delta^{18}O$ signals from fossil tooth enamel carbonate and $\delta^{18}O$ from phosphate is insignificant in many studies, this possibility must be assessed for each case study. Most authors agree that the strongest evidence for isotopic preservation is the occurrence (within a single deposit) of expected differences among ecologically distinct taxa (Lee-Thorp and van der Merwe, 1987; Morgan et al., 1994; Bocherens et al., 1996). In addition, one expects to observe seasonal fluctuations in the oxygen signature from single tooth crowns as teeth typically take several months to develop and mineralise.

The effects of diagenesis on the chemical structure of enamel can be investigated directly by Fourier Transform Infrared Spectroscopy (FTIR). FTIR

[1] Isotopic ratios such as $^{13}C/^{12}C$ and $^{18}O/^{16}O$ are typically expressed in delta (δ) notation as parts per thousand (‰).

analysis is a simple, quick method typically used to characterise biological apatites by providing information on bond strengths and ionic environments (LeGeros, 1981, 1991; Sponheimer and Lee-Thorp, 1999a). The FTIR spectra of enamel and bone for example, differ slightly according to subtle differences in composition and structure. For purposes of FTIR, the most important bonds in biological apatites are the P-O bond in phosphates and the C-O bond in carbonates. Carbonate ions are located in two anionic sites within apatites. Type A carbonates occupy the OH^- position (1540 cm^{-1}) and type B carbonates, which are more abundant, occupy the PO_4 position (1415 cm^{-1}). Changes or alterations in the phosphate and carbonate ions within apatites can be assessed by measuring shifts in the frequency (or wavelength) in the $\nu 4$ PO_4 and the $\nu 3$ CO_3 domain, or by detecting changes in absorbance. The $\nu 4$ phosphate domain contains two important peaks (at 565 cm^{-1} and 605 cm^{-1}) separated by a trough (at 590 cm^{-1}). The Infrared Splitting Index, also called the phosphate crystallinity index (PCI) by Sponheimer and Lee-Thorp (1999a), provides a measure of crystallinity of the apatite structure and can be measured by determining the absorbance in $\nu 4$ PO_4 domain (see section 4.2.2.1). FTIR spectroscopy is also a useful way to detect diagenetic carbonate minerals within fossils (Lee-Thorp and van der Merwe 1987, 1991; Sponheimer and Lee-Thorp, 1999a). FTIR analysis was thus used, prior to isotope analyses, to test whether the enamel apatite from the LBW fossils has retained the structural features of modern enamel.

4.1.1.1 Carbon isotopes

The $\delta^{13}C$ value of plants is a function of the photosynthetic pathway used to fix CO_2 (Park and Epstein, 1960) (Figure 4.1). C_3 photosynthesis is used in all trees, most shrubs and herbs and in grasses that favour a cool growing season. Plants using this pathway discriminate more strongly against the heavier ^{13}C isotope during fixation of CO_2 (as a 3-carbon sugar) and typically have $\delta^{13}C$ values between -20 to -35‰ (Vogel, 1978). In contrast, C_4 photosynthesis occurs in grasses that favour warm growing seasons as well as some herbs and sedges. The $\delta^{13}C$ range for C_4 foliage is -7 to -16‰ (Vogel, 1978). The reason for this is that C_4 plants are extremely efficient at fixing CO_2. The third photosynthetic pathway, the crassulacean acid metabolism (CAM) pathway, occurs in succulents adapted to arid climates only.

CAM plants can fix CO_2 by either the C_3 or C_4 pathway and exhibit $\delta^{13}C$ values intermediate between those of C_3 and C_4 plants. In most ecosystems, CAM plants are a minor component and these plants are therefore of little concern when interpreting the floral composition of palaeoenvironments and the diets of fossil animals.

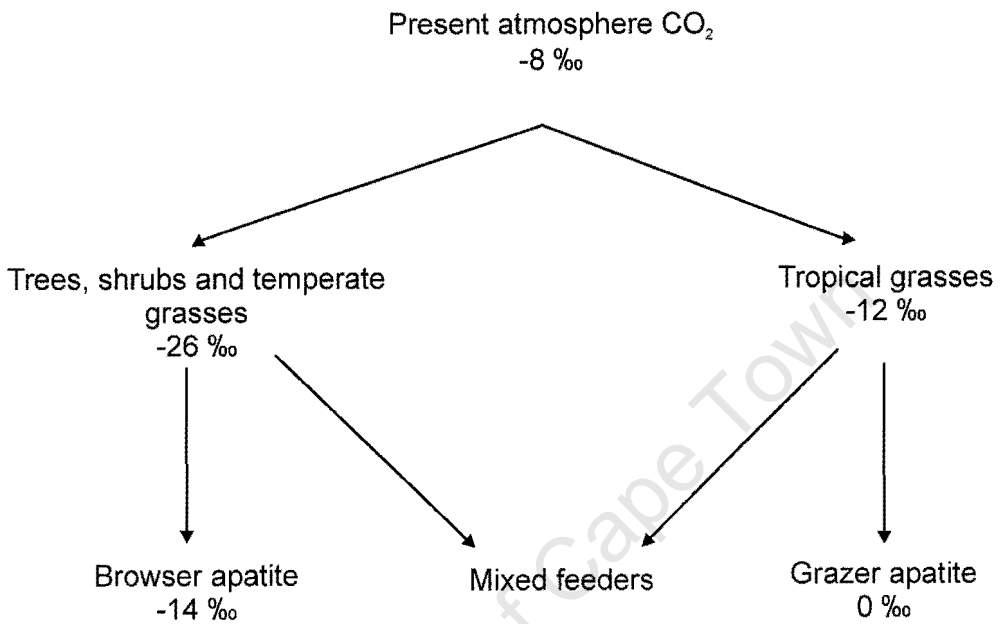

Figure 4.1. Fractionation of $^{13}C/^{12}C$ isotopes in a modern savanna ecosystem (modified from Lee-Thorp, 1989).

When herbivores eat, the $\delta^{13}C$ value of the vegetation they consume is incorporated into their tissues such that the $\delta^{13}C$ value of their tooth enamel reflects their diet, with some additional fractionation[2]. This fractionation value is known and an enrichment in $\delta^{13}C$ between diet and tooth enamel of 12 to 14‰ has been calculated (Lee-Thorp et al., 1989; Cerling and Harris, 1999). Typically, tooth enamel from herbivores eating C_3 vegetation has $\delta^{13}C$ values between -10 and -15‰ whereas herbivores feeding on C_4 tropical grasses have $\delta^{13}C$ values between +2 and

[2] An observable effect generally described in terms of depletion or enrichment of the heavy isotope (Hayes, 1982).

-2‰ (Figure 4.1). Mixed feeders have values between these two extremes. By determining the stable carbon isotope signatures of fossil animals, researchers have successfully placed fossil (and extinct) animals into distinct dietary categories (Lee-Thorp and van der Merwe, 1991; Lee-Thorp et al., 1994; Quade et al., 1995; MacFadden and Cerling, 1996; Cerling et al., 1997a; MacFadden and Shockey, 1997; Cerling et al., 1999; MacFadden et al., 1999; Zazzo et al., 2000). A constraint of the stable carbon isotope analysis is that the method is unable to address more subtle questions, such as whether a grazer preferred fresh grass. Dietary isotopes are recorded at the time of enamel development, and hence reflect the period in the younger animal's life.

The inefficiency of C_3 plants to fix CO_2 makes them more susceptible to abiotic influences than C_4 plants and this variability can indirectly provide additional dietary information. For example, in dense forests, which are invariably C_3 in character, plants growing on the forest floor tend to be depleted in ^{13}C relative to leaves in the canopy (Van der Merwe and Medina, 1991). This is due mainly to photosynthetic recycling of CO_2 produced by forest soil respiration as well as to the increased irradiation and greater evaporation rates experienced by leaves in the canopy. Thus even in C_3 environments, the $\delta^{13}C$ signatures of herbivores eating C_3 plants can provide some indication of where an animal ate – i.e. in an open or closed environment. C_3-grazers feeding in the open country tend to be enriched in $\delta^{13}C$ compared to browsers feeding in the shade of trees and shrubs (Ambrose and DeNiro, 1986).

A complication of the stable carbon isotope method is that modern ecosystems are depleted in ^{13}C by up to 1.5‰ owing to the fossil fuel effect (Friedii et al., 1986; Marino and McElroy, 1991), and there is therefore an apparent offset by this amount when comparing fossil and modern fauna. Some authors report up to 2-3‰ difference between the $\delta^{13}C$ values of modern and fossil ecosystems (Lee-Thorp and van der Merwe, 1987; Cerling et al., 1997b). A second constraint is that $\delta^{13}C$ signatures of tooth enamel do not necessarily translate simply into flora of the local area because some animals are migratory. Such a bias is real when inferences

are based on $\delta^{13}C$ values of large herbivores compared to small ones that tend not to be migratory.

4.1.1.2 Oxygen isotopes

Stable oxygen isotopes from bone or enamel phosphate have been used extensively to provide information on palaeoprecipitation and palaeotemperatures (Longinelli, 1984; Chappell and Shackleton, 1986; Ayliffe and Chivas, 1990; Bryant et al., 1994). $\delta^{18}O$ signatures from phosphate in enamel apatite are less susceptible to diagenesis than $\delta^{18}O_{carbonate}$ because the P-O bond is stronger than the C-O bond. Recently, however, it is has been shown that reasonable biogenic oxygen signals can be obtained from tooth enamel carbonate. $\delta^{18}O$ ratios can reflect local precipitation, short-term seasonal fluctuations and water-related behaviour of fossil animals (Koch et al., 1989; Fricke and O'Neil, 1996; Kohn et al., 1996; Sponheimer and Lee-Thorp, 2001a). The ability to use carbonate signals is useful because these signals are conveniently obtained from evolved CO_2 during the analysis of carbon isotopes ratios and as a result require no additional sampling.

The $\delta^{18}O$ signature of tooth enamel carbonate is directly related to that of body water, which in turn reflects water-usage (uptake and loss) of the animal during tooth development. This method is dependent on the fact that mammals have a constant body temperature. An animal's physiology acts as a filter that regulates the balance between input (plant water, inspired O_2 and drinking water) and output sources (water vapour, CO_2, excretion) of oxygen during enamel formation. Because plant water (e.g. in leaves) and meteoric rainwater have different $\delta^{18}O$ signatures[3], herbivores that obtain most of their water from drinking (i.e. obligate drinkers, which are frequently grazers) can be distinguished from those that obtain water mainly from plants (i.e. non-obligate drinkers, which are usually browsers). Browsers therefore tend to be enriched compared to grazers (Sponheimer and Lee-Thorp, 1999b). Feeding behaviours can also influence enamel $\delta^{18}O$ values *indirectly* since animals feeding during the cooler night temperatures appear to be depleted compared to animals feeding in the hot midday sun. The reason for this is that plant water is not enriched at night (Yakir, 1992). Oxygen isotopes, although not as well understood as

[3] Plant water is enriched compared to meteoric water (Epstein et al., 1977; Yakir, 1992).

carbon isotope pathways, can therefore potentially provide behavioural information about fossil, and particularly extinct animals, which would otherwise not be available. A complication of this technique is that a 2‰ variation in the $\delta^{18}O$ signal has been observed across tooth rows (Bryant et al., 1994), making interpretations where only slight variations in $\delta^{18}O$ values exist difficult.

Perhaps more important in palaeoenvironmental reassessments is the finding that short-term seasonal fluctuations in local precipitation can be determined by serially sampling teeth (especially high crowned hypsodont dentition) from the base of the tooth crown to its tip (Bryant et al., 1994, 1996b; Fricke and O'Neil, 1996; Feranec and MacFadden, 2000; Balasse et al., 2002). This method enables one to determine an animal's feeding and drinking behaviour during the time that the tooth develops. Domestic ungulate molariform teeth typically take 12-16 months to develop and mineralise (cattle: 14 to 20 months (Brown et al., 1960); sheep: 10-12 months (Weinreb, 1964). Bryant et al. (1996a) have shown that the $\delta^{18}O$ of environmental water undergoes a seasonal cycle that is reflected by $\delta^{18}O$ of body water. Low $\delta^{18}O$ values suggest a decrease in output sources of oxygen, which in turn implies that loss of oxygen through water vapour, CO_2 or excretion was reduced. This suggests a wetter period (i.e. rainfall), which would cool down the environment relative to body water and decrease the loss of oxygen. By comparing the lowest and highest $\delta^{18}O$ values along a tooth crown, the amplitude of this seasonal cycle can be determined (Koch et al., 1989; Fricke and O'Neil, 1996) (Figure 4.2).

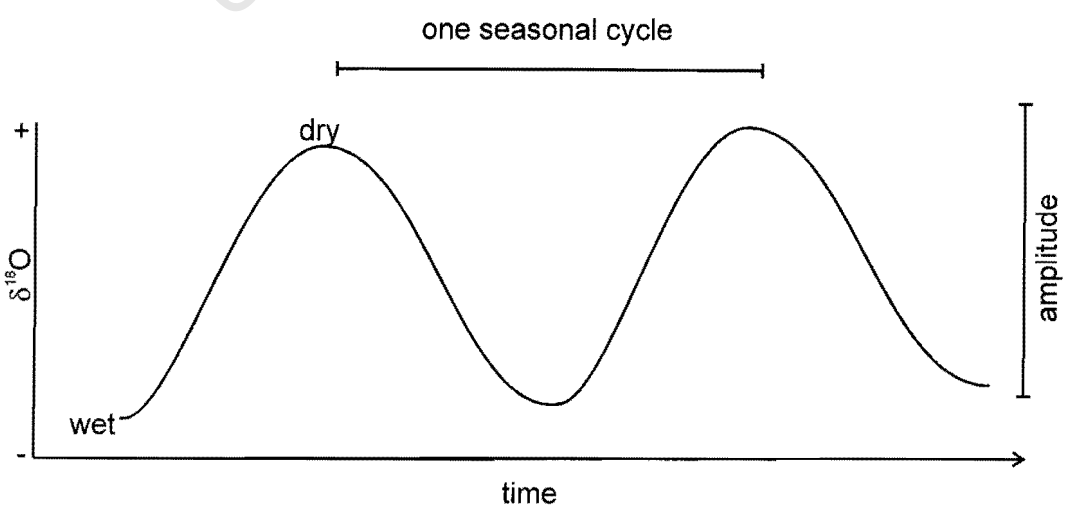

Figure 4.2. Diagram showing how seasonal cycles and amplitude can be deduced from $^{18}O/^{16}O$ ratios.

For LBW, a region where harsh seasonality has been suggested (Hendey, 1981a, 1984), this technique can be extremely valuable in assessing how seasonal the environment was 5 Myr ago. A constraint of this methodology is that $\delta^{18}O$ values across a tooth crown actually reflect variations in drinking behaviour and not rainfall of the area *per se*. During wetter periods animals drink less, as water vapour loss is reduced compared to during drier hotter climates. Caution must therefore be taken when using differences in $\delta^{18}O$ signatures across tooth crowns as a proxy for climate (Bryant et al., 1996a).

4.1.2 Application to the LBW fauna

In order to categorise the diets of fossil animals into those that browse, those that graze, and mixed feeders, the method requires that C_4 grasses are present in the ecosystem under study. Without C_4 grasses the dietary picture is more difficult to interpret. However together with oxygen isotopic signatures some subtle dietary and behavioural preferences can still be determined.

C_4 grasses are favoured in areas were daily maximum temperatures are high (~25°C or more). Today more than 90% of the grasses in South Africa are of the C_4 type (Vogel et al. 1978). However, South Africa has a complex dual climate and floral system (discussed in Chapter 2, section 2.3). LBW is situated in a winter rainfall area at present, which is dominated by coastal fynbos. Grasses are a minor component of this biome and those present are of the cool growing-season C_3 type. Most succulents from the coastal fynbos and the nearby strandveld biomes rarely use the CAM (Crassulacean acid metabolism) photosynthetic pathway (Stock, van der Heyden and Lewis, 1992). CAM plants are rarely eaten by herbivores due to the presence of toxins such as oxalic acid (Owen-Smith and Danckwerts, 1997). The presence of many large bodied grazers at LBW, such as the white rhinoceros, *Ceratotherium praecox*, and the three-toed horse, *Hipparion*, supports the evidence for the existence of a significant and productive grassy component in the ecosystem. The current understanding of the Langebaanweg area is that the subtropical Miocene forests were diminishing at the expense of expanding grasslands during the Early Pliocene (Hendey, 1981a; Coetzee and Rogers, 1982; Hendey, 1983a, 1983b; Scott, 1995). These grasses were assumed to be savanna grasses, but we now know that savanna grasses in South Africa follow the C_4 photosynthetic pathway (Vogel et al.

1978). The assumption that C_4 grasses were present at LBW ~5 Myr ago is in accordance with the C_4 grassland expansion model (Cerling et al., 1997b), which suggests that C_4 grasses could have reached these southerly mid-latitudes by the Early Pliocene.

There are conflicting reports describing the climate regime on the west coast of South Africa during the Early Pliocene, depending on whether they are based on the ocean history or the land history. If the assumption that the large numbers of grazers at LBW were feeding on C_4 grasses (which favour warm growing seasons) is correct, then this implies that a summer-wet/winter-dry climate regime was in place. Several burnt bones at LBW indicate that veld fires occurred during dry months (Hendey, 1981a, 1984). As discussed earlier (Chapter 2, section 2.5), these fires were probably caused by electrical storms, which are common in the summer rainfall area of South Africa today. Marine evidence (albeit limited) does not support this speculation and suggests that early forms of the Benguella Upwelling System may have been present in the Late Miocene (Siesser, 1980). Since upwelling is associated with long-shore south-easterly winds, which are in turn associated with the South Atlantic High, this implies that the current summer-dry/winter-wet climate regime was in place ~ 5 Myr ago. The presence of this climate regime would have prevented the expansion of C_4 grasses to the south-west coast of South Africa.

In summary, this chapter investigates (i) whether C_4 grasses were present 5 Myr ago at LBW and indirectly the climate regime of the area, (ii) the seasonality of the area, and (iii) habitat preferences of several fossil fauna. This chapter aims to provide further insight into the prevailing environment of the LBW area during the Early Pliocene in order to understand the observed pathologies discussed in the subsequent chapters.

4.2 MATERIAL AND METHODS

4.2.1 MATERIAL

Three sivathere (*S. hendeyi*) incisor fragments (PQL 43928, PQL 44045 and PQL 45091A) were analysed by Fourier Transform Infrared Spectroscopy (FTIR) in order to determine if the enamel apatite had been diagenetically altered during fossilisation or over time.

For isotope analyses, six families of fossil animals were analysed, totally sixty-four different tooth fragments (Table 4.1). All teeth originate from the Pelletal Phosphate Member (PPM). Appendix A provides a full list of all the animals sampled and corresponding channel deposits (Bed 3aS or Bed 3aN). Seven samples from modern animals (two from the inland summer-rainfall areas of South Africa and five from the winter-rainfall area) were also analysed. A comparison between modern and fossil giraffids from the winter rainfall area of South Africa would have been ideal but no megaherbivores live in the fynbos areas because of the low nutrient levels of this vegetation. Two samples of sediment surrounding a fossil tooth were also analysed.

For serial sampling across tooth crowns, three sivathere mandibular third molar fragments were selected (PQL 43944, PQL 62733/16 and PQL 62733/57). This tooth type has been shown to best record seasonal fluctuations (Fricke and O'Neil, 1996), mainly because it develops and mineralises after the weaning period in giraffes (Hall-Martin, 1976a). Interference from the mother's $\delta^{18}O$ signature (Fricke and O'Neil, 1996) is therefore completely avoided. In addition, caution was taken to only select teeth that had completed enamel formation (i.e. fully mineralised) because it has been shown that the overall amounts of CO_3^{-2} and HPO_4^{-2} depend on the degree of enamel maturity and that only fully mature enamel has the same chemical and mineral composition (independent of species) (Hiller et al., 1975; Deutsch and Gedalia, 1980; Rey et al., 1991; Bryant et al., 1996a). In cattle for example, immature enamel is composed of 65-70% organic components compared to only 4% in mature enamel (Brown et al., 1960).

Table 4.1. Material used for stable isotope analyses (n indicates number of teeth analysed).

Source	n
Modern Animals (from the summer rainfall area in S.A.)	
Order Artiodactyla	
Family Giraffidae	
Giraffa cameleopardalis (giraffe)	1
Family Bovidae	
Connochaetes taurinus (wildebeest)	1
Modern Animals (from the winter rainfall area in S.A.)	
Order Artiodactyla	
Family Bovidae	
Raphicerus campestris (steenbok)	1
Raphicerus melanotis (grysbok)	1
Damaliscus dorcas (bontebok)	3
Fossil animals (PPM, at LBW)	
Order Artiodactyla	
Family Giraffidae	
Sivatherium hendeyi	25*
Family Hippopotamidae	
Gen. & sp. not determined	15
Family Suidae	
Nyanzachoerus cf. *jaegeri*	4
Family Bovidae	
Kobus sp. (Reduncini)	2
Damalacra sp. (Alcelaphini)	7
Order Perissodactyla	
Family Rhinocerotidae	
Ceratotherium praecox	5
Family Equidae	
Hipparion cf. *baardi*	6
Sediment from a tooth (PPM, at LBW)	2

*There may be some minor contamination with *Giraffa* cf. *jumae* in this sample. Eight of the 25 teeth could not be identified with certainty and may belong to this *Giraffa* species.

4.2.2 METHODS

4.2.2.1 Fourier Transform Infrared Spectroscopy (FTIR)

1.8 mg of enamel was removed from each tooth fragment using a rotary drill equipped with a 2 mm diamond-tipped bit. The enamel powder was ground together with 300 mg Potassium bromide (KBr) by hand using a mortar and pestle, placed in a vacuum hydraulic press and evacuated for 4-5 minutes to remove air bubbles. The sample was compressed under approximately nine tons of pressure for five minutes to make a KBr+enamel disc. An absorbance spectrum was obtained for each disc using a Perkin-Elmer Paragon 1000 spectrometer. Sixty-four scans were taken at a resolution of 8 cm^{-1} and range of 500 to 4000 cm^{-1} as described elsewhere (Regnier et al., 1994; Sponheimer and Lee-Thorp, 1999a). Each spectrum was base-lined at two points in the same manner and analysed using the software package Grams Analyst 1000.

In order to facilitate interpretations of small changes in FTIR spectra, the following indices (after Sponheimer and Lee-Thorp, 1999a) were calculated: type B carbonate (BPI), type A carbonate (API), the relative amount of B to A site carbonate (BAI) and the crystallinity of the sample (reflected by PCI or the Infrared Splitting Index). API and BPI indicate the amounts of type A and type B carbonates relative to phosphate respectively, while BAI indicates the relative amount of B to A site carbonate. PCI is an infrared splitting index, which provides a measure of the crystallinity (i.e. crystal size and strain) of the apatite structure. These indices are determined by measuring the absorbance at particular wavelengths as follows:

$$API = \frac{\text{type A carbonate (1540 cm}^{-1}\text{)}}{\text{phosphate (605 cm}^{-1}\text{)}}$$

$$BPI = \frac{\text{type B carbonate (1415 cm}^{-1}\text{)}}{\text{phosphate (605 cm}^{-1}\text{)}}$$

$$BAI = \frac{\text{type B carbonate (1415 cm}^{-1}\text{)}}{\text{type A carbonate (1540 cm}^{-1}\text{)}}$$

$$PCI = \frac{\text{phosphate } (595\ cm^{-1} + 605\ cm^{-1})}{\text{phosphate } (590\ cm^{-1})}$$

The overall carbonate content of the sample can be determined from BPI values according to the formula, (y = (9.901* BPI) + 0.743 (Sponheimer and Lee-Thorp, 1999b, adapted from LeGeros, 1991), where 'y' is the percentage of carbonate present (by weight).

4.2.2.2 Stable Isotope analyses: bulk and serial sampling

The standard method of isotope analyses outlined by Sponheimer and Lee-Thorp (1999b) was slightly modified in order to take into account the particulars of the matrix at LBW (e.g. high phosphate content) and potential diagenesis at this locality. Approximately 3-5 mg of enamel was removed from a broad basal region of each tooth fragment using a rotary drill fitted with a 1.4 mm diamond tipped bit. Bulk sampling (across a large portion of the crown) is usually carried out in analyses investigating palaeodiets, however, in order to minimise destruction of valuable fossil material, only a basal region of each tooth fragment was drilled. This method has been shown to reliably indicate diet in fossil species (Feranec and MacFadden, 2000). A criticism of this method, however, is that the enamel in this region would "contain" information about similar snapshots of time and may not give an overall dietary indication of the animal. In order to minimise this effect, molar fragments were randomly selected. In addition, sampled teeth were typically collected by bulk screening of mine dump material and therefore are jumbled with respect to stratigraphic position within the PPM deposit.

Pretreatment of the enamel powder was necessary in order to remove organic material (e.g. humates) and exogenous carbonates that may have become incorporated or adhered to the tooth during fossilisation or over time. The enamel was treated as follows: 15% sodium hydrochloride for 30 minutes, followed by 0.1M acetic acid for 15 minutes. Between the addition of each of these solutions, samples were centrifuged at high speed and rinsed in deionised water at least three times before proceeding with the next solution. Samples were then freeze-dried for a

minimum of two hours or overnight. 1.7-1.8 mg of pretreated sample was loaded into individual reaction vessels in a Kiel autocarbonate device. CO_2 was obtained by acid hydrolysis with 100% phosphoric acid (H_3PO_4), collected by cryogenic distillation and measured in a Finnigan Mat 252 mass spectrometer. Isotopic ratios ($^{13}C/^{12}C$ and $^{18}O/^{16}O$) are reported in delta (δ) notation, with $\delta^{13}C$ and $\delta^{18}O$ relative to the PeeDeeBelemnite (PDB)[4] international standard ($\delta = (R_{sample}-R_{standard}) -1 * 1000$ and $R = ^{13}C/^{12}C$ or $^{18}O/^{16}O$). Sample values were corrected using known standards (NBS 18, NBS 20) and secondary standards (CarraraZ and Lincoln limestone). Analytical precision is better than 0.1‰ for both carbon and oxygen isotope ratios. Only ratios obtained from experimental runs that gave voltage readings greater than 1.8V were considered valid. Previous experience with this Kiel device has indicated that the pressure of gas (measured in volts) needs to be greater than this to provide consistent and reliable results. Below this reading, $\delta^{18}O$ values especially are unreliable.

Serial sampling along tooth crowns was conducted by removing enamel starting from the cervical base of the tooth and ending at its tip (Figure 4.3). The number of samples obtained is limited by the size of the tooth and therefore only unworn or slightly worn tooth fragments were used. Ten to seventeen samples were obtained per tooth crown. Enamel was removed from a ± 0.8 mm wide band and each band was ± 1 mm apart. Each sample was treated individually and analysed in the same manner as the bulk sampling method outlined above.

4.2.2.3 Statistical analyses

All statistical analyses were preformed on Statistica (version 6.0). Repeated two-way Students' t-tests for independent samples were conducted to test for significance between populations. The t-statistic, degrees of freedom (df) and *p* value are reported.

[4] The PDB marine carbonate standard, originally derived from a piece of Cretaceous marine fossil, *Belemnitella americana*, from the Peedee Formation in South Carolina, has been exhausted. Today, a nearly identical standard has been prepared by the National Bureau of Standards.

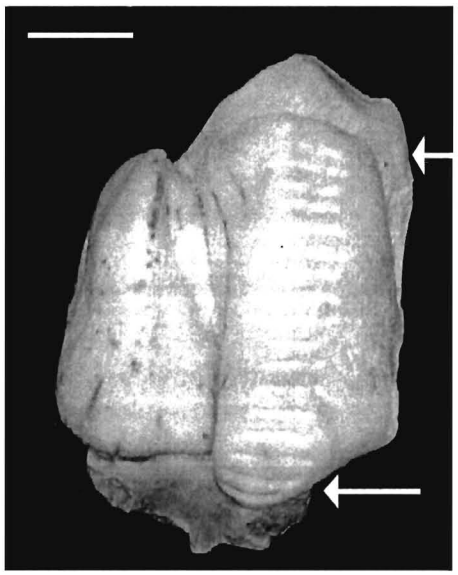

Figure 4.3. A mandibular third molar fragment from *S. hendeyi* showing serial sampling along the tooth crown. Arrows indicate the most basal and most apical drill positions. Seventeen samples were obtained from this tooth. Scale bar represents 1 cm.

4.3 RESULTS

4.3.1 Fourier Transform Infrared analyses

The absorbance spectra of *S. hendeyi* enamel are shown in Figure 4.4. These spectra are very similar to published spectra of Sponheimer and Lee-Thorp (1999a) for modern and 3 Myr old enamel, suggesting that the LBW fossil apatite has not been significantly altered by diagenesis. Shifts in some critical peaks are observed when comparing these fossil spectra with those published for modern enamel (see Table 4.2) but these shifts are very minor, and have been observed previously (Sponheimer and Lee-Thorp, 1999a). No calcite peak (at 711 cm^{-1}) was observed in either modern or fossil spectra.

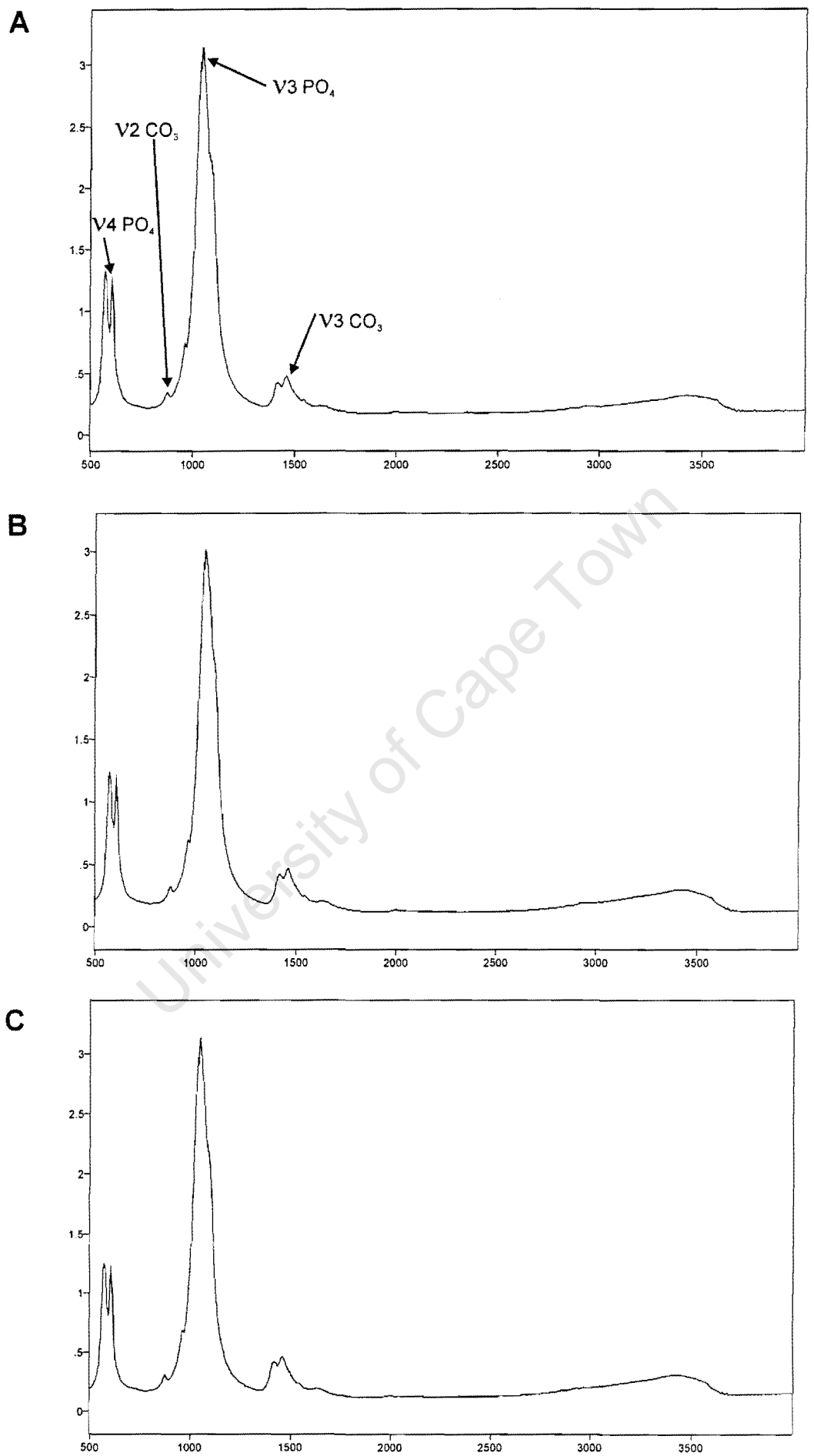

Figure 4.4. Fourier Transform Infrared absorbance spectra of *S. hendeyi* enamel. (A) tooth PQL 43928, (B) PQL 44045 and (C) PQL 45091A. X-axis is wavelength in cm^{-1} and y-axis is absorbance.

Table 4.2. Shifts in the absorbance spectra of modern versus fossil enamel.

Critical peak in extant enamel apatite (Sponheimer and Lee-Throp, 1999b)	Critical peak in fossil *S.hendeyi* enamel apatite
565 cm^{-1}	570 cm^{-1} ± 0.2 cm^{-1}
590 cm^{-1}	589 cm^{-1} ± 0.1 cm^{-1}
605 cm^{-1}	603 cm^{-1} ± 0.4 cm^{-1}
875 cm^{-1}	874.2 cm^{-1} ± 0.3 cm^{-1}
1415 cm^{-1}	1418 cm^{-1} ± 0.5 cm^{-1}
1540 cm^{-1}	1544 cm^{-1} ± 0.4 cm^{-1}

Calculated indices are shown in Table 4.3. The BPI values for sivathere enamel are slightly higher than and significantly different from the published range for fossil animals ($t = 2.24$, $df = 11$, $p<0.05$), indicating that LBW *S. hendeyi* enamel contains slightly increased amounts of type B carbonate relative to phosphate. API values calculated for 5 Myr old sivathere enamel are considerably higher than values for other fossils published by Sponheimer and Lee-Thorp (1999a) ($t = 12.66$, $df = 11$, $p<0.005$) indicating that significantly more type A carbonate is present in the enamel apatite of these LBW giraffids. The A site carbonate peak (at 1415 cm^{-1}) however occurs as a shoulder in the ν_3 carbonate domain and is frequently difficult to measure, resulting in possible errors creeping in when determining the API index. A direct consequence of more type A carbonate is a decrease in BAI, which has elsewhere been used as an indicator of the relative amounts of carbonate substituted in B and A positions and where recrystallinisation has caused shifts. The sivathere enamel also contains increased amounts of overall carbonate compared to published data. The phosphate crystallinity index (PCI) is significantly lower than that reported by Sponheimer and Lee-Thorp (1999a) for fossil enamel ($t = -5.37$, $df = 11$, $p<0.005$). In summary, except for the slightly higher carbonate content in the A-site, the apatite structure of the 5 Myr old sivathere enamel appears reasonably normal.

Table 4.3. Calculated indices from absorbance spectra of *S. hendeyi* enamel shown in Figure 4.2 compared to values published by Sponheimer and Lee-Thorp (1999a) for fossil and modern enamel. For these (published) values both the range and averages (italics) are given.

Accession number	Species	Type	BPI	API	BAI	PCI	CO_3 % wt
PQL 43928	*S. hendeyi*	Fossil	0.341	0.228	1.496	3.012	4.118
PQL 44045	*S. hendeyi*	Fossil	0.361	0.216	1.67	2.988	4.313
PQL 45091A	*S. hendeyi*	Fossil	0.353	0.202	1.75	2.99	4.239
	Various (published)	Modern (n=5)	0.16-0.35 *(0.25)*	0.05-0.12 *(0.08)*	2.9-3.8 *(3.2)*	3.5-3.8 *(3.6)*	2.3-4.2 *(3.2)*
	Various (published)	Fossil (n=10)	0.19-0.34 *(0.26)*	0.043-0.086 *(0.067)*	3.3-5.6 *(4.1)*	3.4-4.1 *(3.6)*	2.6-4.1 *(3.4)*

4.3.2 Stable isotope analyses

All $\delta^{13}C$ and $\delta^{18}O$ values (relative to PDB) are given in Appendix E. Figure 4.5 shows modern, fossil and matrix $\delta^{13}C$ and $\delta^{18}O$ values. The browsing giraffe and grazing wildebeest from the summer rainfall region have C_3 and C_4 signatures respectively. The modern animals from the winter rainfall areas are all grazers and all have $\delta^{13}C$ values indicative of C_3-dominated environments. Average $\delta^{13}C$ and $\delta^{18}O$ values for these animals are -11.1 ± 1.9‰ and -3.6 ± 1.6‰ respectively (n=5) (mean ± standard deviation). The two isotope signatures for matrix are almost identical to one another and were not significantly different from enamel signatures ($t = -1.49$, $df = 64$, $p>0.05$). This could be taken as an indication that the fossil enamel and matrix are equilibrated, except that predictable $\delta^{13}C$ and $\delta^{18}O$ patterning was observed between the taxa.

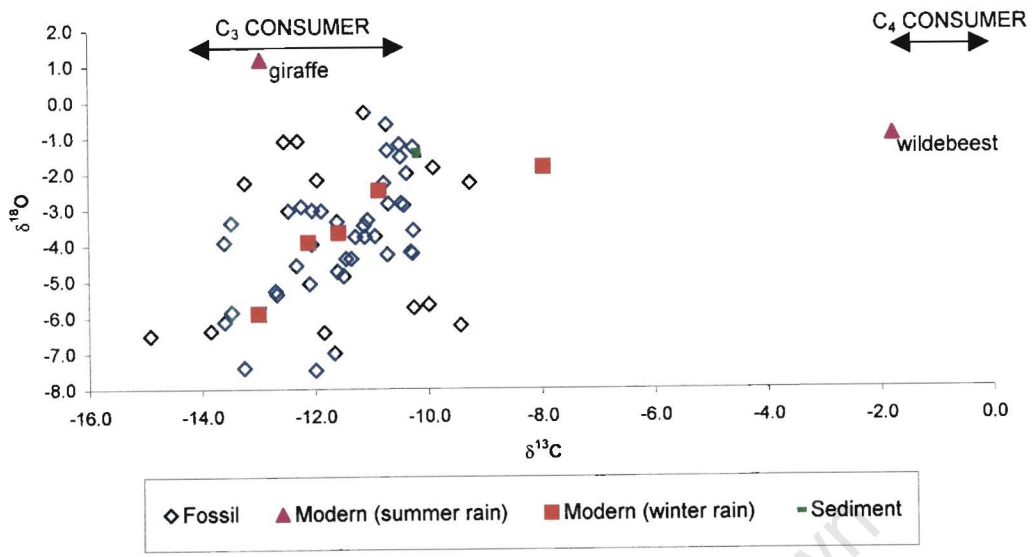

Figure 4.5. $\delta^{13}C$ and $\delta^{18}O$ values for fossil and sediment samples from the Pelletal Phosphate Member at LBW. Values for modern giraffe (*G. camelopardalis*) and wildebeest (*C. taurinus*) from the summer rainfall area of South Africa and bovids from the winter rainfall area are also indicated.

The $\delta^{13}C$ values from fossil tooth enamel cluster between -9.3‰ and -14.9‰ (Figure 4.5). This result indicates that LBW was dominated by C_3 vegetation during the Early Pliocene and that dietary preferences (i.e. browsing versus grazing) could not be determined based on $\delta^{13}C$ values alone. However, together with oxygen values some subtle habitat preferences could be established (discussed in section 4.4.5). Average $\delta^{13}C$ and $\delta^{18}O$ values with standard deviations for each family are shown in Figure 4.6 and Table 4.4. Table 4.4 also gives the range of values for each animal. $\delta^{18}O$ values for the LBW hippopotamus (-5.9 ± 1.0 ‰, n=15) are isotopically distinct ($t = 6.79$, $df = 62$, $p<0.0001$) from all the other animals (-3.2 ± 1.5‰, n=49). The rhinoceros (3.0 ± 1.4‰, n=5) is also significantly different ($t = -2.14$, $df = 47$, $p<0.05$) from the rest of the animals (excluding the hippo) (-4.4 ± 1.2‰, n=44) with respect to $\delta^{18}O$. The giraffids have the widest range of $\delta^{18}O$ values from -0.6‰ to -5.9‰. Half of the equids sampled have $\delta^{18}O$ values below 2‰ while the others have $\delta^{18}O$ values above 4.5‰. Of the Bovidae analysed, the two reduncine teeth have identical $\delta^{13}C$ values (-10.7‰) but quite different $\delta^{18}O$ values (-1.4‰ and -4.3‰). This could indicate different drinking behaviours in these two individuals. That is, one

individual either drank less, possibly because it ate grass with a high water content, or it lived under a wetter climate regime. The alcelaphines on the other hand have wide $\delta^{13}C$ and $\delta^{18}O$ ranges of approximately 3‰ (Table 4.4 and Appendix E). The giraffids, hippos and bovids each have some $\delta^{13}C$ values below -10‰ but the hippos and giraffids are the only animals to have $\delta^{13}C$ values below -13.5‰. On the whole, these two animals have a similar wide range of $\delta^{13}C$ values. The equids, suids and rhinos have similar $\delta^{13}C$ values, whereas bovid values are slightly depleted. The hippos (-11.9 ± 1.5‰, n=15) are statistically significantly different from the bovids (-10.8 ± 0.9‰, n=9) with respect to $\delta^{13}C$ (t = -2.17, df = 22, $p<0.05$). None of the other animals differ significantly from each other with respect to $\delta^{13}C$ values. The sivathere carbon and oxygen signatures do not differ significantly from the giraffid teeth that could not be identified conclusively as belong to the Sivatheriinae (carbon: t = 0.59, df = 23, $p<0.5$; oxygen: t = -0.02, df = 23, $p>0.5$).

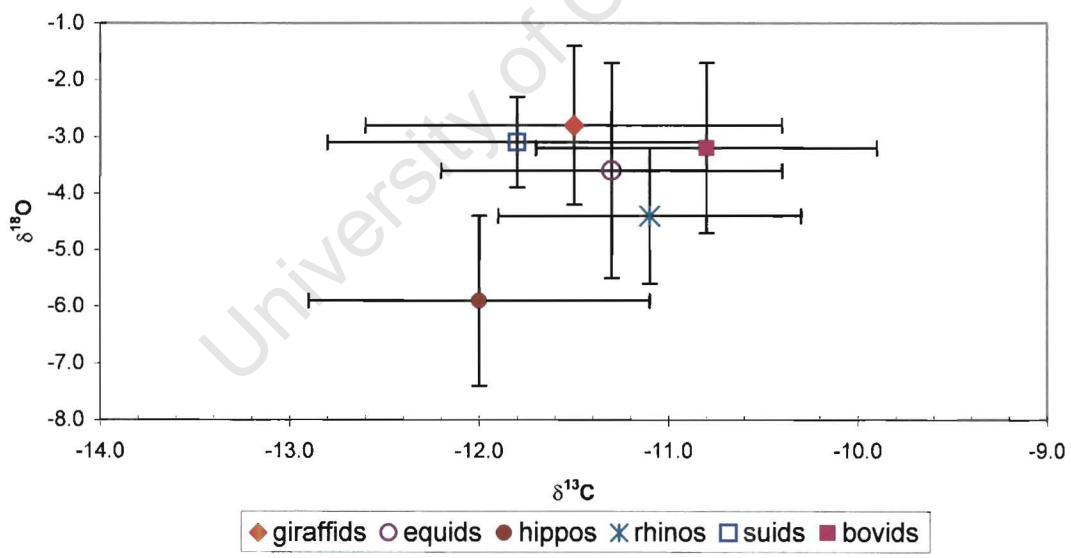

Figure 4.6. Average $\delta^{13}C$ and $\delta^{18}O$ values for LBW fauna. Species are given in Table 4.1.

Table 4.4. Range and mean $\delta^{13}C$ and $\delta^{18}O$ values for each animal analysed. All values are in ppmil (‰). Mean and standard deviations are given.

	n	$\delta^{13}C$ range	$\delta^{13}C$ (mean ± std. dev)	$\delta^{18}O$ range	$\delta^{18}O$ (mean ± std. dev)
Giraffidae					
S. hendeyi	17	-9.9 to -13.6	-11.5 ± 1.2	-0.6 to -5.9	-2.9 ± 1.5
Other giraffids	8	-10.4 to -13.2	-11.8 ± 1.0	-1.1 to -4.0	-2.8 ± 1.2
Bovidae					
Damalacra sp.	7	-9.3 to -12.3	-10.8 ± 1.0	-1.3 to -4.6	-3.2 ± 1.5
Kobus sp.	2	-	-10.7	-1.4 to -4.3	-2.9 ± 2.1
Suidae					
Nyanzachoerus cf. *jaegeri*	4	-10.3 to -12.2	-11.8 ± 1.0	-2.2 to -4.2	-3.1 ± 0.8
Equidae					
Hipparion cf. *baardi*	6	-10.4 to -12.9	-11.3 ± 0.9	-1.3 to -5.6	-3.6 ± 1.9
Rhinocerotidae					
Ceratotherium praecox	5	-10.1 to -11.9	-11.1 ± 0.8	-2.6 to -5.7	-4.4 ± 1.2
Hippopotamidae	15	-9.4 to -14.9	-12.0 ± 1.5	-3.8 to -7.4	-5.9 ± 1.0

Results from serial analyses along sivathere teeth are shown in Figure 4.7 (Appendix F). One data point in PQL 62733/57 repeatedly gave low voltage readings (of less than 1.5 V) indicating that not enough sample gas was produced and that carbonate content was low for this specimen. The $\delta^{18}O$ value from this tooth was therefore discarded. The amplitude of the seasonal cycle (from wet peak, low $\delta^{18}O$ value, to dry peak, high $\delta^{18}O$ value) is 2.0‰ (in PQL 43944) and 2.6‰ (in PQL 62733/16 and PQL 62733/57). The average amplitude is 2.4 ± 0.3‰. In modern animals from the winter rainfall area of South Africa, average seasonal amplitudes from tooth enamel are 3.4‰ (Balasse et al., 2002), significantly higher than 5 Myr ago. The pattern of the seasonal cycle also differs in each tooth. One tooth (PQL 43944) has one relatively long period of depleted values compared to the other two teeth. PQL 62733/16 has two periods of enriched values and one period of depleted $\delta^{18}O$ values whereas PQL 62733/57 has the opposite pattern. $\delta^{13}C$ values are comparatively stable across the tooth crowns except for PQL 43944, which has enriched values at the base of the crown. Stable $\delta^{13}C$ values indicate that diets were fairly consistent during this stage of tooth development.

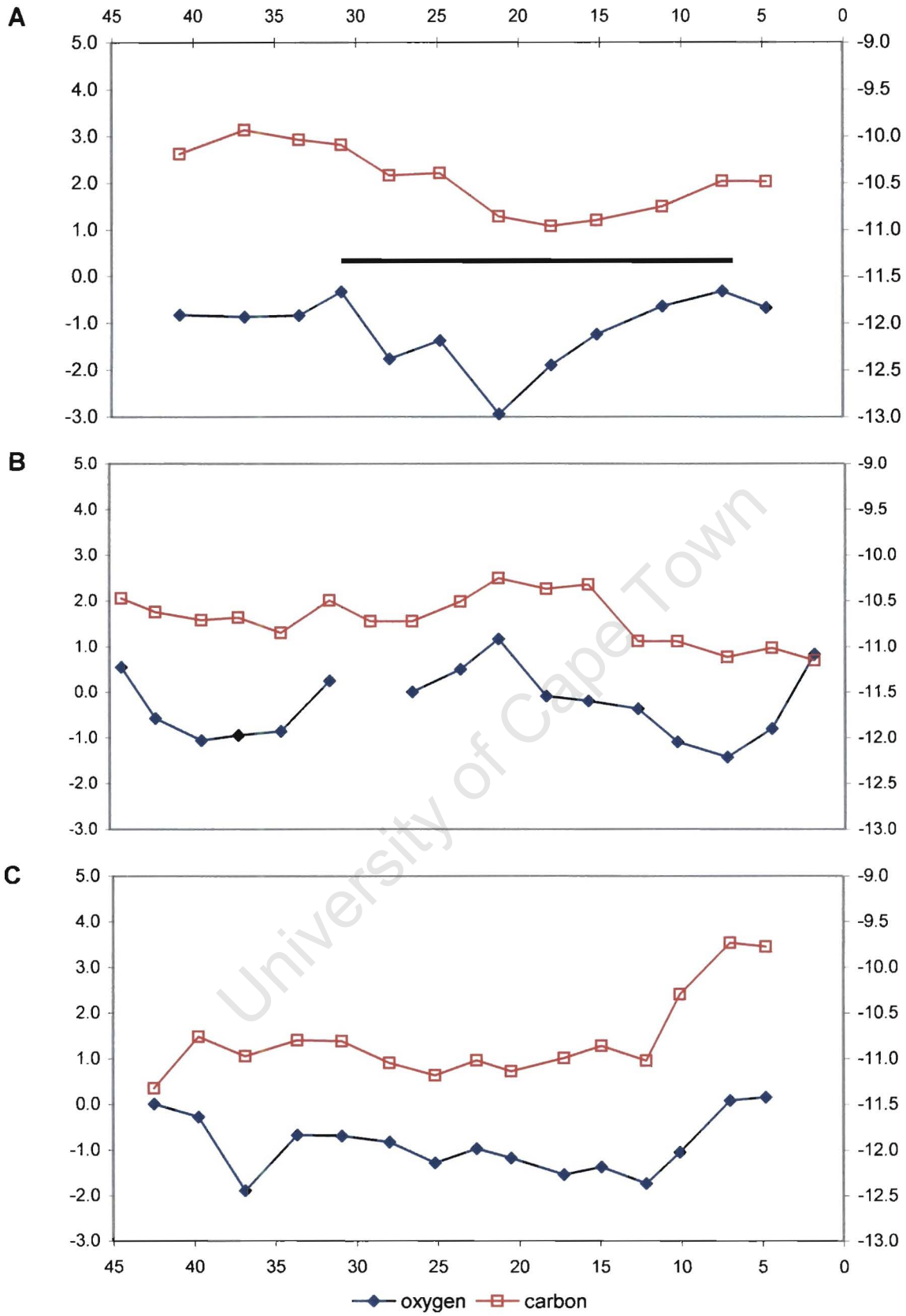

Figure 4.7. Serial isotope analyses along mandibular third molar tooth crowns from *S. hendeyi*. (A) PQL 62733/16, (B) PQL 62733/57 and (C) PQL 43944. The horizontal bar in (A) indicates one seasonal cycle. Y-axis (left) indicates $\delta^{18}O$ values (closed diamonds) and y-axis (right) indicates $\delta^{13}C$ values (open squares). X-axis indicates the distance on the tooth crown (in mm) where samples were taken. The base of the tooth crown is at 0 mm.

4.4 DISCUSSION

4.4.1 Preservation of fossil enamel over time

Preservation of fossil enamel from LBW is indicated firstly by the typical absorbance spectrum obtained for fossil enamel apatite (Figure 4.4), which suggests that the apatite structure and composition has not been altered during fossilisation. Secondly, patterning within the faunal assemblage is observed. For example, significantly depleted $\delta^{18}O$ values for hippos compared to other animals were obtained (Figure 4.5 and 4.6). This has been suggested as a means of testing the validity of the isotope signal (Bocherens et al., 1996). These results provide solid evidence that the fossil enamel has not been diagenetically altered over time, despite the LBW sediment sample yielding similar results to fossil enamel. The latter result may be due to the source of the sediment (i.e. adhering to a tooth), which may be contaminated with some tooth material.

4.4.2 Fourier Transform Infrared Spectroscopy

A limited number of studies have reported FTIR spectra for enamel of fossil and modern animals. Several authors have shown that the overall carbonate content, deduced from the amount of type B carbonate (BPI) and crystallinity (reflected by PCI), do not differ significantly between modern and fossil enamel (Lee-Thorp and van der Merwe, 1991; Sponheimer and Lee-Thorp, 1999a). All calculated indices for the LBW sivathere are significantly different from published modern and fossil values (Sponheimer and Lee-Thorp, 1999a) ($p<0.05$). This may relate partly to the age of the fossil deposit. Increased type A carbonate contents were not observed by Sponheimer and Lee-Thorp (1999a) in any of their fossil enamel samples (see Table 4.3). The increase observed in LBW enamel might be unusual, especially considering the fossilisation conditions and depositional environment at LBW compared to the localities investigated by Sponheimer and Lee-Thorp (1999a) (namely Makapansgat, Florisbad, Swartkrans and Border Cave). These are cave deposits, unlike the fluviatile phosphate-rich deposits at LBW. The increase in the LBW sivathere enamel may therefore represent a real increase in carbonate content under these depositional conditions. If occupation of the A-site by extra carbonates affects the unit cell dimensions as suggested by LeGeros (1991) causing crystal strain and distortions, then the higher A-carbonate at LBW may be related to lower

PCI in some enamels. Carbonate contents as high as 5% (by weight) were reported by Rey et al. (1991) and Rink and Schwarcz (1995) for enamel.

4.4.3 Stable isotopes

Modern $\delta^{13}C$ values for the winter rainfall area from this study (-11.1 ± 1.9‰, n=6) are similar to fossil values (-11.5 ± 1.2‰, n=64). Several authors however, reporting a 2 to 3‰ difference between fossil and modern environments. Similar differences were not observed in this study and this may be the result of the small sample size analysed. These six samples may not be representative of the area.

Average $\delta^{18}O$ values for LBW fossil fauna (-3.8 ± 1.8‰, n=64) cluster near the values one would expect today in the region *if* one back calculates from local rainfall values (-2.8 to -3.8‰ (SMOW[5]), Harris et al., 1999) and take into account the ~30‰ fractionation between meteoric water and body water (Koch, 1998). Zachos et al. (2001) suggest that modern $\delta^{18}O$ values are depleted by less than 1‰ compared to 5 Myr ago due to changes in Antarctic ice volume and temperature. Thus the LBW $\delta^{18}O$ values are consistent with Zachos et al.'s (2001) finding. The $\delta^{18}O$ values obtained for both the LBW fossil fauna and for modern animals from the winter rainfall area of South Africa are however depleted compared to the values obtained by Balasse et al. (2002) for Kasteelberg, a Pleistocene locality ~60 km south-east of Langebaanweg.

4.4.4 Palaeoenvironmental reassessment

According to the C_4 grass expansion model, C_4 grasses had reached low to mid latitudes by the Early Pliocene in both Northern and Southern Hemispheres (MacFadden et al., 1996; Cerling et al., 1997b). Stable carbon isotope results reported here indicate that the expected grazers (eg. alcelaphines, hippopotamus, rhinoceros) fall within the range for C_3 consumers. Since fynbos has a C_3 signature no distinction can be made as to the type of C_3 vegetation that was consumed (browse, graze or fynbos). This finding nevertheless indicates that LBW was a C_3-dominated environment during the Early Pliocene and that C_4 grasses had not extended to this southerly latitude by 5 Myr, if indeed they were ever present.

[5] Relative to Standard Mean Ocean Water ($\delta^{18}O_{SMOW} = (1.03091 * \delta^{18}O_{PDB}) + 30.91$.

Furthermore, the evidence for cool growing C_3 grasslands suggests that a Mediterranean-type climate was established in this region by the Early Pliocene. This result is in agreement with the western European (France and Spain: Cerling et al., 1997b) and eastern Mediterranean (Greece and Turkey: Quade et al., 1995) data that suggests that areas with Mediterranean climates today probably never supported C_4 grasses.

Pollen data from the mid-Miocene Elandsfontein Formation at LBW indicate that fynbos was beginning to establish itself at this time (Scott, 1995). If the climate regime remained unchanged over time, then the reason why C_3 grasslands gave way to fynbos (which is poor in grass) is not clear. It has been suggested elsewhere that a nutrient-rich, more alkaline substrate, which may have supported grasses, was eliminated at some unknown point in time during the Pleistocene (Deacon and Deacon, 1999). Its elimination may have had the effect of opening up a niche for fynbos to flourish.

Analyses of serial isotopes along m3 tooth crowns indicate that one to two cyclical fluctuations in $\delta^{18}O$ values occurred during development of these teeth (Figure 4.7). These can be interpreted as seasonal variations. Since no modern giraffes were available, comparisons with the work of Balasse et al. (2002) on modern and archaeological sheep, cattle, steenbok and eland from Kasteelberg in the south-western Cape is discussed. The amplitudes of the seasonal cycles for *S. hendeyi* m3s are on average 2.4 ± 0.3‰, smaller than amplitudes today (~3.4‰, Balasse et al., 2002). The implication is that the difference between winter and summer was less 5 Myr ago to that experienced in the current climate regime. Thus, although LBW had a Mediterranean-type climate during the Early Pliocene, diagenesis may have smoothed the curves slightly so that the seasons appear less well defined than at present.

In addition, there is great variability in the number of seasonal cycles in each tooth suggesting that the times when isotopic ratios were incorporated (i.e. during tooth development) either did not occur at the same time of year (i.e. same season) in each tooth or that seasonality was not stable. In domestic ungulates, third molars typically take 12-16 months to develop and mineralise (Brown et al., 1960; Weinreb,

1964; Hillson, 1986). If this is applied to *S. hendeyi* (tooth development times for the extant giraffe have not been reported) then this could mean that the observed seasonal cycles occurred within this 12-16 month period, although it is highly unlikely that two seasonal cycles occurred in one year. The long period of depleted $\delta^{18}O$ values in tooth PQL 43944, suggests a long period of wet conditions (i.e. rainfall). In tooth PQL 62733/57, three data points of enriched $\delta^{18}O$ values are reported, suggesting that two seasonal cycles occurred during development of this tooth and that each season (wet versus dry) was of a short duration. Tooth PQL 62733/16 on the other hand has only one seasonal cycle. These findings suggest that environmental conditions were not the same during development of each third molar. Giraffes have their peak number of births in the dry season, although births can occur throughout the year (Sinclair et al., 2000). This means that a particular (giraffe) tooth type can develop under different environmental conditions. The finding reported here of different numbers of seasonal cycles in *S. hendeyi* third molars indicates that if the sivathere had a similar timing of births to that of the extant giraffe then seasonality was possibly variable during development of these teeth and hence also during deposition of the PPM. Unstable seasonality was previously proposed by Hendey (1981a, 1984) based on taphonomic evidence (such as floods and droughts).

In summary, LBW was dominated by C_3 vegetation, which, based on faunal compositions and pollen studies, included mainly open vegetation with some trees. C_3 grasses require cool growing seasons and the implication therefore is that the climate regime was probably winter-wet/summer-dry, similar to current climates. Seasonality however appears to have been slightly unstable.

4.4.5 Niche preferences

In a C_3-dominated environment such as LBW, grazers and browsers cannot be distinguished from one another based on $\delta^{13}C$ values, but some subtle dietary behaviours can be investigated especially when viewed in conjunction with $\delta^{18}O$ values. The lower $\delta^{18}O$ values for the LBW hippos were expected (Bocherens et al., 1996) and suggest that this animal behaved in a similar way to extant hippos (i.e. they wallowed in water pools and were nocturnal feeders). Apart from an indication of the dominant floral type, $\delta^{13}C$ values can indicate whether animals were feeding in

open or closed habitats (Ambrose and DeNiro, 1986). Slightly lower $\delta^{13}C$ values (observed for hippos and giraffids) indicate that these animals were probably feeding under a partially closed canopy where irradiance is reduced. Feeding in open environments where irradiance is high and free mixing of biogenic CO_2 with the atmosphere can occur would result in higher $\delta^{13}C$ values (Quade et al., 1995). The $\delta^{13}C$ values for hippos and bovids are isotopically distinct from each other, indicating perhaps that these animals ate different kinds of C_3 vegetation or plant parts. The equid *Hipparion* cf. *baardi*, suid *Nyanzachoerus* sp. and the bovids (*Damalacra* and *Kobus*) have similar $\delta^{13}C$ values. Because of the large overlap in these values, no clear distinctions regarding niche preferences can be made for these animals.

Variations in oxygen isotope values between animals can indicate the water source or the physiological adaptation of the animal to heat stress. Animals that obtain most of their water directly from plants (like some browsers) can be distinguished from those that obtain their water from direct drinking (like grazers). This is because plant water is enriched in $\delta^{18}O$ compared to meteoric water (Epstein et al., 1977; Yakir, 1992). Differences in $\delta^{18}O$ values can also indicate physiological behaviour relating to cooling. For example, animals (such as hippos) that cool off in water pools and feed at night, greatly reduce oxygen loss and therefore have depleted $\delta^{18}O$ values. The significantly lower $\delta^{18}O$ values for rhinos (-4.4 ± 1.2‰, n=5) compared to other animals (excluding hippos) could therefore suggest that this animal was either a nocturnal feeder, spent time in water pools or drank a lot. Extant white rhinos like to cool off during mid day high temperatures (Kingdon, 1982) and perhaps this behaviour was established in their early ancestor *C. praecox*. It is unlikely that body size could contribute to these slightly depleted values, as the effects of body size are believed to be significant only for small animals (Luz and Kolodny, 1989; Bryant and Froelich, 1995; Kohn et al., 1996). All the LBW ungulates analysed are of a similar medium to large body size. Variable diets for the white rhinoceros, *C. praecox*, have recently been reported (Zazzo et al., 2000). Between 5-4 Myr *C. praecox* in North Africa was a mixed feeder but by 3.5 Myr it was a pure grazer. At Makapansgat (~3 Myr) in the north-east of South Africa, *C. simum* has $\delta^{13}C$ values distinct from bovids in the local ecosystem, which lead to the conclusion that this species of white rhinoceros was a mixed feeder (Sponheimer et al., 2001).

Because of the dominant C_3 signature at LBW, a dietary distinction cannot be made easily. The $\delta^{13}C$ values for *C. praecox* from LBW are not isotopically distinct from the bovids in the local fauna ($t = 0.61$, $df = 12$, $p>0.5$), suggesting that this animal was either a grazer or a browser on the west coast of South Africa during the Early Pliocene. The $\delta^{18}O$ values of the LBW rhinoceros are significantly lower than all the other animals (excluding hippos), supporting the idea that this animal may have been a grazer, since grazers tend to have slightly depleted $\delta^{18}O$ values amongst herbivores (Sponheimer and Lee-Thorp, 1999b). Alternatively, the distinct $\delta^{18}O$ values for the LBW rhinoceros can be considered as support for Klein's suggestion (Klein, 1981, 1982) based on mortality profiles, that the rhinoceros samples have been reworked from an underlying deposit and thus represent different climate and environmental conditions (see Chapter 2, section 2.6.1).

Solounias and co-workers (Solounias et al., 1988; Solounias and Moelleken, 1993b; Solounias et al., 2000) showed, using tooth microwear analyses and premaxillary shape, that the diets of the extinct giraffids are highly heterogeneous with some being mixed feeders and others pure grazers. Recently, a pure C_4 grazing *Sivatherium* species was found at 3-3.5 Myr in Chad, a North African Late Pliocene locality (Zazzo, personal communication 2000), as well as at 1.8 Myr in Olduvai, Tanzania (Van der Merwe, personal communication, 2000). Whether the LBW sivathere with its short neck was a pure grazer or a mixed feeder or a low-level browser cannot be determined based on $\delta^{13}C$ values alone because of the dominant C_3 signature at LBW. However, by comparing $\delta^{18}O$ values to those of taxa from other localities, more subtle distinctions may be possible. The similar $\delta^{13}C$ values to hippos suggest feeding under a partially closed canopy. The average $\delta^{18}O$ values of the sivatheres are most similar to that of the grazing bovids and the suids, and are significantly enriched compared to the hippopotamus. This result indicates that the sivathere is unlikely to have lived in water (similar to hippos) but that it may have fed at night or in the shade (i.e. under a partially closed canopy). Alternatively, *S. hendeyi* was not a browser, as has been assumed (Hendey, 1984). Both explanations are possible. Feeding at night or in the shade results in depleted $\delta^{18}O$ values (compared to other fauna) because evaporation rates and irradiation are reduced. On the other hand, the similar sivathere $\delta^{18}O$ values to the grazing bovids

suggest similar water-related behaviour (i.e. drinking frequently). Cerling et al. (1997a) reported that extant giraffes are enriched compared to contemporaneous fauna, yet Sponheimer and Lee-Thorp (2001) did not observe this phenomenon in the Morea Estate (South Africa) assemblage. They suggest that this difference may relate to different drinking strategies, but nevertheless this complicates behavioural inferences based on $\delta^{18}O$ values. At LBW, the Giraffidae are slightly enriched in $\delta^{18}O$ compared to other fauna, although this difference is not significant. It therefore appears that *S. hendeyi* probably fed under a partially closed canopy. In addition, it may not have been a typical pure browser. The dietary strategy of *S. hendeyi* is further examined using microwear, mesowear and the hypsodonty index in Chapter 7.

4.5 CONCLUSIONS

The results from FTIR spectroscopy and stable isotope analyses indicate that LBW fossil enamel is preserved well and has not undergone significant diagenesis. Furthermore, results show that even subtle differences in stable carbon and oxygen isotope values can shed light on dietary and behavioural differences between taxa. More importantly the findings presented here provide information relating to C_4 expansions in the Southern Hemisphere as well as local climate and vegetation histories. The fact that C_4 grasses did not dominate at 33°S during the Early Pliocene is probably related to the early establishment of the current winter-wet/summer-dry climate regime. Evidence for decreased seasonal amplitudes, less well defined seasons and seasons of various lengths suggest that the local climate was relatively unstable.

Chapter 5

PALAEOPATHOLOGY IN THE HERBIVORES FROM LANGEBAANWEG

5.1 INTRODUCTION

This chapter investigates pathologies in several ungulates from Langebaanweg (LBW) in order to gain insight into prevailing environmental conditions of the time. Hendey (1981b) first noted that enamel hypoplasia is present in numerous teeth belonging to the sivathere, *S. hendeyi* from LBW. In addition, he observed irregular tooth wear in the reduncines (*Kobus* sp.). The aim of this aspect of the study is to determine the extent of defects in several of the LBW fauna from the Pelletal Phosphate Member.

Although this chapter concentrates on dental defects, a number of skeletal elements were also examined for signs of disease, infection or stress that could be indicative of or the result of prevailing environmental conditions. An assessment of the extent of pathologies and the determination of which animals were most affected provides valuable insight into the prevailing health-status of the LBW fauna. For comparative purposes the sivathere (*S. hendeyi*) is included in this chapter, although a more detailed analysis of enamel hypoplasia in this animal is given in Chapter 6.

5.1.1 Pathology in the fossil record

Anthropologists frequently use the analysis of both skeletal and dental defects to obtain health-related information about human populations. Dental defects are however very rarely reported in non-primates (Dobney and Ervynck, 1998; Mead, 1999; Dobney and Ervynck, 2000; Niven, 2002), despite their potential value in providing health-status information. Animal pathologies in the fossil record are however, rarely abundant and infrequently studied.

It is important when dealing with fossil animals to be able to distinguish true pathology from diagenesis. Because the identification of skeletal defects in extant

material is complex (Rothschild and Martin, 1993), making the distinction between a true defect and diagenesis in fossil material is extremely complicated. Hence the assessment of skeletal defects is treated with caution in this chapter. Healed fractures and evidence for scavenging, although easier to identify provide little information on the health-status of a population and were therefore not investigated.

Pathologies can be broadly divided into defects that manifest during growth (such as tooth enamel defects) and those that manifest later in life, usually during old age, such as arthritic disease. Both are useful biological indicators and provide slightly different perspectives on health-status. Evidence for defects that manifested during development can be found in both teeth and bone, while evidence for late onset adult disease only affects skeletal elements. This is because tooth enamel is not remodeled[1] during life and therefore once it has completed development it can no longer 'record' perturbations or disturbances. Bone on the other hand is continually remodeled, so that stress or disease "information" may be incorporated throughout life. Remodeling in bone may however also result in this stress information being lost. The only way tooth defects can be lost is through attrition[2] of the tooth. Teeth therefore provide a permanent record of developmental defects (Goodman, 1991) in comparison to bone.

In general, only diseases in advanced stages manifest in bone, and any wild animal with such a disease would soon be the target of predation. Considering the rarity of pathologies in wild animals and natural predation on these animals, it is unlikely that the remains of many animals with skeletal disease would be found in the fossil record. Some bone pathologies have been reported in fossils but these are mostly isolated cases. For example, osteoarthritis is fairly common in pterosaurs (Bennet, 1989) but uncommon in hadrosaurian dinosaurs, birds and primates (Rothschild and Martin, 1993). Pleistocene marsupials often have osteoarthritis of the ankle (Rothschild and Molnar, 1988). The most frequently reported skeletal pathologies in fossil animals (e.g. in sabre-toothed tigers, mammoths, bears, various primates) appear to be diseases of the spine, such as spondyloarthropathy[3] (Fox,

[1] Remodeling can be defined as the deposition and resorption of tissue.
[2] The process of grinding and chewing food in the mouth for digestion.
[3] This is a category of arthritis often resulting in spinal fusion or asymmetrical arthritis (Rothschild et al., 1993).

1939; Rothschild and Woods, 1989; Rothschild et al., 1991; Rothschild et al., 1993; Dawson and Gottfried, in press). The first occurrence of vertebral end-plate lesions (Schmorl's nodes) in a fossil vertebrate, a Lower Jurassic plesiosaur, was recently reported (Hopley, 2001). Brothwell (1963) lists skeletal pathologies in several Pleistocene mammals. Palaeontologists most often report adult skeletal diseases presumably because adult material is more abundant in the fossil record than juvenile material. These abnormalities are however, rarely investigated in detail and are simply reported and sometimes even ignored. Pathologies that are not fatal are likely to be more common in the fossil record. The advantage of defects that manifest during development is that they have the potential to provide a unique perspective into the health-status of the growing animal.

Non-fatal developmental defects can be observed in both bones and teeth. A disruption of growth in bone results in the development of Harris or stress lines. These are dense transverse lines, visible towards the proximal or distal ends of the diaphysis[4] in radiographs of long bones, and are indicators of general systemic stress. The lines develop as a result of a period of growth arrest followed by growth recovery. Interpretation of Harris lines must however be treated with caution and although they are thought to be indicative of physiological stress, correlations between Harris lines and known stressors are low (Goodman et al., 1984). A constraint of studying stress lines is bone remodeling, which can destroy stress lines that developed early in life. Harris lines have been studied in Pleistocene wolf, coyote, sabre-toothed cat, camel and horse specimens from the Rancho La Brea asphalt deposits in Los Angeles, California (Duckler and van Valkenburgh, 1998). The frequency of Harris lines in the long bones of these animals ranged from one to nearly seven percent.

In teeth, a disruption in the cells (ameloblasts) that lay down (the organic template of) enamel results in a defect known as enamel hypoplasia (EH), while disturbance during the mineralisation (or maturation) phase is known as hypomineralisation (see Chapter 3).

[4] The diaphysis is the shaft of a long bone.

Apart from these developmental enamel defects, gross dental wear irregularities (such as concave wear facets, stepped wear etc.) can also be useful indicators of unusual or abnormal conditions. For example, they could indicate that the normal food source was not available for consumption and that animals were forced to feed on a diet for which they were not well adapted.

5.2 MATERIAL AND METHODS

5.2.1 MATERIAL

Teeth and post-crania belonging to several ungulates from the Pelletal Phosphate Member (PPM) at LBW were examined for defects.

5.2.1.1 Teeth

3069 mainly isolated teeth from five families of ungulates were examined for LEH, irregular tooth wear and gross deformities (Table 5.1). Although permanent teeth were preferentially selected, 375 deciduous teeth were also examined. These teeth form a minor component of each sample. (Deciduous teeth develop prenatally and are therefore unlikely to provide information on prevailing environmental conditions unless defects relate to the maternal health-status). Fossil collections were extremely large for most animals and not all collected material was examined. Complete or partially broken teeth were randomly selected (regardless of tooth type) from the collection for analysis. According to Goodman and co-workers (Goodman et al., 1984; Goodman and Rose, 1990), anterior teeth are preferred for defect analyses, as these teeth appear to be highly susceptible to stress in humans. For the sivathere, *S. hendeyi*, an enormous dental collection exists and therefore only mandibular teeth were examined. However, no distinction between left and right teeth was made, even though opposite jaws develop concurrently and are therefore believed to manifest the same defects during ontogeny (Dobney and Ervynck, 1998). Only erupted teeth in which enamel formation was completed were examined. Large tusk fragments from the hippopotamus (Gen. & sp. not det.) from LBW were also included in the analysis.

The Suidae were not included in this analysis since only a few fragmentary teeth were found in the PPM (Bed 3aS). These teeth may have been reworked from

the underlying QSM deposit (see Chapter 2, section 2.6.1). Teeth belonging to the Equidae were only examined for irregular wear and deformities since these teeth have a thick cementum layer covering the enamel, which completely obscures enamel defects. The indeterminate Bovidae teeth (n = 84), which were identified by Hendey (during sorting) as irregular and possibly abnormal, where kept as a separate Bovidae group in the current analysis as these teeth were not randomly selected.

Table 5.1. Tooth samples. 'n' refers to the numbers of teeth examined.

Animal	Total number	permanent teeth (%, n)	deciduous teeth (%, n)
Family Rhinocerotidae			
Ceratotherium praecox	50	82% (41)	18% (9)
Family Bovidae			
Reduncini (*Kobus* sp.)	43	97.7% (42)	2.3% (1)
Alcelaphini (*Damalacra* sp.)	200	95.5% (191)	4.5% (9)
Bovini (*Simatherium demissum*)	129	90% (116)	10% (13)
Boselaphini (*Mesembriportax acrae*)	183	83.1% (152)	16.9% (31)
Indeterminate	84	81% (68)	19%(16)
Family Hippopotamidae			
Gen. And Sp. not det.	237	82.7% (196)	17.3% (41)
Family Giraffidae			
Sivatherium hendeyi	1759	87.8% (1544)	12.2% (215)
Palaeotragus cf. *germaini*	29	82.8% (24)	17.2% (5)
Giraffa cf. *jumae*	294	88.1 (259)	11.9 (35)
Family Equidae			
Hipparion cf. *baardi*	61	100% (61)	0% (0)

5.2.1.2 Skeletal material

Skeletal material from the four largest ungulates was examined for any evidence of disease, infection or other lesions. In total 244 complete or partial skeletal elements were examined (Table 5.2), and these include elements from all parts of the skeleton (Appendix G). 52% of the complete bones that were studied are

small skeletal elements such as phalanges and digit bones. Of the 125 long limb bones[5] that were analysed, only 34% (n=43) are complete specimens.

Table 5.2. Skeletal material analysed. 'n' refers to the number of bones examined.

Animal	Total number (n)	Number of complete bones (%, n)	Number of partial bones (%, n)
Family Rhinocerotidae *Ceratotherium praecox*	40	7.5% (3)	92.5% (37)
Family Hippopotamidae Gen. and sp. not det.	71	67.6% (48)	32.4% (23)
Family Giraffidae *Sivatherium hendeyi*	102	59.8% (61)	40.2% (41)
Family Equidae *Hipparion* cf. *baardi*	31	38.7% (12)	61.3% (19)

S. hendeyi is the dominant herbivore from the PPM and several complete long bones belonging to this animal are present in the collection. Radiographs of nine metapodials (PQL 45066, PQL 40022, PQL 25864, PQL 14173, PQL 20195, PQL 12472, PQL 45374, PQL 25863, PQL 14228) were examined to determine whether Harris (or stress) lines are present. Only one of these metapodials (PQL 14228) has an unfused epiphysis indicating that it belonged to an immature individual (Figure 5.1).

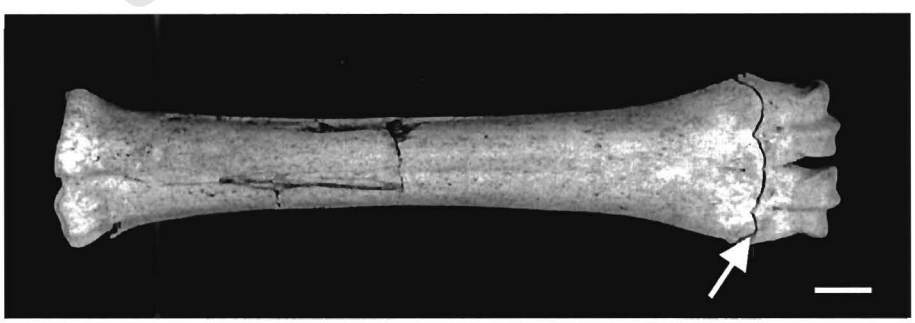

Figure 5.1. An immature metapodial (PQL 14228) belonging to *S. hendeyi.* The arrow indicates the unfused epiphysis. Scale bar represents 3 cm.

[5] These include humeri, femora, radii, ulnae, fibulae, tibiae and metapodials.

5.2.2 METHODS

5.2.2.1 Examination and classification of dental defects

Dental defects include enamel hypoplasia, irregular dental wear and deformities. These defects are distinct from post-depositional damage, which was not recorded. Any variation of the normal wear pattern was recorded as irregular wear – such as concave, stepped, or completely flat occlusal surfaces. A large database of all 3069 teeth was developed, with descriptions of all defective teeth. (The raw data is housed together with the collection at the South African Museum, Iziko Museums of Cape Town, South Africa).

Dobney and Ervynck (1998) suggest oblique lighting should be used to view defects in pigs from archaeological sites. However, in the fossil material from LBW, defects were extremely prominent when viewed with the naked eye in a well-lit room. A magnifying glass was used to confirm the presence of defects in very small bovid teeth as suggested by Goodman and Rose (1990), who believed that a defect not visible with the naked eye is probably too small to reliably record a stress event and is unlikely to be a true enamel hypoplasia.

Enamel hypoplasias were identified as linear or non-linear in accordance with the FDI index (Federation Dentaire International, 1982) (see Chapter 3, section 3.4.1). Linear defects are referred to here as bands of pits or grooves if they are horizontally arranged. All other defects (single pits, diffuse pitting and areas missing enamel) are considered non-linear. Skinner and Goodman (1992) caution that it can be difficult to distinguish normal perikymata[6] from mild hypoplasia, especially if defects are very shallow. Such teeth were classified as "possibly" defective. The FDI index classifies deep single pits that expose underlying dentine as single pits and not as areas missing enamel. In the current study, these deep pits were classified as an area missing enamel so that the subjective distinction between an area and pit was avoided. In addition, in some teeth horizontal arrangements of pits were present that did not extend right across the tooth crown and in others diffuse pitting in a more or less horizontal arrangement was observed. Teeth exhibiting either of these latter

[6] A step-like feature observed on the outer surface of enamel, considered to be the surface manifestation of the incremental enamal layers or Striae of Retzius (Osborn and TenCate, 1983).

defect morphologies were classified as "possibly" defective. The incidence of LEH (i.e. numbers of teeth with these defects) is therefore the minimum level.

Teeth that develop at different times during ontogeny may be exposed to different physiological stress episodes and thus each of these tooth types can provide information about a different period of time. In this chapter, the aim is to assess the extent of pathologies in the fauna, rather than determine the cause of the observed enamel hypoplasia. Therefore, an analysis of defects in each tooth type was not necessary in this initial investigation, although tooth type was recorded where possible. In Chapter 6-8, the cause of the observed enamel hypoplasia is investigated in detail in *S. hendeyi*, the dominant component of the fauna, and only for this animal was tooth type and position in the jaw strictly recorded.

5.2.2.2 Linear enamel hypoplasia analysis

Dobney and Ervynck (1998) record defects on only one surface (i.e. lingual) of pig teeth. They suggest that using the lingual surface may help in identification of linear defects since the crown is highest on this surface (potentially enhancing the resolution of defects) and this surface is flat facilitating height measurements. They conclude that "slight" LEH lines can gradually disappear from the lingual surface due to exposure of this surface to the constantly moving tongue and bolus of food, whereas these lines remain visible on the buccal/labial[7] side. In the analysis of LBW teeth, linear defects were i) in some instances not present on both lingual and buccal surfaces, ii) buccal surfaces more often record defects and iii) in some teeth only lingual linear defects were present. To avoid counting defects that developed as a result of the same stress episode twice, only defects on one surface of a tooth (buccal/labial or lingual) were used in the analysis, although defects on both surfaces were recorded in the database. Buccal/labial surfaces were preferentially chosen, but where a defect was present only on the lingual surface, these defects were included in the calculations of incidence (numbers of teeth with defects) and Tooth Hypoplastic Area Score calculations. Additional defect criteria were recorded for the sivathere (*S. hendeyi*) (see Chapter 6, section 6.2.2).

[7] In anterior teeth (incisors, canines) the surface opposite to the lingual one is referred to as the labial surface whereas in posterior cheek teeth (premolars, molars) this surface is termed the buccal surface.

Tooth Hypoplastic Area Scoring Method

Ensor and Irish (1995) developed a Tooth Hypoplastic Area (THA) scoring method to score linear enamel hypoplasias in human teeth. This method (outlined fully in Chapter 3, section 3.6.2) essentially takes the width of the defect and divides it by two-thirds of the unworn crown height.

In the current analysis, two main changes to the above method were made. Firstly, the THA score for each linear defect was calculated without defining defects as acute or chronic, and all defects are therefore evaluated (without subjectivity) in a similar manner. Secondly, unworn crown heights were not always available for each tooth type in each animal, and actual crown heights were therefore used to calculate THA scores. This gives an actualistic or visible THA score for each tooth and animal that serves adequately in comparisons between animals. Any bias as a result of wear will probably be similar in each population.

The average THA score for an animal was calculated by first calculating a score for each defect on each tooth by dividing the width of the defect by the crown height of the tooth. The sum of these individual defect scores on a crown surface gives the total THA score for a particular tooth. Average THA scores for each animal were then calculated, converted to a percentage and used to compare duration of stress episodes in the different animals. Scores were not calculated for teeth in the "possibly" LEH category and scores reported are therefore minimum scores. All measurements were taken with digital callipers to the second decimal. Defects that were too narrow to measure accurately were assigned a width of 0.2 mm.

Dobney and Ervynck (2000) working on pigs from archaeological deposits show that there are no major differences in defect heights between cusps of the same tooth. In the current study however a preliminary assessment of defective teeth indicated that defects do not maintain a uniform width or height across all cusps and are often slightly wider and higher on the most anterior cusp. For this reason and to maintain consistency, all LEH measurements were taken on the anterior cusp as shown in Figure 5.2. Since enamel development times for most wild extant ungulates are not known, the potential bias this would create when evaluating defects, could not be assessed or avoided. However, the sample of teeth analysed

for each animal here contains a mixture of tooth types and therefore any bias resulting from differences in enamel development rates (a constraint of the THA method, see Chapter 3, section 3.6.2) should be equal for each animal.

5.2.2.3 Examination of skeletal defects

Gross morphology of the post-cranial material was studied for any sign of abnormality, especially of disease or infection. Standard radiographic examination was also conducted (by Dr. Rachel Alexander of the South African Museum), on some complete *S. hendeyi* metapodials.

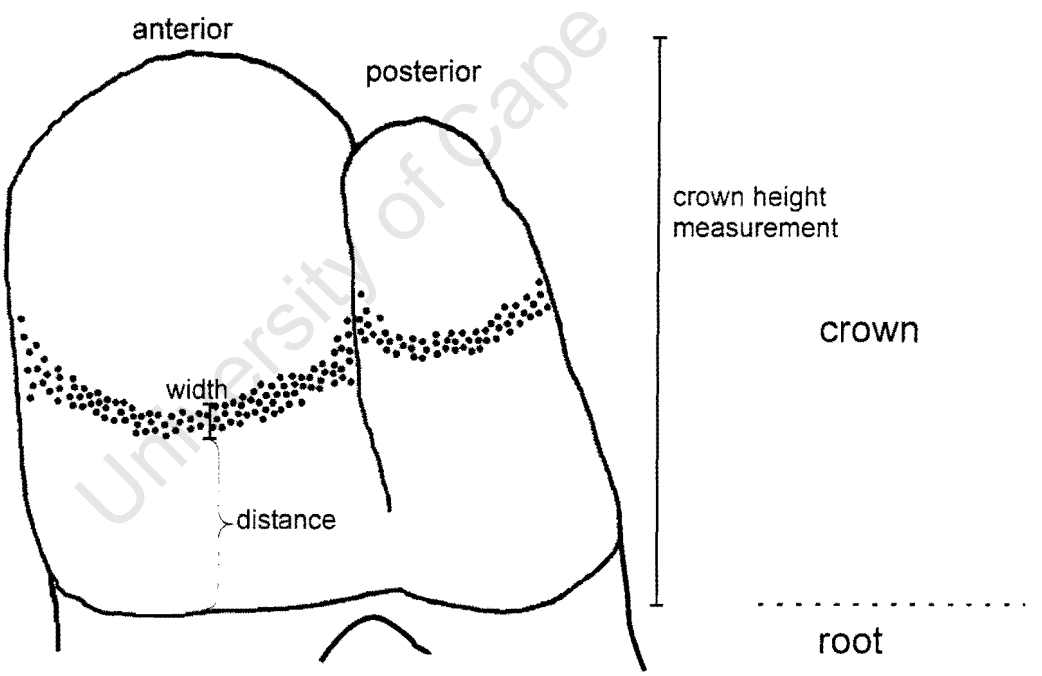

Figure 5.2. Diagram of a mandibular fourth premolar of a giraffe showing where measurements were taken for THA scoring and for the evaluation of age that defects manifested (distance to crown base).

$$\text{THA} = \frac{\text{width of defect}}{\text{crown height}}$$

5.3 RESULTS

5.3.1 Dental defects

Dental defects were found in all animals examined (Table 5.3). Of the 3069 teeth analysed, 1011 teeth have enamel hypoplasia (33.6% excl. equids), seven teeth are deformed and 132 teeth have irregular wear (4.3%). 3.4% possibly have linear enamel hypoplasias (104 teeth). The rest of the teeth are normal. Of the 1011 teeth with enamel hypoplasia, 563 teeth have linear defects and 448 teeth have non-linear defects.

Table 5.3. Numbers of teeth with each type of defect. 'n' refers to the total number of teeth analysed.

	n	LEH	Possibly LEH	Non-linear EH	Irregular dental wear	Deformed teeth
Rhinocerotidae						
C. praecox	50	3	1	0	0	0
Hippopotamidae	237	72	4	31	0	0
Bovidae						
Reduncini *Kobus* sp.	43	9	1	5	4	2
Bovini *S. demissum*	129	12	0	2	4	0
Boselaphini *M. acrae*	183	6	0	3	7	0
Alcelaphini *Damalacra* sp.	200	16	3	6	8	0
Indeterminate	84	8	2	0	38	3
Giraffidae						
Palaeotragus sp.	29	0	1	2	3	0
Giraffa sp.	294	4	2	24	1	0
S. hendeyi	1759	433	90	375	63	2
Equidae						
Hipparion sp.	61	-	-	-	4	0
TOTAL	**3069**	**563**	**104**	**448**	**132**	**7**

83.7% of the non-linear defects identified are present in the teeth of *S. hendeyi* (Figure 5.3). Non-linear defects affect 21.3% of the *S. hendeyi* teeth examined. Examples of a single pit with reduced enamel thickness and multiple diffuse pitting are shown in Figure 5.4 (these defects are described in detail in Chapter 6). Of the remaining animals, the highest incidence of non-linear defects

was found in the hippopotamus (13.1%), the reduncine (11.6%) and *Giraffa* (8.2%). Most of the non-linear defects in the hippo and reduncine are multiple diffuse pitting. This pitting appears to be a fairly common phenomenon in hippo teeth and accounts for 80% of the non-linear defects in this animal. In contrast, in *Giraffa* areas with thin enamel or single pits account for 88% of the non-linear enamel defects. Linear enamel hypoplasia was observed in each of the ungulate families analysed and is discussed in detail in the next section.

Irregular dental wear was observed in only 4.3% of the teeth analysed. The most extreme examples of irregular wear were observed in the bovids, some of which are shown in Figure 5.5. Several incisors have wear facets at the neck of the tooth where the tooth root and crown meet (Figure 5.5A-C). Irregular occlusal wear is shown in Figure 5.5D-J. Some teeth have completely concave occlusal surfaces with high anterior and posterior sides (Figure 5.5D-E) while others have a stepped wear pattern (Figure 5.5F-G) or flat occlusal surfaces (Figure 5.5H).

Only seven deformed teeth were found. Two deformed second molars belong to *S. hendeyi* and the other five cheek teeth belong to the Bovidae (reduncini and the indeterminate Bovidae group) (Figure 5.6). One of the *S. hendeyi* second molars is completely deformed as is shown in Figure 5.6A. The mandibular fragment (PQL 62725) consists of a deciduous premolar, first molar and deformed second molar. The first molar has an area missing enamel on its buccal and lingual surface, as well as a thin deep groove (a LEH) towards the base of this tooth. The deciduous fourth premolar adjacent to this molar is devoid of defects. A developing p4 is visible underlying this deciduous tooth if viewed from the lingual side. The second *S. hendeyi* molar (PQL 45319) has grossly malformed enamel on both buccal and lingual surfaces (Figure 5.6B-C). A bovid third molar (PQL 50739) with a completely deformed posterior and partially deformed middle cusp is shown in Figure 5.6D. Two bovid upper fourth premolars with split buccal cusps were also found (Figure 5.6E).

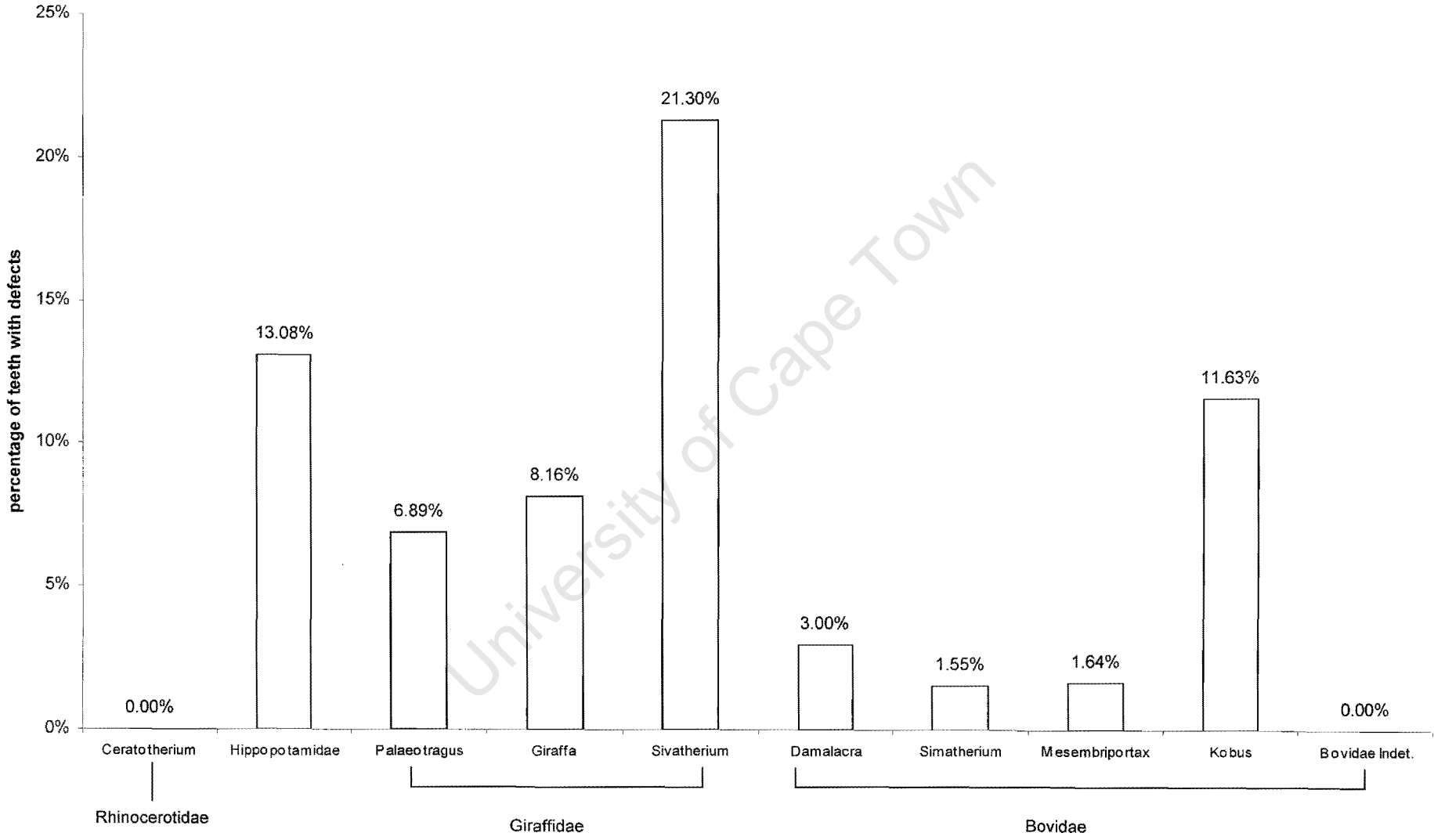

Figure 5.3. Percentage of teeth with non-linear enamel hypoplasia. Numbers of teeth are given in Table 5.3.

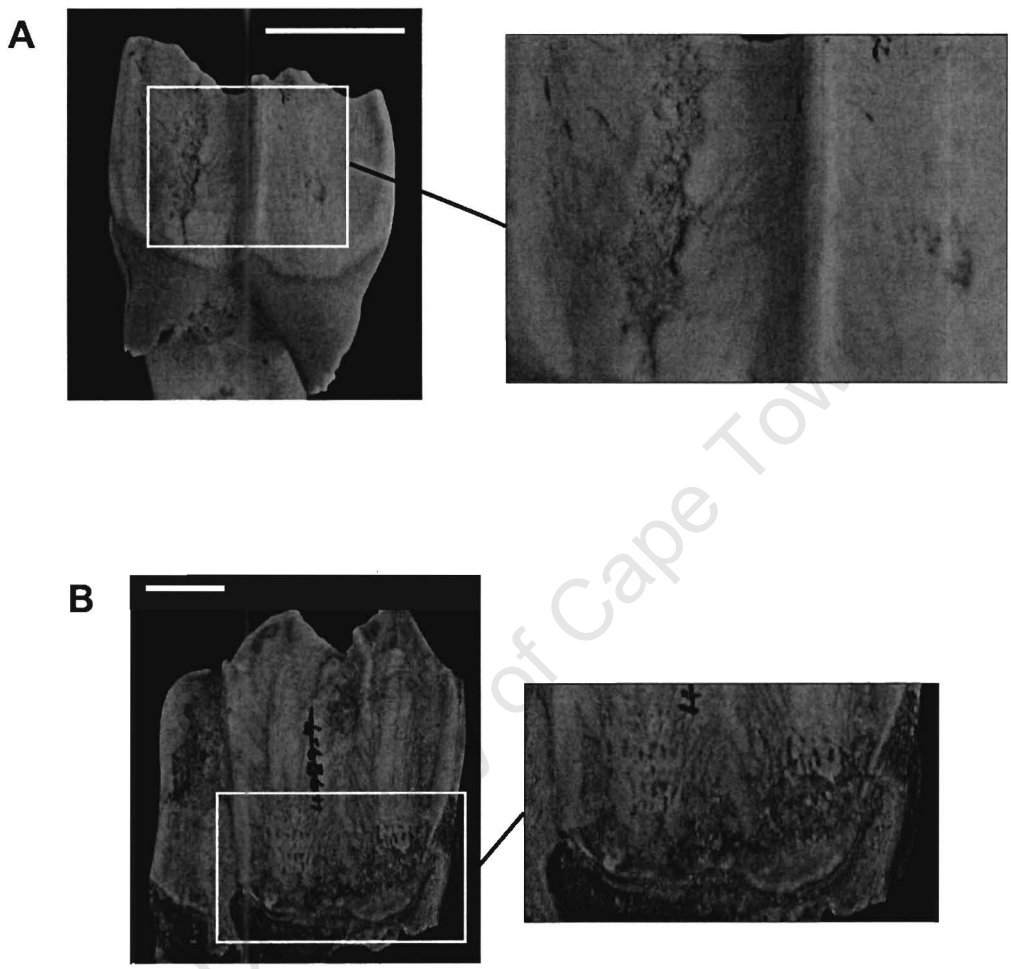

Figure 5.4. Examples of teeth with non-linear enamel hypoplasia. (A) Reduncine upper molar (PQL 31804), lingual surface, showing a long vertical pit extending almost the entire length of the crown, and (B) bovine third molar (PQL 59432) showing diffuse pitting on the lingual surface, at the base of the two most anterior cusps only. Scale bar represents 1 cm.

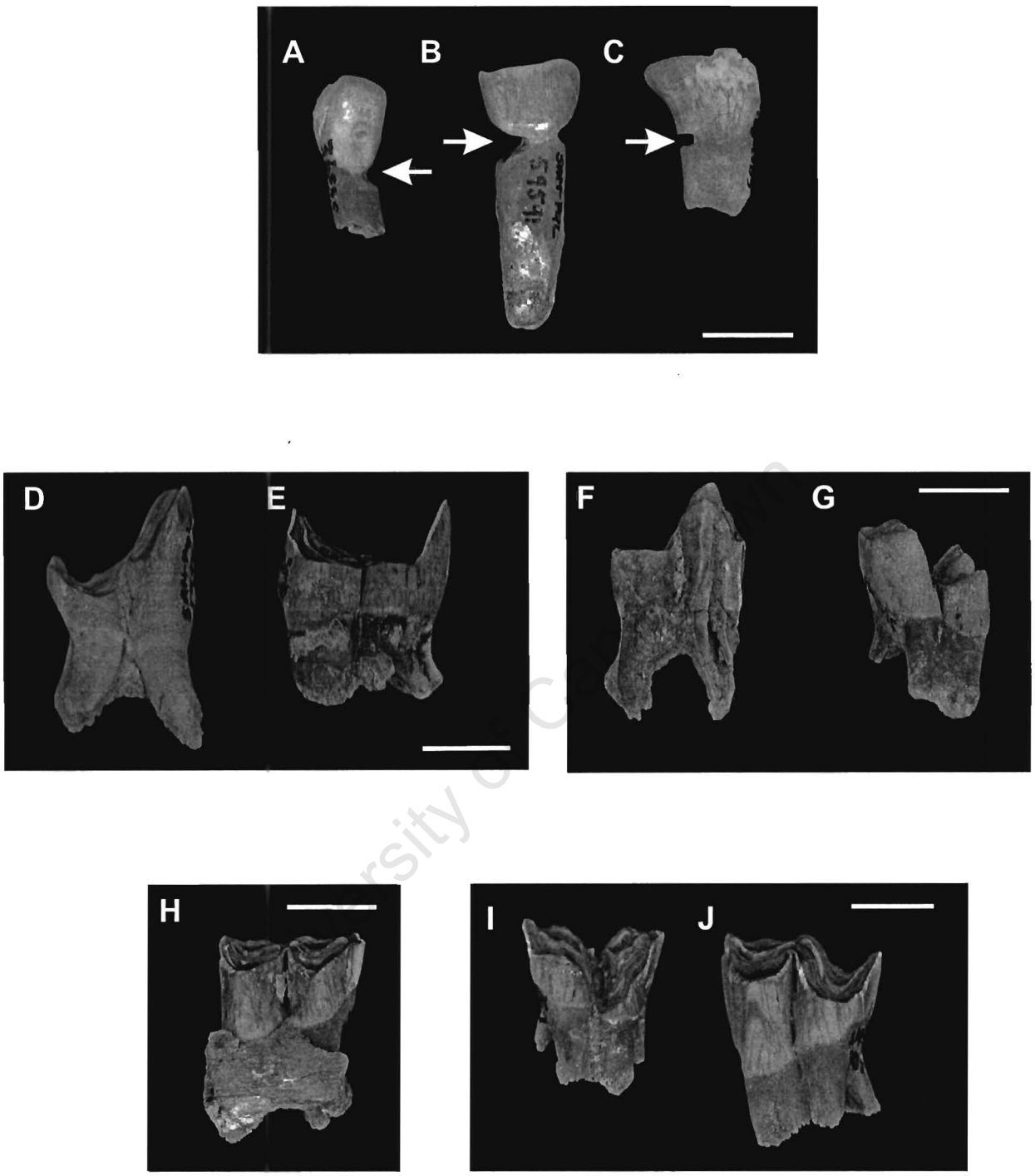

Figure 5.5. Bovid teeth with irregular wear. (A-C) incisors with a wear facet/indentation at the root-crown junction (arrows), (A) PQL 595572, (B) PQL 59591 and (C) PQL 59574. (D-E) molars with concave occlusal surfaces, (D) PQL 59544 and (E) PQL 59547. (F-G) stepped wear in PQL 43914 (F) and PQL 43915 (G). (H) PQL 59545 molar with a flat occlusal surface, (I) PQL 59555 and (J) PQL 59556, molars with milder irregular wear. All scale bars represent 1 cm.

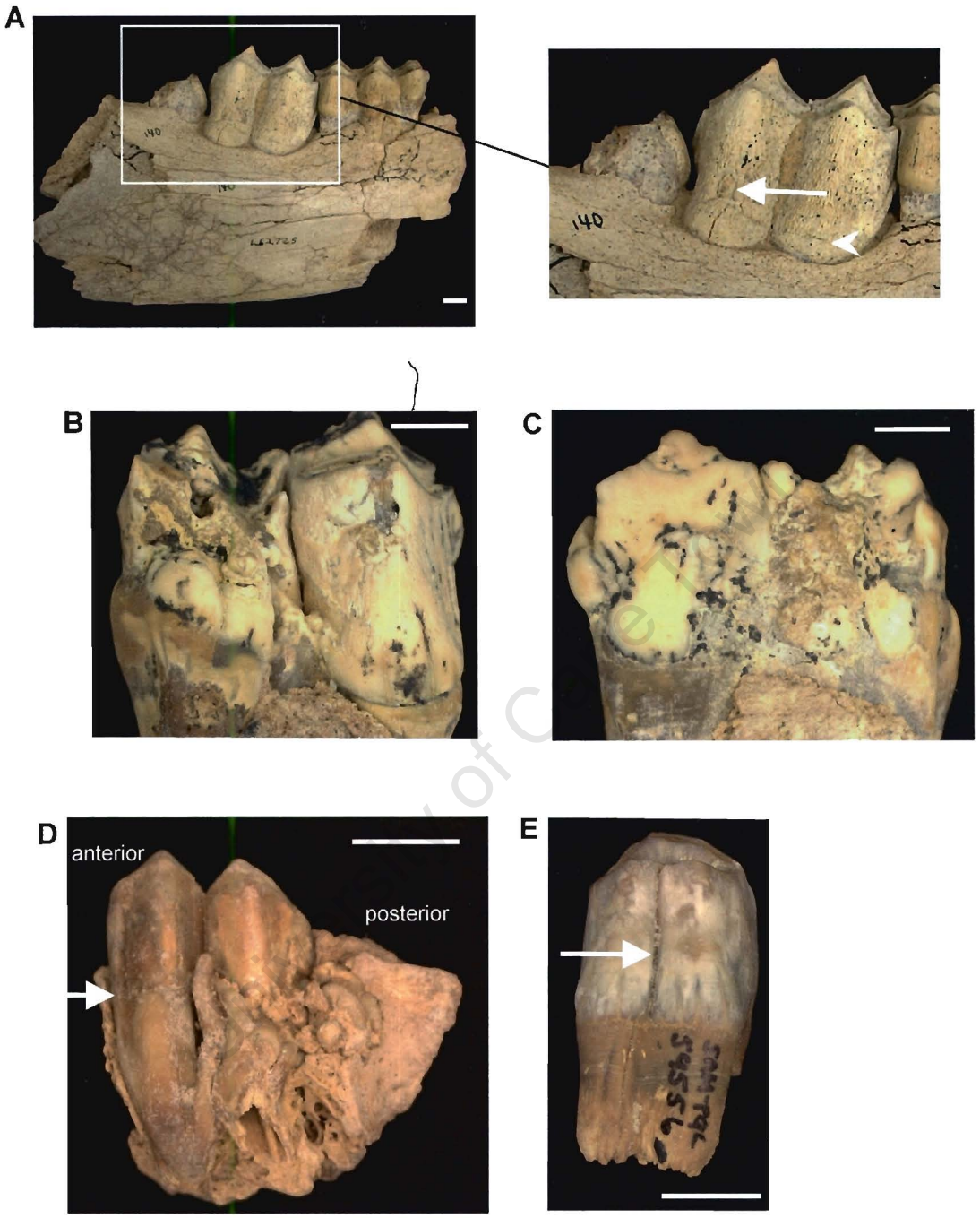

Figure 5.6. Deformed teeth belonging to *S. hendeyi* and Bovidae (indet.). (A) A *S. hendeyi* mandibular fragment (PQL 62725) with a deformed second molar, a first molar and a fourth deciduous premolar. The arrow in the inset indicates an area missing enamel in the first molar, while the arrowhead indicates a deep thin linear enamel hypoplasia groove towards the base of the first molar. (B) and (C) A *S. hendeyi* upper molar (PQL 45319) with malformed enamel, (B) buccal surface and (C) lingual surface. (D) deformed bovid third molar PQL 50739, (E) deformed bovid upper fourth premolar (PQL 59556) with split buccal cusps (arrow). All scale bars represent 1 cm.

5.3.1.1 Linear enamel hypoplasia (LEH)

Morphology: Linear enamel hypoplasia (LEH) was observed as bands of pits or as horizontal grooves. Bands of pits are more prevalent and were found on 86% of defective teeth. Most teeth have only one type of LEH per tooth crown (Table 5.4). However, some hippopotamus and sivathere (*S. hendeyi*) teeth have both types of LEH on the same crown. Examples of LEH in alcelaphine (*Damalacra*), bovine (*S. demissum*), reduncine (*Kobus*) and hippopotamus teeth are shown in Figure 5.7 - 5.9. Bands are generally wider than grooves (compare Figure 5.7B and Figure 5.8).

Table 5.4. Numbers of teeth with each type of linear enamel hypoplasia (bands and/or grooves).

	Grooves only	Bands of pits only	Both grooves and bands
Rhinocerotidae			
C. praecox	1	2	0
Hippopotamidae	3	56	12
Bovidae			
Reduncini *Kobus* sp.	0	9	0
Bovini *S. demissum*	2	10	0
Boselaphini *M. acrae.*	2	4	0
Alcelaphini *Damalacra* sp.	6	10	0
Indeterminate	0	8	0
Giraffidae			
Giraffa sp.	1	3	0
S. hendeyi	65	354	14

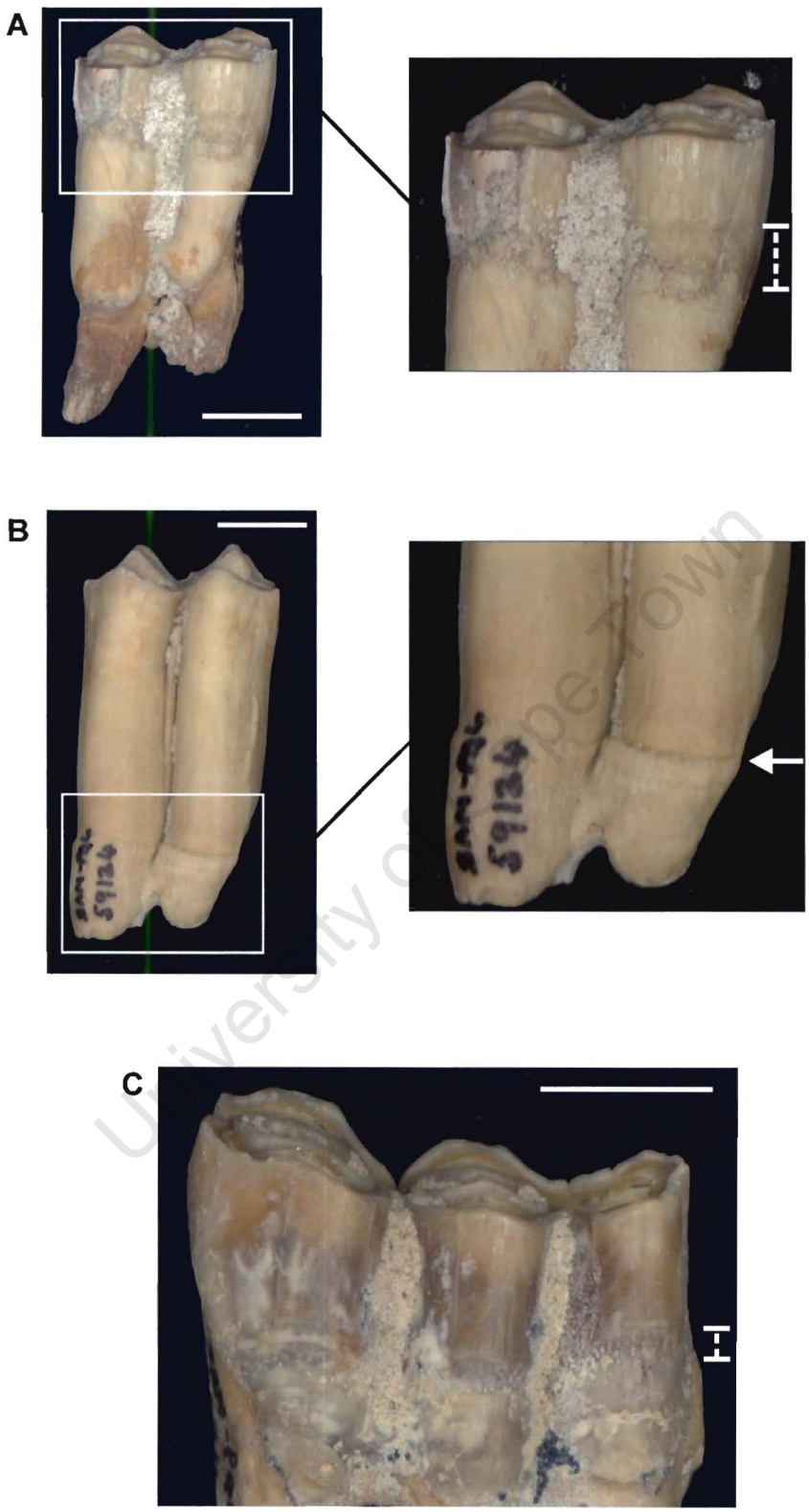

Figure 5.7. Linear enamel hypoplasia in alcelaphine (*Damalacra* sp.) teeth. Dashed vertical bars (in A and C) and arrow (in B) indicate the linear defect in each tooth. (A) PQL 59082, a molar with a band of pits, (B) PQL 59124, a molar with a groove/ridge toward the base of the crown, (C) PQL 59134, a third molar with a band of pits. All scale bars represent 1 cm.

Figure 5.8. A reduncine (*Kobus* sp.) tooth (PQL 10533) with linear enamel hypoplasia and stepped irregular wear. (A) buccal view and (B) lingual view. Dashed vertical lines indicate the width of the LEH. Scale bars represent 1 cm.

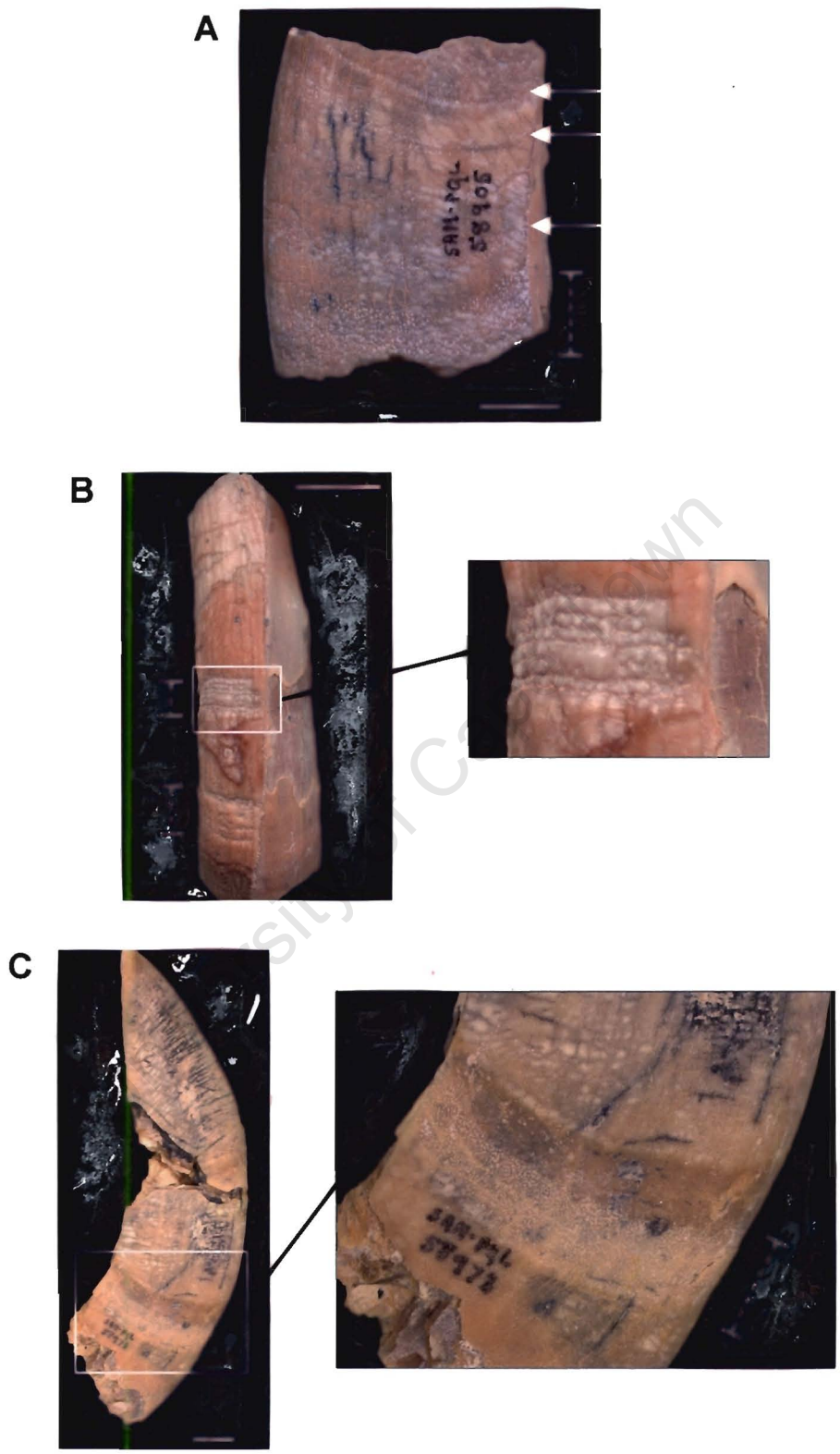

Figure 5.9. Hippopotamus teeth with linear enamel hypoplasia. (A) tusk fragment (PQL 58905), with several linear defects, the basal dashed line indicates a wide band of pits whereas the other three defects (arrows) are fairly narrow. (B) incisor fragment (PQL 51371), dashed lines indicate areas with linear grooves. (C) tusk (PQL 58973), dashed line indicates the width of the linear defect. Scale bars represent 1 cm.

27.7% of the teeth with LEH have more than one linear defect per tooth crown (Table 5.5). Some teeth have as many as ten grooves (hippo tusks) and five bands of pits (hippo and *S. hendeyi* teeth) on a tooth crown (Figure 5.9). The location and width of the defects on the tooth crowns are highly variable. An analysis of LEH location on a tooth crown, distribution in each tooth type and a detailed high-magnification morphological description is provided for *S. hendeyi* teeth (see Chapter 6). Here only width is considered further.

Table 5.5. Numbers of teeth with one or more linear defects on a single tooth crown.

	One defect	Two defects	Three defects	Four defects	Five or more defects
Rhinocerotidae *C. praecox*	3	0	0	0	0
Hippopotamidae	48	11	6	4	3
Bovidae					
Reduncini *Kobus* sp.	8	1	0	0	0
Bovini *S. demissum*	12	0	0	0	0
Boselaphini *M. acrae*	4	1	1	0	0
Alcelaphini *Damalacra* sp	16	0	0	0	0
Indeterminate	8	0	0	0	0
Giraffidae					
Giraffa sp.	4	0	0	0	0
S. hendeyi	304	86	33	7	3

Incidence: The overall incidence of LEH in the LBW fauna is 18.7% (563 out of 3008 teeth excluding the Equidae[8]). Since deciduous and permanent teeth develop at different times (prenatally versus postnatally) in ungulates, combining these two samples is not favourable in an evaluation of incidence. Only six deciduous teeth have linear defects (Appendix H) giving a deciduous teeth incidence of 1.6%. The overall incidence of LEH in the permanent teeth is 21.1% (557 out of 2633 teeth, excluding the equids), significantly greater than that of the deciduous teeth. The incidence of LEH in the permanent dentition of each animal is highly variable ranging

[8] Enamel defects were not investigated in this animal (see section 5.2.1.1).

from 0% to ~30% (Figure 5.10). The hippopotamus and sivathere have the highest incidence of LEH in permanent teeth (29.6% and 28.0% respectively) while very few linear defects were found in teeth belonging to *Palaeotragus* and *Giraffa*. The reduncines (*Kobus*) have an incidence of 21.4% and all other animals have a low incidence of LEH (< 12%). The reported incidence for the hippo may be an underestimate as tusk fragments less than 100 mm in length were excluded from this calculation. If these ten fragments are included as representing individual teeth then the incidence of LEH in this animal increases to 34.7%.

THA score: The average THA score for each animal is shown in Figure 5.11. The hippopotamus and reduncines have the highest scores (greater than 33%) indicating that on average more than 33% of each defective tooth crown is occupied by a linear defect. The rest of the Bovidae and the Giraffidae (*S. hendeyi* and *Giraffa*) have THA scores of 15-25%, and the rhinos have the lowest average score of 3.1%. The teeth belonging to Bovidae (indet.) have a high THA score of 72% but these eight teeth are severely defective and were isolated from the general collection. As they constitute a biased sample they are not included in Figure 5.11. An overall average THA score for all the Bovidae is 35.2% similar to that obtained for the hippopotamus. The minimum and maximum tooth scores for each animal together with the average scores shown in Figure 5.11 are reported in Table 5.6. Minimum THA scores are less than 2% for all animals except the boselaphine *M. acrae* where the minimum score for any tooth was 5%. For hippo, reduncines (*Kobus*) and sivathere (*S. hendeyi*) THA scores reach maximum values (of 100%) indicating that in some teeth linear defects occupy the entire tooth crown. Maximum scores for the other bovids and *Giraffa* are between 40-60%. The rhino has a maximum score on any tooth of only 7%, which is substantially lower than that for any tooth in the other animals.

If all hippo tusk fragments are included in this THA calculation, then the average THA score for this animal increases to 34.7%, which is only very slightly greater than 33.9%. However, if any of these fragments belong to the same tooth then the average THA score for this animal could be greater than this value.

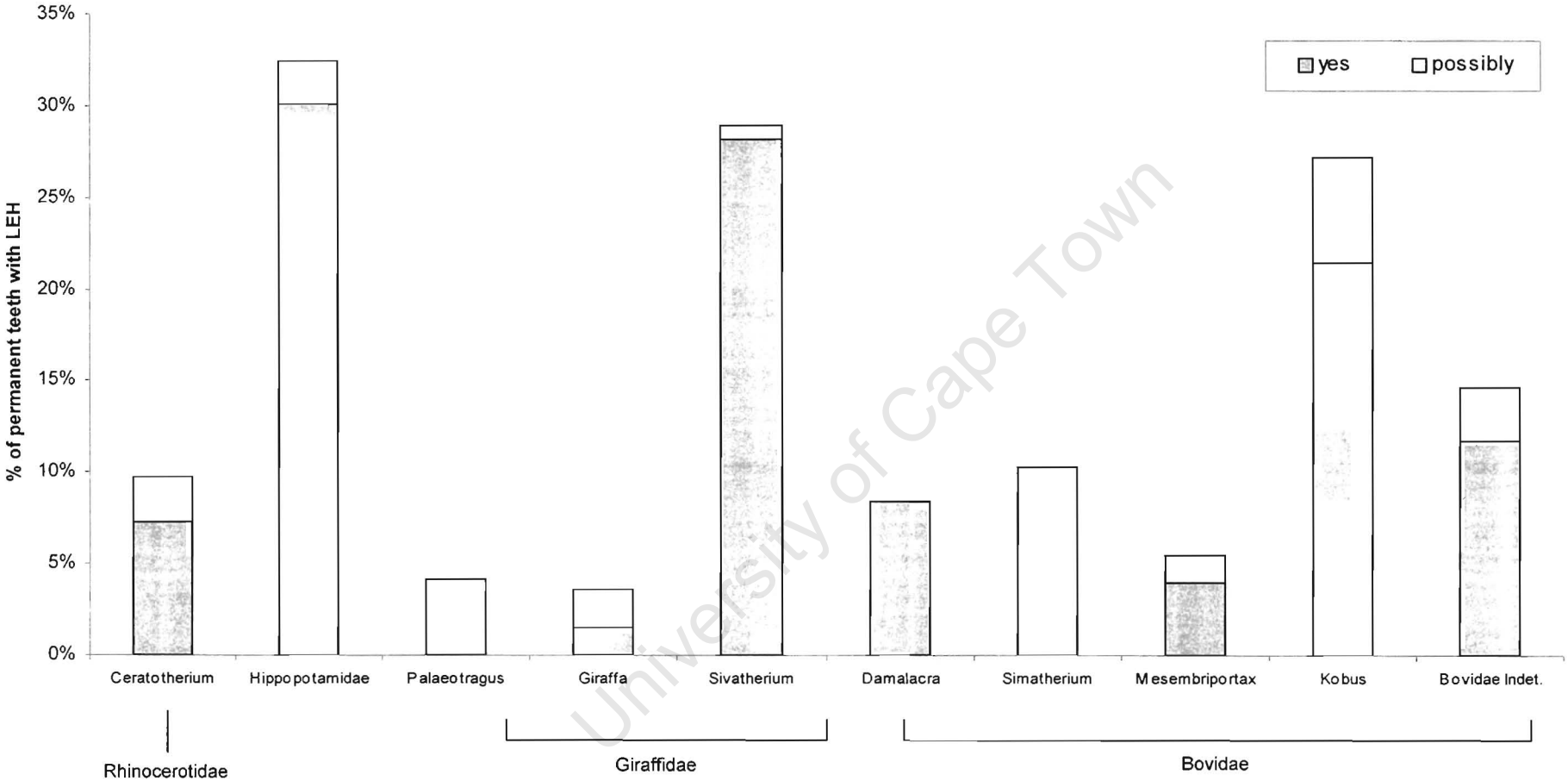

Figure 5.10. Incidence of linear enamel hypoplasia in the permanent teeth of several ungulates at LBW. Numbers in parentheses refer to the numbers of permanent teeth with LEH and the total number of permanent teeth analysed (see Table 5.1). *Ceratotherium praecox* (3, 41), Hippopotamidae (not det.) (58, 196), *Palaeotragus* cf. *germaini* (0, 24), *Giraffa* cf. *jumae* (4, 259), *Sivatherium hendeyi* (433, 1544), *Damalacra* sp. (16, 191), *Simatherium demissum* (12, 116), *Mesembriportax acrae* (6, 152), *Kobus* sp. (9, 42), Bovidae Indet. (8, 68). For the Hippopotamidae, ten small fragments are excluded.

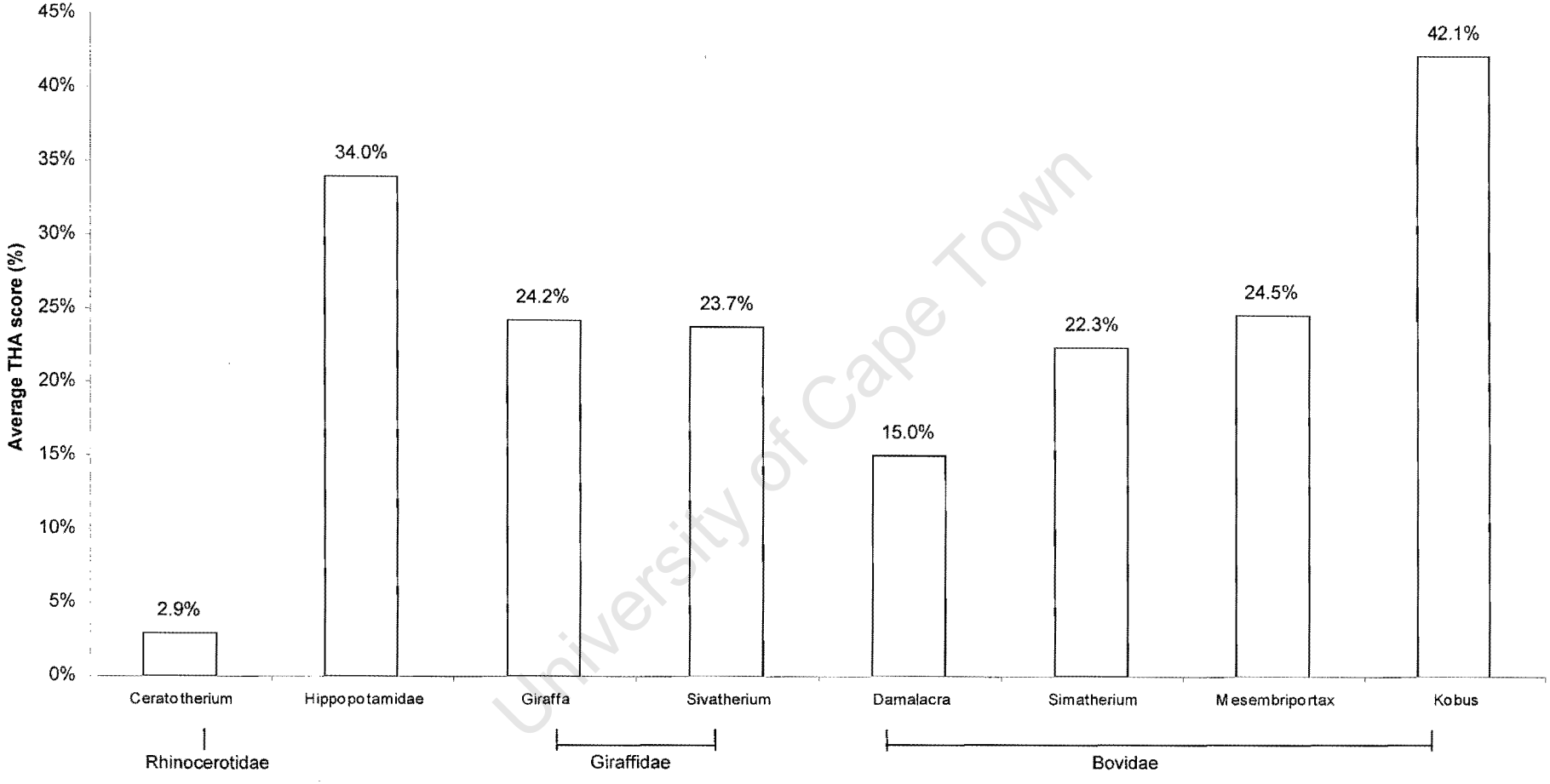

Figure 5.11. Average Tooth Hypoplastic Area scores (expressed as a percentage) for LBW ungulates with linear enamel hypoplasia. Species and numbers of teeth as in Figure 5.10.

Table 5.6. Maximum and minimum individual tooth scores for each animal.

	Minimum THA score	Maximum THA score	Average THA score
Rhinocerotidae			
C. praecox	0.4%	7%	2.9%
Hippopotamidae	1.3%	100%	33.9%
Bovidae			
Reduncini *Kobus* sp.	1.2%	100%	42.1%
Bovini *S. demissum*	1.3%	53.7%	22.3%
Boselaphini *M. acrae.*	5%	48.1%	24.5%
Alcelaphini *Damalacra* sp.	1.4%	41.9%	15%
Indeterminate	32%	100%	72%
Giraffidae			
Giraffa sp.	1.3%	60.5%	24.2%
S. hendeyi	0.4%	100%	22.6%

5.3.2 Skeletal evidence for stress

None of the 244 bones examined show any signs of severe defects, disease, lesions or infections. In most cases only the proximal or distal ends of bones were present so that examination of skeletal defects was restricted to those defects affecting the articular surfaces, such as arthritis of the joints and eburnation[9].

Only one element, a hippopotamus cervical vertebra (PQL 33853), has mild osteophytic outgrowths (Figure 5.12) consisting of an osteophytic ridge on the ventrolateral aspect and another osteophytic spike on the anterior side of the vertebra. Osteophytic growths in vertebrae generally represent a spinal disease known as *spondylisis deformans* rather than arthritis (Rothschild et al., 1993). A single phalanx II belonging to *S. hendeyi* was also found with some very small possibly osteophytic growths (PQL 13169C, not shown). No Harris (stress) lines were observed in any of the nine *S. hendeyi* metapodials that were X-rayed by R. Alexander.

[9] Eburnation results from continually grinding away of the articular cartilage until no cartilage is left and finally the bones rub together to give a polished finish, and which creates pain at the joint.

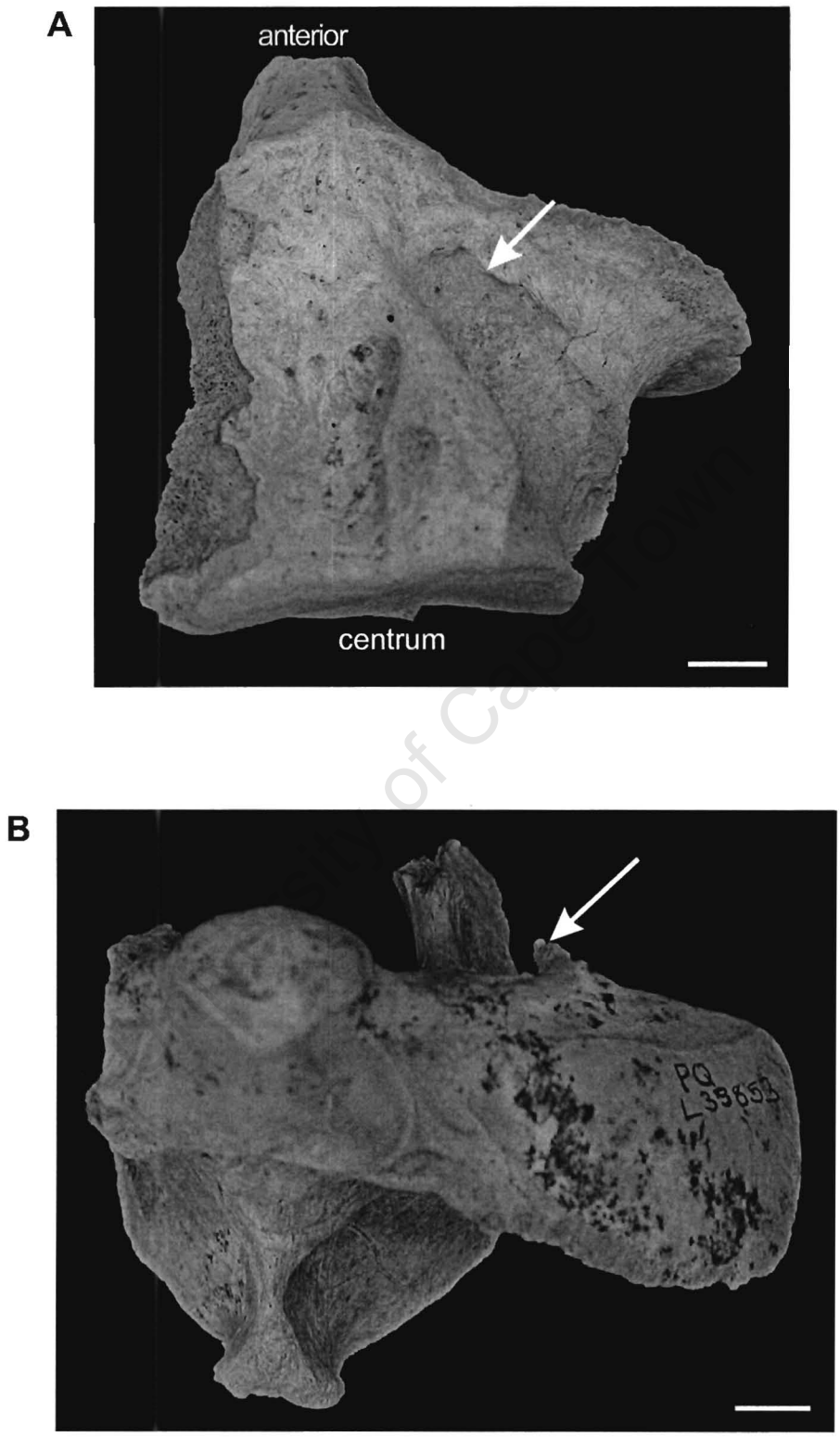

Figure 5.12. A partial second cervical hippopotamus vertebra (PQL 33853) with osteophytic outgrowths. (A) an osteophytic ridge (arrow) on the lateroventral aspect of the vertebra (ventral view shown) and (B) an osteophytic spike (arrow) on the posterolateral side (anterior view shown). Scale bars represent 1 cm.

5.4 DISCUSSION

The lack of evidence for skeletal disease in the ungulates of LBW indicates that the local fauna was relatively healthy. This is further substantiated by the fact that no Harris (stress) lines were found in any of the *S. hendeyi* metapodials that were analysed. However, this does not necessarily imply that no systemic stress was ever experienced, since these lines could be "lost" during bone growth and/or remodeling. Dental defects were however frequently observed and are therefore useful as a tool to understand the health-status of the animal populations at LBW during the Early Pliocene.

Dental defects such as non-linear enamel hypoplasia and irregular dental wear are fairly common, affecting 18.9% of the teeth analysed. Of all the teeth with these defects, most teeth (75.5%) belong to the sivathere, *S. hendeyi* (Table 5.3). Irregular dental wear, although low in number in most animals, is most common and extreme in the Bovidae. The observed concave and step-wear could be the result of malocclusion of the upper and lower jaws in a few individuals only. The odd incisor wear at the tooth neck may however relate to grooming behaviour. McKenzie (personal communication, 1999) has noted this wear pattern in wild bovids. During grooming, as hairs are pulled between the incisors, a wear facet at the neck of these teeth develops. Geophagia[10] and osteophagia[11], techniques employed by extant ungulates to correct mineral imbalances (Langman, 1978; Milewski and Diamond, 2000) may also result in irregular dental wear, if sufficient nutrients are not available in the vegetation. The cause of the non-linear defects and irregular wear therefore remain uncertain.

Deformed teeth were rarely observed and are usually the result of mechanical obstruction during tooth development (Fortelius, 1985). The completely deformed *S. hendeyi* second molar (PQL 62725) and the bovid upper premolars with split buccal surfaces (Figure 5.6A and 5.6E, respectively) are probably the result of a genetic defect as these are known to result in the loss of dental characteristics and even teeth (Fortelius, 1985). The other partially deformed teeth (a sivathere m2 and

[10] Licking the ground or chewing on soil.
[11] Chewing on bones from carcasses in the field.

a bovid m3) (Figure 5.6B-D) are more likely to be the result of mechanical obstruction to the developing tooth crypt.

Linear defects are fairly prevalent in the faunal assemblage at LBW, despite initial reports by Hendey (1981b) indicating that these defects were only present in the sivathere, *S. hendeyi*. LEH was found in all animals examined, except *Palaeotragus* (where only a few possibly defective teeth were found). This latter result may be because of the small sample size examined for this animal, rather than a real absence. Only five deciduous teeth have LEH indicating that the *in utero* period and first few months of life were stress-free in the majority of animals. These defective deciduous teeth belong to the hippo and boselaphine (*M. acrae*) and may be the result of a stressful birth or even a stressful prenatal period in some individuals. LEH associated with stressful birth periods have been reported in a Miocene rhinoceros (Mead, 1999). Further analyses of these defects (such as histological examination of tooth sections to locate a neonatal or birth line could elucidate their causes but because of the low number of affected deciduous teeth (possibly in only five individuals), this analysis was not conducted. In permanent teeth, LEH was observed in almost all tooth types examined (Appendix H). These defects are unlikely to relate to local trauma or inherited conditions in every animal, and hence a more general physiological (systemic) stress is likely to be responsible for the observed defects. The presence of LEH has frequently been interpreted to indicate that affected animals are not only more stressed but also less well adapted to conditions than those without these defects (Goodman, 1991).

27.7% of the defective teeth have more than one linear defect on their crown. This suggests that the stress episodes associated with defects were periodic and of a relatively short duration (i.e. compared to the time it takes for a tooth to develop). More favourable conditions probably prevailed between these stress episodes as defects are separated by enamel with a normal appearance. Several distinct LEH present in the continually erupting hippopotamus tusks indicate that stress periods were not confined to the developing years of an animal's life but that they extended into adulthood. It therefore appears that although each individual stress episode was relatively short (periodic), these stress episodes occurred frequently throughout the

life of the animals. Further support for this is provided by evidence that as many as 5-10 linear defects were observed on the same tooth crown.

The highest incidence of LEH in permanent dentition was observed in the sivathere (*S. hendeyi)* (28%), the hippopotamus (Gen. & sp. not det.) (29.6%) and the reduncines (*Kobus* sp.) (21.4%). LEH as a result of systemic stress can be the result of a number of phenomena, but since nutritional stress is the most commonly reported cause for LEH (Goodman et al., 1980; Goodman and Rose, 1990), initial attempts were made to determine whether the incidence of defects correlated with dietary preference. The diets of the sivathere and reduncine at LBW have not been determined directly, although the hippopotamus is likely to have grazed on riverside grasses. (The diet of the LBW fauna is discussed in Chapter 2, section 2.6 and summarised in Appendix D, while the diet of *S. hendeyi* is explored in Chapter 7). Results indicate that animals with similar diets (e.g. grazing hippopotamuses versus grazing alcelaphines) are not equally affected (Figure 5.10) and there therefore does not appear to be a simple correlation between incidence of LEH and diet. A more general cause for the systemic stress underlying the LEH probably exists. Differences in incidence between animals with similar diets may therefore relate to differences in behaviour and/or tolerance levels for stressful conditions. Thus those animals that are least affected (e.g. the rhino, *C. praecox*) were probably better adapted to conditions than those animals that are more greatly affected (e.g. the hippopotamus). Alternatively, it has been suggested that the rhinoceros teeth from Bed 3aS may have been reworked from the underlying QSM deposit (Klein, 1982), suggesting that this animal lived under different (i.e. possibly more favourable) environmental conditions.

There are two main complications of the current analysis. First, the PPM deposit, from which the teeth originate, together with the underlying QSM deposit is thought to span not more than 0.5 Myr (Hendey, 1981b, 1984). Although deposition of the PPM may be far less than this, this means that several populations of animals, living at different times and under different conditions, could have been analysed. Incidence may therefore not be a good indicator of the health-status of any one population's existence. The second complication to the analysis is that the cause of the observed LEH in each animal, or even in each tooth type, cannot be determined

from the current analysis, i.e. there is no way of determining whether the observed LEH in each animal (or tooth type) is the result of the same stress episode. A general cause for the systemic stress is likely, but there may be a few exceptions. The main aim of this aspect of the study was to determine which animals were affected by pathologies, what the pathologies are and their extent in each population. The cause of the observed linear defects is investigated in detail in Chapters 6-8. THA scores may be more useful in indicating the degree to which animals were stressed. Average THA scores were highest for the hippopotamus and reduncine (*Kobus*) and lowest for the rhinoceros (*C. praecox*). Only three rhino teeth have defects and their low THA scores indicate that even these individuals were only mildly affected.

It is possible that the stress episode responsible for the defects in the rhinoceros at LBW could be attributed to a different phenomenon to that which caused the defects in all or some of the other animals. Mead (1999) reports LEH in Miocene black rhinos (*Teleoceras*) from Nebraska and in one extant rhinoceros (*Diceros bicornis*) skull. He speculates that the defects in the fourth premolars (33% affected) of *Teleoceras* are associated with a stressful calf-cow separation. All extant rhinos exhibit the behaviour of driving the calf away before the birth of the next offspring at a time when the fourth premolar is developing. Perhaps the LEH observed in *C. praecox* at LBW can be attributed to a similar event. However, if the diagnosis of the LEH in Mead's study is correct, then many more rhino teeth should be affected by LEH at LBW. The extremely low incidence of LEH therefore suggests that this defect is probably not associated with calf-cow separation (i.e. Mead's diagnosis of LEH may be incorrect). Mead does caution that his diagnosis is speculative. The single extant rhinoceros skull investigated by Mead, also has LEH on the fourth premolars. This brings to light one of the major constraints of LEH analysis in fossil animals – the lack of comparative databases of extant wild animals. The incidence of LEH in extant ungulates has not been studied, and without such a database, interpretation of defects in the fossil record becomes extremely difficult.

Some animals have a low incidence of LEH but medium to high THA scores (e.g. *Giraffa*) indicating that those individuals that were exposed to physiological stress were exposed for a relatively long period of time. If a general cause of the

LEH is accepted, then two explanations exist as to why some *Giraffa* individuals (for example) are affected severely and others are unaffected. Either these two groups of *Giraffa* (affected and unaffected) lived at different times within the 0.5 Myr time span suggested for the PPM (Hendey, 1981b, 1984); or these LEHs are not the result of a general systemic stress such as nutrition, but rather of a more confined event such as a birth or weaning stress.

The enamel pitting observed in the LBW fauna closely resembles that documented for fluoride toxicosis. In addition, irregular wear, which is also associated with fluoride toxicosis, was observed in some teeth. Since not all bones (or parts of a bone) are equally affected by osteofluorosis (Shupe et al., 1984), the lack of evidence for skeletal pathologies in the LBW post-cranial elements does not necessarily mean that fluoride toxicosis did not occur. It is possible that dental defects are related to high fluoride levels in drinking water. Rock phosphate was available for erosion and reworking in the phosphate deposit at LBW (Dingle et al., 1979) and it is known that rock phosphates contain fluoride in high enough quantities (42 000 ppm) to cause fluoride toxicosis (Moller, 1982). It seems plausible therefore that fluoride may have leached out of the rock phosphate lining the river channel. Perhaps, during wet months, when the river was fast flowing, the fluoride concentrations in the water would be diluted by rainwater. In dry months fluoride would be concentrated and may have reached levels that disrupt ameloblasts during enamel formation. Kierdorf and Kierdorf (1997) suggest that teeth and bones developing under constrained conditions (i.e. winter) are more likely to act as a sink for fluoride, as this is the time when reduced body and skeletal growth occurs. It is virtually impossible however, to determine for certain whether high fluoride levels can be linked to these defects because of diagenesis. (The possible incorporation of fluoride into the apatite of defective enamel is investigated in Chapter 6).

5.5 CONCLUSIONS

In summary, the results presented in this Chapter indicate that

i) almost all the ungulates at LBW were affected with dental defects and that these defects are more prevalent in some animals than in others;

ii) defects (such as linear enamel hypoplasia) are likely to relate to physiological (systemic) stress episodes, which were not responsible for the death of the animals;

iii) these stress episodes were periodic and present throughout development of adult dentition and beyond, and

iv) although a general cause of the stress episode is likely, linear defects do not appear to correlate with diet (i.e. nutritional stress).

In order to fully understand the observed enamel hypoplasia, an understanding of the environmental contexts under which these defects manifested is required (Goodman, 1991). Chapters 6-8 focus exclusively on the enamel hypoplasia observed in the most abundant herbivore from the PPM deposit, namely *S. hendeyi*. In Chapter 6, an analysis of the affected tooth types is conducted, which enables an evaluation of the timing of stress episodes during the juvenile and sub-adult years of life to be made. In order to enhance interpretations stemming from this analysis, the diet of *S. hendeyi* is investigated in Chapter 7. Finally, Chapter 8 further explores the environmental conditions that prevailed during the manifestation of defects in this animal as well as possible behaviours (such as weaning), which may be attributed to some of the observed defects. In addition, possible migration of the less affected animals (such as the rhinoceros) is also investigated.

Chapter 6

ENAMEL HYPOPLASIA IN *SIVATHERIUM HENDEYI*

6.1 INTRODUCTION

This chapter investigates enamel hypoplasia in *S. hendeyi* in detail. 24.6% of *S. hendeyi* teeth have linear defects and 21.3% have non-linear defects (see Chapter 5, Table 5.3). *S. hendeyi* is the dominant herbivore in the fossiliferous Pelletal Phosphate Member at LBW and understanding the underlying cause(s) of the observed defects in this animal will shed light on conditions under which they manifested. First an analysis of the defects in each tooth type is presented. Since only defects that manifest at the same ontogenetic age can be related to the same stress event, it is important to analyse the prevalence, size and position of defects on all tooth types separately. An analysis of the height of the defect from the root-crown junction and its width will provide information on the timing and duration of each stress event, respectively. In this way particular stress periods during development can be determined. The eruption sequence of *S. hendeyi* is also investigated. The second aspect of this study is to investigate the enamel hypoplasia microscopically using both light and scanning electron microscope techniques. An analysis of enamel ultrastructure in the extant giraffe (*Giraffa camelopardalis*) is presented for comparative purposes.

A comprehensive introduction to enamel hypoplasia was given in Chapter 3 and therefore this introduction only provides pertinent information to evaluate the defects in *S. hendeyi*. The size of each *S. hendeyi* tooth type is presented in the following chapter (Chapter 7) together with an assessment of the diet of this animal.

6.1.1 Elucidating enamel hypoplasia in *Sivatherium hendeyi*

The key to interpreting enamel hypoplasia is to have knowledge of the tooth development and eruption sequence of the animal concerned. For extinct taxa, knowledge of the tooth eruption pattern is rarely available and is dependent on the taphonomic situation, preservation state, numbers of complete jaws and comparative

analyses of closely related extant taxa. The tooth eruption pattern in most extant animals is known and therefore attempts to determine the ages at which LEH manifests in fossil animals relies heavily on this knowledge. More important however, is the knowledge of the tooth developmental sequence and timing, which unfortunately is only known for a limited number of ungulates. No studies have reported linear enamel hypoplasia in extant wild animals, other than those associated with fluoride toxicosis (Shearer et al., 1978; Kierdorf et al., 1993, 2000).

A further investigation into fluoride as a contributing factor to the observed LEH was conducted, even though no bone lesions characteristic of fluoride toxicosis were observed in any of the LBW fauna studied in Chapter 5. This was felt to be warranted since i) an association between LEH and irregular wear has been reported in animals ingesting excessive fluorides (Shupe et al., 1984, Kierdorf et al., 1993; Kierdorf and Kierdorf, 1997; Kierdorf et al., 2000), ii) only a few complete post cranial specimens were available for examination and fluorotic lesions may therefore have remained undetected, iii) the dental defects in the Langebaanweg fauna are morphologically very similar to those reported as a result of excessive fluoride ingestion, and iv) seasonal migrations of wild animals can result in intermittent periods of ingestion of fluorides resulting in several linear defects per crown (Shupe et al., 1984), a phenomenon frequently observed in the LBW fauna (Chapter 5).

Although fluoride is present in small amounts within normal enamel and plays an important role in preventing tooth decay and the development of caries, excess fluoride entering during tooth development may result in fluoride toxicosis. Fluoride ions are highly mobile and may also enter the apatite after death of the animal (i.e. during or after fossilisation). Diagenetic addition of fluoride would most likely result in the formation of a fluorapatite over time. Once fluoride ions have entered the hydroxyapatite, they are tightly held in position (LeGeros, 1981) and are not easily lost through diagenesis. There are two main ways to test for fluoride in biological apatites. Ion microprobe analysis detects fluoride concentration in a sample, but cannot detect where the fluoride is situated (i.e. within the crystal lattice or surface-bound). This method is therefore unable to determine whether fluoride has been diagenetically incorporated during fossilisation (and has formed a fluorapatite), or whether it merely adhered to the tooth. Infrared absorption spectroscopy on the

other hand detects the ionic environment (such as interactions between ions) within the apatite structure and can therefore be used to detect the effects of fluorination on ionic interactions as well as to detect fluorapatite (Regnier et al., 1994). Since FTIR was already being used to investigate the structure of normal sivathere enamel, in order to determine the extent of diagenesis (see Chapter 4), it seemed logical to use this method to attempt to determine whether excessive fluoride ions are present in defective enamel, since the effects of fluoride incorporation into enamel apatites are known. Moreover, none of the methods discussed above can differentiate between *in vivo* and post-depositional incorporation of fluoride ions.

Trombe (1972) found that fluoride ions have an affinity for the OH^- site (also the type A carbonate site) and displace all other ions within the crystal lattice. This has the effect of increasing crystallinity and the ultimate size of the apatite crystals as well as decreasing crystal strain and solubility (Kay et al., 1964; LeGeros, 1981, 1991). Crystal size and strain are reflected in the infrared splitting index (PCI) (Sponheimer and Lee-Thorp, 1999a) described in Chapter 4. Okazaki (1983) showed that with increasing degrees of fluorination, the *conformation* of carbonate ions and not carbonate content was disturbed. This conformational change was observed by a shift in the carbonate ions at 875 cm^{-1} (the $\nu 2\ CO_3$ domain) to a lower frequency. (This shift is also observed in fluorapatites (Regnier et al., 1994)). Fourier Transform Infrared analyses were therefore applied to defective *S. hendeyi* enamel and the absorbance spectrum was compared to that of normal *S. hendeyi* enamel (presented in Chapter 4). This analysis should indicate whether alteration in enamel apatite structure and composition contributes to the defective morphology of the tooth crown.

6.1.2 The teeth and eruption sequence of *Giraffa camelopardalis*

Giraffe teeth are characterised by having very rugose[1] enamel (Singer and Boné, 1960, Hall-Martin, 1976a). The dental formula for giraffes is:

$$\text{Deciduous teeth} = \frac{0.0.3.0}{3.1.3.0} = 20$$

[1] Uneven, rough enamel.

$$\text{Permanent teeth} = \frac{0.0.3.3}{3.1.3.3} = 32$$

The deciduous lower dentition of each side of the mouth consists of three incisors (di1, di2, di3), one canine (dc) and three premolars (dp2, dp3, dp4). Only premolars are present in the maxilla (dP2, dP3, dP4). The permanent dentition consists of upper premolars (P2, P3, P4) and molars (M1, M2, M3), whereas the lower dentition consists of incisors (i1-i3), one canine (c), three premolars (p2, p3, p4) and three molars (m1, m2, m3). (Lower case is used for lower teeth and upper case for upper teeth). The canines are bilobed and are separated from posterior cheek teeth (premolars and molars) by a diastema[2]. During chewing, the anterior teeth (incisors and canines) make contact with the maxillary pad. The incisors and canines have a single root, which slopes backwards. Lower cheek teeth have two roots (an anterior and a posterior one) whereas upper teeth have three roots (two lateral and one medial). Both anterior and posterior roots of lower molars and the medial root of uppers have a tendency of fusion into fangs (Singer and Boné, 1960).

The eruption sequence of the extant giraffe (*G. camelopardalis*) is known from two studies, Singer and Boné (1960) and Hall-Martin (1976a), and is summarised in Figure 6.1.

The sequence of eruption for mandibular and maxillary teeth is not identical. In giraffes, the maxillary sequence is less rigid and is not always a simple reversal of the mandibular sequence as is common in ungulates. Since only mandibular *S. hendeyi* teeth were examined, only this eruption sequence will be discussed further.

At birth, the deciduous teeth are in an advanced stage of eruption. Both the deciduous and permanent premolars erupt in a regular succession from posterior (fourth premolar) to anterior (second premolar) (Hall-Martin, 1976b). The permanent molars on the other hand erupt in reverse order from first (anterior) to third (posterior). The eruption sequence of the permanent lower premolars is not rigid and in some reports the second premolar was the first to erupt (Singer and Boné, 1960;

[2] An area of the jaw (between the canine and premolars) lacking teeth.

Hall-Martin, 1976a). The permanent incisors erupt in a regular succession from first (central) to third (lateral). I1 appears during the eruption and maturation of m3 and is always present by the time m3 has completed its growth. I2 appears only after all the molars have erupted and at the same time as the premolars appear. I3 only erupts after all the premolars have erupted. I1 can be completely erupted before di2 and di3 are replaced. The permanent canine is the last tooth to erupt in giraffes and its eruption indicates adulthood.

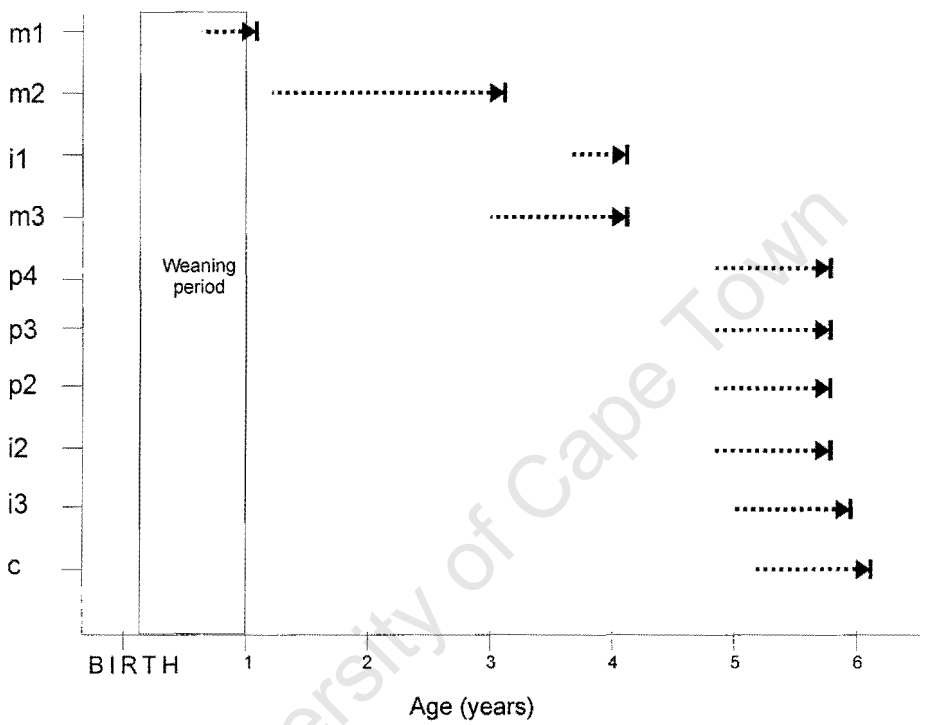

Figure 6.1. The eruption sequence of the mandibular permanent dentition of *G. camelopardalis* (from Hall-Martin, 1976a). Dashed arrows indicate the period of eruption.

Hall-Martin (1976a, 1976b) attempted to assess the chronological age of eruption of giraffe teeth based on available known-age material and cementum growth line counts. He defined the age of eruption as the time when cusps begin to emerge above the alveolar margin. 63 decalcified histological sections through giraffe first molar roots were examined for incremental lines in dentine and cementum (Hall-Martin, 1976b). Dentine lines were clearly distinguishable for counting in only ten sections. Of these none were in agreement with the results of the cementum count or with known ages, however, it did appear that older animals had more lines than younger ones. Numerous difficulties in counting cementum lines were also encountered, mainly due to the high degree of accessory and split lines. Split lines have been reported in other animals (Spinage, 1967, Grimsdell, 1973). Eruption

lines found by Spinage (1967) in *Kobus defassa* (waterbuck) were not found to be a feature in giraffes (Hall-Martin, 1976b). The staining of cementum bands/lines varied between teeth and even between sections of the same tooth, making counting very difficult. Unfortunately few details of tooth development (such as the age at which it commences) are provided in this study, other than that the postnatal development of the first molar is slow.

6.2 MATERIAL AND METHODS

6.2.1 MATERIAL

1759 *S. hendeyi* teeth were examined morphologically for enamel hypoplasia defects (see Chapter 5, Table 5.1 and Appendix H). Care was taken to include a reasonable number of all tooth types (n>45 for each deciduous tooth type and n>85 for each permanent tooth type).

Two sivathere tooth fragments (PQL 44053 and PQL 59598) with linear enamel hypoplasia pitting were analysed by Fourier Transform Infrared analyses and results were compared to those obtained for normal *S. hendeyi* teeth discussed in Chapter 4.

In order to investigate the microstructure of linear defects both histology and scanning electron microscopy was applied. Ten *S. hendeyi* incisor tooth fragments with defective enamel (Table 6.1) were prepared for histological examination (method in section 6.2.2.3) in order to confirm whether defects manifested during the laying down phase of enamel formation and to determine whether the characteristic accentuated Striae of Retzius were visible underlying surface defects. Two of these fragments with defects were badly preserved and were discarded from subsequent analyses. One normal sivathere incisor (PQL 59599) and one normal *G. camelopardalis* incisor (GIR N) were also sectioned. Linear defects that were sectioned include bands of pits and grooves in five defective incisors (PQL 58674, PQL 58741, PQL 58679, PQL 58762, PQL 58763). One tooth (PQL 58672) with a shallow linear groove in the middle of the crown, which was classified as possibly LEH, was also sectioned. Two non-linear defects in tooth PQL 58681 and PQL 58675 were also examined histologically.

Table 6.1. Material used for histology and scanning electron microscopy (SEM) analyses. All accession numbers preceeded by 'PQL' belong to *S. hendeyi*.

Tooth fragment	Defect type	Histological section cut	SEM
PQL 58674, incisor	Band of pits	Longitudinal	-
PQL 58741, incisor	Band of pits	Longitudinal	-
PQL 58679, incisor	Band of pits	Transverse	Transverse
PQL 58762, molar	Deep, wide groove	Longitudinal	-
PQL 58763, molar	Deep, wide groove	Longitudinal	-
PQL 58672, incisor	Shallow, wide groove	Longitudinal	-
PQL 58681, incisor	Diffuse multiple pits	Transverse	Transverse and longitudinal
PQL 58675, incisor	Area missing enamel	Longitudinal	-
PQL 58658, incisor		-	Transverse
PQL 58663, incisor		-	Transverse
PQL 59599, incisor	Normal	Longitudinal	-
G. camelopardalis (GIR N), incisor	Normal	Longitudinal	Transverse

Once the scanning electron microscopy method had been established (method in section 6.2.2.3 below), four *S. hendeyi* incisor tooth fragments (PQL 58679, PQL 58681, PQL 58663, PQL 58658) and one *G. camelopardalis* incisor fragment (GIR N) were examined. Two of the sivathere fragments (PQL 58679 and PQL 58681) were also examined histologically. The enamel prism pattern of one sivathere incisor (PQL 58663) was examined and compared to that of the extant giraffe incisor.

For a comparative analysis of enamel hypoplasia in extant giraffes (*G. camelopardalis*), all giraffe skulls (n = 13) housed at the South African Museum, Iziko Museums of Cape Town, were examined (Table 6.2). Most skulls do not have the full dental set and are missing the anterior incisors and canines. A total of 268 teeth were examined noting their origin (i.e. wildlife reserve/national park or zoo). The reason for this is that animals living in captivity (zoos) may suffer from physiological stress (e.g. nutritional stress), which could manifest as linear enamel

hypoplasia. The estimated age in the table below is based on the presence of deciduous and/or permanent teeth. The tooth types present in each specimen are given in Appendix I.

Table 6.2. Modern giraffe specimens from the South African Museum, Iziko Museums of Cape Town. (WR = wildlife reserve, C=captive (zoo) animal).

Specimen number	Origin	Estimated age
ZM 39558	Villiersdorp (C)	Juvenile
ZM 39204	Safariland, South Africa (WR)	Juvenile
ZM 36851	Unknown	Sub-adult
ZM 39795	Safariland, South Africa (WR)	Sub-adult
ZM 35365	Unknown	Sub-adult
ZM 33540	Unknown	Sub-adult
ZM 39692	Witvlei, Namibia (WR)	Adult
ZM 35363	Unknown	Adult
ZM 36655	Tygerberg Zoo (Z)	Adult
ZM 35364	Unknown	Adult
ZM 36654	Phalaborwa (WR)	Adult
ZM 37058	Unknown	Adult
ZM 17176	Northern Zimbabwe (WR)	Adult

6.2.2 METHODS

The procedure used for the identification and classification of defects and the methods used for Fourier Transform Infrared analysis were outlined in Chapter 5 (section 5.2.2) and Chapter 4 (section 4.2.2.1), respectively. Defect widths and THA scores for *S. hendeyi* teeth were also presented in the previous chapter. The following additional methods were used to analyse dental defects in *S. hendeyi* and *G. camelopardalis*.

6.2.2.1 Additional measurements

The height from the root-crown junction to the base of each defect on each tooth as well as the distance between linear defects were measured in the same manner as width measurements in Chapter 5 (i.e. in the mid-region of the anterior cusps). The position of each defect on the tooth crown reflects the age at which the defect manifested; the width of each defect reflects the duration of the stress

episode, and the distance between defects reflects the time lapsed between stress events. These three measurements were therefore used to elucidate the possible causes of the systemic stress episodes in each tooth type. Unfortunately in the absence of knowledge about the monthly increment of enamel in the extant giraffe, the time lapsed between stress periods and the duration of stress episodes are expressed in millimeters of enamel.

In order to determine the distribution of linear defects on *S. hendeyi* teeth, the percentage of defects on each third of the tooth crown was calculated by dividing the average unworn crown height of each tooth type into three equal regions (a cervical third, a middle third and an occlusal third) as in Goodman and Rose (1990). The midpoint of each defect was used in this analysis and was calculated by adding half its width to the height measurement from the root-crown junction. This analysis provides a good determination of the general distribution of defects over the tooth crown.

For a more detailed analysis and in order to pinpoint more accurately the age at which defects manifest, the height of linear defects was analysed further. The percentage of defects in each 2 mm of the tooth crown was calculated and peak heights at which defects occur determined. (For example, a tooth with an average unworn height of 30 mm was divided into fifteen 2 mm categories and the percentage of defects in each 2 mm category was determined and plotted).

Average measurements for defects are reported together with standard errors and number of defects (n) as follows (mean ± std. error, n). The incisors, i1, i2, and i3 could not be identified as to their position in the jaw (see Chapter 7, section 7.2.2.1) and are therefore grouped together as "incisors". In addition, a sample of first and second mandibular molars could not be sorted based on their buccolingual and anteroposterior measurements (see Chapter 7, section 7.2.2.1) and these teeth have therefore been excluded from all analyses, except for the overall incidence of defective teeth.

6.2.2.2 Projected Tooth Hypoplastic Area score analysis

An overall Tooth Hypoplastic Area (THA) score for *S. hendeyi* (reported in Chapter 5, section 5.3.1.1) was calculated by dividing the defect width by the crown height of the tooth. This score will be referred to here as the actualistic THA score. The THA score method originally developed by Ensor and Irish (1995) used two-thirds of the unworn crown height [3] to calculate the percentage of tooth crown that is defective. Since the sample size for *S. hendeyi* teeth is large, average unworn crown heights for each tooth type could be determined and are reported in Chapter 7, Table 7.3. The crown heights of all defective teeth were measured and since most of these teeth are not worn to two-thirds of the unworn crown height, the original method of Ensor and Irish (1995) was adapted as follows. A projected THA score that takes the observed occlusal wear of each tooth into account was calculated by multiplying the width of each defect by a height index. A maximum index of one was used throughout. The formulae for calculating the actualistic and projected THA scores are summarised below.

$$\text{Actualistic THA score} = \frac{\text{Width of defect}}{\text{Actual crown height}}$$

$$\text{Projected THA score} = \text{Width defect} * \text{height index} \qquad \text{where,}$$

$$\text{height index} = \frac{\text{Average unworn crown height}}{\text{Actual crown height}}$$

This projected THA score thus represents a minimum THA score for each tooth, whereas the actualistic THA score represents the actual observable THA score (i.e. the percentage of defective crown that can be observed directly). Average projected and actualistic scores per tooth type are compared and used for inter-tooth comparisons. For canines the THA score is least accurate because of the large difference in the size of the two lobes of this tooth. The slight difference in unworn crown height between buccal/labial and lingual surfaces is believed to be insignificant

[3] This was done to take occlusal wear into account.

in this analyses considering that average THA scores for each tooth type are calculated.

A potential constraint in comparing defect widths in different tooth types is that the apparent duration of the stress episode (indicated by the width of the defect and the THA score) may be overestimated for tooth crowns that develop faster (Ensor and Irish, 1995). Without knowledge of the monthly increment of enamel in each tooth type of the giraffe, the determination of the THA analysis and the duration of stress episodes in each tooth type is an estimate at best.

6.2.2.3 Microscopy

Histology

Histological sections were made according to standard procedures (Chinsamy and Raath, 1992). Teeth were embedded in araldite resin (EC103) with hardener (HY951) (resin: hardener, 3:1). The samples were placed in a vacuum for 4 minutes to remove bubbles and then placed in cold water overnight to prevent overheating during the hardening process. The resin block was then cut, either longitudinally or transversely, to expose the defect. The block was prepared for sectioning by grinding the selected surface on sandpaper of decreasing roughness (320, 600 and 1200 grit size). This surface was then polished using Struers OP-U suspension fluid to remove all scratches and the resin block glued, using a resin adhesive (Epotek), to a frosted histological slide. A section of approximately 2 mm was cut on a Buehler (Isomet 11-1180) low speed saw using a diamond-impregnated blade. The section was then ground in the same way as the resin block. By periodically viewing the section during the grinding process an optimal thickness was reached when light just penetrated through the section. After polishing, the sections were viewed on a standard bifocal petrographic microscope under non-polarised and/or polarised light. Most teeth were cut longitudinally in a buccolingual direction (Table 6.1).

Incremental lines were counted at 4x and 10x magnification since striae are more easily visible at low magnifications (Hillson, 1986).

Scanning Electron Microscopy

In order to optimise the scanning electron microscopy (SEM) method for fossil teeth, several SEM methods were tested on enamel fragments. Before etching, fragments were either treated with Bouins solution for 6 hours (the standard method for preparing modern material for SEM analysis) (S. Marshall, personal communication, 2000) or left untreated (Hoffman et al., 1969). After this initial preparation, fragments were embedded in araldite resin (as recommended by Martin and Wahlert, 1999) and etched in a range of HCl concentrations (2-7%) for various periods of time (0-30 seconds). Optimum results were obtained by embedding the untreated tooth fragment in resin and etching in 7% HCl for 3 seconds (the method recommended by Martin and Walhert, 1999). This method allows for the selection of a precise area for analysis, as the resin block can be accurately cut to expose the defects. To avoid a methodological bias, the same methodology was applied to both fossil and modern teeth. The method used is outlined below.

1. Embed tooth in araldite resin as for histological analyses,
2. Cut the resin block to expose the required surface/defect,
3. Grind away any excess resin and tooth enamel so that a small resin block is produced that fits onto the SEM stub. (Typically these were approximately 4 mm by 4 mm),
4. Polish the surface of interest as for histological sections,
5. Etch the specimen in 7% HCl for 3 seconds,
6. Mount the specimen on a SEM stub,
7. Gold coat and view the specimen according to standard SEM procedures. A JSM 5200 scanning electron microscope was used and specimens were viewed at a working distance of 20 or 48 mm at 15-25 kV (kilovolts).

6.2.2.4 Statistical analyses

All statistical tests were performed on Statistica (version 6.0). Mean values and standard errors are reported throughout this Chapter. Where Student's t-tests are performed these are two-tailed tests for independent samples. Other statistical tests (one-way ANOVA, chi-squared) are also used and in each case the relevant statistics are given. For one-way ANOVA analyses, normal distribution of data was first tested and if necessary the data was transformed.

6.3 RESULTS

Enamel hypoplasia is prevalent in *S. hendeyi* with an overall incidence (percentage of defective teeth) of 46%. Except for deciduous incisors, where sample size is small, it occurs in all tooth types and affects both permanent and deciduous teeth (Figure 6.2). Deciduous teeth only have non-linear enamel defects. The percentage of deciduous teeth with defects ranges from 6.3% to 29.4% in dp3 and dc respectively, with an average prevalence in deciduous teeth of 19.1%. Permanent teeth have both linear and non-linear defects and the overall incidence of defects ranges from 40.4% (in p2) to 74.8% (in m3). Non-linear defects in permanent dentition reach a maximum incidence of 57.8% (in m3) and a minimum incidence of 27.8% (in p2), whereas linear defects range between 19.8% and 34.8% in p2 and m3s respectively. Actual numbers of teeth affected for each tooth type are given in Appendix J. There is a strong correlation between linear and non-linear defects with 69% of teeth with linear defects also having non-linear defects. Some teeth have non-linear defects closely associated with linear defects (Figure 6.3). The incidence and morphology of each defect is described below. The results of histological and SEM analyses are given in section 6.3.4.

6.3.1 Non-linear enamel hypoplasia in *S. hendeyi*

Non-linear enamel hypoplasia was commonly observed in all tooth types (except di). Single pits and areas missing enamel (aplasia) are the most prevalent defect in deciduous teeth, whereas multiple pits are the most common defect type in permanent teeth (Appendix J).

6.3.1.1 Enamel aplasia (areas missing enamel)

Morphology: Areas missing enamel are typically irregular in shape (Figure 6.4) and average 4.9 mm ± 0.4 mm (high) by 4.3 mm ± 0.4 mm (wide) (n=97). A few caries-like areas (with rough edges) were also found on the labial surface of anterior teeth (Figure 6.4C). Defects are largest in the largest tooth type, the third molar. Seldom is there a corresponding area of aplasia at the same height on the opposite tooth surface. According to Goodman and Rose (1990) enamel aplasia may occur as wide grooves that expose underlying dentine. Only ten wide deep grooves (all of which are in molars) were found in the *S. hendeyi* collection comprising 1759 teeth. As these grooves are linearly arranged across the tooth crown, they have been

included in the linear enamel hypoplasia analysis, even though they expose underlying dentine.

Incidence: Enamel aplasia was observed in all tooth types, affecting both permanent and deciduous teeth (Figure 6.4E). The incidence in deciduous teeth is statistically different to that observed in permanent teeth using a Chi-squared test ($p<0.005$, $x^2 = 10.64$, df = 1). Dp3 have the lowest incidence of 4% while 10-15% of dp2, dp4 and dc's are affected with this defect. In the permanent teeth, the m3's have the highest incidence (11%) compared to less than 5% in the other permanent tooth types.

Distribution: In deciduous canines, enamel aplasia is located only on the posterior lobe of the tooth and neither tooth surface (labial or lingual) has significantly more defects than the other. Only one tooth has this defect on both sides of the same lobe. In dp2s, 60% of the defects are on the buccal surface while in dp4s all these defects are located on the lingual side of the crown. The position of this defect on any deciduous tooth crown is highly variable, however on average they are higher in dp4s than in dp2s.

In third molars 73% of the areas missing enamel are located on the middle cusp and the same percentage are present on the lingual surface of this tooth. These defects are on average large (62.2 mm^2) and most occur on the lower third of the tooth crown. The sizes and positions of these defects vary considerably in each permanent tooth.

6.3.1.2 Isolated pits

Morphology: The morphology of single pits (that do not expose underlying dentine) is consistent, having rounded edges and typically being very small (6.65 $mm^2 \pm 1.0$ mm^2, n=229). Some larger pits with thin enamel (12 in total) were recorded in incisors, canines and third molars (Figure 6.5A). By definition these were classed as single pits as they did not expose underlying dentine but may however represent mild enamel aplasia.

Incidence: Isolated pits are present in both deciduous and permanent teeth and are most prevalent in the permanent third molar (20%), canine (18.6%) and deciduous second premolar (17%)(Figure 6.5B). The incidences of this defect in the other mandibular teeth are less than 10%.

Distribution: In deciduous canines, single pits are more prevalent on the lingual surface (67%), whereas in deciduous premolars, 81% of the defects are on the buccal/labial surface of the tooth. Their locations on tooth surfaces are highly variable.

In the permanent molars, canine and incisor this defect is much more prevalent on the buccal/labial surface of the tooth crown (>88% of these defects occur on this surface of the tooth, n= 122), whereas in the permanent premolars almost half of the defects occur on the lingual surface (46%, n=37). Defects in this tooth are located on both anterior and posterior lobes, with the posterior lobe having slightly more pits. In the third molar they are most common on the middle and posterior cusps and least common on the anterior cusp. In the permanent incisor single pits are all located on the labial surface of the tooth. These pits are located at variable heights on the tooth crown.

6.3.1.3 Multiple non-linear pits

Incidence and morphology: Multiple pits were classed as either diffuse or tight (i.e. close together) (Figure 6.6). Since tight pits were not arranged linearly around the tooth they were not considered linear defects and are included here, even though these pits were as close to one another as those in linear bands. Diffuse pitting can occupy a large portion of the tooth crown whereas tight pitting typically occurs in small patches. The incidence of teeth with tight multiple pits is low (<6% in any tooth type) compared to diffuse pitting (<50%) (Appendix J). In deciduous teeth only the canine has diffuse pitting (7.8%), whereas all permanent tooth types have both types of multiple pits (Figure 6.6). The incidence in these teeth ranges from 11.7% (m1) to 48.2% (m3) with the highest incidence (>40%) in m3 and p4.

Distribution: Only four deciduous canines have diffuse pitting, most of which were located on the posterior lobe, between 3 mm and 8 mm from the base of the tooth. In the first and second molars multiple pits are present on both cusps and on either side of the tooth. These patches of pits are all within 10 mm of the base of the tooth. Only a few teeth have multiple pits at a similar height, size and cusp on both sides of the same tooth. 74% of the m3s with this defect type have the defect within 2 mm of the base of the crown, but the maximum height of these defects is recorded at 28.2 mm, about two-thirds of the total unworn crown height. In incisors this type of defect typically occurs in the middle of the crown and these areas are of variable sizes. In canines, multiple (non-linear) pits are only slightly more common on the posterior lobe and most (~76%) occur between 6 mm and 15 mm from the base of the crown. In second and third premolars this defect occurs equally on both lingual and labial surfaces, whereas in the fourth premolar 65% of these defects occur on the lingual surface. These defects occur at similar heights in each premolar. In p2, average height of the defect from the base of the crown is 7.6 mm ± 0.5 mm (n=53), in p3 it is 10.5 mm ± 0.9 mm (n=79) and in p4s the average height is 8.7 mm ± 2.5 mm (n=61). A one-way ANOVA showed that the results for each premolar are statistically different ($p<0.05$, $F=23.23$, $df=2$).

6.3.1.4 Short or oblique grooves

The morphology of short oblique defects is fairly consistent (Figure 6.7) and they occur on both buccal/labial and lingual tooth surfaces. The greatest incidence of short grooves in any tooth type was found in the first and second molars (~16%). Less than 6% of the other tooth types have this defect. Short grooves occur at variable heights and on both anterior and posterior cusps of the molars. In the deciduous dentition, only canines have short grooves and these are very rare (<2%).

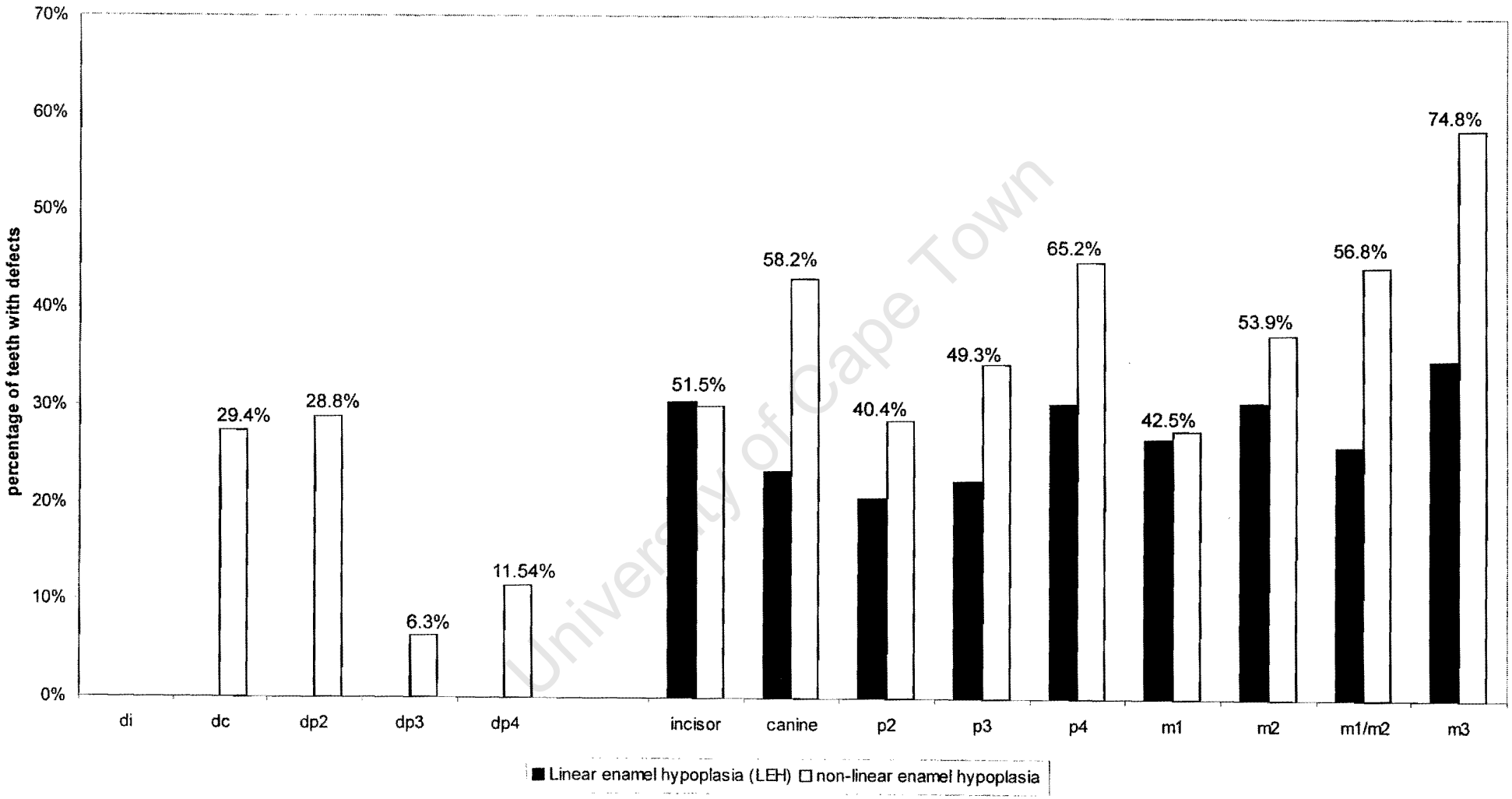

Figure 6.2. Percentage of defective *S. hendeyi* teeth with linear and non-linear enamel hypoplasia. The percentages above the bar indicate the combined incidence of enamel hypoplasia in each tooth type.

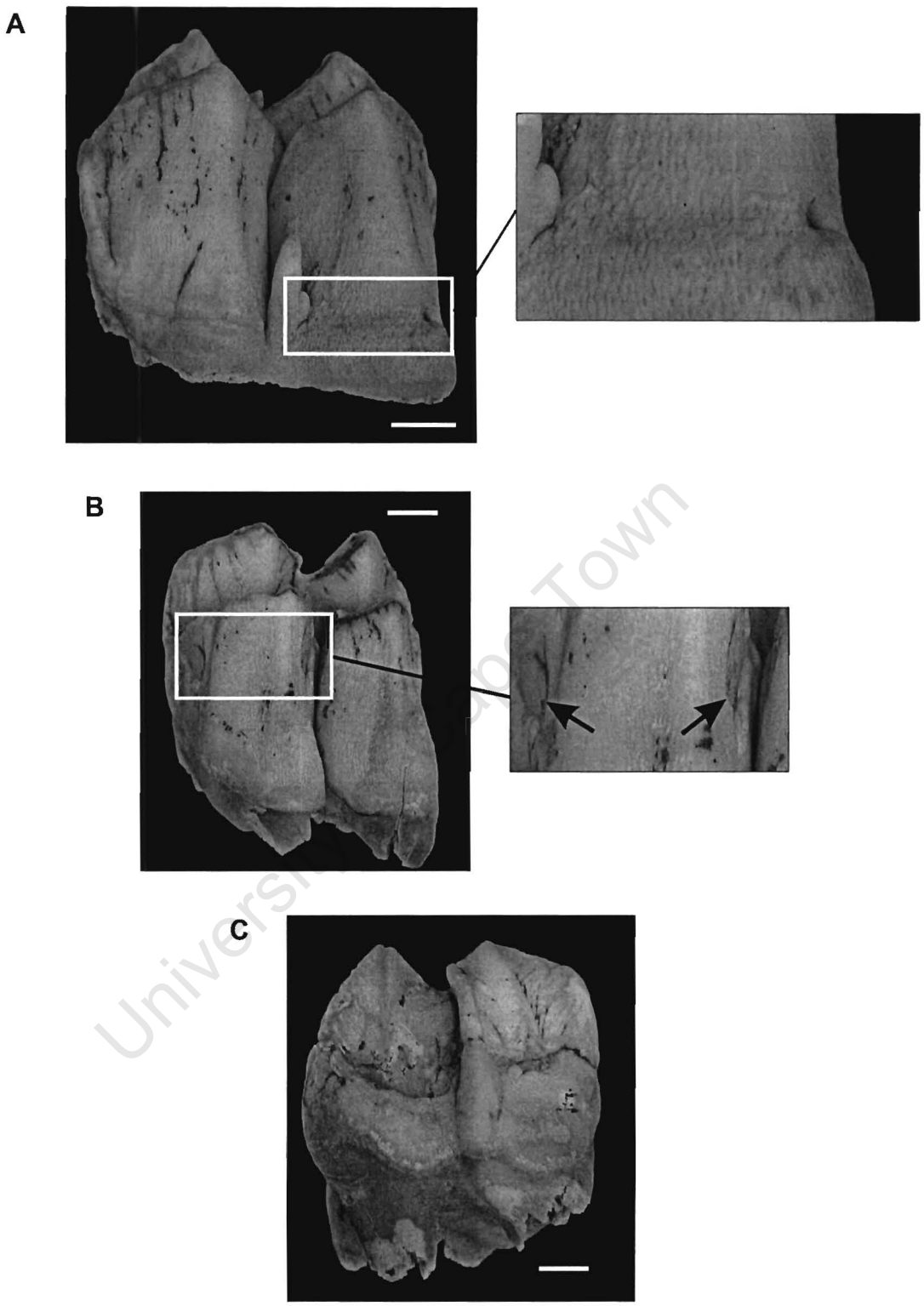

Figure 6.3. *S. hendeyi* teeth with linear and non-linear enamel defects at similar heights on the tooth crown. (A) PQL 44916 with a groove leading into/from a small area missing enamel. (B, C) a molar (PQL 58781) with three single pits on buccal surface (B) (arrows in inset indicate two of these pits) and a deep wide groove at a similar height on the lingual surface (C). Scale bars represent 1 cm.

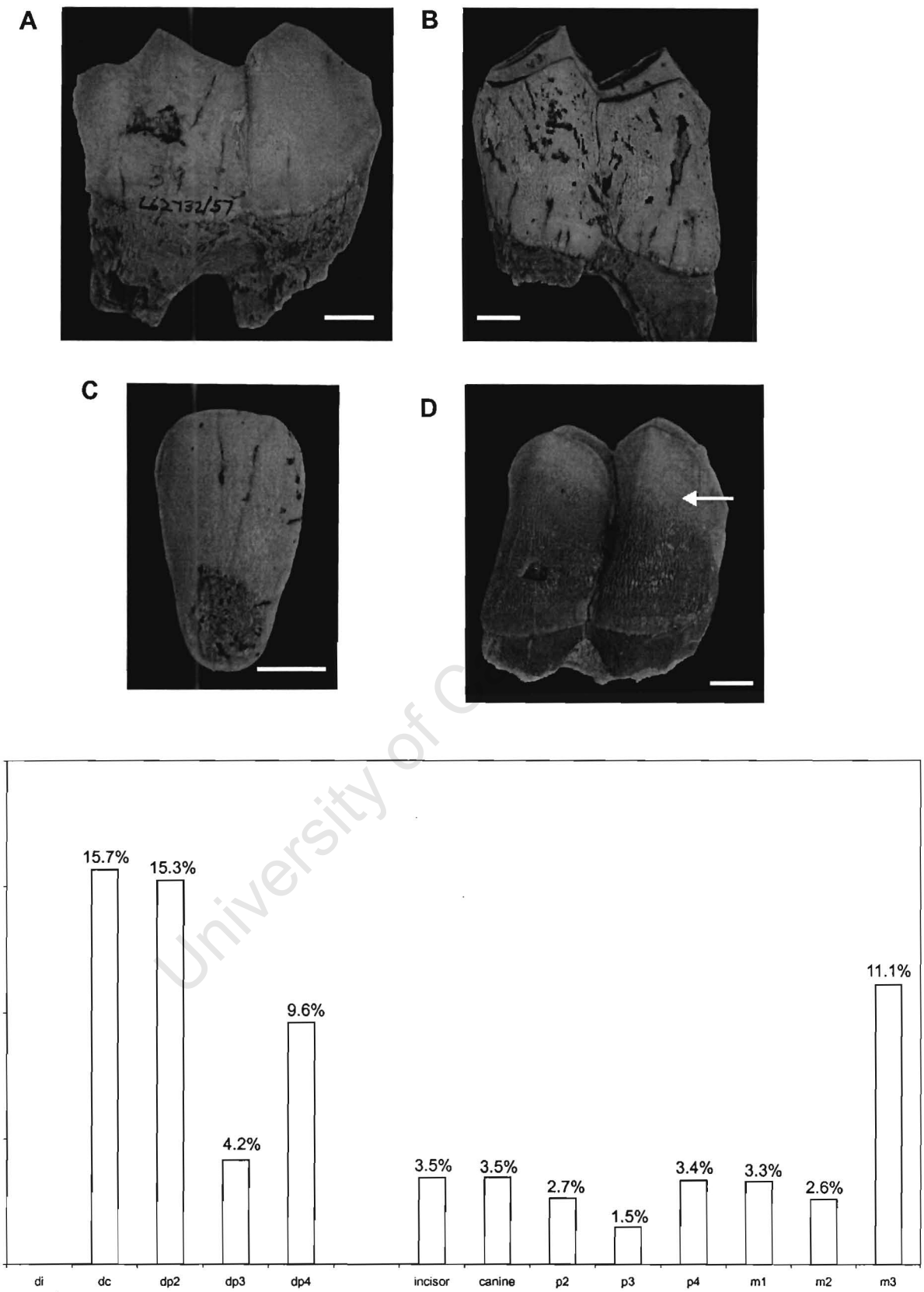

Figure 6.4. Enamel aplasia in *S. hendeyi* mandibular teeth. (A) Lingual surface of a molar (PQL 62732/57) showing an irregular area missing enamel, (B) buccal surface of a molar PQL 44941), (C) a caries-like defect in an incisor (PQL 40066), and (D) a buccal defect on an unmineralised molar crown (PQL 62738/50). Arrow indicates the mineralisation front. Scale bars represent 1 cm. (E) Percentage of teeth with enamel aplasia.

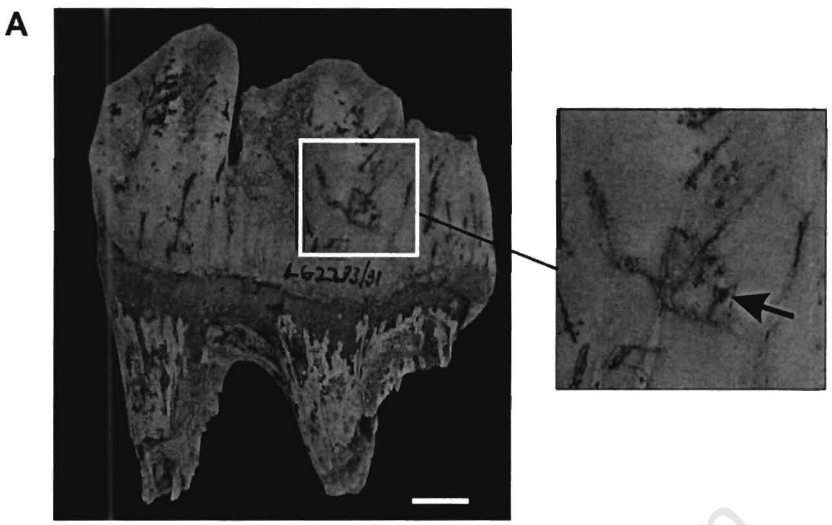

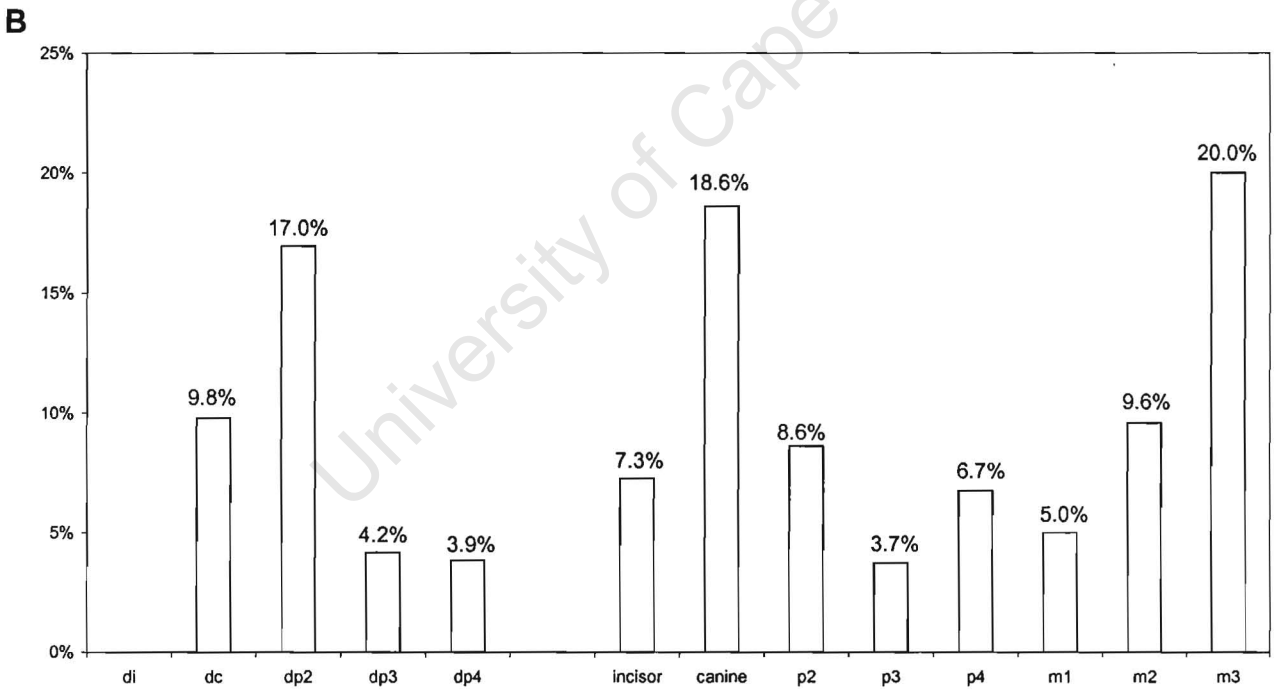

Figure 6.5. Isolated single pits in *S. hendeyi* mandibular teeth. (A) a shallow pit (arrow in inset) on the lingual surface of a third molar (PQL 62233/31). Scale bar represents 1 cm. (B) Percentage of teeth with single pits.

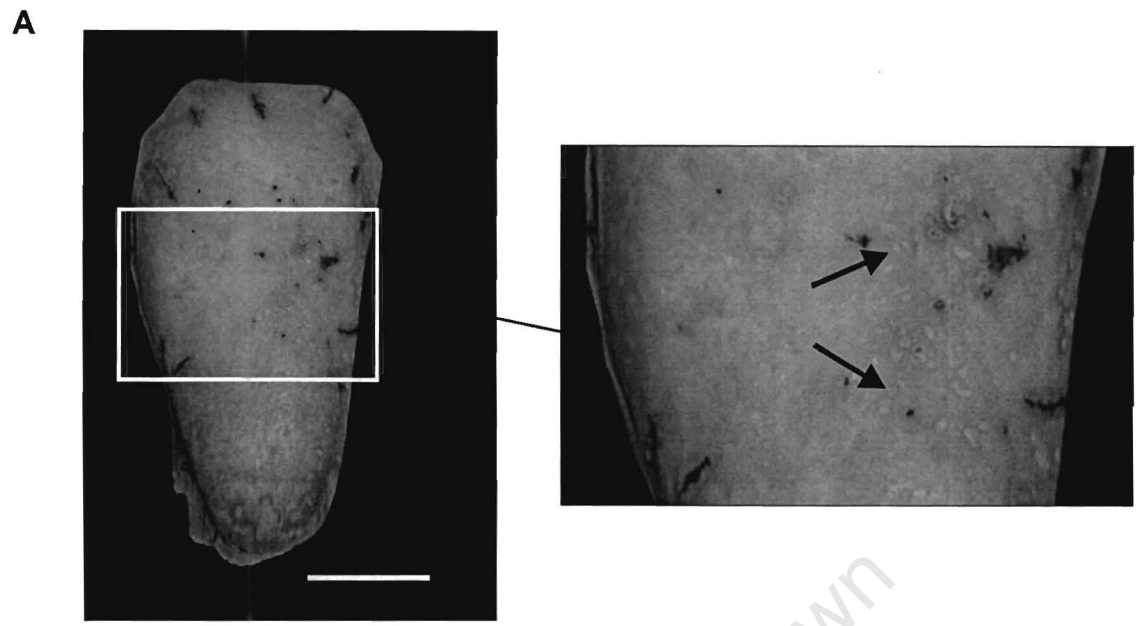

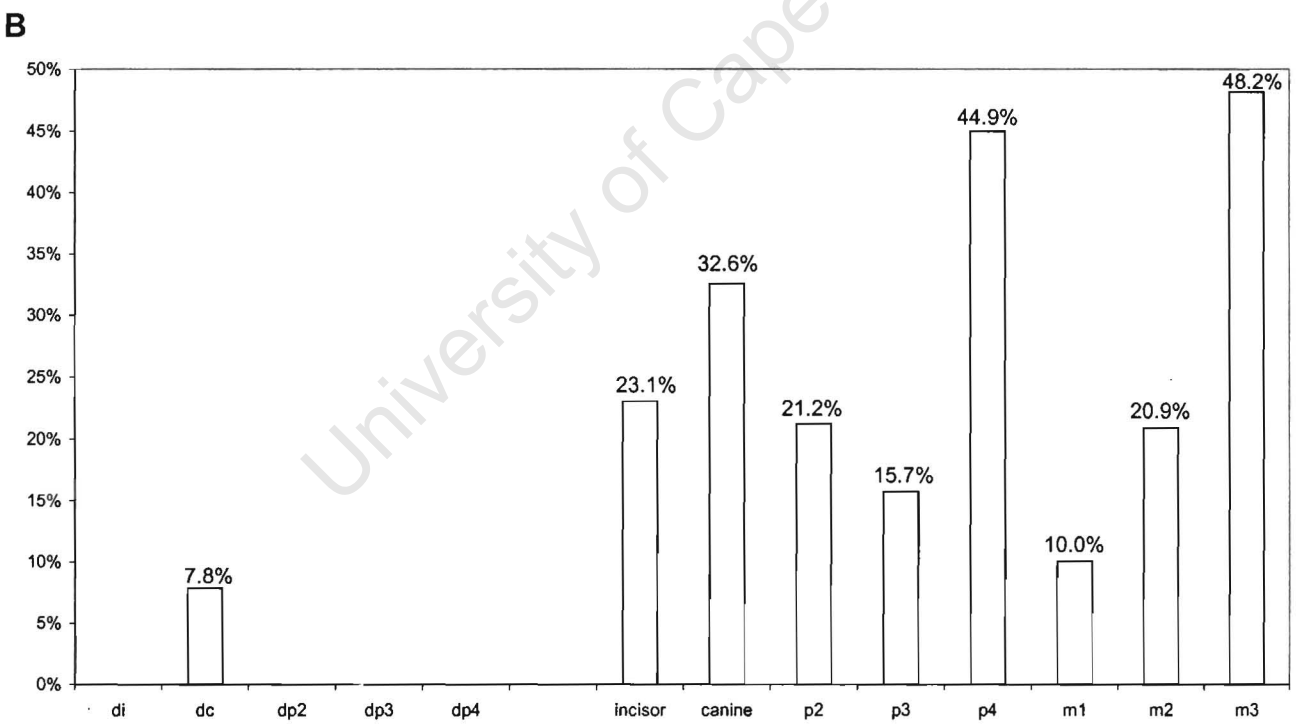

Figure 6.6. Multiple non-linear pits in *S. hendeyi* mandibular teeth. (A) incisor (PQL 44139) with multiple pits (arrows) on labial surface. Scale bar represents 1 cm. (B) Percentage of teeth with defects.

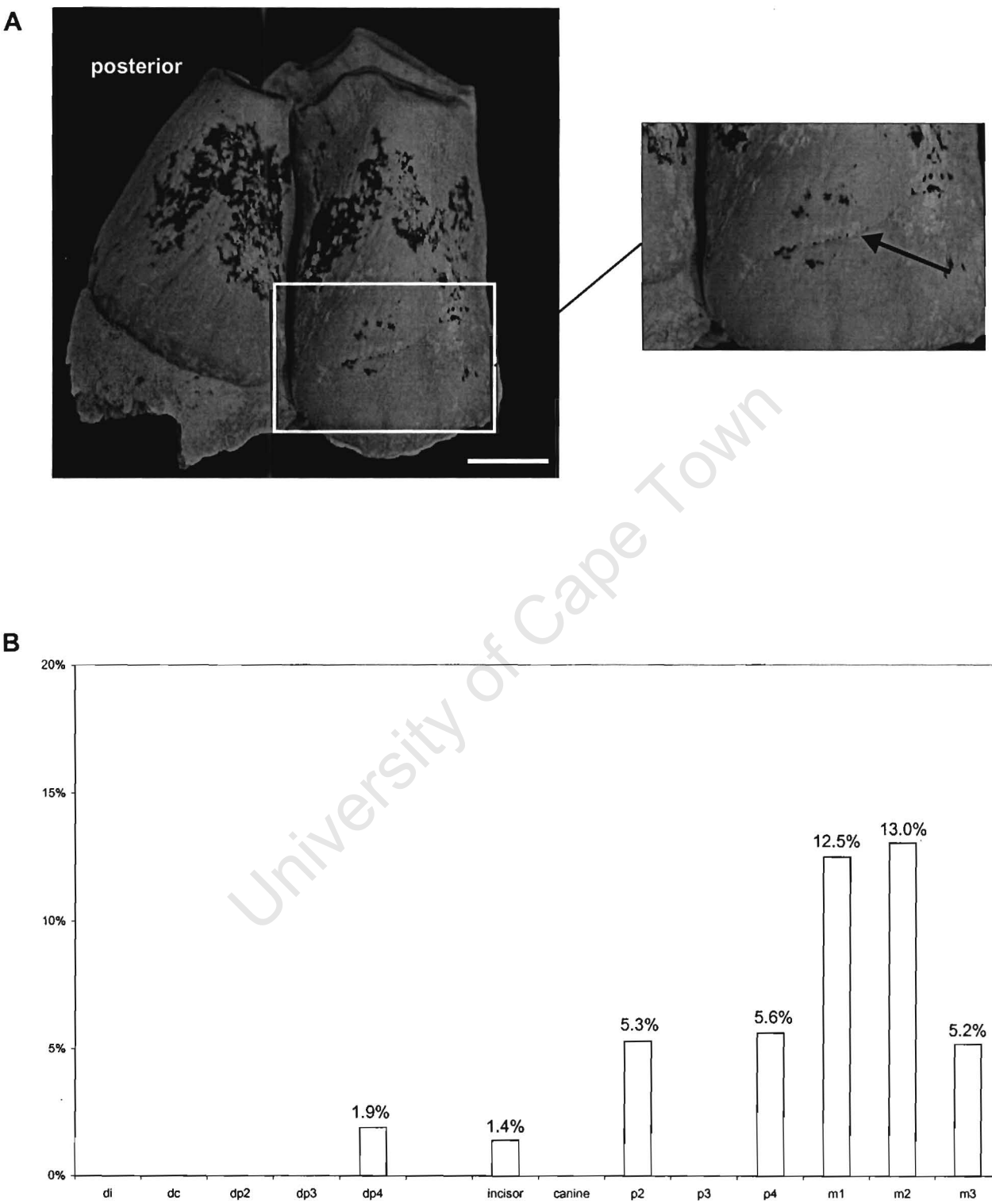

Figure 6.7. Non-linear short grooves in *S. hendeyi* mandibular teeth. (A) a third molar fragment (PQL 62733/49) with anterior cusp missing. Arrow indicates a short oblique groove on the buccal surface of the middle cusp. Scale bar represents 1 cm. (B) percentage of teeth with short grooves.

6.3.2 Linear enamel hypoplasia in *S. hendeyi*

6.3.2.1 Gross morphology

Bands of pits are rarely reported in the published literature yet they are the dominant LEH type (~ 80%) in *S. hendeyi.* A close association between grooves and bands was sometimes observed, with either pits being present within a groove or grooves running into bands on one part of the tooth crown. The occurrence of the grooves compared to bands is however different in each tooth type (Figure 6.8). Grooves are particularly common in the first molars (~67%) and about half of the second molars have this type of LEH. In the other permanent teeth, less than 20% of the defects are grooves. Grooves are typically narrow. In multiple t-tests applied to each tooth type, grooves are significantly narrower than bands of pits in all tooth types ($p<0.05$), except p2 and p3. (Appendix K gives the t-statistic, probability value and degrees of freedom for each tooth type). In ten teeth extremely deep wide grooves that expose the underlying dentine are present running circumferentially around the tooth (Figure 6.9). These defects may also be considered enamel aplasia. The width of LEH defects is discussed in more detail below (section 6.3.2.4).

The morphology of bands of pits is similar in all tooth types (Figure 6.9C-F). These pits are small, close together and are arranged linearly across the tooth surface. The size of the individual pits within each band are however not uniform throughout the band's width (Figure 6.10). Some bands have large pits towards the base of the band and others have smaller pits in this region. This difference in pit size relates to the number of ameloblasts that are disrupted, so that larger pits indicate more disruption compared to smaller ones and may indicate whether the stress episode started more severely (or more abruptly) than it ended.

6.3.2.2 Incidence and distribution of linear enamel hypoplasia

The percentage of *S. hendeyi* teeth examined with linear enamel hypoplasia (LEH) is 24.7 %. However, only one deciduous tooth (dp4) was recorded as possibly having a linear defect, whereas all permanent tooth types have this defect. The incidence in the permanent dentition alone is 28.3%. The prevalence of this defect in the molars and incisors (~30%) is higher than that in the premolars and canines

(~23%) although many p4's are affected (see Figure 6.2). The lowest incidence in any tooth type was 19.9% (p2). A large number of first molars are possibly defective.

The distribution of linear defects over each tooth surface was highly variable. Only 34.2% of the teeth with these defects have defects on both the buccal/labial and lingual surface. In teeth with linear defects right around the crown, the defects on the lingual surface are on average about 1 mm lower (0.2 ± 0.2 mm, n=163) and 1.0 mm ± 0.3 mm (n=163) narrower than linear defects on the buccal/labial surface. Single lingual defects (i.e. without corresponding buccal/labial defects) were less frequently observed (in only 2.5 % of teeth).

6.3.2.3 Tooth Hypoplastic Area scores

Average projected Tooth Hypoplastic Area (THA) scores indicating the minimal THA score for each tooth type are presented in Table 6.3 together with actualistic THA scores calculated previously (Chapter 5). Projected scores range from 0.03 (i.e. 3%) in m1 to 0.4 (~40%) in p2s and the average score for *S. hendeyi* is 0.24. That is on average defective teeth have ~24% of the tooth crown covered by disrupted/disturbed enamel. The observed actualistic scores are greater than projected (minimum) THA scores as expected.

Table 6.3. Average projected and actualistic Tooth Hypoplastic Area scores for *S. hendeyi*.

Tooth Type	Actualistic THA	Projected THA
Incisors	0.35	0.34
Canines	0.37	0.34
p2	0.41	0.39
p3	0.31	0.26
p4	0.33	0.28
m1	0.03	0.03
m2	0.08	0.08
m3	0.20	0.19
AVERAGE	**0.26**	**0.24**

There is a tendency for anterior teeth to have larger projected scores than posterior teeth. If viewed in order of tooth eruption, the later erupting teeth have progressively higher scores than earlier erupting teeth (Figure 6.11). A one-way ANOVA indicates that the projected THA scores are statistically different ($F = 15.143$, $p<0.001$, $df = 7$).

6.3.2.4 Widths of defects and the duration of stress episodes

The width of each linear defect in each tooth type reflects the duration of the stress events and is reflected in the THA scores (see section 6.3.2.3). The average maximum and minimum widths of both bands and grooves for each tooth type are shown in Figure 6.12. Grooved defects are on average 1.5 ± 0.2 mm (n = 170) wide while bands of pits are substantially larger, at 7.2 ± 0.2 mm (n = 682). (Results of statistical analyses were reported in section 6.3.2.1). The first molar, which has predominantly grooved LEHs, has the narrowest defects, averaging 1.3 ± 0.2 mm wide (n=56) (Table 6.4). On average, the widest defects were observed in the canine, p2 and p3.

Table 6.4. The average widths and heights of linear enamel hypoplasia in *S. hendeyi*. Means and standard errors are reported. 'n' is the number of defects measured. Numbers in parenthesis refer to numbers of bands/grooves measured. (No grooves were observed in canines).

Tooth Type	n	Average height of defect	Average width of defect	Average width: bands	Average width: grooves
Incisors	338	6.8 ± 0.3 mm	6.8 ± 0.3mm	7.4 ± 0.3 mm (303)	1.9 ± 0.5 mm (35)
Canine	41	9.3 ± 1.1 mm	7.8 ± 0.9mm	7.8 ± 0.9mm	-
p2	66	7.2 ± 0.7 mm	8.3 ± 0.8mm	8.5 ± 0.8 mm (64)	1.8 ± 0.2 mm (2)
p3	58	9.9 ± 1.2 mm	8.6 ± 0.9mm	9.0 ± 0.9 mm (55)	1.0 ± 0.8 mm (3)
p4	68	11.3 ± 0.9 mm	7.3 ± 1.1mm	8. 0 ± 1.2 mm (61)	0.7 ± 0.3 mm (7)
m1	56	7.1 ± 0.5 mm	1.3 ± 0.2mm	3.3 ± 0.5 mm (18)	0.4 ± 0.04 mm (38)
m2	68	8.3 ± 0.9 mm	3.4 ± 0.6mm	5.3 ± 0.9 mm (33)	1.7 ± 0.5 mm (35)
m3	114	10.3 ± 0.8 mm	5.2 ± 0.4mm	6.3 ± 0.5 mm (90)	0.7 ± 0.3 mm (24)

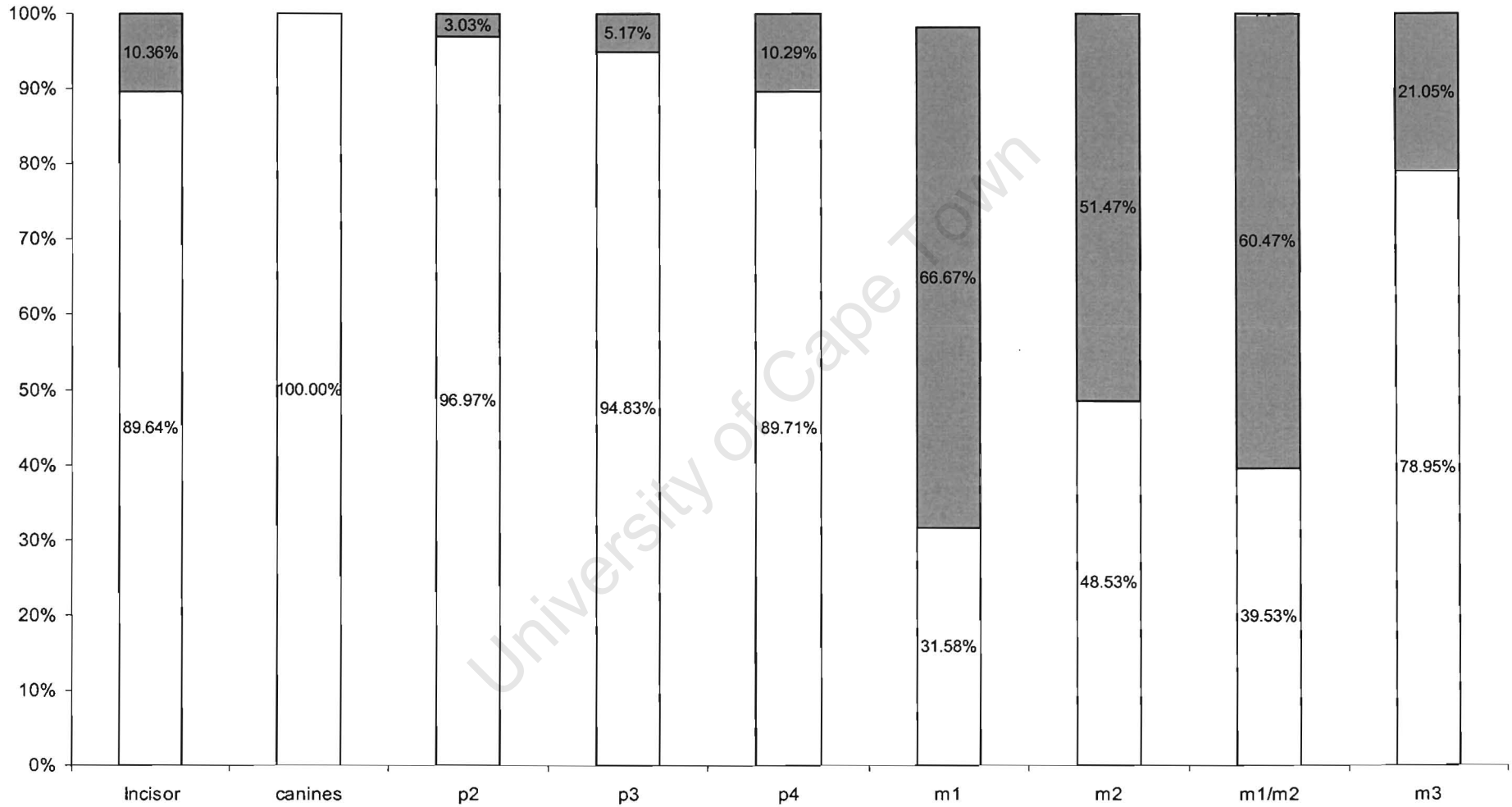

Figure 6.8. Types of linear enamel hypoplasia in *S. hendeyi* mandibular teeth. The percentage of teeth with bands of pits (open bars) and grooves (closed bars) is shown.

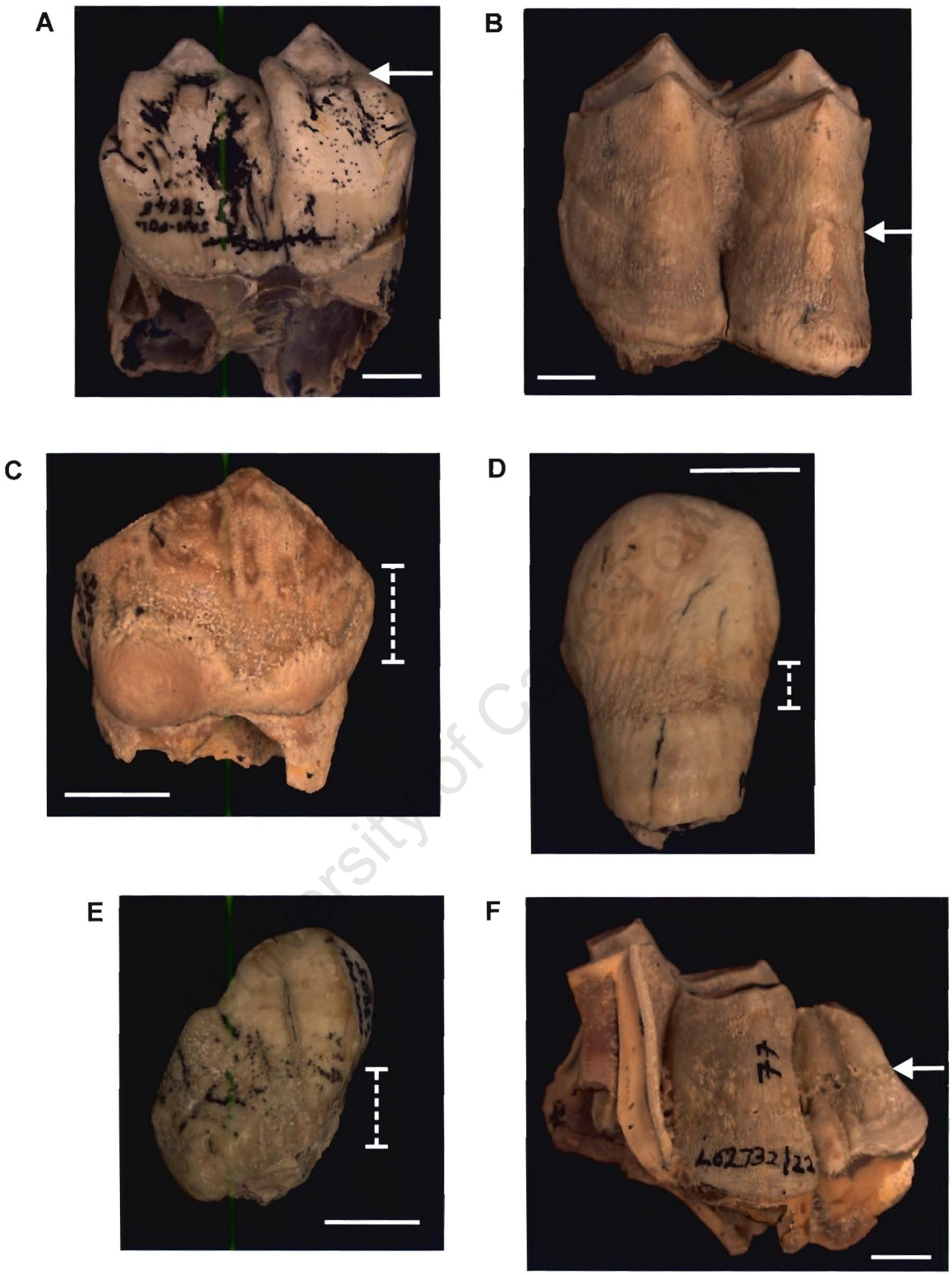

Figure 6.9. Linear enamel hypoplasia in *S. hendeyi*. (A) a wide groove exposing underlying dentine at the top of the lingual crown of a molar (PQL 58848), arrow. (B) a narrow groove on buccal surface of a molar (PQL 62727/24), arrow. (C) a third premolar (PQL 58109) with a wide band of pits, dashed vertical bar. (D) an incisor (PQL 44162) with a band of pits in the middle of the crown (labial surface), dashed vertical bar. (E) a canine (PQL 49905) with a large band of pits in the lower half of the crown (labial surface), dashed vertical bar. (F) a third molar (PQL 62732/22) with a narrow band of pits extending in the middle of the crown (buccal surface), arrow. Scale bars represent 1 cm.

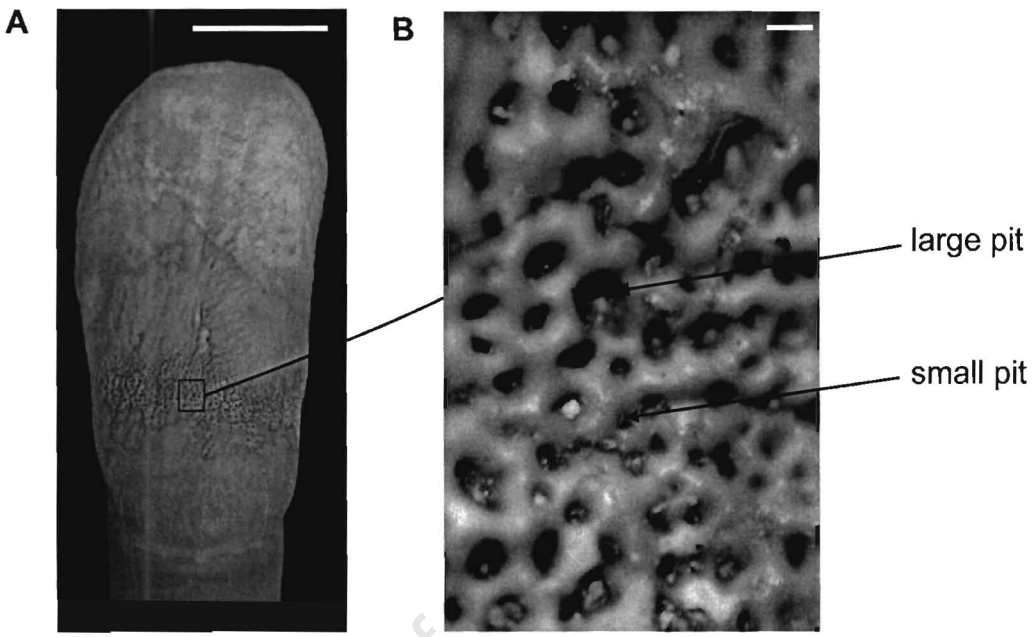

Figure 6.10. Linear enamel hypoplasia in a *S. hendeyi* incisor. (A) PQL 44091 and (B) inset in (A). Scale bars represent 10 mm in (A) and 277 μm in (B).

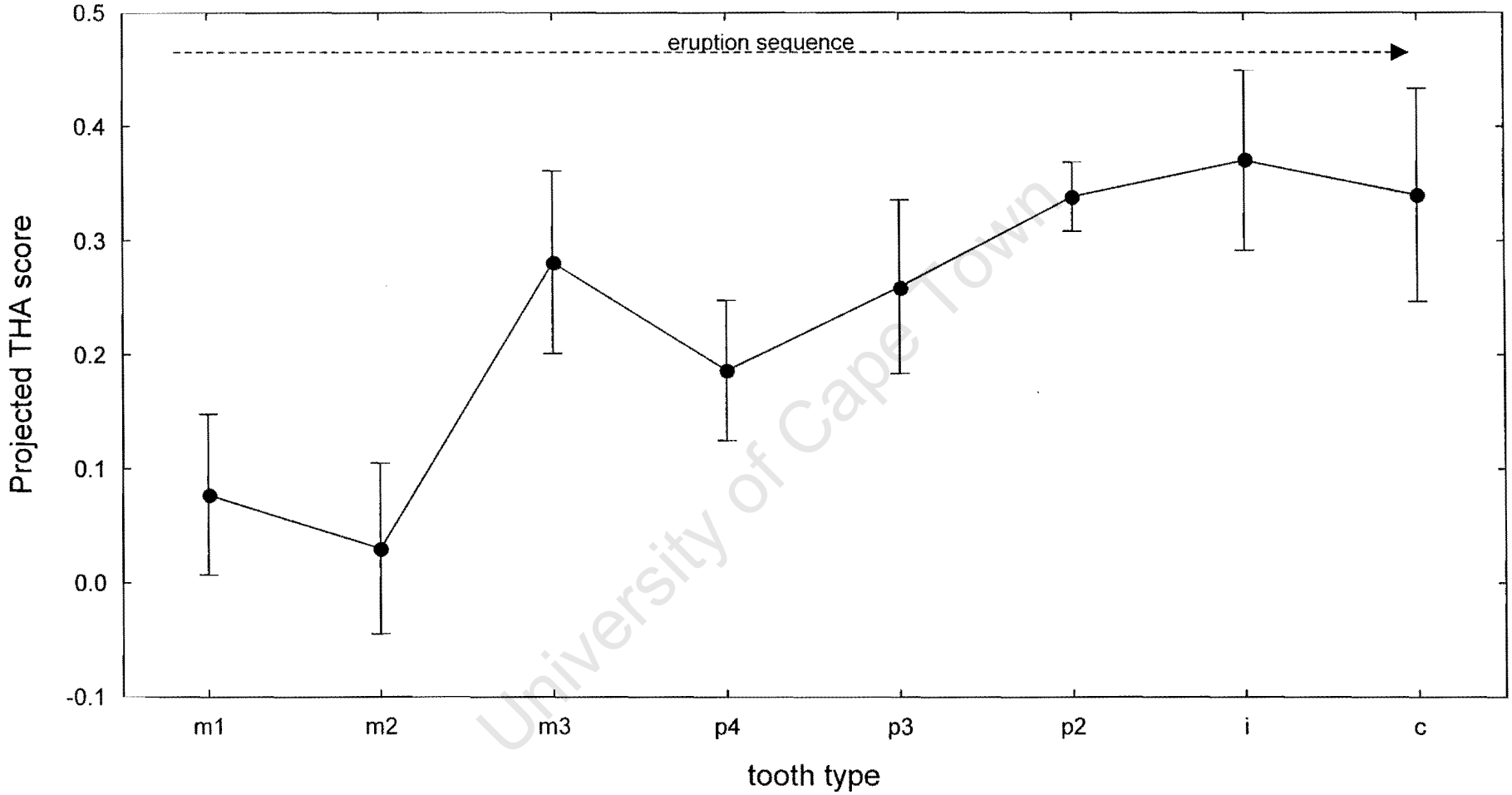

Figure 6.11. Average projected Tooth Hypoplastic Area (THA) scores for *S. hendeyi* teeth, in order of tooth eruption. Vertical bars indicate 95% confidence intervals.

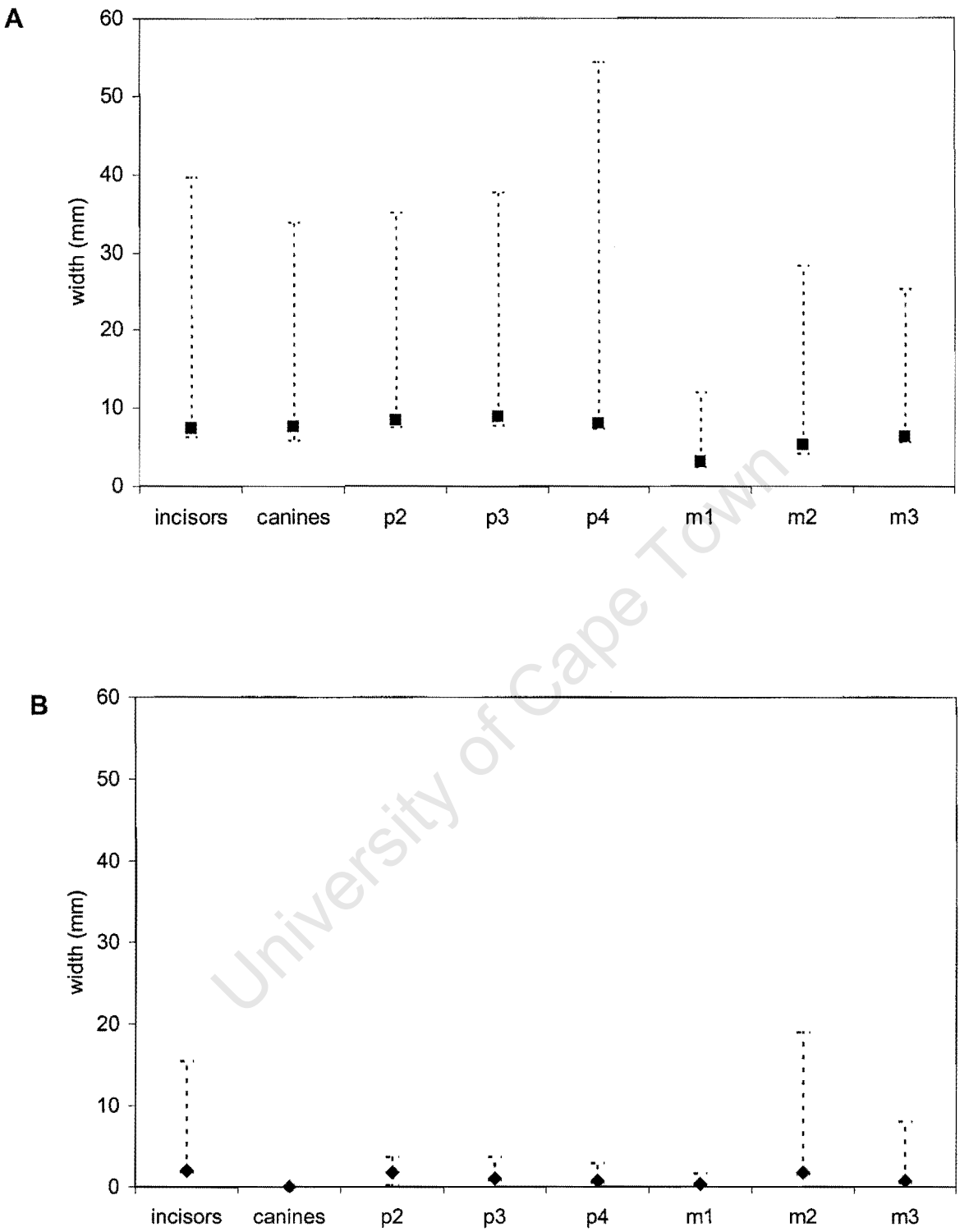

Figure 6.12. Widths of linear enamel hypoplasia in *S. hendeyi* teeth. (A) bands of pits and (B) grooves. The data point indicates the average defect width and the vertical line represents the range of values.

6.3.2.5 Heights of defects and the timing of stress events

The average heights of linear defects on each tooth crown are given in Table 6.4. The distribution of unique defects (i.e. that relate to particular stress episodes) throughout the dentition of *S. hendeyi* is shown in Figure 6.13 (insets). In the earlier erupting teeth (m1, m2, m3) LEHs are more common in the cervical third of the tooth. In the p4 and p3, similar numbers of linear defects were found in the middle and cervical portion of the tooth. In the p2 and incisor, the middle portion of the tooth crown has the most defects whereas in the canine LEHs are evenly spread over the entire tooth crown. There appears to be a tendency for LEHs to be confined to the cervical portion of the tooth posteriorly (in the mouth). No LEHs were found in the occlusal third of the first molar coinciding with *in utero* development.

In almost all tooth types, the average height of bands (11.1 ± 0.3 mm, n=682) and grooves is similar (9.3 ± 0.4 mm, n=170). The averages per tooth type are given in Table 6.6. Only in the second premolars are these two defect morphologies located in different segments of the tooth. In p2's two grooves are present at 14 mm and 17 mm from the base of the root-crown junction, whereas bands are present at a height of 6.9 ± 0.7 mm (n=64) on average.

In order to analyse the location of unique defects more accurately, the percentage of defects in 2 mm categories was determined (Figure 6.13, graphs). The defects in the incisors and canines are distributed more or less evenly across the tooth crowns and no height preferentially records defects. Over 55.6% of the defects in the p2 are located at a height of 9 - 15 mm from the base of the tooth crown. The third premolar has 21% of the defects located 7 - 10 mm and another 21% of the defects at 15 - 18 mm from the base of the crown, indicating possibly two regions at which defects are common. In the fourth premolar over a quarter of the defects are located at a height of 10 - 14 mm from the base of the crown. 93% of the defects in the first molar are present in the lower 15 mm of the crown. The second molar records most defects (73%) within 8 mm of the base of the tooth crown whereas in the third molar 49% of the defects are present 8 - 20mm from the base of the crown.

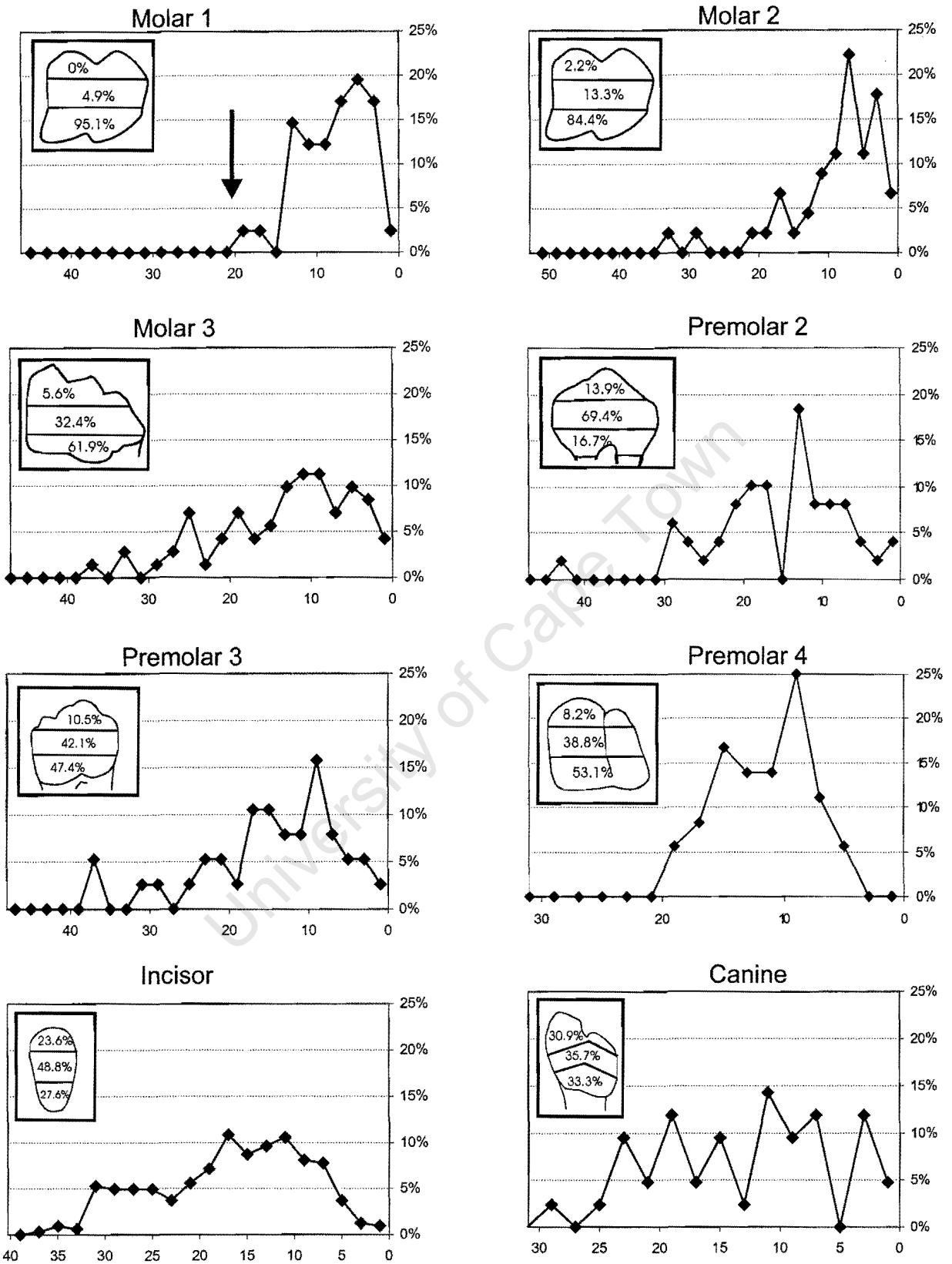

Figure 6.13. Distribution of linear enamel hypoplasia in *S. hendeyi* mandibular teeth. The percentage of linear defects on each third of each tooth is shown in the insets. The percentage of defects in each 2 mm of the tooth crown for each tooth type is plotted in the graphs. The arrow in the first molar graph indicates birth.

6.3.2.6 Periodicity and the number of defects per tooth crown

Many teeth have more than one defect per tooth crown (Table 6.5) and the maximum number recorded on a single tooth crown was five. This was observed in one incisor and one third molar. The majority of defects (~65%) however, occur singly. On average each defective tooth has 1.75 to 2.1 linear defects. Although several defects on a tooth crown suggests an episodic stress event, if these events are very close together, tooth development may not resolve them, and hence a single (wide) defect would be visible. In some cases where several linear defects are present on the buccal/labial surface, only one defect is present on the lingual surface. (This lingual defect would correspond to one of the defects on the opposite surface). In other teeth one broad defect was present on the buccal/labial surface but on the lingual surface two or three narrower LEHs were present, corresponding to the height of the buccal/labial defect. 52% of the defective p4s and 48% of incisors have two or more defects per crown. About 30% of canines and m3s have more than one defect per tooth crown, yet only 10% of p2s share this phenomenon. This is the lowest percentage recorded out of all tooth types.

Table 6.5. The percentage of teeth with one or more linear defects on a single tooth crown. The number in parenthesis refers to the number of teeth. The total number of defects per tooth type are given in Table 6.4 above.

Tooth Type	One defect	Two defects	Three defects	Four or more defects
Incisors	55.4% (107)	28% (54)	13% (25)	3.6% (7)
Canines	70% (14)	10% (2)	10% (2)	10% (2)
p2	90% (27)	6.7% (2)	3.3% (1)	0%
p3	73.3% (22)	23.3% (7)	3.3% (1)	0%
p4	48.2% (13)	29.6% (8)	22.2% (6)	0%
m1	81.8% (27)	12.1% (4)	3% (1)	3% (1)
m2	77.2% (27)	17.1% (6)	5.7% (2)	0%
m3	64.4% (29)	29% (13)	2.2% (1)	4.4% (2)

The distance between bands (on the buccal/labial surface) is highly variable compared to the distances between grooves (Table 6.6). No two grooves were further than 12 mm apart, regardless of tooth size. Canines and premolars do not have more than one groove on a tooth surface. Using a two-tailed Student's t-test for independent samples on each tooth type, the average distance between bands and between grooves is significantly different in incisors and third molars only (incisors: $t = -2.04$, $p<0.05$, $df = 115$; m3: $t = -2.71$, $p<0.05$, $df = 16$). The distance between bands and between grooves is not statistically significant for first and second molars. The other tooth types do not have more than one groove on a tooth crown.

Table 6.6. Distance between linear defects on the buccal/labial tooth surface. Distances between bands are given with distances between grooves in parenthesis where present.

Tooth type	Minimum distance between defects (mm)	Maximum distance between defects (mm)
Incisors	2.2 (2.2)	23.7 (12)
Canines	4.4	16.9
p2	1.9	7.3
p3	3.6	33.6
p4	0.8	16.3
m1	2.8 (1)	5.6 (8)
m2	3.6	12.3
m3	3.2 (0.4)	23.4 (8.3)

6.3.3 Fourier Transform Infrared Analyses

The Fourier Transform Infrared spectra for the two defective *S. hendeyi* enamel samples (PQL 59598 and PQL 44053) are similar to those of normal *S. hendeyi* enamel (compare Figure 4.4 in Chapter 4 to Figure 6.14). The absorbance of the $^{Y}3$ PO_4 is especially high in one defective tooth PQL 44053 (Figure 6.14A). Noise in the $^{Y}3$ CO_3 of tooth PQL 59598 made it impossible to determine the absorbance at wavelength 1540 cm^{-1} and hence type A carbonate content. The calculated indices (introduced in Chapter 4, section 4.2.2.1) are shown in Table 6.7. The indices for normal sivathere enamel reported in Chapter 4 are repeated here for comparison only.

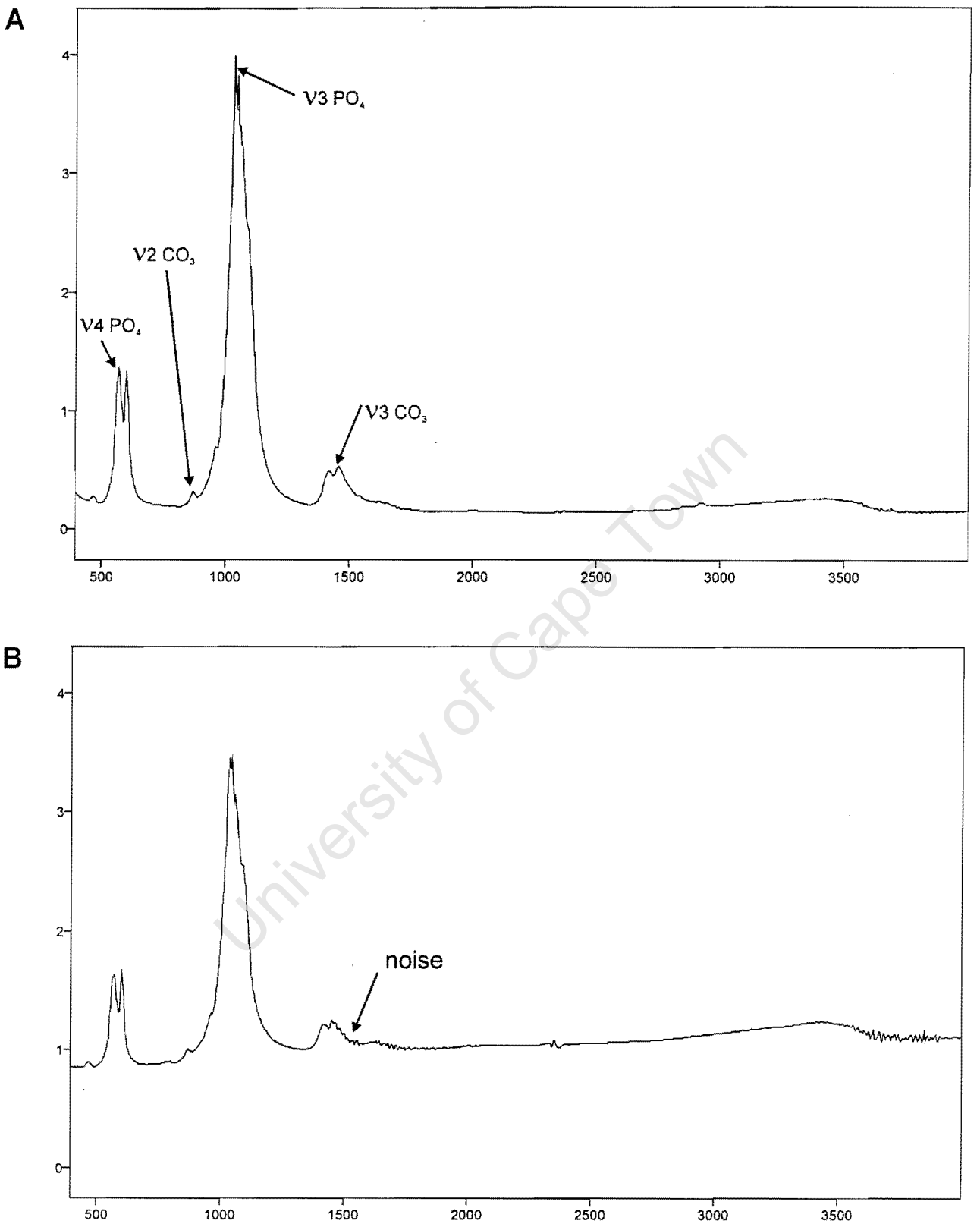

Figure 6.14. Fourier Transform Infrared absorbance spectra for defective *S. hendeyi* enamel. (A) PQL 44053 and (B) PQL 59598.

Table 6.7. Absorbance indices for defective and normal *S. hendeyi* enamel (indices were defined in Chapter 4). Mean ± standard deviation is given for normal enamel.

Accession number		BPI	API	BAI	PCI	% CO2 by wt
PQL 44053	Defective	0.391	0.203	1.701	2.938	4.609
PQL 59598	Defective	1.138	-	-	2.465	12.083
(from Chapter 4)	Normal	0.352 ± 0.01	0.215 ± 0.01	1.523 ± 0.33	2.99 ± 0.01	4.215 ± 0.1

The carbonate content and phosphate crystallinity index (PCI) for tooth PQL 44053 are similar to those for normal enamel. However, the indices for PQL 59598 differ markedly from both normal sivathere enamel and from tooth PQL 44053, especially in the amount of type B carbonate (reflected by BPI) and the overall carbonate content. The phosphate crystallinity index (PCI), which measures the crystallinity of the apatite, is reduced in this tooth. The heights of the peaks at 595 cm^{-1} and 605 cm^{-1} (the $\nu 4$ PO_4 domain), which is used to calculate the PCI index, are different in each defective tooth (Figure 6.14). In the normal enamel spectrum (Figure 4.4A, Chapter 4) and in defective tooth PQL 44053, the first peak (595 cm^{-1}) is slightly higher than the second (at 605 cm^{-1}). In PQL 59598, however, this difference in peak size is altered – the second peak (605 cm^{-1}) is greater than the first (595 cm^{-1}) (i.e. the ratio is greater than 1). Increased resolution of the $\nu 3$ phosphate (at ~1045 cm^{-1}) is also observed in the defective enamel spectra (Figure 6.14) compared to normal enamel. The $\nu 2$ carbonate peak at 874.2 cm^{-1} (Table 4.2, Chapter 4) in normal *S. hendeyi* teeth is shifted to a slightly lower frequency in the defective teeth. These peaks are positioned at 873.2 cm^{-1} and 871.5 cm^{-1} respectively, for tooth PQL 44053 and PQL 59598.

6.3.4 Microscopy of defects

Defective enamel:

Examination of histological results revealed several interesting observations. In all sections cut through linear bands of pits (PQL 58679, PQL 58674, PQL 58741) deflections in the incremental lines underlying defects were observed (Figure 6.15). The latter two of these teeth were sectioned longitudinally. In PQL 58674, where the band of pits is located towards the top of the tooth with normal enamel cervically, incremental lines underlying the pits are accentuated compared to the lines visible cervically to the defect (Figure 6.15A). These accentuated lines are darker than the "normal" incremental lines. The lines immediately below the defects deflect with the pit outline whereas those that are deeper deflect very little (or not at all) but are equally dark. The same phenomenon was observed in the tooth (PQL 58741) with bands of pits at the base of the crown, except that the accentuated lines are cervical to the normal incremental lines (not shown). In the transverse section through pits (PQL 58679), dark accentuated lines are located above lighter unaccentuated "normal" lines (Figure 6.15B). That is, normal incremental lines are present near the enamel-dentine junction, and these lines are only accentuated from about the middle of the enamel to the outer surface. This indicates that systemic stress was only experienced later, during the latter part of the laying down process.

In the two teeth with deep wide linear grooves (PQL 58762, PQL 58763) the incremental lines deflect on either side of the groove and converge towards the defect (Figure 6.15C). In both of these teeth deflections in dentine incremental lines are present underlying the groove. In the tooth with a shallow groove (PQL 58672) (not shown) the incremental lines are unfortunately not clearly resolved but it appears as if the same phenomenon is observed as for bands of pits, with incremental lines deflecting in the region underlying the groove only.

The incremental enamel lines in the tooth with diffuse multiple non-linear pits (PQL 58681, Figure 6.15D) also deflect underneath the pit and are equally accentuated. These pits are about half as deep (~125 µm) as those in the bands of pits (~250 µm).

In SEM analyses of enamel pits, the orientation of the enamel prisms underlying pits was not altered in any of the tooth fragments examined (Figure 6.16). Enamel prisms are arranged parallel to one another and perpendicular to the surface. The entire depth of enamel was examined.

Normal enamel:

Incremental lines in normal sivathere enamel are more or less parallel to one another. These lines were not always equally visible throughout the enamel of one tooth and often patches of obscure lines were present. Incremental lines in both the normal sivathere incisor (PQL 59599) as well as in the enamel surrounding defects in other teeth were counted (Table 6.8). The number of incremental lines per µm enamel in incisors is 0.02-0.03 lines/µm. In the molar fragment the count was 0.04-0.05 lines/µm. (Results from SEM analyses of normal enamel are presented in section 6.3.5.2. in order to compare them with *G. camelopardalis*).

Table 6.8. Analysis of normal *S. hendeyi* enamel. The number of incremental lines (n) and total enamel thickness was counted and measured.

Tooth	n	Enamel thickness (µm)
PQL 59599, incisor	19	875
PQL 58679, incisor	42	1 400
PQL 58675, incisor	42	1350
PQL 58763, molar	86	1625
PQL 58762, molar	54	1250

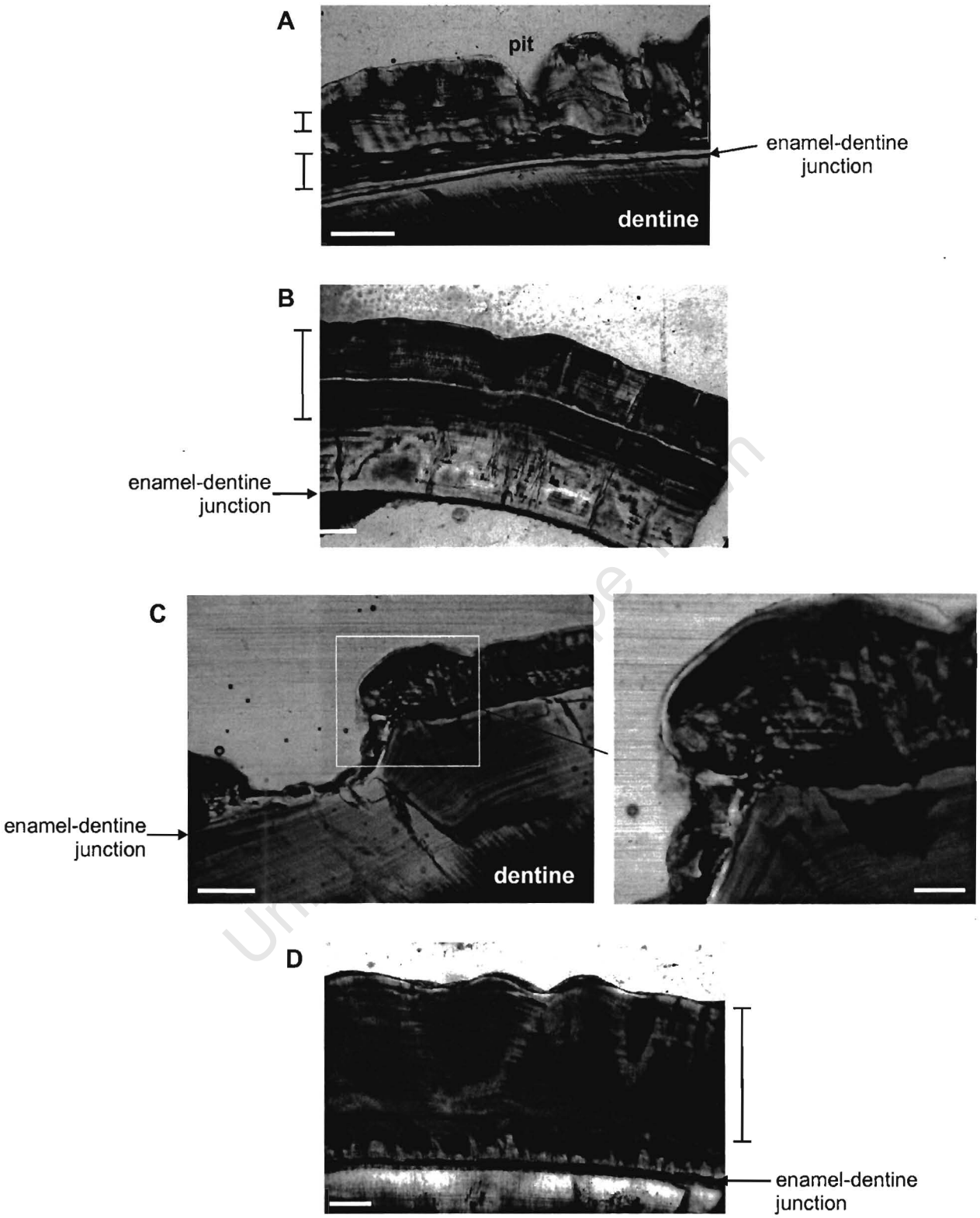

Figure 6.15. Histology of enamel hypoplasia in *S. hendeyi*. Enamel is above dentine in all sections. Vertical bars indicate deflecting incremental lines. (A) longitudinal section through a band on pits in an incisor (PQL 54674) showing deflecting incremental lines below the pit. Scale bar = 500 μm. (B) transverse section through pits in an incisor (PQL 58679) showing a small deflection of the incremental lines below the pit. Scale bar = 375 μm. (C) section through a deep groove in a molar fragment (PQL 58763). Incremental lines in both the enamel and underlying dentine deflect in the region of the groove. Scale bar = 850 μm. Inset, Scale bar = 475 μm. (D) transverse section through diffuse pits in incisor (PQL 58681) showing deflecting incremental lines in upper enamel. Scale bar = 385 μm.

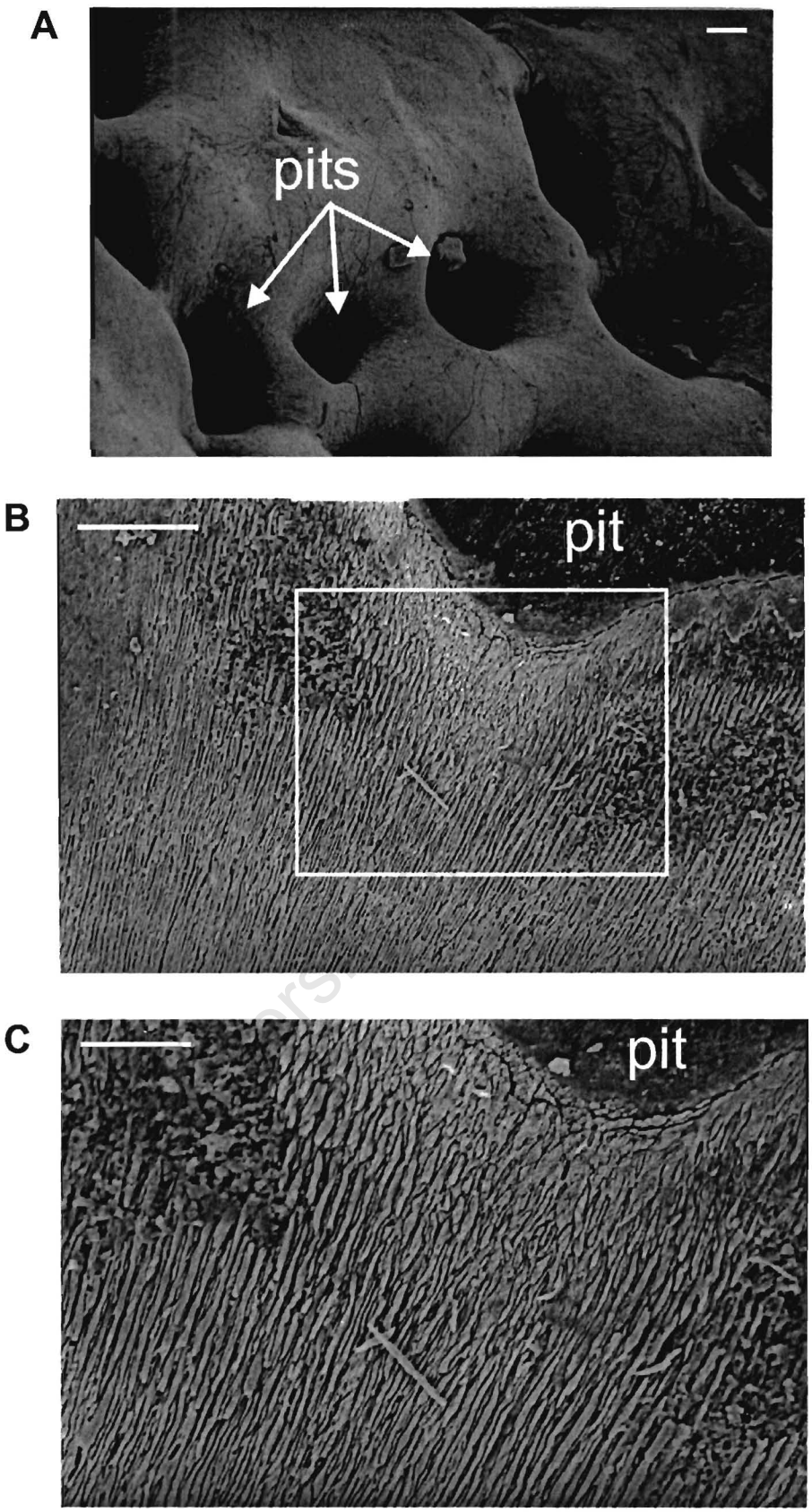

Figure 6.16. Scanning electron micrographs of enamel hypoplasia in *S. hendeyi*. (A) low magnification of the unetched surface of tooth PQL 58670 showing pits in the enamel, scale bar represents 100 μm. (B) transverse section through a pit showing the enamel prisms underlying the pit (PQL 58681), scale bar represents 100 μm. (C) Inset in (B) showing the parallel alignment of enamel prisms below the pit, scale bar represents 500 μm.

6.3.5 Comparisons with *Giraffa camelopardalis*

The location at which most defects occur on each tooth crown together with the tooth eruption sequence for the giraffe is crucial in elucidating the cause of the stress event in each tooth type.

6.3.5.1 Tooth eruption sequence

Two mandibles (from sub-adult individuals) with both deciduous and permanent teeth present were found in the collection. In both of these the deciduous premolar(s) are in wear and the broken mandible exposes the underlying developing permanent premolar(s). In one mandible, which is part of an *in situ* exhibit at Langebaanweg, the two deciduous premolars and the permanent first and second molars are present and in wear (Figure 6.17). The third molar is unworn and is at an advanced stage of eruption. Underlying the deciduous premolars, the tip of each of the permanent premolars has fully mineralised (Figure 6.17, arrow). In the second smaller mandible fragment (PQL62725) only the dp4 and m1 are present and in wear (see Figure 5.6A in Chapter 5). (The m2 is deformed). Underlying the deciduous fourth premolar, the permanent p4 is just visible. The eruption sequence presented by both mandibles is consistent with that of the giraffe and if eruption timings are the same then both these animals are approximately four years old.

6.3.5.2 Enamel Microstructure

Enamel from *G. camelopardalis* and *S. hendeyi* was compared to determine whether the enamel prism patterns are similar (Figure 6.18A-D). In *S. hendeyi*, prisms are smaller (3.8 µm by 2.5 µm), have a slightly different prism shape and are surrounded by thicker prism sheath(s). The prism arrangement in the fossil enamel is somewhat disorganised and appears to be a mixture of Pattern 2 and 3. In the extant giraffe, the typical Pattern 2 prism arrangement is present. Evidence for decussation (Hunter-Schreger bands) was found in the enamel of *S. hendeyi* (Figure 6.18E). According to von Koenigswald et al. (1987), the earliest presence of true Hunter-Schreger bands was in the Early Palaeocene (~60 Myr) mammals and therefore the presence of these bands in *S. hendeyi* enamel is not unexpected. In the extant giraffe, the prisms are organised with little interprismatic enamel and are about 6.7 µm by 3.3 µm in size.

In histological sections, the enamel was much thinner in *G. camelopardalis* (GIR N1) compared to *S. hendeyi* (PQL 59599). Labial incisor enamel in the mid region of the tooth crown was about 1.13 mm in the extant giraffe and about 1.65 mm in the sivathere.

6.3.5.3 Enamel defects

The incidence of enamel hypoplasia in *G. camelopardalis* was high in terms of affected individuals but low in terms of affected teeth (Table 6.9). Out of the thirteen individuals examined, nine have teeth with defects. Linear defects however affected only ten teeth (three different tooth types) in three individuals (ZM 35364, ZM 36851, ZM 36655) whereas non-linear defects were observed in eleven teeth (six tooth types) in eight individuals (Table 6.9). The percentage of permanent teeth with linear or non-linear defects was the same, 6%. Single pits were more prevalent compared to the other non-linear types of defects. Only one deciduous tooth was defective with a non-linear defect.

Major differences between mandible and maxilla and between left and right jaws were observed. In general non-linear defects were isolated (occurring in only one tooth in the jaw or skull) compared to linear defects. In only one tooth was a non-linear defect present in both left and right upper teeth. The incidence of defects in the maxilla compared to the mandible was not identical. No non-linear defects, for example, were observed in any mandibles. Linear defects observed in both lower first molars (of ZM 35364), were not present in the upper first molars. In comparison, ZM 36851 has linear defects in three of the four first molars. The maxilla of ZM 36655 is most defective (mandible not available) with P2, P4, M1 and possibly M2 having linear defects. The third premolar, however, which develops almost concurrently with the other premolars, has non-linear defects. In all three giraffes with linear defects, the defects occur within 5 mm from the base of the first molar consistent with the position of linear defects in *S. hendeyi*.

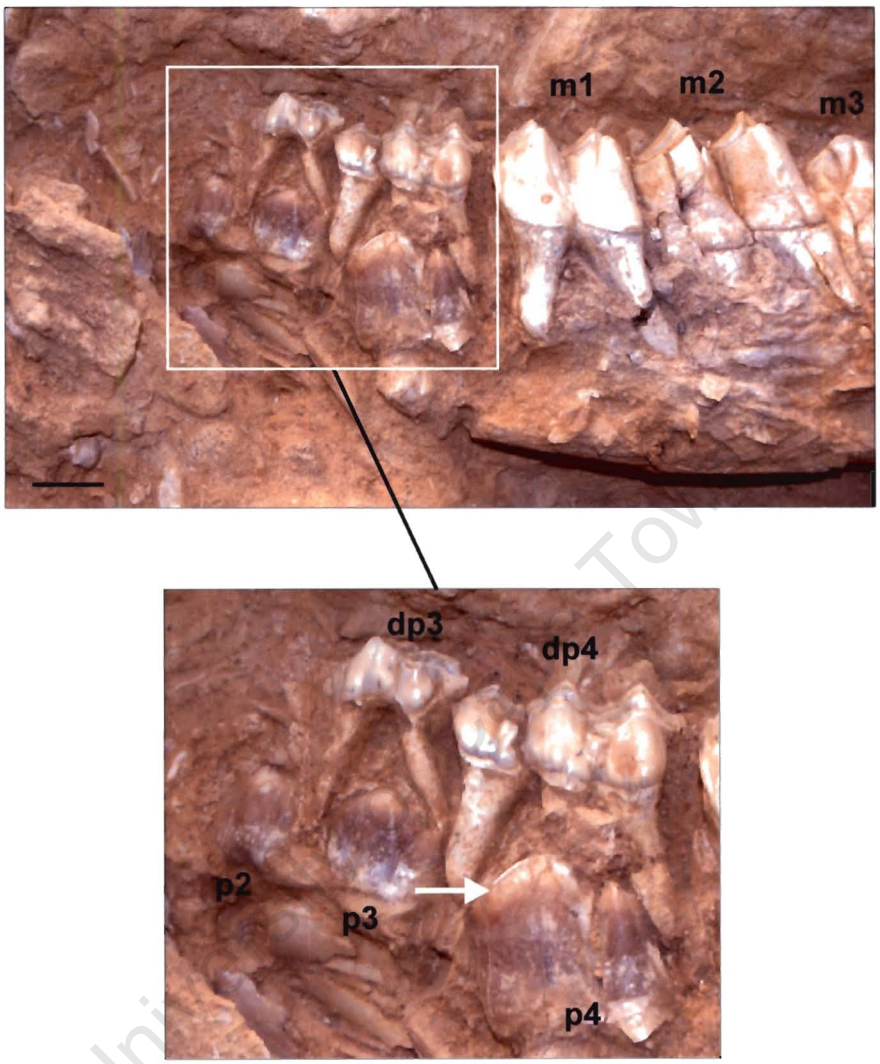

Figure 6.17. The *in situ S. hendeyi* mandible belonging to a sub-adult individual. Note the permanent p2-4 tooth crowns visible between the roots of the deciduous premolars (dp3 and dp4). The permanent m1 and m2 are in wear. Scale bar represents 3 cm. The arrow in the inset indicates the mineralisation front in the permanent p4. The tips of the permanent p3 and p2 are also mineralised.

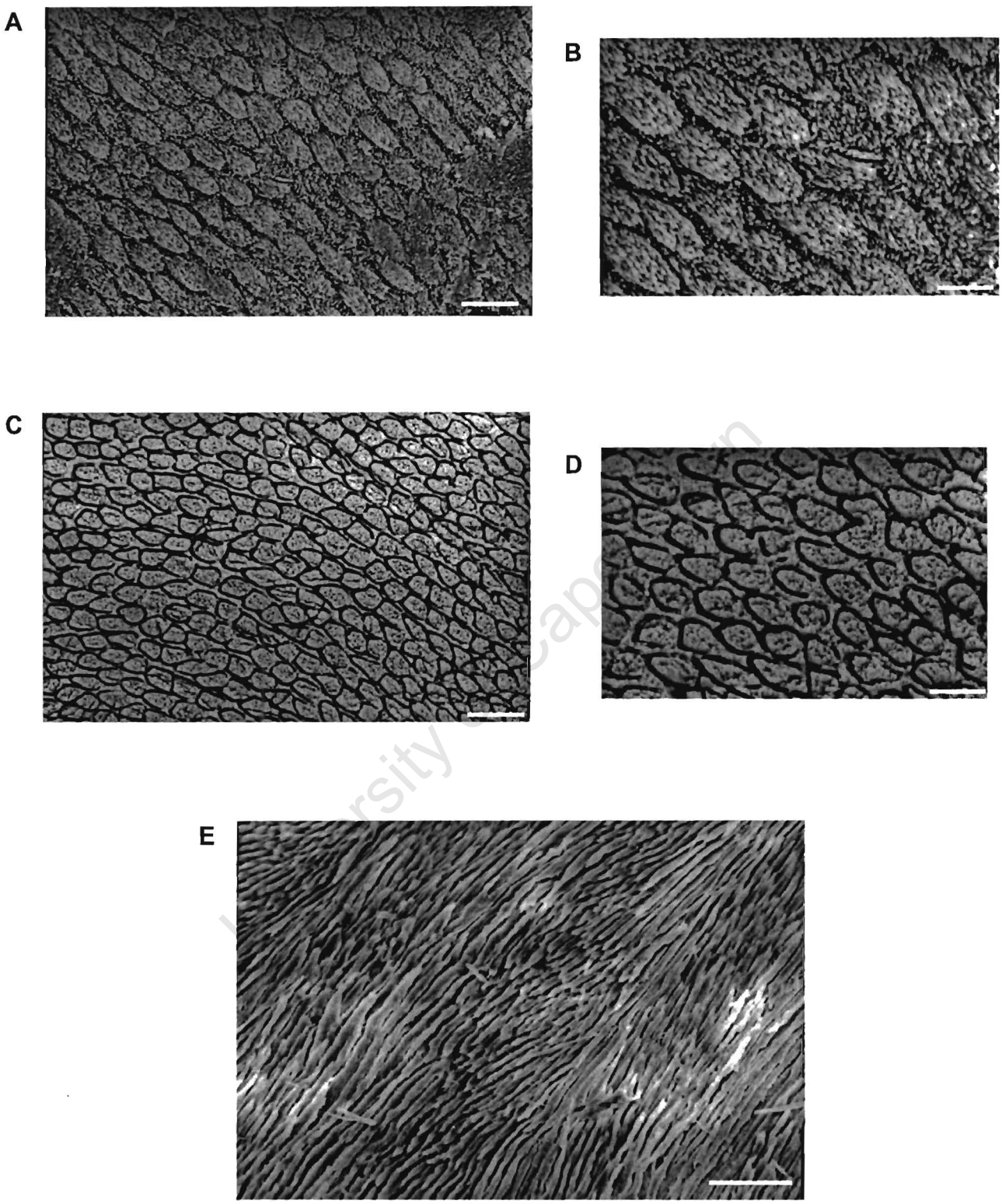

Figure 6.18. Scanning electron micrographs of giraffid enamel showing the prism arrangement. (A, B) *G. camelopardalis* surface enamel. (C, D) *S. hendeyi* surface enamel. (E) transverse view of *S. hendeyi* enamel showing prism decussation. Magnification in (A, C) is 1 500x and scale bars represent 10 μm. Magnification in (B, D) is 3 500x and scale bars represent 5 μm. In E, magnification is 500x and scale bar represents 50 μm.

Table 6.9. Enamel hypoplasia in *G. camelopardalis.* (ZM 36655 does not have an associated mandible). Samples are from the comparative mammal collection at the South African Museum, Iziko Museums of Cape Town.

Accession number	Tooth type	Defect
ZM 36655	Upper P2 (left and right)	LINEAR groove
	Upper P3 (left and right)	NON-LINEAR single pit
	Upper P4 (left and right)	LINEAR band of pits
	Upper M1 (right)	LINEAR band of pits
	Upper M2 (left)	possibly LINEAR groove
ZM 36851	Upper M1 (left and right)	LINEAR groove
	Lower m1 (left)	LINEAR groove
ZM 35364	Lower m1 (left and right)	LINEAR groove with pits
	Upper M1 (right)	NON-LINEAR aplasia (2)
		NON-LINEAR diffuse pits
	Lower m2 (right)	possibly LINEAR groove
	Upper M2 (right)	possibly LINEAR groove
ZM 35363	Upper P3 (left)	NON-LINEAR aplasia
	Upper P4 (left)	NON-LINEAR aplasia
ZM 37058	Upper M2 (right)	NON-LINEAR single pit
ZM 17176	Upper M1 (left)	NON-LINEAR single pit
	Upper M2 (left)	NON-LINEAR single pit
ZM 36654	Upper P3 (left)	NON-LINEAR aplasia
ZM 39692	Upper M3 (left)	NON-LINEAR aplasia
ZM 39795	Upper dP4	NON-LINEAR single pit

6.4 DISCUSSION

6.4.1 Morphology and aetiology of defects

The gross morphology of enamel hypoplasia in *S. hendeyi* is consistent with that reported for humans (Goodman and Rose, 1990), fossil and archaeological non-primates (Dobney and Ervynck, 1998; Mead, 1999; Dobney and Ervynck, 2000; Niven, 2002) and for wild boar and cervids subjected to fluoride contamination (Kierdorf and Kierdorf, 1989; Kierdorf et al., 1993, 1996, 2000). The type of linear defects (grooves or bands of pits) in each of the above studies was not assessed and figures show only grooved defects. Bands of pits are however, always associated with fluorotic alterations in the teeth of wild boar and cervids. Only 20% of the linear defects in *S. hendeyi* are grooves. The gross morphology of these defects most closely resembles those reported for animals with dental fluorosis (discussed further below). Grooves are the result of more severe/intense stress periods than bands of pits (Goodman and Rose, 1990) because pits are surrounded by normal enamel (which is laid down by undisrupted cells) whereas in grooves all ameloblasts in the region of the groove are disrupted. (If grooves are deep enough to expose underlying dentine, then the disruption is also more severe). The depth of a defect is therefore a good indicator of the severity of the stress episode causing that defect. Grooves are significantly narrower than bands of pits indicating that associated stress episodes, although intense, were probably of a shorter duration than those associated with bands, which are generally wider.

In the sivathere sample, few teeth have lingual defects indicating that either this surface has a reduced susceptibility to defects or that lingual defects are "lost" due to abrasion resulting from the constantly moving tongue and food bolus (as suggested by Dobney and Ervynck, 2000). Some teeth have more than one lingual defect and these defects are at a similar height to a single broad buccal/labial defect, suggesting that defects on the lingual surface are more resolved. It is unlikely that the enamel on each surface develops at different rates since in *S. hendeyi* teeth that are still in the process of enamel formation (see Chapter 3, Figure 3.4) the matrix production front is at a similar height on each surface.

The microstructure of enamel hypoplasia has only been investigated in humans (Goodman and Rose, 1990) and in wild extant animals with fluorosis (Shearer et al., 1978; Kierdorf et al., 1993; Kierdorf and Kierdorf, 1997; Kierdorf et al., 2000). Non-linear and linear defects are both the result of a disruption in ameloblasts and as such the histological features associated with LEH and non-linear defects are similar. Incremental (growth) lines in enamel form as a consequence of the enamel laying down process pausing regularly during development similarly to the growth arrest lines in bone. The parallel, unaccentuated (light) incremental lines in normal *S. hendeyi* enamel, indicates the normal rhythm of enamel secretion. Since an incremental line forms as a result of natural growth arrest, an accentuated incremental line indicates severe growth arrest. These accentuated lines are present below surface pits but only appear to deflect near the base of the pit (Figure 6.19). This indicates that initially (when accentuated, non-deflecting lines are formed), severe growth arrest occurs, followed by a growth phase. This repeats several times until a point at which the ameloblasts are disrupted. This disruption results in a reduction in the enamel secretion rate (Kierdorf et al., 1993) and thus deflection of accentuated lines. As these disrupted ameloblasts experience more periods of severe growth arrest, they are ultimately destroyed and can no longer produce enamel, even at a reduced rate. Once enamel is no longer produced the depth of the pit is reached. These observations agree with the threshold model proposed by Goodman and Rose (1990). Repeated episodes of severe growth arrest followed by growth, eventually results in a disruption of the ameloblasts that ultimately results in surface defect formation. This means that the systemic stress was experienced early on during enamel formation (below the bottom of the pit) and that depth of a pit only indicates the point at which a threshold level of stress was experienced. In summary, the degree and duration of disruption to ameloblasts can be determined by the angle at which the accentuated incremental lines bend, by the number of deflecting lines and by the location of these lines within the enamel.

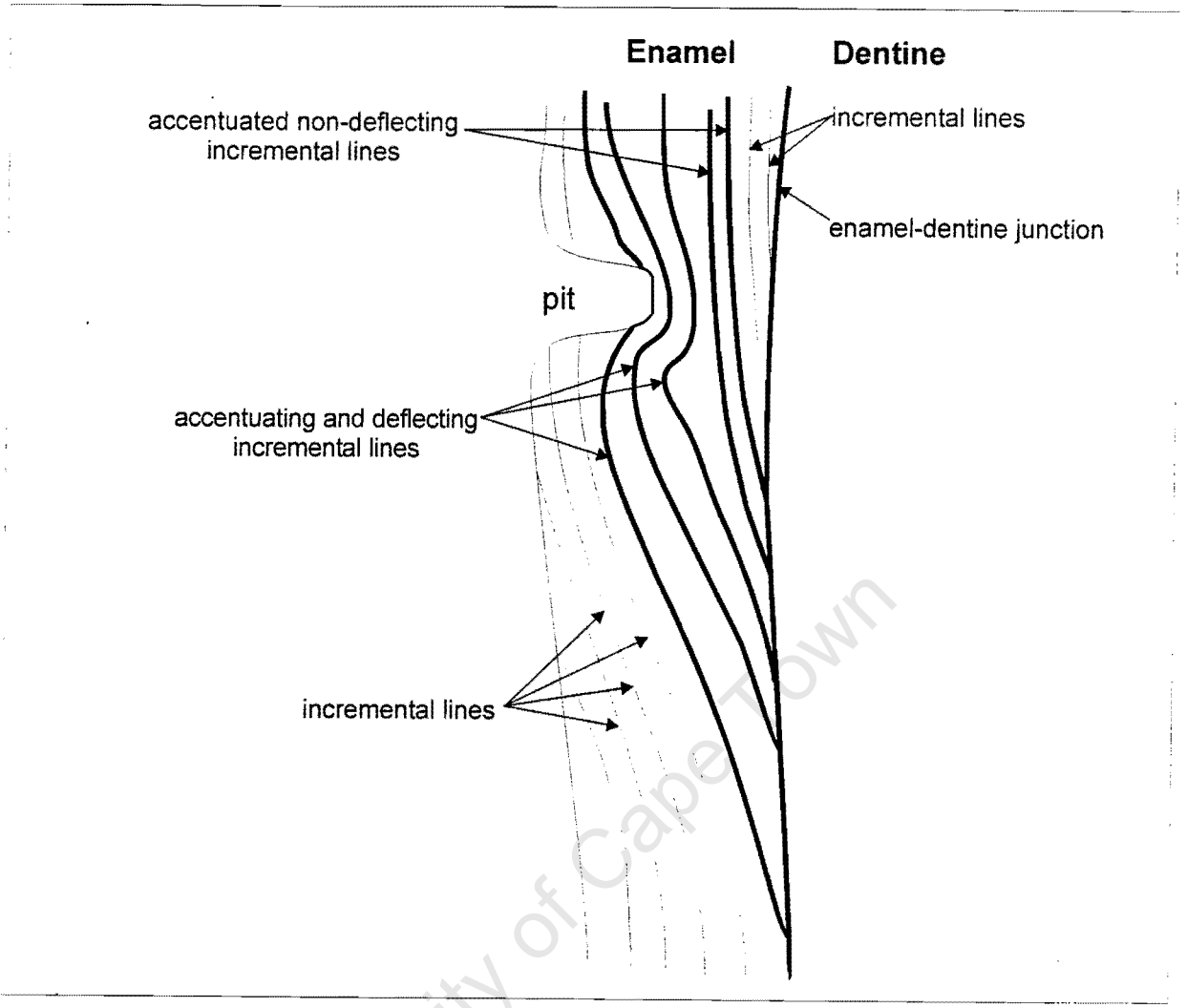

Figure 6.19. A schematic diagram of the incremental lines underlying a defect/pit.

In teeth with single pits or with enamel aplasia, ameloblasts are completely disrupted by the insult at some point during development so that no subsequent enamel is laid down in this region. Adjacent cells are unaffected and normal enamel is laid down cervically to the defect. For example, the deflections in incremental lines underlying diffuse pits are similar (but less marked) than those underlying pits in linear bands. Any disruption of cells however indicates that the associated stress episodes were relatively severe (Goodman and Rose, 1990).

The histological features of enamel hypoplasia reported here are consistent with those of Kierdorf and co-workers (Kierdorf et al., 1993, 1996; Kierdorf and Kierdorf, 1997; Kierdorf et al., 2000) as a result of excess fluoride intake. According to these authors accentuated incremental lines are hypomineralised and aprismatic. Hypomineralised lines have been observed in human teeth as well (Boyde, 1972)

and result from Tomes' processes that have lost their distal ends. Because ameloblasts continually grow these processes and constantly produce cell membranes, normal prismatic enamel is laid down adjacent to this hypomineralised aprismatic band (Kierdorf et al., 1993). The fact that normal enamel develops cervically to a defect indicates that not all ameloblasts are irreparably damaged. Scanning electron microscopy of linear defects in *S. hendeyi* indicates that prism angles were not altered and thus that enamel *mineralisation* proceeded normally. Incremental lines were not easily visible in SEM micrographs and no hypomineralised lines/bands of enamel were observed underlying the defects.

Dentine deflections were only observed underlying deep, wide LEH grooves (Figure 6.15C). This indicates a disruption in both dentinoblasts and ameloblasts early in development. This disruption was present when the cells in this region began laying down enamel and continued throughout development. In the case of dentinoblasts, these cells laid down dentine at a slower rate than adjacent cells resulting in a bending of the dentine incremental lines. Ameloblasts however, were severely disrupted and completely destroyed so that no enamel was laid down in this region. This is consistent with findings by Goodman and Rose (1990) in human teeth.

The size of the enamel hypoplasia is thought to depend solely on the number of ameoloblasts that are disrupted (Goodman and Rose, 1990), i.e. a wide defect is the result of a disruption in a larger number of cells than a smaller defect. Variations in defect widths in the different tooth types may however relate to their rate of development and not to cell number *per se.* For example, in *S. hendeyi*, the number of incremental lines per micron of enamel is much higher in incisors than in molars (Table 6.8) indicating that the rate of enamel formation was faster in the anterior teeth. Unfortunately the molar fragment could not be distinguished into molar type and may be a fragment from the slow developing first molar (Hall-Martin, 1976a). In addition, the enamel prism arrangement in the extant versus the extinct giraffid is not the same. In primates, Pattern 1 prisms are associated with slow secretion and Pattern 3 with faster enamel secretion (Martin, 1981). However, von Koenigswald and Sander (1997) caution that i) a single tooth may have different enamel prism patterns but that one pattern is usually dominant and ii) that the prism patterns

described by Boyde (1964) insufficiently cover the great variety of structures seen in mammalian enamel and are therefore inadequate as enamel microstructure descriptions. Further analyses are therefore required to elucidate whether this prism pattern difference is real or merely indicative of variation within the tooth.

Since width does not strictly reflect duration of stress events because of the complications tooth development rates create, the interpretation of the duration of stress events must be treated with caution. In addition, histological analyses supports the threshold model for defect manifestation and indicates that systemic stress is experienced earlier than is indicated by defect depth or size. The first molar has a slow growth (in giraffes) (Hall-Martin, 1976a) and the defects in this tooth are narrowest, indicating that the related stress events were short and intense. (Wider defects would be expected in teeth that develop at faster rates).

6.4.2 Elucidating enamel hypoplasia in *S. hendeyi*

Caries-like defects are rare in *S. hendeyi* indicating that the condition of teeth was good. The high prevalence of both linear and non-linear enamel hypoplasia however indicates that stress episode(s) were experienced during tooth development. The interpretation of defects relies heavily on the timing of eruption and development of teeth. The eruption sequence in the sivathere and extant giraffe appear to be similar, but the precise timing of events may be different in these two animals, especially since sivathere teeth are about a third larger than those of extant giraffes. The interpretation of enamel hypoplasia in the sivathere has therefore to be extrapolated from extant giraffe behaviour (and the timing of tooth development).

Deciduous teeth and the top thirds of first molars are completely devoid of linear defects. Since the first molar undergoes most of its development before birth, these results indicate that the *in utero* period was stress-free.

The consistent presence of thin grooves towards the base of the first molar in both *S. hendeyi* and *G. camelopardalis* suggests a similar and consistent short, intense stress episode. This defect is very likely to relate to systemic stress associated with either birth or weaning. Both events represent critical periods of physiological and nutritional stress to the calf (Rodney, 1983) and both have been

associated with LEH in other animals. Birth stress has been documented in Miocene rhinos (Mead, 1999), whereas weaning stress has been reported in humans and primates (Corruccini et al., 1985; Goodman and Rose, 1990; Moggi-Cecchi et al., 1994) as well as in archaeological pigs (Dobney and Ervynck, 2000). Weaning in extant giraffes and the okapi can start as early as 2-3 weeks of age and can be completed within one month (Hall-Martin, 1976b; Reason, 1991). The length of the weaning period however is dependent on the nutritional content of available food and weaning periods of as long as 12 months have been reported in extant giraffes living under unfavourable conditions (Hall-Martin, 1976b). It is extremely difficult to determine whether the observed linear defects in this tooth are associated with birth and/or the onset of weaning, as the timing of these two events are very close. Thin sectioning may elucidate this problem since neonatal lines have been observed in some mammalian teeth developing at birth (Klevezal, 1996). Mead (1999) attempted this strategy to confirm their hypothesis of birth stress in the Miocene rhino dp4, but failed to find a neonatal line in this tooth.

Other defects that may relate to birth are the localised defects in the deciduous premolars. These teeth are at an advanced stage of eruption at birth and these non-linear defects may result from direct trauma to the developing tooth during the prenatal period. Localised defects in human deciduous canines are ultimately the result of poor maternal diet (Skinner, 1986; Skinner and Hung, 1986). If this hypothesis is correct then evidence for poor maternal diet should be detectable in the later erupting teeth. The *S. hendeyi* dp2s have the highest incidence of defects and are the last of the deciduous teeth to erupt.

The development of the m2 in extant giraffes overlaps with m1 development so that the m2 undergoes some of its development during the weaning period. This tooth begins developing at around 1 year of age and erupts at 3 years (Hall-Martin, 1976a). If a weaning stress was responsible for the observed linear defects in this tooth, then these defects should be located towards the top of the tooth crown. 84% of the defects in this tooth are located toward the bottom of the tooth crown. The peak height of defects is 5-8 mm from the base of the tooth. This suggests that weaning is unlikely to be responsible for these defects unless weaning in *S. hendeyi* did not occur at the same time as that in extant giraffes (weaning is further

investigated in Chapter 8). If the nutritional content of the vegetation at LBW was unfavourable to sivatheres then weaning would most likely be prolonged and the defects in this tooth could then relate to the end of the weaning period, a time when the mother is reluctant to let her calf suckle anymore. The end of weaning is likely to be a stressful event to calves. However, if *S. hendeyi* had a flexible birthing season that coincided with the rainy season (as in extant giraffes, Sinclair et al., 2000) then weaning would probably take place at a time when vegetation is flourishing (and not under unfavourable conditions).

Linear defects were observed in all later erupting teeth (m3 onwards) indicating that some other stress period(s) prevailed. The only other phenomena that have been reported to cause LEHs are fevers associated with severe illness (domestic animals: Miles and Grigson, 1990), stressful calf-cow separations (fossil rhino: Mead, 1999), nutritional stress (primates, humans, archaeological pigs: Blakey et al., 1994; Dobney and Ervynck, 2000; Niven, 2002), and stress associated with mating (archaeological pigs: Dobney and Ervynck, 2000). It is unlikely that calf-cow separation is a stressful event for modern giraffes because the independent juvenile does not permanently separate from the mother but remains in the herd. Modern giraffe calves stay in a "crèche" during the first few months of life (3-4 months in giraffes), and begin to move around with adults as early as 6 months. Stress associated with mating on the other hand is difficult to determine. Male giraffes reach sexual maturity at around 3 years and females tend to fall pregnant for the first time at around 4 years and 7 months in the wild (Hall-Martin, 1976a) so that any stress associated with mating should be reflected in the m3, premolars and incisors. It is, however, virtually impossible to establish the timing of this possible stress event in these teeth in the sivathere. If mating was stressful (and seasonal) then one LEH on each of these teeth *could* have developed in association with this event. The heights at which most defects occur in the premolars (Figure 6.13) coincides with the time when mating occurs in extant giraffes. More than one LEH on the tooth crowns of these teeth however, indicate that there was some other underlying (or additional) stress event occurring during development of these teeth. The LEHs in these teeth are of the banded type (i.e. milder) and wide, indicating that this stress episode (whatever it was) was less intense but more prolonged than that experienced during development of the m1. In addition, 35% of teeth have more than one defect

indicating that stress episodes were episodic and perhaps interspersed with more favourable periods.

No specific event can therefore be closely linked to the observed linear defects in *S. hendeyi.* This, together with the finding that enamel defects are widespread in the Langebaanweg fauna (Chapter 5), suggests that adverse conditions prevailed at times. The gross morphology and enamel microstructure of defective enamel closely resembles those observed in association with enamel hypoplasia in wild boar and cervids suffering from fluorosis (Shearer et al., 1978; Kierdorf and Kierdorf, 1989; Kierdorf et al., 1993, 1996, 2000). This together with the irregular wear observed in *S. hendeyi* and other fauna (reported in Chapter 5) suggests that fluoride contamination may have contributed to the manifestation of these defects. The source of a possible fluoride contamination may be fluoride leaching out of rock phosphates (Dingle et al., 1979) that lined the river channel, Pelletal Phosphate Member, at Langebaanweg from where the material in this study originates.

Fourier Transform Infrared analyses did not reveal any obvious differences in the absorbance spectra for defective *S. hendeyi* enamel compared to normal sivathere enamel, indicating that apatite structure is not grossly altered. Fluoride ions typically occupy the OH^- position (also the A carbonate position) (Trombe, 1972) so that a reduction in the amount of type A carbonate and overall carbonate content might be expected. Since the incorporation of fluoride ions and carbonate ions has the opposite effects (LeGeros, 1991), Sponheimer and Lee-Thorp (1999a) suggest that a reduction in type A carbonate content will decrease solubility and increase crystallinity. In addition, the incorporation of fluoride ions into enamel apatites causes a shift in the ν_2 carbonate peak to a lower frequency (Okazaki, 1983).

The type A carbonate content of defective tooth PQL 44053 is slightly reduced compared to normal enamel. (Noise in this region of tooth PQL 59598 prevented type A carbonate from being measured). A corresponding slight reduction in the splitting index (PCI), which is a measure of crystallinity, is present in both defective teeth, but is especially significant in PQL 59598. A reduction in type A carbonate is however reported to cause an increase in crystallinity (Trombe, 1972; LeGeros,

1981) and therefore the meaning of these results is unclear. The reduction in PCI (hence crystallinity) is more substantial and suggests that fluoride ions are unlikely to be present in sufficient quantities in the apatite from defective enamel to have a significant influence. An alternative explanation is that both fluoride ions and carbonate ions have been incorporated. This explanation is supported by the increase in overall carbonate content observed in both PQL 44053 and PQL 59598). Since the effects of each of these incorporations are opposite, they cancel each other out so that the ionic environment within the apatite (and the FTIR spectra) will appear normal. Reduced PCI values are also expected to coincide with lower resolution of the phosphate peaks in the $\nu 3$ PO_4 domain (LeGeros, 1991). This is the opposite of what is observed (Figure 6.14B), suggesting that some diagenetic alteration may have taken place. According to Lee-Thorp (personal communication, 2001), the ratio between the $\nu 4$ phosphate peaks in enamel changes if diagenesis has taken place (due to the rearrangement of phosphate ions during recrystallisation). In modern and unaltered fossil enamel samples, the first peak (565 cm^{-1}) is larger than the second (605 cm^{-1}) and as fossilisation proceeds, this ratio may change. The peaks in one defect tooth (PQL 44053) are similar to that of normal enamel. The altered ratio of these peaks in tooth PQL 59598, however, indicates that there has been some rearrangement of the phosphate ions in this tooth. In addition, the slight shift in the $\nu 2$ carbonate peak to a lower frequency in both defective teeth suggests that the conformation of carbonate has been altered and that some fluoride ions may have been incorporated.

In summary, from FTIR results there is no clear evidence for the presence of excessive fluoride in the defective teeth. The only possible exception is the very small shift in the $\nu 2$ carbonate peak. This shift is however more likely due to fossilisation than the presence of fluoride. In tooth PQL 59598, the high carbonate content, noise in the $\nu 3$ carbonate domain and the change in peak heights in the $\nu 4$ phosphate domain suggests that although apatite structure is preserved, diagenesis has occurred to some degree in this tooth. Thus FTIR results suggest that despite defects closely resembling the gross morphology of defects associated with fluorosis, alone FTIR analyses cannot resolve the question of whether fluorosis is responsible for the observed defects, although this appears unlikely. Not all the teeth of animals that are exposed to high levels of fluoride develop dental fluorosis. Teeth that

develop *in utero* and/or during weaning (i.e. the first molar in cervids) exhibit only minor fluorotic alterations (Kierdorf and Kierdorf, 1997). The first molar in giraffes, which develops during the weaning period, is the least affected tooth in *S. hendeyi*. The defects in this tooth (towards the base of the crown) are likely to be associated with weaning and/or birth. Further analyses are perhaps required to confirm whether abnormally high levels of fluoride are not present in these teeth. Even though enamel hypoplasia is fairly widespread in the LBW fauna (Chapter 5), some other widespread adverse condition/event may have been responsible since excessive fluoride was not detected. This is further investigated in Chapter 8.

6.4.3 Insights from extant comparative data

In extant giraffes, non-linear defects are typically isolated (enamel aplasia and single pits) occurring in one jaw (mandible or maxilla) and on one side of the mouth only. These defects are therefore likely to be the result of isolated localised physical disruption to ameloblasts during enamel formation. Only one patch of non-linear multiple pits was recorded (ZM 35364) in a right M1 whose counterpart (right m1) has a linear groove with pits. This suggests that patches of non-linear multiple pits may in fact be remnants of linear defects that have lost their anterior or posterior ends due to abrasion by the food bolus. Hence the incidence of defects reported must be viewed as an absolute minimum.

Linear defects in extant giraffes are not recorded in any of the animals originating from wildlife reserves, suggesting that the incidence in wild extant giraffes is extremely rare. This may be why no studies report these defects in wild populations. In these giraffes, neither stressful births nor stressful weaning periods were experienced. The three individuals with LEH originate from a zoo (ZM 36655) and unknown localities (ZM 36851, ZM 35364). All three have linear defects in the first molar. The zoo animal has defects in both the premolars and first molars, indicating that the overall health-status of this animal was poor and it is possible that enduring an early stress makes an animal more susceptible to stress events later in life, as suggested by Goodman and Rose (1990).

In one individual with LEH in the first molar (ZM 36851), only three of the four first molars have the defect. The fourth may have developed later or slightly ahead,

"missing" the stress episode. Alternatively, all first molars may not be equally susceptible to stress events. In ZM 36655, the p2 and p3, which usually develop concurrently, have different defects. The p2 has a linear defect, while the p3 has non-linear defects. The mandibular p2 and p3 are however devoid of defects. This indicates that different teeth, in the same jaw, can have different susceptibilities to stress episodes. This difference in susceptibility has been suggested by Goodman and Rose (1990) in studies on human teeth. In addition, *S. hendeyi* anterior teeth typically display the widest defects and the highest THA score, similar to that observed in human dentitions (Ensor and Irish, 1995; Goodman and Rose, 1990), and may therefore be more susceptible to enamel hypoplasia than posterior teeth. Goodman and Rose (1990) further report that even within a tooth, there appears to be differences in the manifestation of defects. This was also found to be present in *S. hendeyi.* A single tooth with a linear defect on the lingual surface and three areas of aplasia on the buccal surface was found (Figure 6.3, PQL 58781), indicating that different parts of the same tooth are not equally susceptible to stress episodes.

6.5 CONCLUSIONS

The prevalence of enamel hypoplasia in *S. hendeyi* is similar to that recorded for Hippopotamidae and higher than that recorded for all bovids, rhinos and other giraffids (see Chapter 5). Since wild extant giraffes do not have these defects, some major adverse stress episode(s) must have prevailed at Langebaanweg.

The correlation between linear and non-linear defects is also high in *S. hendeyi* and suggests that both these defect types should be recorded in analyses of enamel hypoplasia. Dobney and Ervynck (1998) suggested, in order to reduce sample size and duplicate counting, that only one jaw, one side of the mouth and one tooth surface should be investigated. From the results presented here, it is best to analyse all available teeth in analyses of linear enamel hypoplasia and not to ignore non-linear defects, especially if sample size is not large. In theory all teeth that develop during the stress period should manifest a defect (Dobney and Ervynck, 1998) however, modern data presented here suggest that this is not strictly true. In many teeth, several LEHs were observed on one tooth crown (Table 6.5) indicating that these stress episodes were periodic and possibly interspersed with more favourable times. It is possible that these stress events were seasonal. Modern

giraffes are particularly stressed at the end of the dry season mainly because their preferred food, the *Acacia*, looses its leaves at this time so that food is scarce (Hall-Martin, 1976a). Giraffes can die of starvation if the rains do not come soon enough. It is therefore possible that the defects in the sivathere are directly related to nutritional stress during times when foods were scarce and by analogy during drier conditions. There, however, does not appear to be a simple correlation between dietary preference and incidence of LEH or THA score (Chapter 5).

In summary, the results of this enamel hypoplasia analysis in *S. hendeyi* indicate that

i) deciduous teeth devoid of LEHs indicate non-stressful *in utero* development and pregnancies. The localised EH in these teeth may indicate poor maternal diet and that the foetus suffered from some physical trauma during birth or shortly thereafter;
ii) intense periods of stress experienced during the later development of the m1 are likely to be associated with weaning or birth;
iii) m2 defects are unlikely to be associated with weaning;
iv) milder and perhaps more prolonged stress events were experienced soon after weaning (m2 onwards);
v) stress events are periodic and perhaps seasonal.

Results show that only the first molar defects relate to behavioural stress and that no other behavioural stress events (e.g. calf-cow separation, mating etc) can be associated with defects in the other permanent teeth. It appears as if prevailing conditions were poor, periodically; yet nutrition is not solely responsible for the observed defects (Chapter 5). The diet of *S. hendeyi* and the environmental conditions under which defects manifested are investigated in Chapter 7 and 8, respectively.

Chapter 7

DIET OF *SIVATHERIUM HENDEYI*

7.1 INTRODUCTION

In this chapter the diet of *S. hendeyi* is investigated using three different approaches – hypsodonty index (Janis, 1988), mesowear (Fortelius and Solounias, 2000) and a new low magnification microwear method (Solounias and Semprebon, 2002). These three independent dietary assessments each determines diet over a different timescale and each thus provides a different perspective on the dietary regime of sivatheres. The unworn tooth morphology (and hypsodonty index) essentially reflects the results of evolution on the geological time-scale, whereas the gross wear pattern (investigated by mesowear) reflects an overall impression of the diet of the animal. The analysis of microscopic wear facets of enamel on the other hand reflects the diet of the last few "meals" prior to death (Solounias et al., 1994). The average tooth size of each *S. hendeyi* mandibular tooth is also reported in this chapter.

7.1.1 Tooth morphology of Giraffidae teeth

Teeth can be categorised based on overall shape (selenodont, lyphodont, bunodont) and/or on crown height (hypsodont, mesodont, brachyodont). All teeth belonging to animals in the Order Artiodactyla are selenodont, as opposed to lyphodont or bunodont. Selenodont teeth have more or less concentric, longitudinally flattened cusps whereas lyphodont teeth have either transverse or combined longitudinal and transverse cusps. Bunodont teeth essentially have blunt, separated cusps, such as those of omnivores and frugivores (Janis, 1988). Teeth that have a crown height that exceeds its anterior-posterior dimension are called hypsodont and the base of the tooth crown of these teeth is contained within the body of the jaw. Hypselodonty is a special case of hypsodonty and refers to rootless teeth, which have crowns that continue to grow throughout life of the individual. Hippopotamus and elephant tusks are examples of hypselodont teeth. Brachyodont teeth are low crowned and the individual cusps are united into lophs. The root-crown junction of these teeth is visible just above the bony tooth socket in dry specimens. The term mesodont is used to describe teeth that are more high crowned than brachyodont

teeth but which are not hypsodont. Giraffidae teeth are selenodont (in terms of shape) and brachyodont (in terms of crown height).

In addition to tooth categories, each cusp and wear facet on each tooth type has a distinct name, making the nomenclature of teeth terminology rich. The cusps of mammalian teeth were named by Arambourg (1947) (Figure 7.1). The main (or primary) cusps are called cones in the maxillary teeth and conids in the mandibular teeth. The lingual ones in the maxillary teeth are from anterior to posterior, the protocone and the hypocone and in mandibular teeth are the paraconid, metaconid and entoconid. Buccal cusps are the paracone and metacone (in maxillary teeth) and the protoconid and hypoconid (in mandibular teeth). Secondary cusps are also named as shown in Figure 7.1. In extant giraffes, several cusps and styles have lost their individuality and have fused into crests or lophs (Hall-Martin, 1976b). With gradual attrition, the pointed crests of the apex of each loph is level in the anterior-posterior plane while at the same time broadens along the buccolingual axis.

Singer and Boné (1960) noted that African Sivatheriinae have significantly larger teeth than extant giraffes (*Giraffa camelopardalis)* and that the length of the premolar-molar series is ~ 60% of the length of the jaw, compared to only 40% in extant giraffes. They suggest that there may be a selective advantage in a broader grinding surface for side-to-side masticatory movements.

7.1.2 Diet of extant Giraffidae

The two extant species of Giraffidae - the okapi (*Okapia johnstoni*) and the giraffe (*G. camelopardalis*) – are both nearly exclusive browsers taking leaves, fresh shoots, flowers, pods and fruits from trees (Apps, 1986). The okapi inhabits forests in central Africa, whereas the long-necked giraffe favours woodland habitats but does not occur where the canopy is completely closed. Giraffes are independent of water if fresh green food is available and can occur in very arid areas.

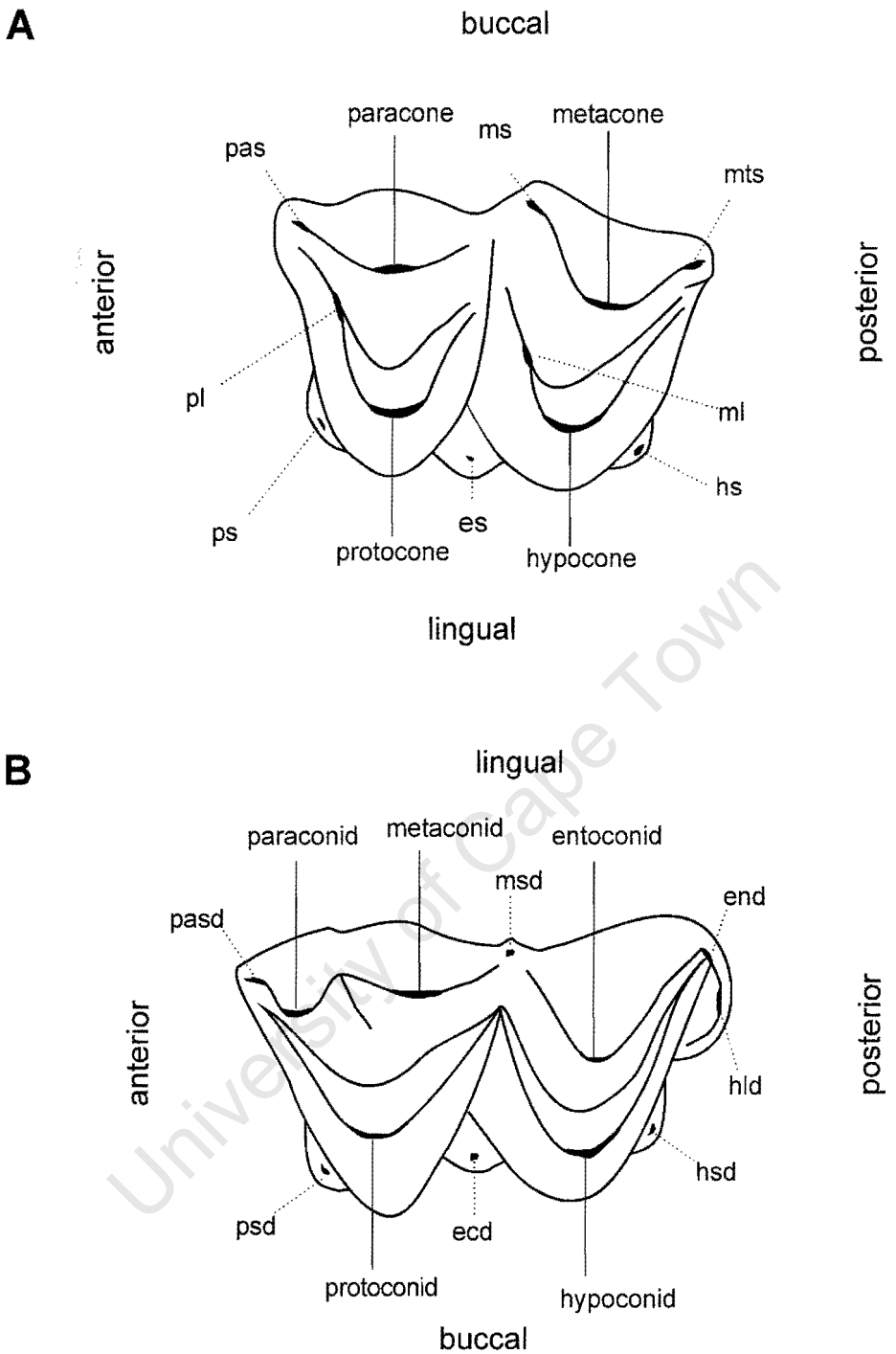

Figure 7.1. Schematic representation of giraffid molars (modified from Singer and Boné, 1960). (A) upper molar, (B) lower molar. Primary cusps are labelled in full, secondary cusp are abbreviated as follows.

Upper molar		Lower molar	
Paraconule	pl	Hypoconulid	hld
Metaconule	ml	Protostylid	psd
Parastyle	pas	Ectostylid	ecd
Mesostyle	ms	Hypostylid	hsd
Metastyle	mts	Parastylid	pasd
Protostyle	ps	Metastylid	msd
Entostyle	es	Entostylid	end
Hypostyle	hs		

7.1.3 Dietary assessments based on teeth

The dietary interpretation of fossil mammalian teeth was previously based largely on comparisons with extant animals (the taxonomic uniformitarian approach) (e.g. by Hendey, 1976, 1981b, 1983a, 1984 for the LBW fauna). However, in the last decade several other methods for determining the diet of extinct animals have been developed. Throughout this chapter, the general classification of dietary classes are defined as follows: browsers take <10% grass, grazers take <10% browse and all other animals are classified as mixed feeders (Hofmann and Stewart, 1972).

Stable carbon isotope analyses have been extensively applied to determine the diets of extinct fauna (Lee-Thorp, 1989; Thackeray and Lee-Thorp, 1992; MacFadden and Cerling, 1994; Bocherens et al., 1996; Cerling et al., 1997a; Cerling et al., 1999; Sponheimer et al., 1999, 2001). Several constraints of this method exist. Firstly, in order to use this method to distinquish between C_3 browsing and C_4 grazing, knowledge that C_4 grasses are present in the ecosystem is required, as well as good preservation. At Langebaanweg, C_3 grasses dominate (see Chapter 3). Secondly, the stable isotope method is slightly destructive (Chapter 3). Another approach of determining whether fossil animals ate C_3 or C_4 grasses is to examine the phytoliths that adhere to teeth. Phytoliths are biogenic opaline silica bodies present in plant cells and are diagnostic for some plant taxa. For C_3 and C_4 grasses, the phytoliths do not differ fundamentally, but where assemblages are well preserved, the identification of phytoliths to family level is possible, enabling a distinction between C_3 and C_4 grasses to be made (Akersten et al., 1988; Bozarth and Hofman, 1998; Gobetz and Bozarth, 2001). Morphological methods to determine diet, relying for instance on premaxillary shape (Solounias et al., 1988; Solounias and Moelleken, 1993a, 1993b; Dompierre and Churcher, 1996) or the ratio of muzzle width to palatal width (Janis and Ehrdardt, 1988), require good anatomical preservation. According to Solounias and co-workers (Solounias et al., 1988; Solounias and Moelleken, 1993a, 1993b) the shape of the premaxillae of grazers is generally wider and less pointed than that of browsers, allowing the intake of more food per bite and less selectivity. Mixed feeders tend to have premaxillae that are intermediate in shape between those of browsers and grazers. In addition, broader muzzles have been associated with the need for a large daily intake of food as seen in grazers (Janis and Ehrdardt, 1988), whereas browsers have narrower muzzles,

which are required for more selective foraging. All morphological characteristics are essentially the product of evolution and as such each animal also has some "evolutionary baggage" that influences the shape of the premaxilla. The disadvantage of morphological methods is that morphology is strongly influenced by phylogeny.

Apart from the methods outlined above, several authors have analysed the patterns of tooth wear and the wear facets left by food (in enamel) to determine diet (Walker et al., 1978; Gordan, 1982; Grine and Kay, 1988; Solounias et al., 1988; Teaford, 1988; Teaford and Robinson, 1989; Hayek et al., 1992; Solounias and Hayek, 1993; Solounias and Moelleken, 1993a; Bernor et al., 1999; Solounias and Semprebon, 2002). Enamel is the most wear resistant dental tissue and this resistance depends largely on the alignment of enamel prisms (discussed in Chapter 3). As soon as a tooth emerges above the gingiva (or gums) it is subject to wear in the mouth, which can be the result of abrasion and/or attrition. The former results from food to tooth contact in contrast to the latter, which is caused by tooth-to-tooth contact. Both types of wear forces act on teeth at all times (Solounias and Semprebon, 2002), but some species have stronger forces of abrasion than attrition and others have stronger attritive forces. In browsers, for example, abrasion is relatively low and attrition is high, whereas in grazers, abrasion is high and attrition is relatively low (Solounias and Semprebon, 2002). Since wear is cumulative over time, it is also used to age teeth in fossil assemblages.

The three methods of assessing the diet of *S. hendeyi* described in this chapter are: (i) unworn tooth morphology and the hypsodonty index, (ii) mesowear analysis and (iii) a light microscope microwear method. Each of these methods are discussed below.

7.1.3.1 Unworn tooth morphology and the hypsodonty index

Although hypsodonty (high-crowned) is generally associated with an abrasive grazing diet (McNaughton et al., 1985), no correlation between lifespan and degree of hypsodonty in living mammals has been found (Fortelius, 1985). Janis (1988) conducted the first quantitative analyses of extant ungulate teeth in order to determine whether tooth crown height does indeed correlate with an abrasive diet.

The hypsodonty index (HI), which is based on crown height and width (see methods 7.2.2.3), of several distinct dietary categories are shown in Table 7.1. Grazers appear to be significantly different from all other feeding types. Mixed feeders in open habitats and fresh grass grazers have the next highest mean HI. Mixed feeders in closed habitats, regular browsers and selective browsers are indistinguishable from each other. However, mixed feeders in closed habitats have a higher mean hypsodonty value than omnivores. In addition Janis (1988) showed that grit accumulated with food when feeding is a more important determinant of the level of hypsodonty than the proportion of fibrous (abrasive) grasses in the diet. (I.e. animals feeding close to the ground in open habitats have high hypsodonty values). Mixed feeders in closed habitats have low hypsodonty values similar to browsers feeding close to the ground, and high-level browsers have the lowest HI values. Although Janis (1988) observed that HI appears to be greater in smaller animals, this could not be substantiated statistically. However, to avoid possible errors Janis (1988) cautions that when comparing HI of fossil ungulates with extant taxa, one should use animals of approximately similar body size.

Hypsodonty is affected by both attritive and/or abrasive forces (Solounias et al., 1994; Solounias and Semprebon, 2002) and is regarded as an overall proxy for diet, but not as a reliable indicator. Fortelius and Solounias (2000) showed that the hypsodonty index is only 60% accurate in determining the diets of extant ungulates.

Table 7.1. Hypsodonty indices for different dietary groups (Janis, 1988).

Diet type	n	Mean HI ± std. error	Range
Grazers	11	4.78 ± 0.21	3.8-6.1
Mixed - open habitat	40	3.89 ± 0.12	2.5-5.3
Fresh grass grazers	8	3.20 ± 0.26	1.9-4.1
Mixed - closed habitats	21	2.05 ± 0.11	1.1-3.0
Regular browsers	13	1.65 ± 0.09	1.2- 2.3
Selective browsers	3	1.5 ± 0.08	1.3 - 1.7
High level browsers	7	1.28 ± 0.18	0.8 - 2.2
Omnivores	6	1.16 ± 0.06	1.0 - 1.3

According to Janis (1988) the term brachyodont should be restricted to ungulates with a HI of less than 1.5, mesodont ungulates have a HI of between 1.5 and 3.0 and the term highly hypsodont should be used for hypsodont species with a HI of more than 4.75. Almost all living ungulates that fall into the last category are grazers. Fortelius and Solounias (2000) however, partitioned ungulate species into these three categories of diet differently. Their tripartite subdivision of hypsodonty index was, however, for convenience only and is therefore subjective. Their division allows the hypsodonty of most taxa to be determined by direct observation. They defined mesodont artiodactyls as having hypsodonty indices of between 2.6 and 3.4, brachyodont artiodacyls have indices of 2.5 or lower and hypsodont teeth have indices of 3.5 and higher. Although there does not appear to be a consensus on the HI associated with each tooth morphology type, most authors agree that HI are not good determinants of diet and should not be used in isolation (Fortelius and Solounias, 2000).

7.1.3.2 Mesowear analyses

Mesowear analyses are based on a combined result of the relative amounts of attritive and abrasive wear on occlusal dental enamel. This relatively new method of dietary assessment has reported to accurately determine the diet of 64 species of extant ungulates (Fortelius and Solounias, 2000). It has further been applied to fossil equids (Fortelius and Solounias, 2000; Kaiser et al., 2000). The mesowear technique is dependent on two variables that are observable on the buccal side of teeth, namely cusp relief and cusp shape. Cusp relief is defined as the relative difference in height between cusp tips and inter cusp valleys. Low relief is the result of high attritive and abrasive forces as seen in exclusive grazers. Cusp shape is the result of the relative contribution of abrasion and attrition to the total wear and refers to the shape of the apex of the cusp, which can be rounded, blunt or sharp. It is independent of hypsodonty. Sharp cusps indicate that attrition predominates, whereas for blunt cusps attrition is almost completely masked by abrasion. Cusp relief and cusp shape are not entirely independent but converge at the low, blunt end of the spectrum. These variables are described in more detail in methods section 7.2.2.4.

Fortelius and Solounias (2000) found that browsers and mixed feeders generally have high occlusal relief and no browser with less than 80% high relief was found. No extant grazer has more than 40% sharp cusps and no browser or mixed feeder has more than 10% blunt cusps. In this study mesowear identified four main dietary groups from abrasion-dominated to attrition-dominated: grazers, graze-dominated mixed feeders, browse-dominated mixed feeders, and browsers. By combining HI with mesowear, the accuracy of dietary interpretations of extant species was ~ 75% accurate. However, hypsodonty and mesowear tend to sway dietary classifications in opposite directions. Hypsodonty pulls the result towards a more conservative classification[1] while mesowear pulls it toward a more radical classification[2].

A constraint of the mesowear technique is that it cannot distinguish between the different particles causing abrasion (i.e. dust/grit versus food). Fortelius and Solounias (2000) therefore suggest using mesowear determinations of diet in combination with microwear analyses. This is the approach taken in the current analysis.

7.1.3.3 Microwear analyses

Microwear analysis is a technique based on the analysis of microscopic wear facets. It was identified almost two decades ago and relies on the relative proportion of pits versus scratches seen in scanning electron micrographs of occlusal enamel. This method essentially reflects the "last" meal (i.e. couple of meals) of an animal before death and has been applied extensively to determine the diet of fossil animals (Walker et al., 1978; Solounias et al., 1988; Teaford, 1988; Hayek et al., 1992; Solounias and Hayek, 1993; Solounias and Moelleken, 1993a; Bernor et al., 1999). A constraint however is that well preserved, undamaged occlusal surfaces are required. Recently, Solounias and Semprebon (2002) have established a low magnification method for examining these microwear facets. This simplified method uses high-resolution casts of wear surfaces that can be easily examined under the light microscope. The method is described fully in section 7.2.2.5.

[1] Where species with doubtful diets are classified as mixed feeders.
[2] Where doubtful species are classified as extreme grazers or browsers.

Solounias and Semprebon (2002) found that the average number of scratches is more diagnostic of diet than pit counts. They define traditional browsers as having 0-17 scratches and traditional grazers as having more than 17 scratches per unit area (0.5 mm by 0.5 mm). However, Solounias and Semprebon (2002) found that many species did not fall into the expected categories. For example, they found that half the teeth of *Okapia johnstoni* have counts of 17.5 to 28 scratches, yet it is a browser. By introducing four additional variables of microwear (scratch texture, cross scratches, large pits, and gouges), which have not been identified by previous microwear studies, they were able to further resolve the dietary spectrum into five categories – with browsers at one end, grazers at the other end and a transitional browsing-grazing group in the middle. This transitional browser-grazing zone comprises additional browser and grazing species as well as mixed feeders. Solounias and Semprebon (2002) find no patterning when comparing the microwear variables of hypsodont, mesodont and brachyodont ungulates, however, general agreement with mesowear results was obtained. Table 7.2 gives average pit and scratch counts for dietary categories identified by Solounias and Semprebon (2002).

Table 7.2. Average number of pits and scratches for extant ungulates (from Solounias and Semprebon, 2002). Means ± standard deviations are given. 'n' refers to the number of species in each category.

	Average pits	**Average scratches**	**n**
Grazers	11.42 ± 6.4	25.51 ± 3.42	9
Mixed feeders	19.55 ± 9.7	20.57 ± 5.4	20
Browsers-leaf dominated	16.30 ± 9.6	10.16 ± 3.5	7
Browsers-fruit dominated	24.88 ± 6.23	21.0 ± 4.33	16
Browsers dry habitats	44.80 ± 27.7	12.8 ± 2.7	4
Elephants	12.9 ± 4.3	26.32 ± 2.6	2
Hippopotamus	15.86	25.43	1

Results show that browsers have distinct scratches, which are clearly separated from one another by areas of enamel with no scratches. In contrast, in grazers scratches are often superimposed on top of one another with no non-scratched enamel in between. Thus this enamel appears duller in appearance. For this reason, Solounias and Semprebon (2002) indicate that they may have undercounted scratches in grazers. Browsers also appear to have mostly fine

scratches compared to open country grazers that have more coarsely textured scratches. This finding lead Solounias and Semprebon (2002) to suggest that C_3 plants may be finer than tropical C_4 grasses. C_4 plants are high in fibre and contain cells with large bundle-sheaths compared to C_3 plants (Heckathorn et al, 1999). These structural characteristics increase the leaf resistance of C_4 plants to shearing and tearing, and hence one would expect them to leave coarser scratches in enamel than C_3 plants. Typical grazers are defined as having few small pits, a narrow range of scratches, and a mixture of fine and coarse scratches within the same tooth. Mixed feeders were polarised into low-scratch versus high-scratch groups depending mostly on the relative amounts of browse versus grass consumed in their diet. Seasonal mixed feeders have similar results to those of traditional browsers when they browse, however when they graze, these same animals have more pits and a greater dispersion of coarse scratches. It is possible that more pits may be a consequence of these wear facets remaining longer on the occlusal enamel surface, whereas additional scratches are "added" or superimposed during the grazing phase (Solounias and Semprebon, 2002).

Fortelius and Solounias (2000) also found that animals inhabiting dry habitats (for example camels) have an unusually high number of small pits and a very low number of fine scratches. They suggest that grit accumulated with food may affect microwear facets by excessively scarring the enamel with coarser (deeper and wider) scratches, rather than by excessive pitting. That is, animals that incorporate grit with food, such as those feeding close to the ground, have coarse scratches.

A constraint of this methodology is that unlike with the traditional scanning electron microscope (SEM) microwear method where counts are made from SEM micrographs, there is no actual record of the areas counted or the morphology of microwear features. Microphotography of these features has proved to be very problematic (Solounias, personal communication, 2002) because pits and scratches require different optimal lighting conditions. On the other hand, the main advantage of the light microscope method of examining microscopic wear facets is that it is much quicker and more cost effective than the traditional SEM method.

Although most authors agree that no single method of dietary assessment is superior, there are problems when trying to use more than one method. For example, authors using different tools identify different trophic feeding types so that methods cannot easily be compared. Janis (1988) identifies dry grass grazers, fresh grass grazers and high-level browsers, whereas Solounias and Semprebon (2002) could not find a matching pattern to these trophic types and identified leaf-dominated browsers, fruit-dominated browsers, mixed feeders and grazers. Despite the complexity this creates when comparing the different dietary assessment methods, each method approaches diet from a different angle and therefore together will provide a better understanding of the diet of an extinct species than any single method used in isolation.

7.1.4 Diet of fossil Giraffidae

The diet of fossil Giraffidae was until recently thought to be similar to that of extant giraffes (i.e. that they were committed browsers), however Solounias and co-workers (Solounias et al., 1988 Solounias and Moelleken, 1993b) have shown, using traditional tooth microwear analyses and premaxilla shape, that the diets of fossil Giraffidae are highly heterogeneous. Many giraffids can be classified as grazers, including the following Sivatheriinae – *Bramatherium megacephalum* and *Sivatherium giganteum.* One mixed feeding Sivatheriinae, *Giraffokeryx punjabensis,* and two browsing sivatheres (*Hallodotherium duvemoyi* and "*Palaeotragus" primaevus*) were also identified. Amongst the Giraffinae and Palaeotraginae there are also grazing and mixed feeding forms. According to Solounias et al. (2000), different dietary strategies for Sivatheriinae (compared to extant giraffes) are not unexpected considering their short-necks, stout metapodials and large body size. They further suggest that amongst the sivatheres there was a transition in diet from a more primitive mixed feeding behaviour (seen in the ancestral *Giraffokeryx punjabensis)* to a grazing feeding strategy (seen in sivathere descendants). In addition this grazing was probably taking place within forested habitats. Their data therefore suggests that grazing was taking place before the expansion of C_4 grasslands at around 6 to 8 Myr (Cerling et al., 1997b), and thus that these giraffids were grazing on C_3 grasses, which are the dominant type in wooded environments. The only African Sivatheriinae *sensu lato* investigated in this study, the Miocene

"*Palaeotragus*" *primaevus* (Fort Ternan, Kenya) was found to be a browser, indicating that by this time the browsing feeding strategy was retained.

The diet of the Early Pliocene sivathere, *S. hendeyi*, is not only important to help elucidate dental defects (reported in Chapter 4 and 6) but also because it should provide clarity on the evolution of feeding strategies of African Sivatheriinae, especially in Southern Africa where no data is currently available.

7.2 MATERIAL AND METHODS

7.2.1 MATERIAL

The database of *S. hendeyi* teeth available for examination was listed in Table 5.1, Chapter 5). To obtain average tooth dimensions of *S. hendeyi* teeth, the following unworn or slightly worn teeth were measured. Permanent teeth: 338 incisors, 36 canines, 68 p2s, 47 p3s, 27 p4s, 9 m1s, 6 m2s and 16 m3s. Deciduous teeth: 5 incisors, 19 canines, 6 dp2s, 2 dp3s. No unworn dp4s were available and average crown height of these teeth could not be determined, however 46 worn dp4s were measured to obtain buccolingual and anteroposterior dimensions. A single almost complete mandible was recently excavated at the *in situ* LBW dig site (at the West Coast Fossil Park), and this jaw was also measured.

Isolated first and second molars were sorted according to the dimensions of twelve associated specimens (Appendix L). The hypsodonty index was determined based on the measurements for 11 unworn or very slightly worn m3s (Appendix M). A single unworn *G. camelopardalis* m3 was also measured.

According to Fortelius and Solounias (2000), the mesowear pattern is stable after 20 to 30 individuals and gives a fairly reasonable approximation after about 10. Thirty maxillary and thirty mandibular second molars (M2 and m2, respectively) were therefore selected for mesowear analyses. Although this method was initially established on M2s (by Fortelius and Solounias, 2000), its robusticity was evaluated by applying the method to m2s as well. For microwear analysis 53 m2s were analysed. The accession numbers of these teeth are provided in Appendix N and O respectively, together with raw data.

7.2.2 METHODS

7.2.2.1 Sorting *S. hendeyi* teeth

The majority of S. *hendeyi* teeth were sorted into tooth types during early excavations. The incisors (i1, i2, i3) were unsorted and could not be sorted further into their relative positions in the jaw since no complete *S. hendeyi* mandible with anterior teeth in tact has been found. In addition, the average anteroposterior and buccolingual dimensions of these teeth in *G. camelopardalis* overlap with one another (Singer and Boné, 1960, and own observations). The measurements for deciduous incisors also overlap with permanent incisor dimensions in the extant giraffe, so these teeth were not easily distinguishable from one another, hence the small sample size.

According to Singer and Boné (1960), the diagnosis of Sivatheriinae teeth is complicated by the great breadth of the tooth near the root-crown junction and because of fusion of the cones/conids at different wear stages. Isolated m1 and m2s were sorted according to anteroposterior and buccolingual measurements.

7.2.2.2 Tooth Dimensions

Teeth with unworn crown heights were measured in order to determine the average dimensions of each tooth type. Maximum unworn crown heights, anteroposterior lengths and buccolingual widths were measured to the second decimal place using digital callipers. The dental index of each tooth type was calculated by dividing the buccolingual dimension by the anteroposterior one, and is expressed as a percentage. Roots were seldom present in isolated teeth and therefore were not analysed. The length of the *in situ* mandible from the West Coast Fossil Park was also measured from the anterior to posterior end and the tooth row length was measured from the anterior aspect of the canine to the posterior aspect of the last visible molar (the m2).

7.2.2.3 Hypsodonty index determination

The hypsodonty index (HI) for *S. hendeyi* was determined according to Janis (1988) as follows:

$$HI = \frac{\text{unworn m3 height}}{\text{m3 width}}$$

For both fossil and extant specimens, the unworn m3 height was measured on the anterior cusp from the base of the crown to tip of the protoconid. Width was measured from the outer protoconid to the outer entoconid, according to the method of Janis (1988). Statistical analyses were performed using Statistica (version 6.0).

7.2.2.4 Mesowear analyses

The mesowear method developed by Fortelius and Solounias (2000) was used to determine the average diet of *S. hendeyi* based on cusp relief and cusp shape. Cusp or occlusal relief is the relative difference in height between cusp tips and valleys and was calculated by dividing the distance from the valley base to cusp tip by the crown height as shown in Figure 7.2A. Measurements were taken with digital callipers to the second decimal place. For selenodont forms, the limit between high cusp relief and low relief was arbitrarily set at 0.1 (Fortelius and Solounias, 2000). Cusp shape describes the apex of the buccal cusp (protoconid or hypoconid for lower teeth; paracone and metacone for upper teeth) and is described as sharp, blunt or rounded (Figure 7.2B). Cusp shape was determined by direct observation of the degree of facet development. A sharp cusp is pointed with no rounded edges, a rounded cusp has a distinctly rounded tip without planar facet wear but with facets on the lower slopes, and blunt cusps lack distinct facets altogether. The percentage of rounded, sharp and blunt cusps in the sample of *S. hendeyi* teeth analysed was then determined for the species. Finally, these variables were plotted against hypsodonty index as recommended by Fortelius and Solounias (2000) since combining HI with mesowear produces more accurate dietary determinations.

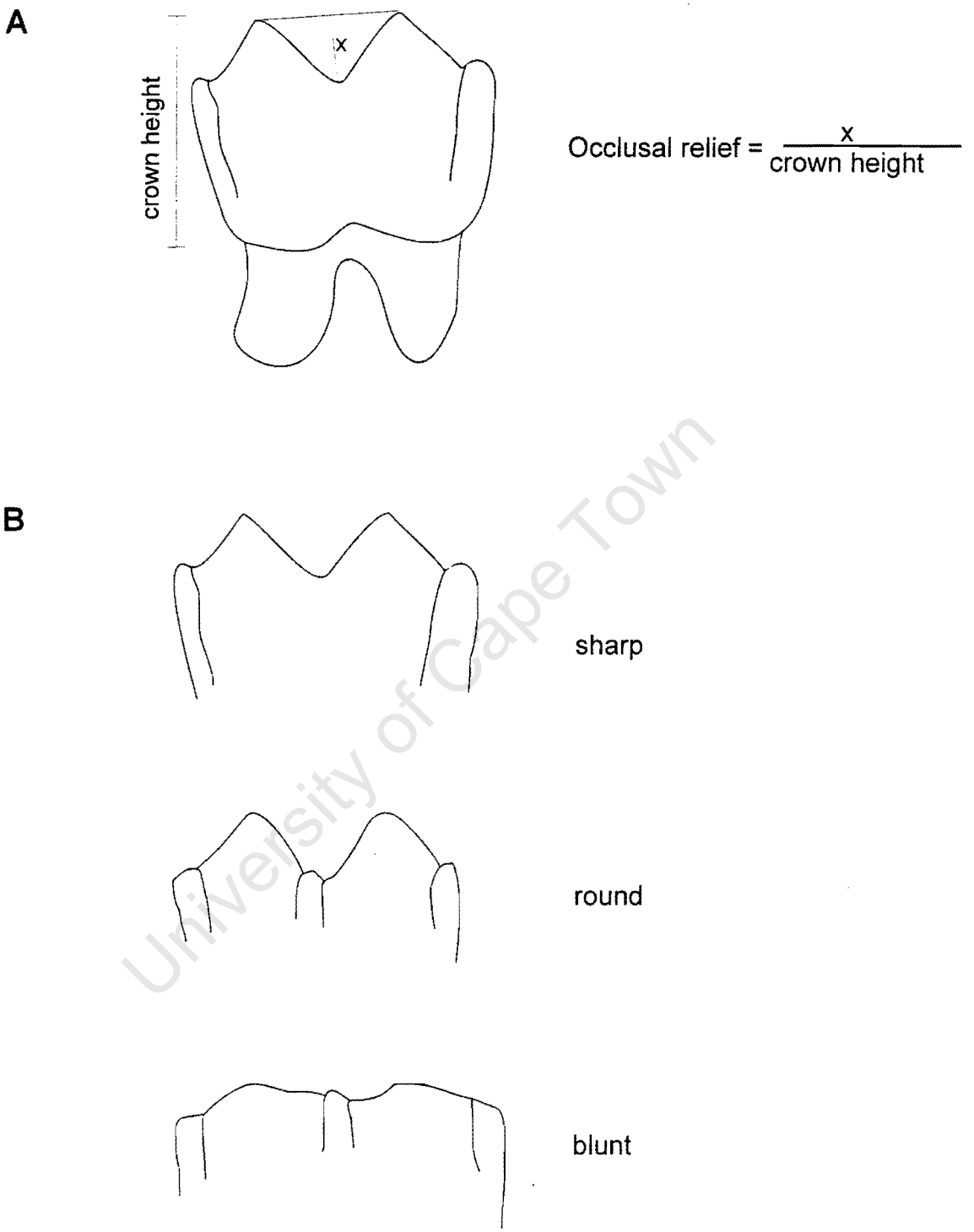

Figure 7.2. Diagram showing mesowear variables. (A) cusp or occlusal relief, which is calculated by dividing the height of a valley between two adjacent cusps (x) by the total crown height of the tooth. (B) cusp shape can be sharp, round or blunt.

7.2.2.5 Microwear analyses

The light microscope method for examining microwear scar topography established by Solounias and Semprebon (2002) was used and is outlined below.

Teeth were cleaned with cotton swabs dipped in 95% alcohol and allowed to dry. The occlusal surface of each tooth was then moulded twice using high precision polyvinylsiloxane dental impression material (President Plus Jet Regular Body, Surface Activated 4605 – Coltene/Whaledent Inc.). The first mould was not analysed and was considered a final cleaning step. The second mould was sent to the U.S.A and clear epoxy casts were made by Nikos Solounias (New York College of Osteopathic Medicine) according to the procedure outlined in Solounias and Semprebon (2002). These casts were then returned to South Africa and examined for microwear scarring. The microwear features on the casts were examined using a stereomicroscope. Oblique transmitted bright field lighting illuminated scratches optimally whereas pits, which are highly reflective, were best viewed using spot-lights shone directly onto the reflective surface. Using an eyepiece fitted with an ocular graticule, pits and scratches were counted in four graticule quadrants equating to 0.5 mm by 0.5 mm, at 35x magnification (as in Solounias and Semprebon, 2002). Counts were made in two representative areas of the enamel band as recommended by Solounias and Semprebon (2002) to standardise the methodology. The average number of pits and scratches per cast was then determined and used to obtain an average for the species. Pits were also classified as small or large. If more than four large pits were present in the counting fields then pits for that tooth were recorded as large. Scratches were qualitatively scored by determining whether i) only fine scratches were present, ii) only coarse scratches were present, or iii) whether a mixture of fine and coarse scratches were present within the counting area. The presence of four or more cross scratches per counting area was also recorded, as well as the presence of four or more large, deep elongated pits, which were classified as gouges.

Solounias also examined these casts for microwear facets independently and results were compared in order to test the method for intra-observer differences (see section 7.3.4.1).

The relative proportion of browsing versus grazing for the species as a whole was determined by calculating the percentage of teeth with more than 17 scratches (indicating grazing) and those with less than 17 scratches (indicating a browsing phase). The average pit and scratch counts for each phase was also calculated. Statistical analyses were performed using Statistica (version 6.0).

7.3 RESULTS

7.3.1 Tooth size

22% of the isolated m1 and m2s could not be sorted because buccolingual and anteroposterior measurements of m1 and m2s overlap (Figure 7.3 and Appendix L).

The average sizes of *S. hendeyi* mandibular teeth are given in Table 7.3. The most complete mandible in the collection is shown in Figure 7.4. The mandible measures 0.6 meters from the anterior to posterior end and the tooth row length from canine to m2 is 0.45 meters.

7.3.2 Hypsodonty index

The hypsodonty index obtained for the extant giraffe is 1.19 (25.29 mm/ 21.10 mm), which is identical to the published value of 1.2 (Janis, 1988). The hypsodonty index for the two unworn *S. hendeyi* third molars is 1.46 and 1.55, giving an average HI of 1.51 ± 0.06 (n =2). Raw data is provided in Appendix M. However, in order to increase sample number slightly worn m3s were subsequently included. This had the effect of decreasing the average HI to 1.30 ± 0.1 (n = 9). The range for this sample is 1.22 to 1.55. These two average HI are however, statistically different (two-tailed Student's t-test for independent samples, t = -2.91, df = 9, $p<0.05$), and therefore for all subsequent analyses the HI for completely unworn teeth is used.

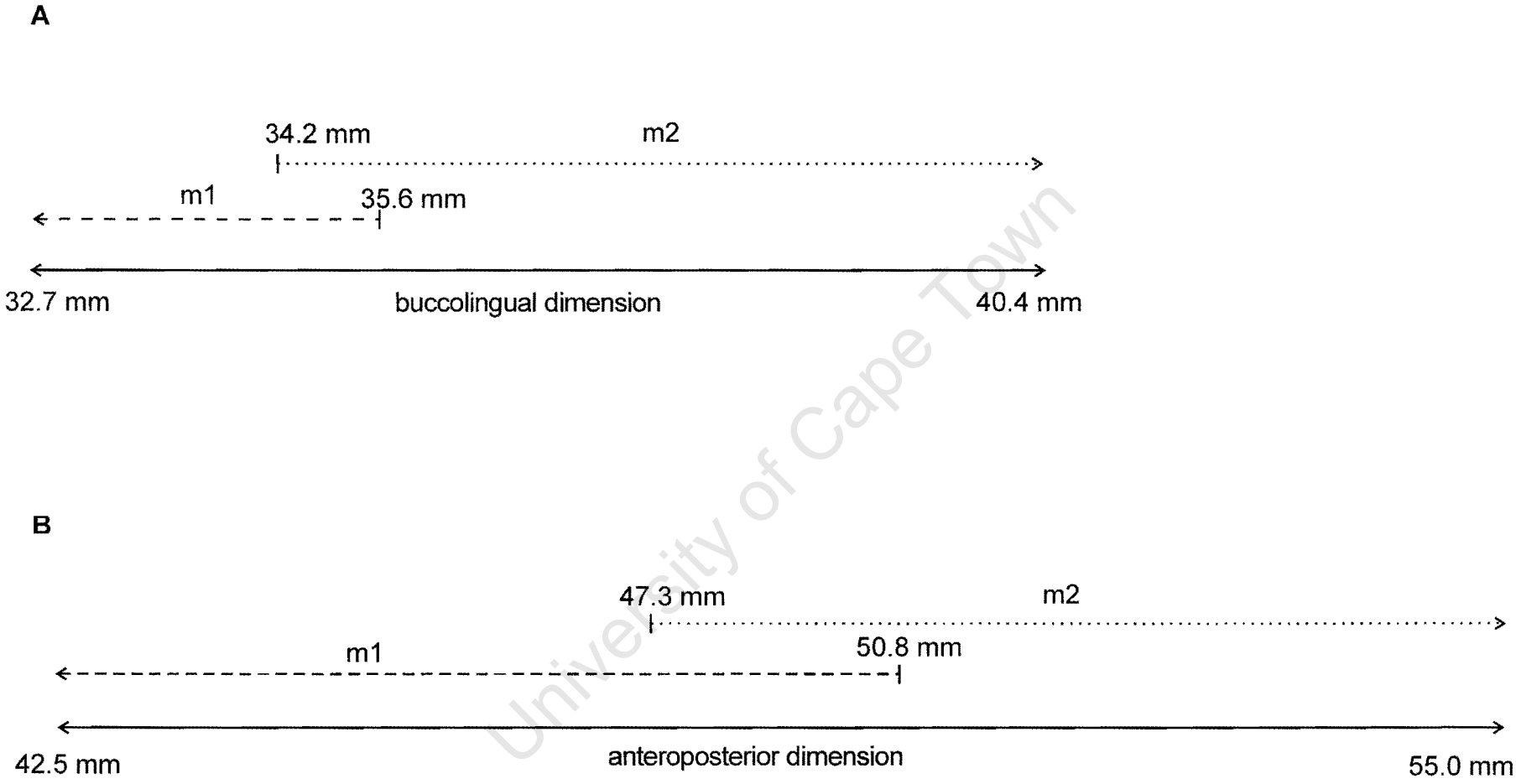

Figure 7.3. Dimensions used to distinguish mandibular first and second molars of *S. hendeyi.* (A) buccolingual dimensions and (B) anteroposterior dimensions. First molar (m1) range is indicated with dashed line and second molar (m2) range is indicated with a dotted line.

Table 7.3. Average unworn crown height, buccolingual and anteroposterior measurements of *S. hendeyi* mandibular teeth. Numbers in parentheses indicate range of values from minimum to maximum. 'n' indicates the number of teeth measured. All measurements are given in millimeters. Dental index is calculated by dividing the buccolingual measurement by the anteroposterior measurement (after Singer and Boné, 1960).

Tooth type	Crown height	Buccolingual	Anteroposterior	Dental index (%)	n
di	27.51 (25.6 - 30.8)	11.92 (11.1 - 13.1)	17.27 (16.4 - 19.1)	69.1 (66.5 - 74.9)	5
dc	19.03 (12.7 - 23.1)	8.88 (8.0 - 10.1)	22.08 (19.3 - 25.4)	40.4 (33.7 - 46.3)	19
dp2	17.34 (13.8 - 21.64)	11.17 (9.6 - 13.6)	23.62 (20.9 - 26.5)	47.3 (43.0 - 54.0)	6
dp3	19.48 (19.0 - 20.0)	16.89 (15.8 - 18.0)	34.08 (33.8 - 34.3)	49.5 (46.7 - 52.4)	2
dp4*	-	26.27 (21.9 - 34.4)	55.17 (47.7 - 64.8)	47.6 (40.5 - 54.9)	46
i1-i3	33.94 (21.1 - 23.1)	17.52 (11.8 - 26.7)	20.52 (16.7 - 28.7)	85.6 (57.1 - 127.9)	338
c	27.41 (21.4 - 30.9)	14.18 (9.1 - 15.6)	27.32 (23.1 - 31.6)	52.0 (39.5 - 63.0)	36
p2	24.99 (21.1 - 31.0)	16.25 (13.8 - 19.2)	29.13 (25.4 - 33.2)	55.9 (48.6 - 66.7)	68
p3	37.86 (20.9 - 48.0)	29.94 (22.1 - 29.8)	39.17 (34.7 - 45.1)	66.3 (56.4 - 77.9)	47
p4	41.23 (29.2 - 47.1)	30.58 (24.6 - 34.1)	43.33 (34.9 - 47.9)	70.7 (64.2 - 81.7)	27
m1	43.17 (40.3 - 46.2)	32.07 (29.9 - 34.9)	48.61 (44.9 - 51.6)	66.2 (58.0 - 77.8)	9
m2	45.25 (39.8 - 52.8)	38.66 (35.1 - 49.9)	54.33 (50.8 - 57.8)	71.3 (62.3 - 91.8)	6
m3	42.53 (31.9 - 46.7)	32.24 (28.6 - 35.0)	65.34 (54.7 - 69.0)	50.2 (46.6 - 57.0)	16

* no unworn dp4s were available and therefore measurements for worn teeth are given.

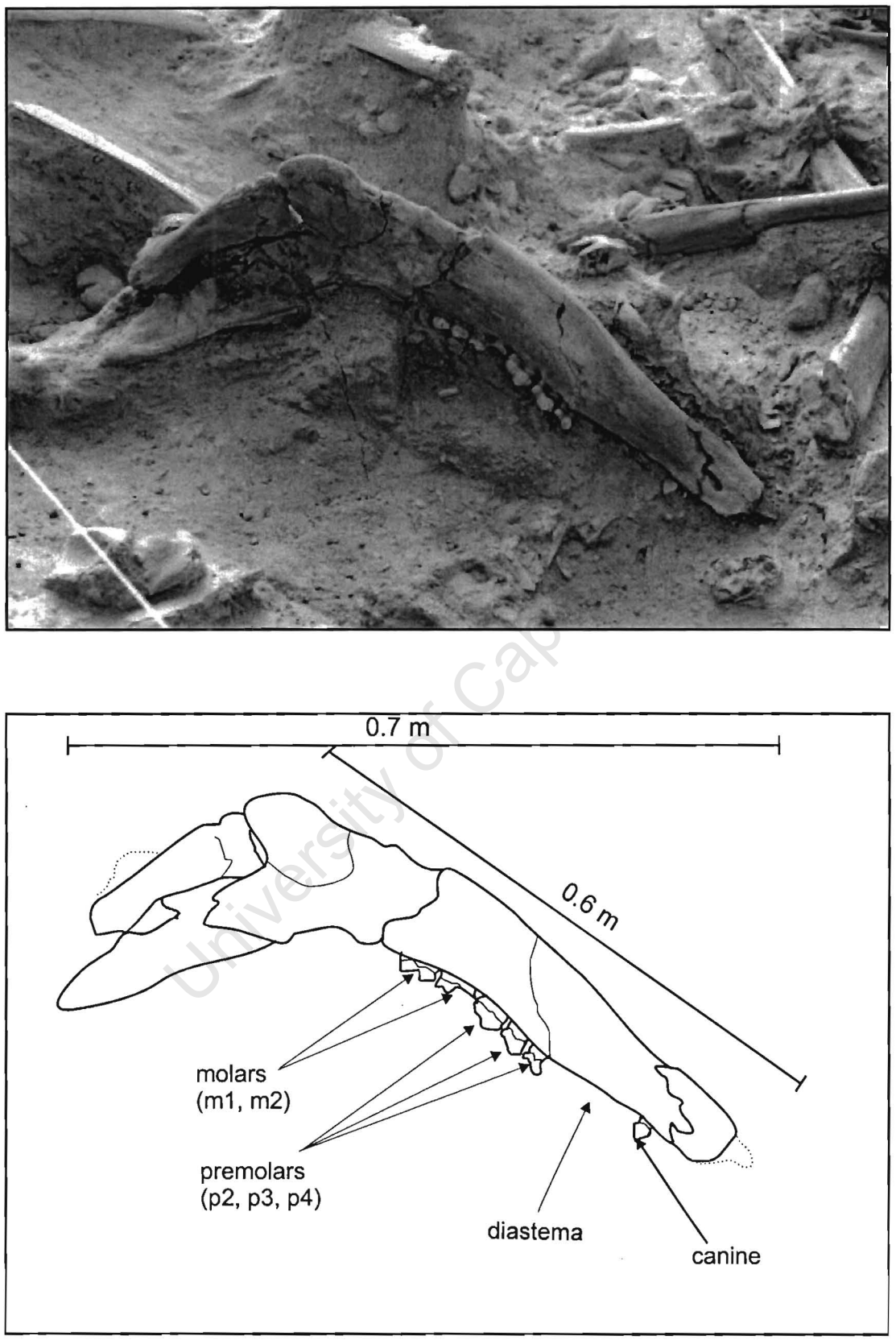

Figure 7.4. The most complete *in situ S. hendeyi* mandible at the West Coast Fossil Park. (A) photograph of the mandible and (B) outline of the mandible in (A), the permanent teeth and mandible size are indicated.

7.3.3 Mesowear analysis

The raw data for each mesowear variable is provided in Appendix N. The average occlusal relief for upper teeth is 0.221 ± 0.04 (n = 30) and ranges from 0.136 to 0.341. That is, all *S. hendeyi* teeth have high relief (according to the arbitrary division between low and high relief set at 0.1 by Fortelius and Solounias, 2000). In terms of cusp shape, *S. hendeyi* has 63% round cusps, 37% sharp cusps and no blunt cusps.

Very similar results were obtained for lower teeth. Average occlusal relief is almost identical to that for upper teeth (0.221 ± 0.03, n = 30). There is however some difference in cusp shape between upper and lower teeth (Figure 7.5). Lower teeth have slightly more rounded (77%) and fewer sharp (23%) cusps than upper teeth. No blunt cusps were observed in the entire sample.

7.3.4 Microwear analysis

Average values for each microwear variable are given in Table 7.4 and raw data is provided in Appendix O. A comparison of my results with those obtained by Solounias (for the same casts) is provided in section 7.3.4.1. The average number of pits and scratches for *S. hendeyi* was 27.5% and 11.2% respectively per unit area. Pit and scratch counts per counting area varied greatly from tooth to tooth. Pit counts ranged from 3 to 70 and scratch counts ranged from 1 to 36 per counting area. Examples of these microwear facets are show in Figure 7.6. In *S. hendeyi* large pits were present in 41.5% of teeth and are more common than cross scratches and gouges. Scratch textures also differed markedly between teeth with some teeth having only fine scratches (35.8%), some having only coarse scratches (20.8%) and some having both fine and coarse scratches (43.4%).

Most *S. hendeyi* teeth (92%, n=49) had scratch counts less than 17 (indicating browsing) whereas some (8%, n=4) have scratch counts greater than 17 (indicating grazing). The average pit and scratch counts for each feeding phase are shown in Table 7.5.

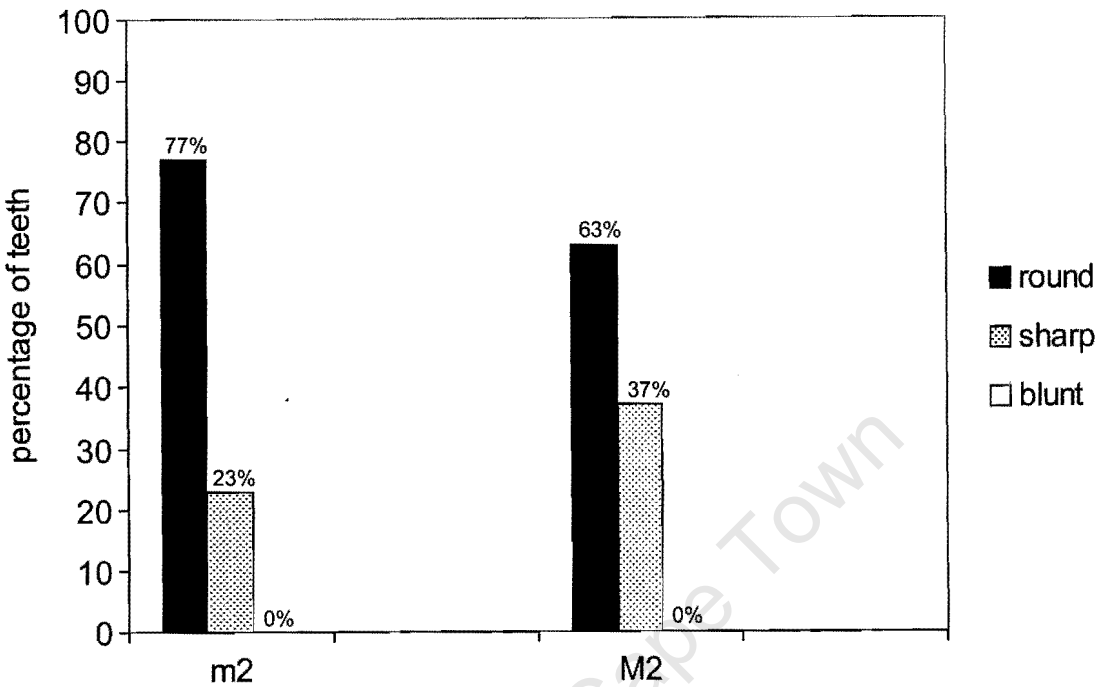

Figure 7.5. Mesowear cusp shape results for *S. hendeyi* lower (m2) and upper (M2) molars.

Table 7.4. Microwear data for *S. hendeyi*. Average number of pits and scratches are reported. The percentage of large pits (LP), cross-scratches (CS), gouges (GOU), fine, coarse and mixed scratch textures are also reported.

	N	pits	scratches	LP	CS	GOU	Fine	Coarse	Mixed
S. hendeyi	53	27.5	11.2	41.5	9.4	18.9	35.8	20.8	43.4

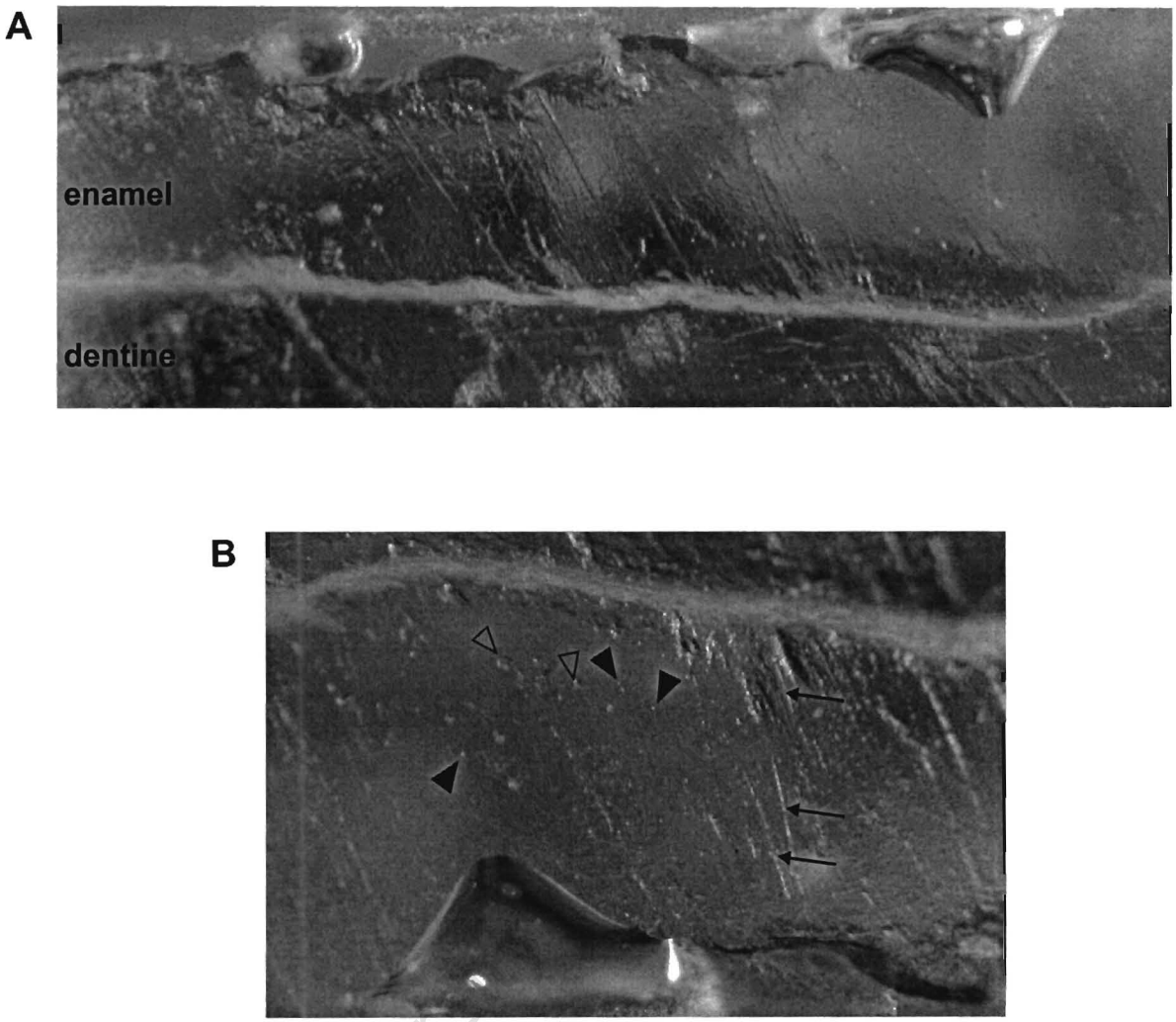

Figure 7.6. Microwear facets on casts of *S. hendeyi* m2s. (A) low magnification showing enamel band with many scratches and a few small reflective pits. (B) Higher magnification of an enamel band. Arrows indicate scratches and arrowheads indicate pits. Both small (closed arrowheads) and larger pits (open arrowheads) are indicated. Scratches are more common on the right of the field shown and pits are common in the middle of the field shown. Magnification in (A) is 27.5x and in (B) is 58.5x.

Table 7.5. Proportion of browsing and grazing in *S. hendeyi*. Average numbers of pits and scratches are given for each phase.

	Browsing phase		Grazing phase	
	Pits	**Scratches**	**Pits**	**Scratches**
S. hendeyi	27.0	10.3	33.0	21.6

7.3.4.1 Robusticity of the microwear method

The microwear data for *S. hendeyi* was compared to the data obtained by Solounias (NS) in his analysis of the same casts (Appendix P). The average number of pits and scratches obtained by Solounias are 20.5% pits and 15.8% scratches. Each of these averages is statistically different from those obtained in the current analysis (two-tailed Student's t-test for independent samples: for pits, t = 2.41, df = 103, $p<0.05$; and for scratches: t = -3.87, df = 103, $p<0.05$). In addition, NS obtains 40% teeth (n = 21) with grazing signatures (more than 17 scratches) and 60% of teeth (n = 31) with browsing signatures (less than 17 scratches). The two-tailed Students' t-test for independent samples indicates that only pit counts for the browsing phase are significantly different when comparing my data with that obtained by NS (t = 2.21, df = 78, $p<0.05$).

7.4 DISCUSSION

7.4.1 *S. hendeyi* teeth

In the original description of *S. hendeyi* by Harrris (1976b), buccolingual and anteroposterior dimensions were reported for 23 mandibular teeth (two dp3s, two dp4s, one p2, three p3s, five p4s, five m1s, two m2s and three m3s) and no unworn crown heights were reported. Since a very large collection of *S. hendeyi* teeth have since been recovered, the dimensions reported in the current analysis are more accurate as they are based on much larger sample sizes (Table 7.3). The dental index for each *S. hendeyi* tooth type is very similar to those reported for African Sivatheriinae (excluding *S. hendeyi*) by Singer and Boné (1960) (Figure 7.7).

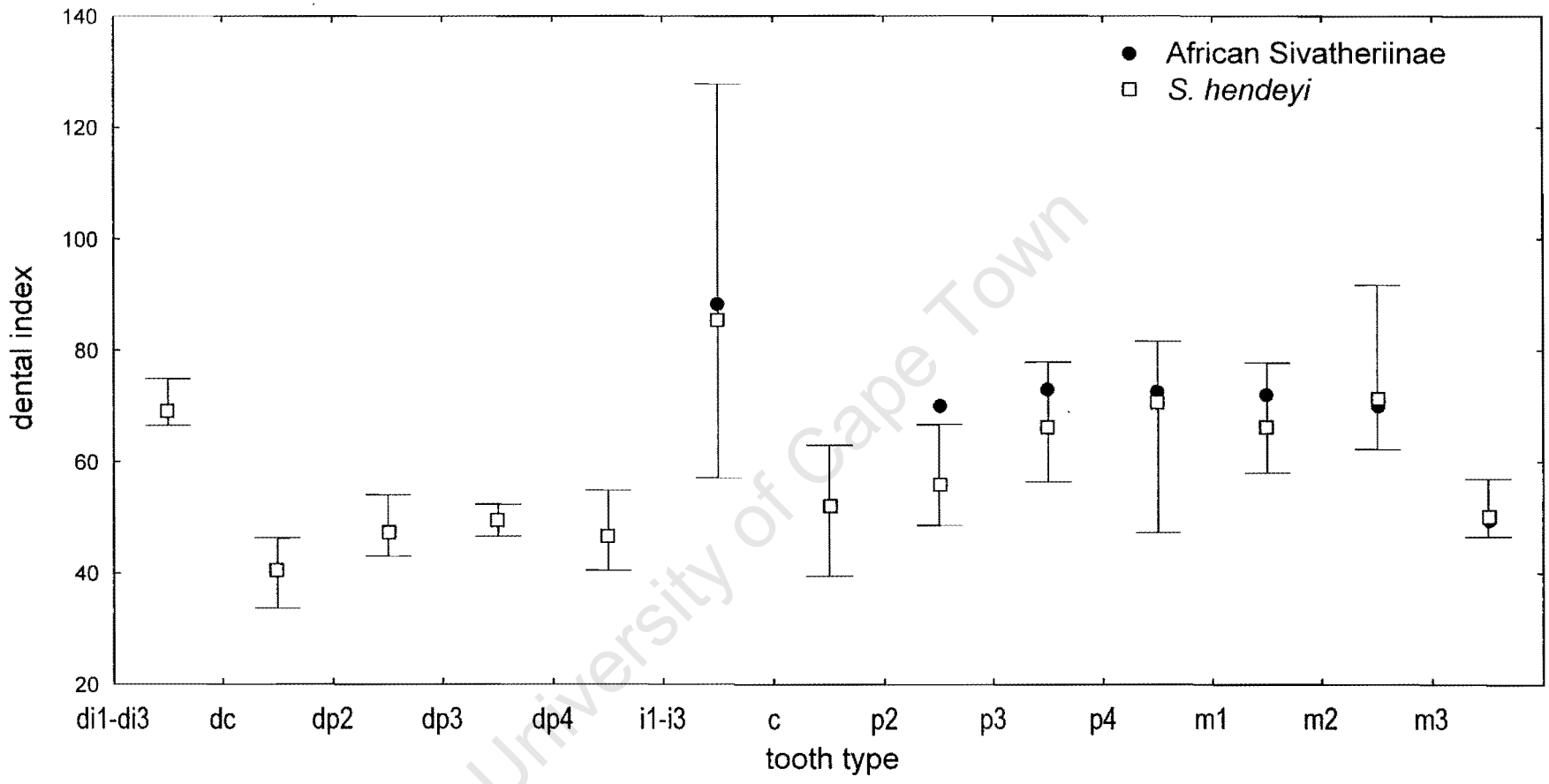

Figure 7.7. Dental index of *S. hendeyi* mandibular teeth compared to African Sivatheriinae (excl. *S. hendeyi*) (from Singer and Boné, 1960). Average dental index for *S. hendeyi* (open squares) and range of values (vertical bars) are given for each tooth type. Average dental index for African Sivatheriinae (closed circles) are also given.

7.4.2 Dietary assessment of *S. hendeyi*

7.4.2.1 Hypsodonty index

The HI for *S. hendeyi* falls within the category of ' brachyodont' as defined by both Janis (1988) and Fortelius and Solounias (2000), as expected from tooth morphology. It also falls within the range for mixed feeders in closed habitats, and all types of browsers (regular, selective and high-level) as determined by Janis (1988) (Figure 7.8) and is most similar to the average for selective browsers (Table 7.1). By comparing the HI of *S. hendeyi* (HI = 1.51) to the published HI of 127 species of living ungulates (Janis, 1988), *S. hendeyi* HI is most similar to that of two cervids, *Capreolus capreolus* (roe deer) and *Blastocerus dichotomus* (Janis, 1988). These two animals were classified by Janis (1988) as mixed feeders in closed habitats. However, both of these animals have body weights of less than 150 kg, which is significantly smaller than that estimated for *S. hendeyi* (~2 500 kg) (P. Haarhoff, personal communication, 2000). Since Janis (1988) suggests that HI of fossil taxa should be compared to animals of similar body size, the similarity between these species must be treated with caution. Janis (1988) however, could not prove a correlation between body size and HI. In addition, there are only very few living ungulates with body masses equivalent to that of *S. hendeyi*. This sivathere was larger than *G. camelopardalis* (~ 1075 kg) and most similar in body weight to the living rhinoceroses (*Rhinoceros unicornis*, *Rhinoceros sondaicus* and *Diceros bicornis*) (Janis, 1988). The published HI of these animals is 1.2 for *G. camelopardalis*, 1.59 for *R. unicornis*, 1.72 for *R. sondaicus* and 2.24 for *D. bi*cornis (Janis, 1988). Thus in terms of HI alone, the diet of *S. hendeyi* falls between that of *G. camelopardalis* and *R. unicornis*. The extant giraffe is a high-level browser, whereas the rhinoceros is a mixed feeder in closed habitats.

In summary the HI of *S. hendeyi* is most similar to that of mixed feeders in closed habitats, and browsers. Hypsodonty indices are however regarded as unreliable indicators of diet if used in isolation (Janis, 1988; Fortelius and Solounias, 2000).

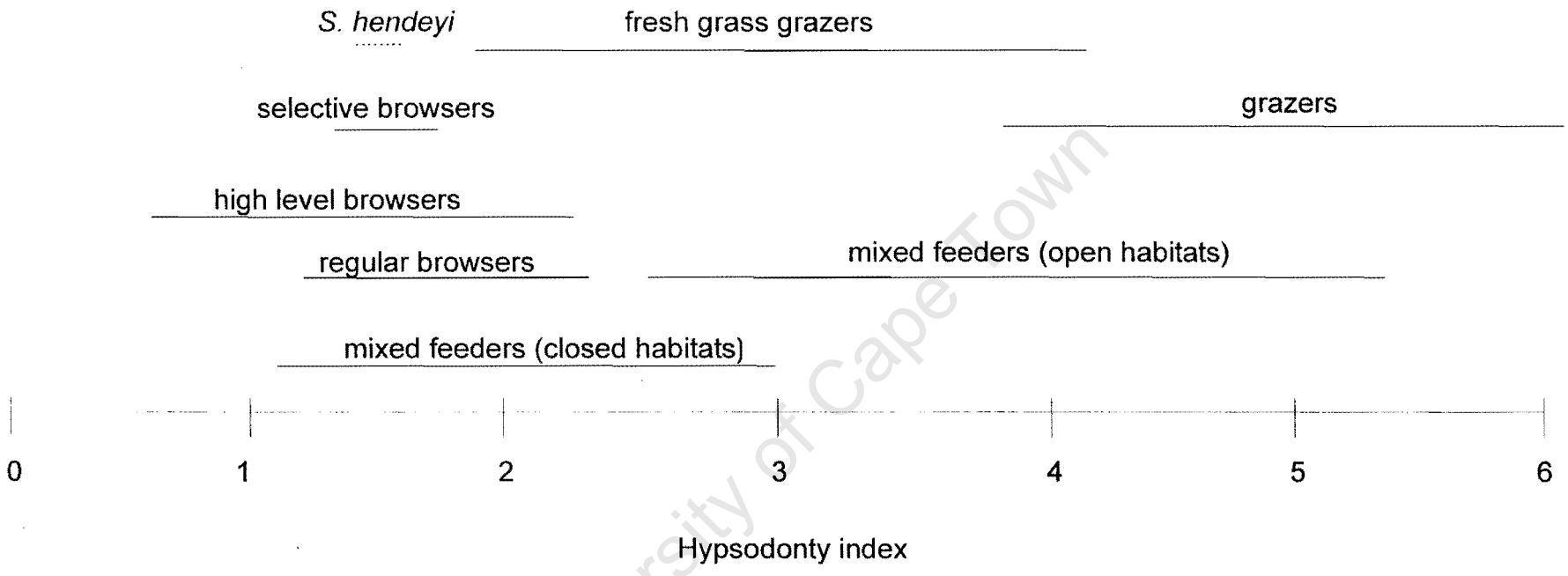

Figure 7.8. Hypsodonty index of *S. hendeyi* compared to those of extant ungulates (from Janis, 1988). *S. hendeyi* range is indicated with a dashed line.

7.4.2.2 Mesowear analysis

The differences in cusp shape for upper and lower teeth (Figure 7.5) is expected and is a direct result of the relative proportions of abrasive and attritive forces these teeth are subjected to during life. Since Fortelius and Solounias (2000) showed that combining HI with mesowear performs better than either alone, HI has been included in the mesowear analysis. The results for both upper and lower teeth (Appendix N) are plotted against mesowear variables obtained by Fortelius and Solounias (2000) for 64 extant ungulate species. Bivariate plots for the three dietary classes of percentage high occlusal relief against HI (Figure 7.9), indicates that *S. hendeyi* falls within the range for browsers, at the end of the range for mixed feeders and out of the range for grazers. The same result is obtained when cusp shape is plotted against HI (Figure 7.10). That is no similarities with grazers were found.

According to Fortelius and Solounias (2000), many browsers and mixed feeders have high occlusal relief and no blunt cusps as in *S. hendeyi*. In comparison with mesowear variables reported by Fortelius and Solounias (2000), *S. hendeyi* is most similar to two browsers, *Ammodorcas clarkei* (dibatag) and *Litocranius walleri* (gerenuk) and four mixed feeders (*Camelus dromedarius* (dromedary), *Ourebia ourebia* (oribi), *Tetracerus quadricornis* (chousingha) and *Tragelaphus angasi* (nyala)). However, only the gerenuk has a similar hypsodonty index (of 1.32), but Janis (1988) reports that this animal has an exceptionally low HI for a bovid. Cusp shape for *G. camelopardalis* (74% sharp cusps and 26% round cusps) (Fortelius and Solounias, 2000) is quite different to that of *S. hendeyi* indicating that this extinct giraffid did not have the same feeding strategy as extant giraffes.

Thus from mesowear analysis (combined with hypsodonty), *S. hendeyi* is most similar to browsers, although there are also some similarities with mixed feeders. No evidence indicates a grazing feeding strategy.

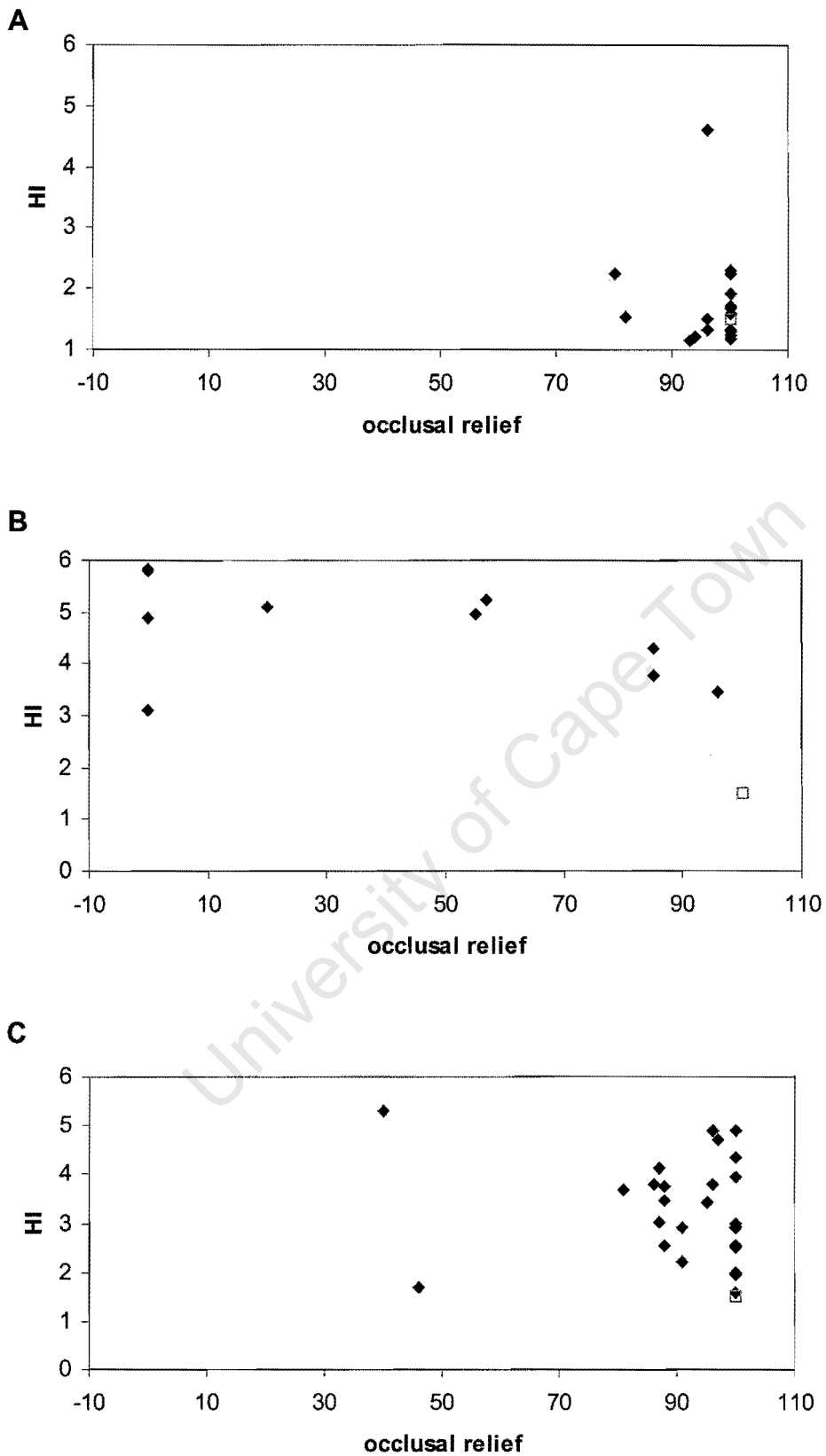

Figure 7.9. Bivariate plots of percentage high occlusal relief against hypsodonty index (HI). (A) browsers, (B) grazers and (C) mixed feeders. Data from Fortelius and Solounias (2000) (closed diamonds) and *S. hendeyi* (open squares).

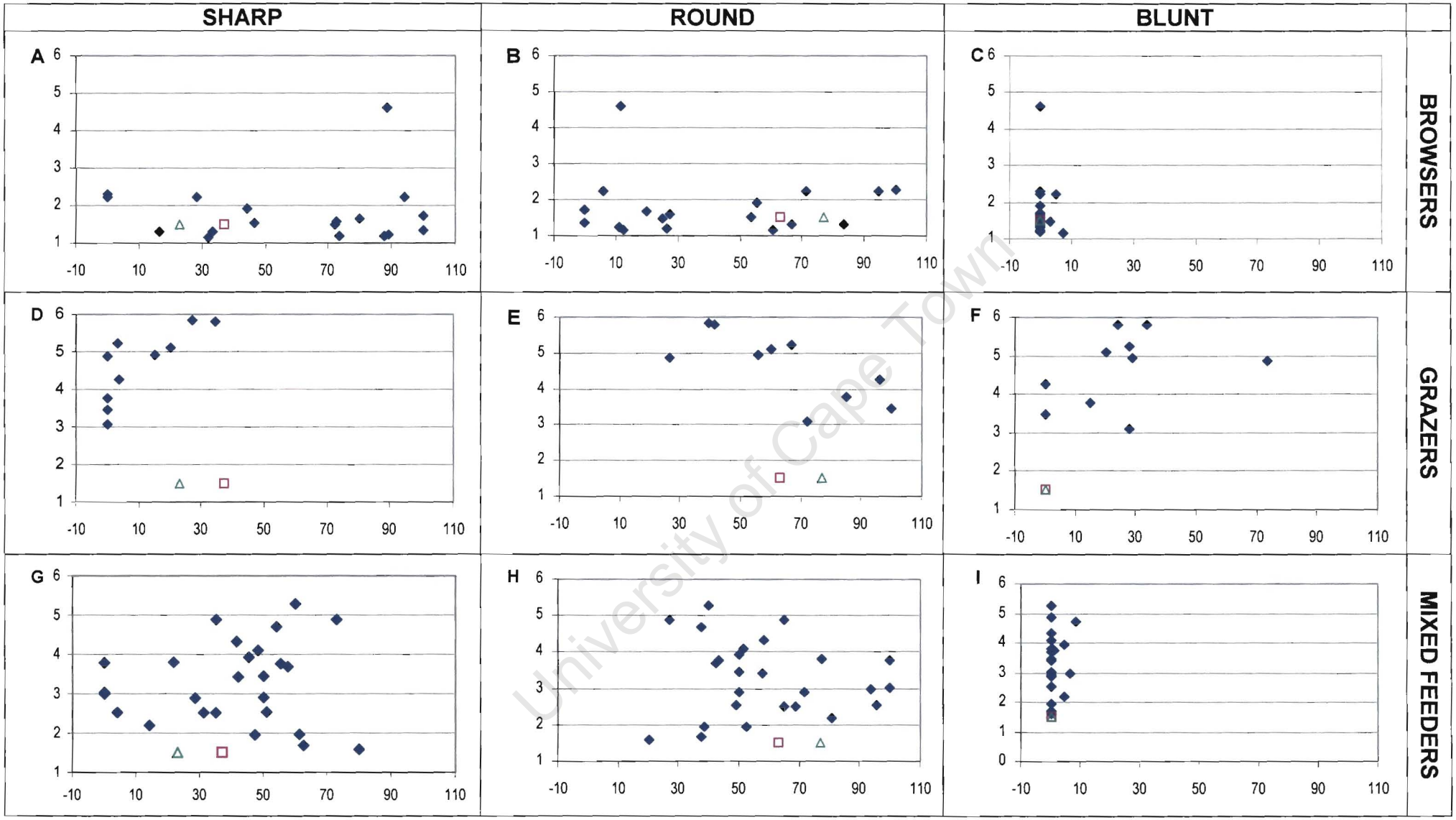

Figure 7.10. Mesowear analyses of the diet of *S. hendeyi*. *S. hendeyi* data for lower (open squares) and upper (open triangle) teeth are plotted against 64 ungulate species (closed diamonds) from Fortelius and Solounias (2000). A, B, C browsers, D, E, F are grazers, and G, H and I are mixed feeders. In all graphs, y-axis represents hypsodonty index and x-axis represents one of the three mesowear variables (percentage sharp cusps in A, D, G; percentage round cusps in B, E, H, and percentage blunt cusps in C, F and I).

7.4.2.3 Microwear analysis

The percentage of scratches and pits for the sivathere cannot be compared to those obtained using the SEM microwear method, since the level of magnification at which counts are made are very different. Since only one study has used this light microscope method, only a limited number of comparisons can be made. It is unlikely that taphonomy (such as tumbling) would cause regular parallel scratch marks as observed here and these scratches therefore most likely relate to feeding strategy. Microwear data obtained for *S. hendeyi* were compared to data obtained by Solounias and Semprebon (2002) for 50 extant ungulate species (Figure 7.11).

S. hendeyi has on average 27.5% pits suggesting that it belongs in the browser class. Solounias and Semprebon (2002) however, have shown that pit counts alone cannot discriminate browsing from grazing ungulates. Taking both average pits and average scratch counts into account, *S. hendeyi* falls on the browser side of a division between traditional grazers (more than 17 scratches) and traditional browsers (less than 17 scratches) (vertical line, Figure 7.11). Since *S. hendeyi* has teeth with scratch counts less than 17 and teeth with scratch counts between 17 and 29.5, it cannot be placed with the traditional browsers. Instead it falls within the transitional browser-grazing group together with some fruit-dominated browsers, leaf-dominated browsers and mixed feeders (seasonal and regional). Actual scratch and pit counts for *S. hendeyi* are most similar to the moose *Alces alces* (11.2% scratches, 27.5% pits) and the gerenuk *Litocranius walleri* (11.8% scratches, 27.1% pits) (data from Solounias and Semprebon, 2002) both of which are browsers with leaf-dominated diets. The mixed feeder, *Cephalus niger*, is the next most similar species to *S. hendeyi* in terms of scratch and pit counts (9.43% scratches, 28.86% pits). Thus in summary, based on scratch and pit counts alone, *S. hendeyi* has similarities with browsers and mixed feeders.

Solounias and Semprebon (2002) however, also show that seasonal and regional mixed feeders show a greater dispersion of scratch numbers than typically seen in grazers and a higher number of pits on average. *S. hendeyi* has a wide range of scratch counts (from 1 to 34 per counting area) and a high number of pits (up to 70), supporting the result that it could have been a seasonal mixed feeder.

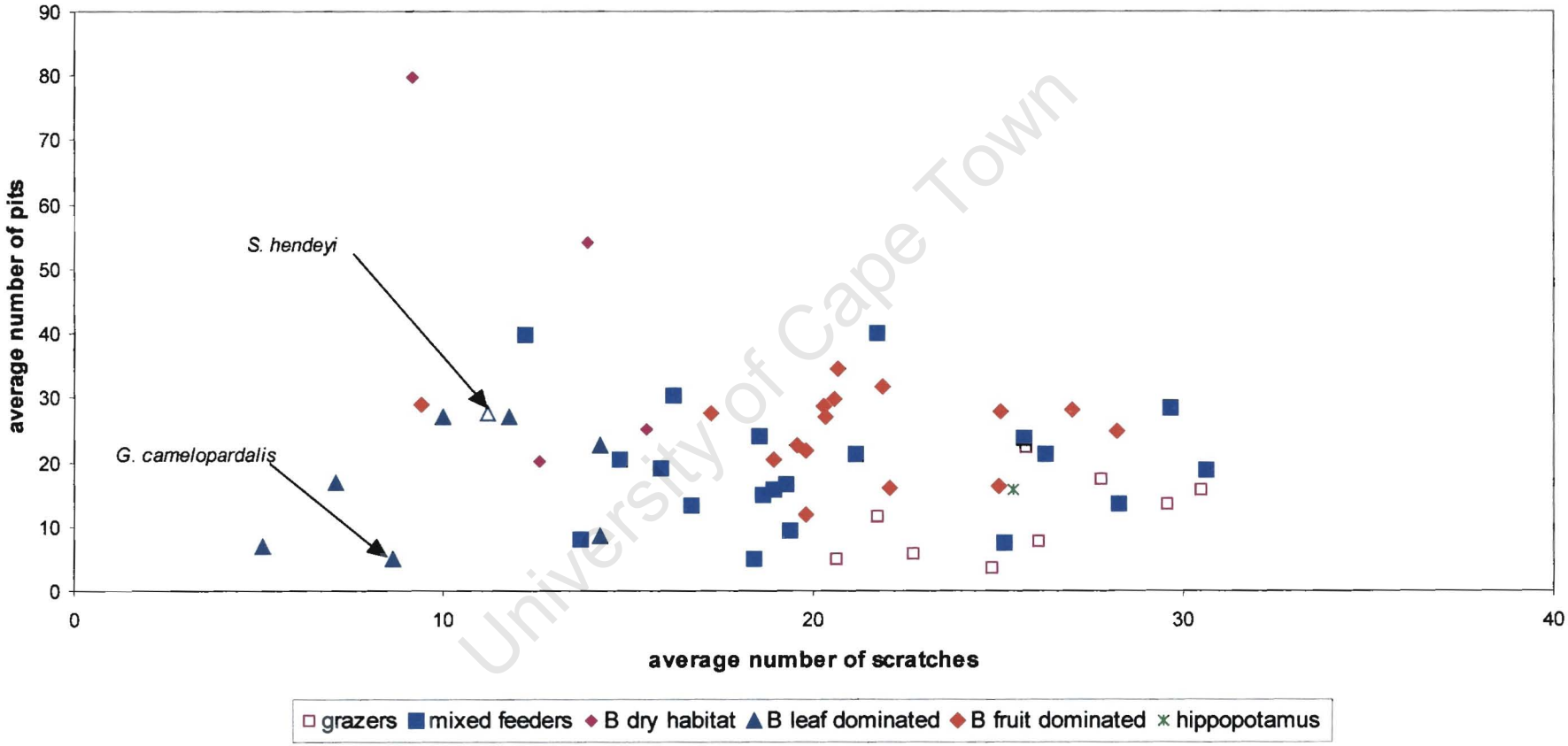

Figure 7.11. Microwear data for *S. hendeyi* (open triangle) compared to extant ungulates (from Solounias and Semprebon, 2002). The vertical line represents the cut-off point between traditional browsers (less than 17 scratches) and traditional grazers (> 17 scratches). Browsers (B) in dry, leaf-dominated and fruit-dominated habitats are shown.

Although scratch counts for individual *S. hendeyi* teeth indicate that values fall into two categories – grazing (> 17 scratches) and browsing (< 17 scratches), only four teeth were found with more than 17 scratches on average and these counts may therefore be outliers. In establishing the dietary ranges, Solounias and Semprebon (2002) had to eliminate some data that was an outlier to an observable pattern. At most one specimen per taxon was eliminated in this way. In the current analyses no recorded data has been ignored.

Microwear can also distinguish browsing from grazing based on scratch textures. Solounias and Semprebon (2002) suggest that grazers and graze-dominated mixed feeders possess tooth surfaces that are abrasion dominated (and have coarse scratches) and that attrition is more apparent in browser-dominated mixed feeders and browsers (which have predominately fine scratches). Only half (54.9%) of *S. hendeyi* teeth have only fine scratches on an enamel band. Mixed scratch textures are present in 33.3% of the teeth, indicating that *S. hendeyi* was not an exclusive browser. Solounias and Semprebon (2002) determined that mixed feeders show two distinct forms of microwear, one typical of browsing and one typical of grazing. Thus it appears that based on scratch texture, some *S. hendeyi* individuals were browsing (fine scratches only), some grazing (coarse scratches only) and some have features of both feeding types (mixed scratches). The percentages of fine, coarse and medium scratches are most similar to the mixed feeder, *Ourebia ourebia* (oribi). However this animal has different average numbers of pits and scratches (21% each) to the sivathere.

In summary, microwear data indicates that *S. hendeyi* was probably a seasonal mixed feeder. Although, average scratch and pit counts are most similar to browsers, scratch textures and scratch patterns indicate that this sivathere was probably a seasonal mixed feeder. In addition, at least four teeth with grazing-type signatures were noted. Solounias and Semprebon's (2002) method correctly classified all extant browsers in their database but only 38% of mixed feeders. The correct classification is less reliable for mixed feeders because these animals incorporate a relatively high percentage of browse in their diet and may therefore be misclassified as browsers. Since microwear scratch textures and pattern suggest a mixed feeding behaviour, this is probably the more likely correct classification of

S. hendeyi. Microwear represents the last few meals of an animal prior to death and since the accumulation at Langebaanweg represents a number of populations or cohorts of animals that accumulated over 0.5 Myr (Hendey, 1981b, 1984), it is highly likely that animals died at different times of the year (i.e. they were feeding on different types of diets prior to death). This may account for the large differences in scratch and pit counts for individual *S. hendeyi* teeth.

Robusticity of the microwear method

Comparisons of data for microwear analyses determined independently by Solounias and myself indicate that the average scratch and pit counts each of us obtained are statistically different. In addition the proportion of time spent browsing versus grazing, which is about 60:40 as determined by Solounias, is different to the proportion obtained in my analysis (92% browsing to 8% grazing). Despite this difference, Solounias's results also indicate that *S. hendeyi* was a seasonal mixed feeder. The average pit and scratch counts (obtained by Solounias) are most similar to two mixed feeders, *Tragelaphus scriptus* (12.6% scratches, 20.1% pits) and *Gazella granti* (14.8% scratches, 20.5% pits), which are both seasonal mixed feeders. Thus, Solounias's results steers the dietary strategy of *S. hendeyi* more towards mixed feeding than my own analysis.

Despite the overall results being similar, the robusticity of the method must be questioned since significantly different results were obtained. The intra-observer differences in counting for this method have not yet been established and should be further investigated. There are a number of avenues where subjectivity creeps into the analysis. The first is that counts are made in two "representative" areas on each cast, which are chosen by the observer. The microwear facets along a single enamel band differ markedly and perhaps more representative areas should be selected. This would serve to minimise intra-observer differences assuming no other biases are present. It is unlikely that pits and scratches were identified incorrectly and therefore the differences in average pit and scratch counts are likely to relate to the counting areas chosen. The identification of large versus small pits, gouges and scratch texture are also subjective. None of these microwear features were quantified by Solounias and Semprebon (2002) or shown in figures. As a

recommendation, microwear features should in future be quantified (e.g. by using image analysis) or at the least the range in scar morphology for each feature should be provided. This would reduce intra-observer differences greatly.

7.5 CONCLUSIONS

All three dietary assessments of *S. hendeyi*, indicate that this animal was not an exclusive or typical grazer. In addition, the results of all three methods show similarities with browsing as well as with mixed feeding. Although HI is not a perfect indicator of dietary strategy, the HI for *S. hendeyi* is most similar to that of mixed feeders from closed habitats as well as browsers. Mesowear indicates *S. hendeyi* is more likely a browser although results also fall at the end of the range for mixed feeders. Microwear data indicates that *S. hendeyi* was not an exclusive or typical browser and that it most likely was a seasonal mixed feeder tending to browse. Stable isotope results (presented in Chapter 4) for sivathere enamel support the finding that *S. hendeyi* was not a typical browser and suggests that it ate vegetation under conditions of reduced irradiance (see Chapter 9, section 9.2 for further discussion).

Both the mesowear approach, which uses HI, and the microwear approach have different advantages. Mesowear determination is very easy and quick, but provides limited information regarding diet apart from placing the animal into grazer, browser or mixed feeding groups. The microwear method on the other hand, is more complex and more time consuming than mesowear (but less so than the traditional SEM method), yet it provides far more information regarding the diet of an animal. As more variables are determined each providing a different clue to the overall diet, a reasonably accurate determination of diet can be made. The details of this method however need further refinement since intra-observer differences were significant.

Although the microwear method provides the highest resolution in terms of diet, this can actually complicate the dietary evaluation, since for example the feeding strategies of male and female giraffes are somewhat different (Young and Isbell, 1991). Males are more common in forest and taller, thicker vegetation whereas females prefer more open habitats (Young and Isbell, 1991). The relative proportions

of woody species consumed also changes depending on the social structure of their group.

Another area in which uncertainties in the methodology may occur is the origin of the extant ungulates used as a comparative database on which *S. hendeyi* microwear and mesowear variables were superimposed, is not clear. These specimens are housed in American and Canadian museums, and many originate in Africa. However, the south-western region of South Africa is dominated by a unique fynbos vegetation. Scott (1995) showed that fynbos was beginning to establish itself during the period of deposition of the Pelletal Phosphate Member at ~5 Myr. The microwear facets that this vegetation would cause is not known and therefore interpretations of what is causing the observed gouges, cross scratches, large pits, coarse scratches etc. is not clear. Solounias and Semprebon (2002) suggest that C_4 grasses produce coarser scratches compared to C_3 grasses, yet almost 50% of *S. hendeyi* teeth have coarse scratches (20% have only coarse scratches and 33% have coarse and mixed scratches). The local environment at Langebaanweg was C_3-dominated (Chapter 4) and this inconsistency may therefore relate to feeding on C_3 fynbos plant types. Determining the wear facets that fynbos produces is not easily accomplished as few extant ungulates live in fynbos areas of South Africa today. In terms of the evolution of Sivatheriinae diets from grazing to mixed feeding and browsing (Solounias et al., 2000), a mixed feeding strategy for *S. hendeyi* is plausible.

Chapter 8

INSIGHTS INTO ENAMEL HYPOPLASIA FROM STABLE LIGHT ISOTOPES

8.1 INTRODUCTION

The morphological examination of dental pathologies in the herbivores from Langebaanweg (LBW) (Chapter 5) shows that enamel hypoplasia is widespread in the local fauna and that some animals are significantly less affected (i.e. the rhinoceros, alcelaphines, boselaphines and bovines) than others (i.e. the hippopotamus, sivatheres and reduncines). This finding does not appear to correlate with dietary strategy. The extensive examination of this defect in *S. hendeyi* (Chapter 6) further indicates that these enamel defects are more likely related to environmental conditions than to behavioural events (except possibly in the early erupting first molar). The climatic conditions that prevailed during development of the enamel hypoplasia in *S. hendeyi* (reported in Chapter 6) is investigated in this chapter by means of stable carbon and oxygen isotopes obtained from teeth with defects. The possibility that less affected animals migrated out of the unfavourable area is also investigated by means of strontium isotope ratios from tooth enamel.

8.1.1 Stable isotopes and the timing of dental defects

Analyses of stable oxygen isotopes from enamel apatite carbonate obtained from tooth crowns reflect seasonal changes during tooth development in both modern and fossil animals (Koch et al., 1989; Bryant et al., 1994, 1996b; Fricke and O'Neil, 1996; Feranec and MacFadden, 2000; Balasse et al., 2002). Chapter 4 shows that $\delta^{13}C$ and $\delta^{18}O$ values for the LBW faunal assemblage varied according to predictable patterns (e.g. hippos are significantly depleted). In addition, variations in $\delta^{18}O$ values across tooth crowns were found indicating that diagenesis has not obscured the seasonal $\delta^{18}O$ values. The amplitude of the seasonal cycles during *S. hendeyi* m3 development was more than 2‰ (see Figure 4.7, Chapter 4). This is similar to the seasonal cyclicity recorded for modern and archaeological sheep and cattle from the south-western region of South Africa (3.4‰)(Balasse et al., 2002).

In order to determine whether differences in seasonal patterns could account for (or be associated with) defects, serial $\delta^{18}O$ signatures across defective *S. hendeyi* m3 tooth crowns were obtained and compared with those obtained previously for normal unaffected teeth. To my knowledge, this approach of using stable isotopes as a tool to investigate conditions under which dental defects manifested has not been applied previously.

One complication however, is that enamel defects manifest during the initial *laying down* phase of the organic template of enamel, whereas apatite formation and hence incorporation of carbonate proceeds from this point until the end of mineralisation. In domestic sheep for example three waves of mineralisation occur (Suga, 1982). Hence a defect at a certain position on the tooth crown represents a stress episode that occurred during the initial secretion of enamel protein, whereas the $\delta^{18}O$ composition reflected at the same point on the crown (in the mineral) represents an accumulation of the isotope signal over a longer period of time. Thus defect position and $\delta^{18}O$ values do not give information about exactly the same time period during ontogeny, nevertheless they are broadly synchronous.

High-resolution $\delta^{18}O$ analyses were also used to determine whether defects located towards the base of the *S. hendeyi* second molar (Chapter 6, section 6.3.2.5) are related to weaning. In extant giraffes this tooth erupts at around one year and its early development coincides with weaning (from 2 weeks to 1 year of age) (Hall-Martin, 1976a) (see Figure 6.1, Chapter 6). In order to determine when during tooth development weaning occurred in *S. hendeyi* and whether the subsequent stress episodes were linked to weaning or to seasonal changes, serial $\delta^{18}O$ analyses were conducted on *S. hendeyi* second molars. Some authors (Fricke and O'Neil, 1996; Wright and Schwartz, 1999) have reported that the weaning transition is detectable in $\delta^{18}O$ (from enamel carbonate) because milk (from the mother) is significantly enriched in ^{18}O compared to drinking water, resulting in higher $\delta^{18}O$ in suckling calves compared to weaned calves and adults. Defects present at the base of the *S. hendeyi* first molar (Chapter 6, section 6.3.2.5) were not investigated further by means of serial $\delta^{18}O$ analyses. This is because it is likely from their basal positions on the tooth crown that these defects can be attributed to an early event such as a

stressful weaning or birth period, considering the timing of these events in extant giraffes (Hall-Martin, 1976a). Until now, no previous study has investigated the weaning behaviour of Pliocene fossil mammals based on stable oxygen isotope ratios and none have used this technique to evaluate linear enamel hypoplasia.

8.1.2 Strontium isotopes as an indicator of migration

Strontium (Sr) is an alkaline earth element that has no demonstrable biochemical or physiological function, although it is present in soils, plants and animals. It commonly substitutes for calcium and undergoes fixation in the crystalline lattice of hydroxyapatite in both bone and teeth (Likins et al., 1960). The use of $^{87}Sr/^{86}Sr$ isotope ratios from teeth and bone to assess diets and to study migration patterns of populations is a recently developed technique (humans: Ericson, 1985; Sealy, 1989; Sealy et al., 1991; Price et al., 1994; Sillen et al., 1995; Ezzo et al., 1997; Price et al., 2001; elephants: Koch et al. 1995; mammoths and mastodons: Hoppe et al. 1999; salmon: Kennedy et al. 1997; Ingram et al. 1999) originally derived from geochemistry. The decay of rubidium (^{87}Rb) to strontium (^{87}Sr) is used to date rocks. Older rocks have enriched $^{87}Sr/^{86}Sr$ signals compared to rocks that have formed more recently. Although strontium isotope ratios change over the geological time-scale, over short time-scales the strontium isotope ratio of the sea is relatively constant due to continual mixing of the isotopes. Therefore marine organisms have a strontium ratio of 0.70923, similar to seawater (DePaolo and Ingram, 1985).

During growth, small quantities of strontium from plants and surface water are incorporated into the bones and teeth of animals. Because of the relative stability of geological strontium compositions over time, the strontium isotopic signal obtained from these tissues is assumed to be identical to that of the geological substrate on which they were feeding/drinking at the time (Sealy, 1989). Sealy and Sillen (work in progress), however, caution that several factors can influence how similar biological strontium ratios are compared to those from the local geology. For example, soils that are derived from more than one geological formation (such as those from river channels) may have complex strontium isotope ratios. Sea mists may deposit marine-derived strontium on land and hence complicate the signals obtained from terrestrial organisms living near the coast. Diagenesis may also possibly affect

strontium signatures. Archaeological seal bones buried in terrestrial deposits near the sea lose their marine-derived strontium over time and acquire instead the signature of the matrix in which they are buried (Nelson et al., 1986). Sillen (1990) however showed that the sample preparation method used by Nelson et al. (1986) caused severe alterations to the crystallinity and crystal structure of the fossil bones.

Strontium isotope ratios obtained from enamel carbonate are preferred since enamel is not remodelled during growth and therefore retains the strontium isotopic signal throughout life. These ratios reflect the strontium intake at the time that enamel mineral formed (i.e. during tooth development in the juvenile animal). Thus if the $^{87}Sr/^{86}Sr$ signal of the geological substrate in one area differs from that of adjacent rock types, then by measuring the strontium isotope ratios, one can deduce the area in which the animals were living during their growing years. In addition, strontium is not biologically fractionated (Gosz et al., 1983) due to the very small relative mass differences of the strontium isotopes.

The south-western region of South Africa consists largely of pre-Cambrian Malmesbury sediments, and the sandstones, quartzites and shales of Table Mountain as well as more recent coastal marine sands (Figure 8.1). Each of these geological substrates can be distinguished based on their $^{87}Sr/^{86}Sr$ signatures (Table 8.1). The marine sands as well as animals/plants that live in the sea or near the coast have strontium ratios similar to that of the seawater (Sealy, 1989). Inland terrestrial animals (from ancient shales and sandstones) on the other hand, have slightly enriched $^{87}Sr/^{86}Sr$ values. Sealy et al. (1991) has shown that the strontium isotope ratios from modern human bone are sensitive enough to distinguish between geological substrates in the south-western regions of South Africa.

Table 8.1. The $^{87}Sr/^{86}Sr$ range for the geological substrates of the south-western region of South Africa investigated by Sealy et al. (1991). ('n' indicates sample size).

Substrate type	**$^{87}Sr/^{86}Sr$ range**	**n**
Recent marine sands	0.70938-0.71124	6
Table mountain sandstones and quartzites	0.71543-0.71746	2
Malmesbury shales	0.71777-0.71794	2

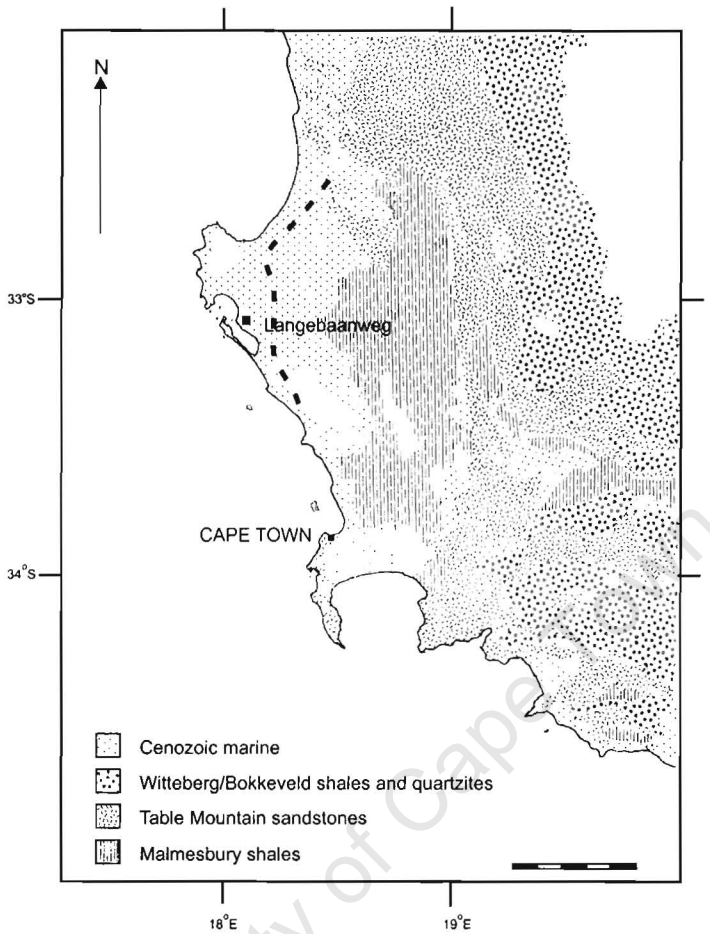

Figure 8.1. Geology of the south-western region of South Africa (modified from Sealy, 1989). The dashed line indicates the approximate position of the coastline during the Early Pliocene (see Chapter 2 for further details of sea-level changes during the Tertiary Period). Scale bar represents 5 km.

Strontium isotope ratios from human bone and fossil enamel have been used to investigate both the dietary and migratory patterns of populations in the past (Sealy, 1989; Sealy et al., 1991; Price et al., 1994; Ezzo et al., 1997; Sillen et al., 1998; Price et al., 2001; Balasse et al., 2001, 2002). Since Langebaanweg is situated near the border between two geological substrates (i.e. marine sands and Malmesbury sediments) (Figure 8.1) and since these geological substrates are relatively stable through time and have distinct $^{87}Sr/^{86}Sr$ signatures, evidence for the

geology of the local habitat during tooth development and possibly migration may be detected from analyses of tooth enamel strontium ratios (if the original isotopic composition has been preserved). Balasse et al. (2001) used this tool to evaluate migration patterns of cattle from a Late Stone Age (1100 B.P. to 1860 B.P.) site (Kasteelberg) in the south-west region of South Africa. Chapter 4 showed that the enamel apatite of several of the LBW fauna is reasonably well preserved since both carbon and oxygen isotope results show predictable patterning within the fauna. In addition, the apatite structure has been preserved over time (see Chapter 4, section 4.4.1). It therefore seems reasonable that strontium isotopes are also preserved.

Two complications exist when using of $^{87}Sr/^{86}Sr$ ratios from the LBW fossils. Firstly strontium isotopes have not previously been applied to fossil material older than the Pleistocene (~2 Myr) to study migration (Sillen et al., 1995, 1998). In these studies, Sillen and co-workers investigated strontium ratios from fossil bone and obtained plausible results. Since enamel is subjected to less alteration during diagenesis than bone (Ayliffe and Chivas, 1990; Lee-Thorp and van der Merwe, 1991; Quade et al., 1992; Thackeray and Lee-Thorp, 1992; Bryant et al., 1994; Lee-Thorp et al., 1994; Sponheimer and Lee-Thorp, 1999a), reasonable strontium ratios should be obtainable from fossil enamel 5 Myr old. Secondly, isotope ratios (even if they are preserved) may be complex because the fossils under study were recovered from a river channel deposit whose sediments may be acquired from diverse sources along the river before being deposited in the floodplain area. This means that animals that are likely to have grazed in the floodplain areas (such as the alcelaphines, *Damalacra* sp.) may have complex strontium ratios. In addition, the close proximity of the sea during the Early Pliocene can result in marine-derived strontium being incorporated into some fossils. For these reasons only a preliminary investigation of the potential usefulness of strontium isotopic ratios to evaluate the local (geological) habitat and possible migration patterns of two of the LBW fauna – namely the sivathere (*S. hendeyi*) and rhinoceros (*C. praecox*) – was conducted. These animals have different incidences of enamel hypoplasia with the sivathere severely affected compared to the rhinoceros.

8.2 MATERIALS AND METHODS

8.2.1 MATERIAL

Three *S. hendeyi* lower third molars (PQL 62733/62, PQL 62733/61, PQL 62733/13) with linear enamel hypoplasia were used for serial isotope analyses. PQL 62733/62 and PQL 62733/13 have single linear defects, although the defect in PQL 62733/62 is much wider than that in the latter tooth. PQL 62733/61 in contrast has three narrow defects on the tooth crown.

In order to determine whether the linear defects at the base of the second molar could be attributed to weaning, *S. hendeyi* m2s were also analysed by serial sampling. Five normal *S. hendeyi* m2s (PQL 43988, PQL 44046, PQL 43982, PQL 62738/22, PQL 43985) and one normal *G. camelopardalis* m2 (UCT 8174[1]) were selected for this analysis.

For strontium analysis, a single *S. hendeyi* molar tooth fragment (PQL 62733/61) with three narrow linear defects (the same tooth used for oxygen isotope analyses) and a rhinoceros (*C. praecox*) tooth fragment (PQL 41297) were analysed.

8.2.2 METHODS

The method of drilling along a tooth crown from its base to its tip in order to obtain a high-resolution stable isotope series was outlined in Chapter 4 (section 4.2.2.2).

For strontium isotope analyses, the tooth fragment was placed in a chamber connected to a Perkin Elmer/Sciex ICP-IMS (inductively coupled plasma mass spectrometer) (Elan 6000). Enamel was removed by laser ablation using a Cetac LSX 200 laser. The laser scanned the enamel surface at a speed of 10 μms^{-1} and twenty-five replicate readings in each position (A-D) were taken (Figure 8.2). The four samples (A-D) were taken at four different (equally spaced) positions along each tooth crown, such that position A is towards the base of the tooth and position D is towards the top of the tooth. The average of these replicates was then standardised

[1] This specimen was donated from Skukuza, Kruger National Park, South Africa.

against an in-house natural mineral apatite of known $^{87}Sr/^{86}Sr$ (0.71145). Strontium ratios are typically reported to five decimal places. Analytical precision of this instrument is better than 5%.

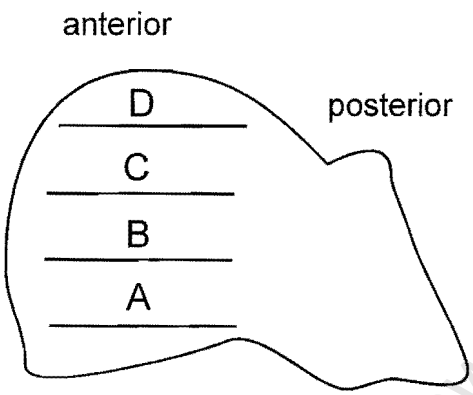

Figure 8.2. A diagram showing where strontium ratios were taken on the anterior cusp of a *S. hendeyi* fourth premolar (lingual surface). Each horizontal line denotes the line along which the 25 replicate samples were taken. The average of each of these 25 ratios gives the ratio for each position, A-D. A-D are approximately 7 mm apart.

8.3 RESULTS

8.3.1 Oxygen isotope series in second molars

$\delta^{18}O$ values and corresponding $\delta^{13}C$ values from samples taken across *G. camelopardalis* and *S. hendeyi* second molars are given in Appendix Q and shown graphically in Figure 8.3 and 8.4, respectively. In the extant giraffe, a distinct positive shift in $\delta^{18}O$ values towards the top of the second molar was observed (arrow, Figure 8.3). This indicates that the weaning period ended during development of this portion of the tooth crown. This is expected based on the weaning behaviour of extant giraffes (Hall-Martin, 1976b). Corresponding $\delta^{13}C$ values are relatively constant across the tooth crown, except for a positive shift in one value (dashed line, Figure 8.3). This shift in $\delta^{13}C$ occurs slightly lower on the tooth crown to the weaning signal and suggests that weaning was followed by a short dry period.

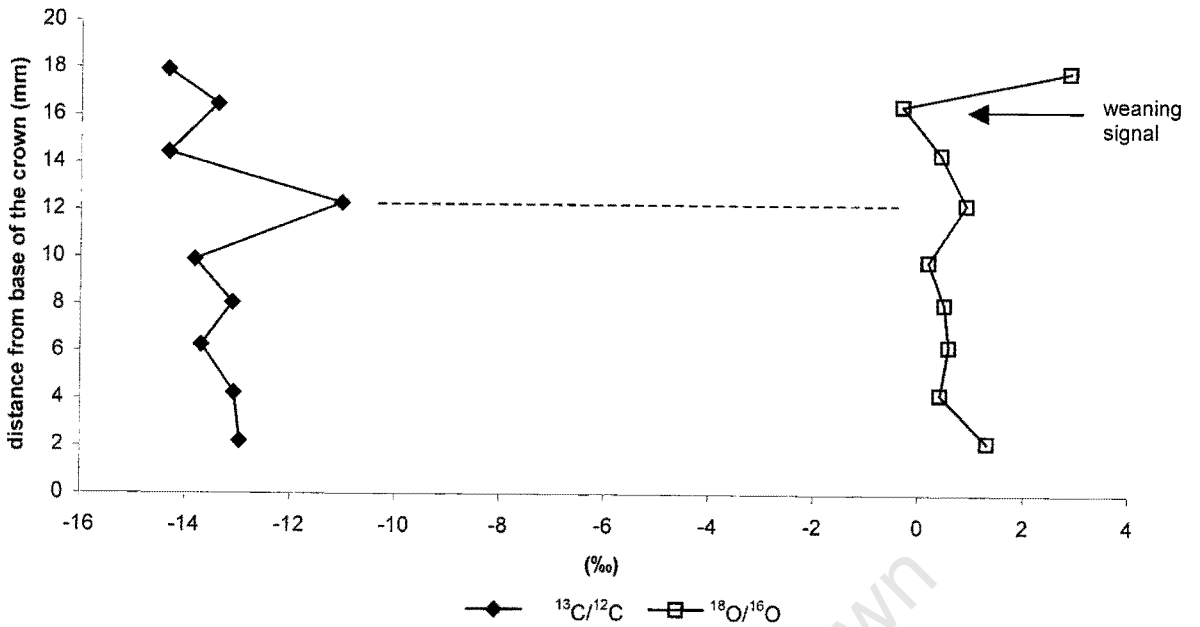

Figure 8.3. Stable carbon and oxygen isotopic ratios obtained from the mandibular second molar of an extant giraffe, *G. camelopardalis* (UCT 8174). The arrow indicates the position at which $\delta^{18}O$ values change abruptly and the weaning signal is detected. The dashed line indicates the position at which $\delta^{13}C$ values are depleted.

Similar positive shifts in $\delta^{18}O$ values were observed at the top of four out of the five *S. hendeyi* m2s (arrow, Figure 8.4A). One tooth (PQL 43985) however shows no significant enrichment of ^{18}O anywhere along the tooth crown. $\delta^{13}C$ values for three of the five sivathere teeth (PQL 43988, PQL 43982, PQL 62738/22) are reduced in the region with ^{18}O enrichment (Figure 8.4B) (i.e. towards the top of the tooth crown). One tooth (PQL 44046) shows little variation in carbon values across the tooth crown whereas another tooth (PQL 43985) is markedly enriched in ^{13}C towards the top of the tooth. This latter tooth however does not show the characteristic positive shift in $\delta^{18}O$ values observed in the extant giraffe and other sivathere teeth. In addition, the amplitude of the shift (i.e. the difference between the highest $\delta^{18}O$ value at the top of the tooth crown and the lowest $\delta^{18}O$ value) is greater than 2‰ in each tooth (except PQL 44046). The largest amplitude was observed in tooth PQL 43988, where a shift of 5.7‰ was detected across the tooth crown.

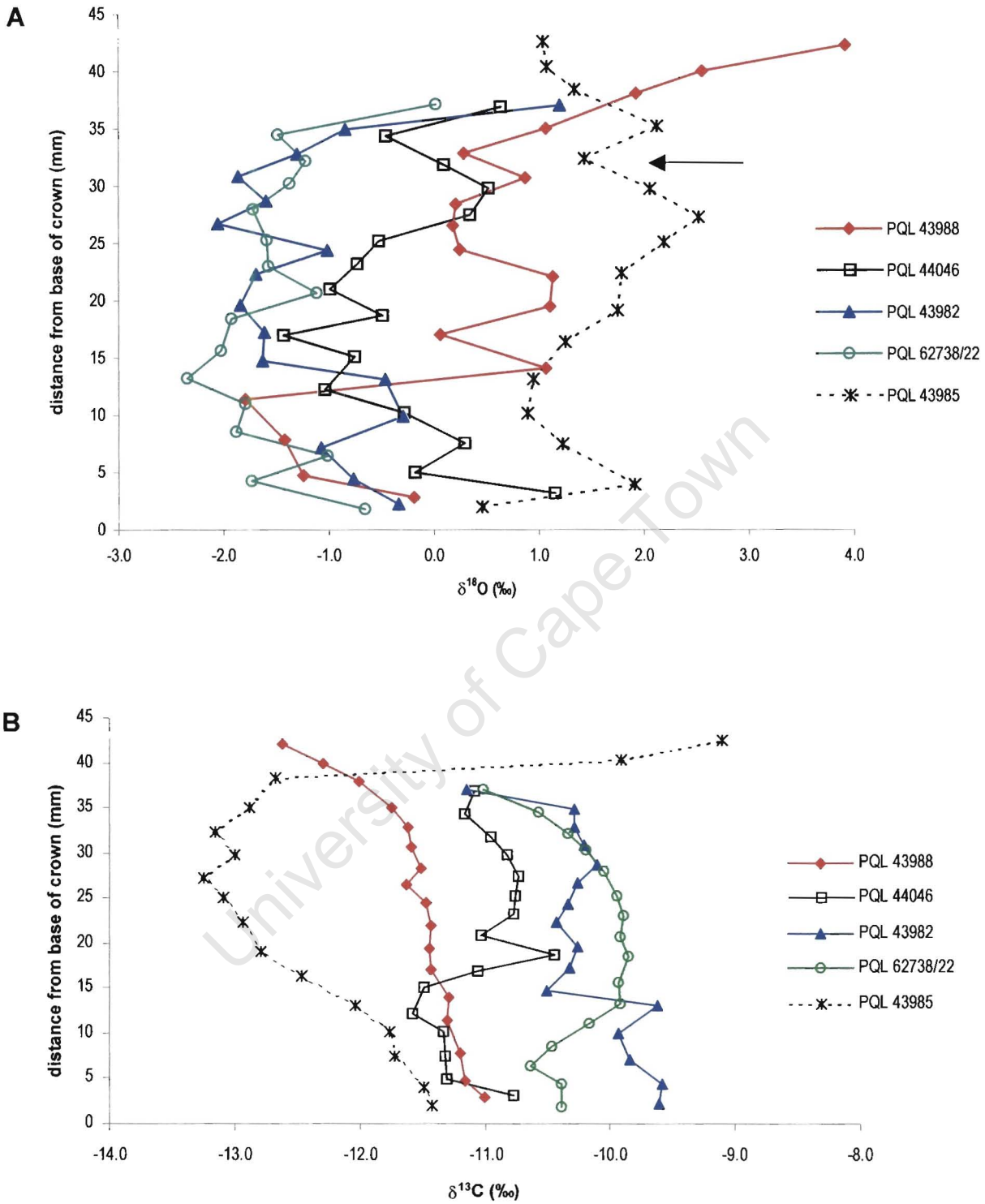

Figure 8.4. Stable isotope results from *S. hendeyi* mandibular second molars. (A) oxygen and (B) carbon isotope ratios. The arrow in (A) indicates the position at which $\delta^{18}O$ values shift abruptly in all teeth, except PQL 43985.

8.3.2 Analysis of defective *S. hendeyi* teeth

Stable oxygen isotope ratios from serial sampling across defective tooth crowns are shown graphically in Figure 8.5. Appendix R gives both $\delta^{18}O$ and $\delta^{13}C$ values. In each of the three defective teeth analysed, the amplitude of the seasonal cycle (i.e. the difference in $\delta^{18}O$ values from the top and bottom of the seasonal cycle) is narrow (Figure 8.5). The lowest seasonal amplitude of 0.9‰ occurs in tooth PQL 62733/62 which has the broadest defect affecting over 36% of the tooth crown (Figure 8.5A). In tooth PQL 62733/61, seasonal amplitude is low (0.9‰) in the area with three narrow defects, while it is 1.7‰ in the broad basal portion of this tooth (Figure 8.5B). The pattern is less similar for tooth PQL 62733/13, where a negative $\delta^{18}O$ shift corresponds with a linear enamel hypoplasia at the base of the tooth crown (Figure 8.5C). $\delta^{13}C$ values are relatively constant across each third molar with fluctuations of a maximum 1.5‰ across tooth crowns (Appendix R). Only one data point, towards the base of tooth PQL 62733/62 is slightly depleted in $\delta^{13}C$.

8.3.3 Strontium isotope analyses

Results of strontium isotope analyses are shown in Figure 8.6. The average $^{87}Sr/^{86}Sr$ value for the rhinoceros tooth was 0.71549 ± 0.0009 (n=4) and for the sivathere tooth 0.71176 ± 0.0005 (n=4). These two averages are significantly different (Two-way Student's t-test for independent samples, $p<0.05$, t = 7.151491, df = 6). The mean strontium ratios at each position (A-D) on both the sivathere and rhinoceros tooth crowns are variable (Figure 8.6). The variation in the twenty-five replicate samples at each position, are shown by the box and whiskers in Figure 8.6. Large standard deviations in the third decimal place were obtained at each position on the tooth crown.

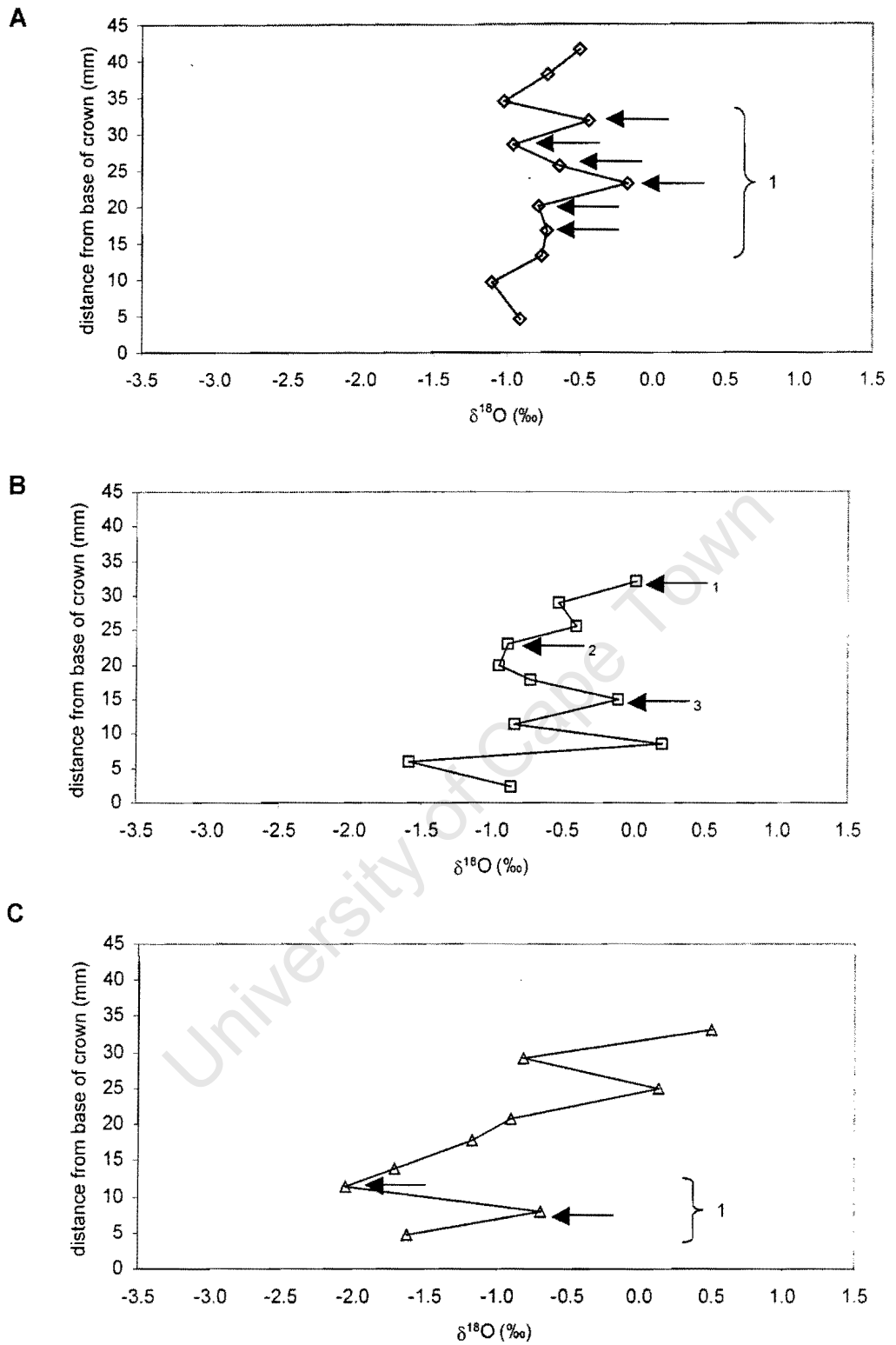

Figure 8.5. Stable oxygen isotope values across defective m3 tooth crowns of *S. hendeyi*. (A) PQL 62733/62, (B) PQL 62733/61 and (C) PQL 62733/13. The position of the defects on each tooth are indicated with arrows. (A) has one broad defect, (B) has three narrow defects and (C) has one medium-sized defect towards the base of the tooth.

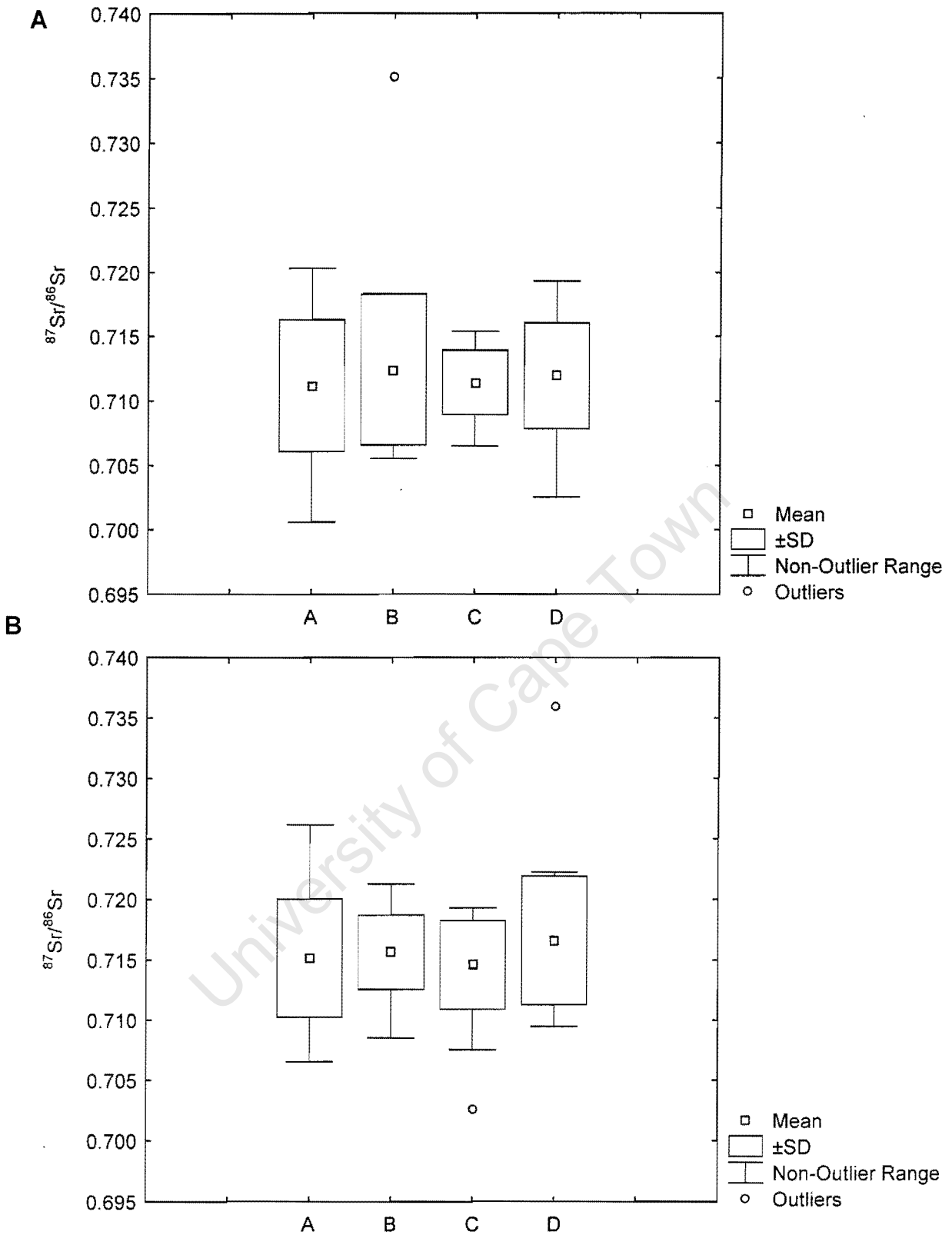

Figure 8.6. Box and whisker plots showing the $^{87}Sr/^{86}Sr$ values of replicate samples at each position on the tooth crown. (A) sivathere, *S. hendeyi*, and (B) rhinoceros, *C. praecox*. The x-axis denotes the position on the tooth crown where samples were taken (see Figure 8.2). Mean, standard deviations (SD) and non-outlier range are shown.

8.4 DISCUSSION

8.4.1 Weaning behaviour of *S. hendeyi*

Results demonstrate that a weaning signal indicated by relatively enriched ^{18}O values can be detected in second molars of both a modern giraffe and the extinct sivathere (arrows in Figure 8.3 and 8.4A). Most of the *S. hendeyi* teeth (four out of five) show that weaning occurs during development of the top of the tooth crown, similar to that in extant giraffes. Thus the sivathere from LBW was weaned at a similar ontogenetic age to extant giraffes. Furthermore, this result indicates that the linear enamel hypoplasia, which is evident towards the base of this tooth type and not at the top of the crown, is unlikely to relate to weaning and must be due to some other external cause. Environmental stress is a likely explanation (see Chapter 6, section 6.4.2 and below).

8.4.2 Environmental contexts under which defects manifested

The normal seasonal cycles of *S. hendeyi* teeth (m3s) were reported in Chapter 4 (Figure 4.5). $\delta^{18}O$ values in three teeth ranged from -3‰ in the wet season to +1‰ in the dry season giving an inferred seasonal amplitude of more than 2‰. Balasse et al. (2002) report similar seasonal amplitudes for modern and archaeological sheep, cattle, steenbok and eland living in the south-western part of South Africa. Isotopic ratios from serial samples taken across defective tooth crowns (shown in Figure 8.5) however indicate that the amplitude of the seasonal cycle is significantly reduced compared to that in normal teeth. In the most defective tooth (PQL 62733/62) the seasonal amplitude is only 0.9‰. That is, the difference between the wet and dry part of the seasonal cycle is less marked over the period tooth crowns take to develop. The duration of crown development and mineralisation for giraffid third molars is unknown, however, most ungulate third molars take 12-16 months to develop (cattle: 14 to 20 months, Brown et al., 1960; sheep: 10-12 months, Weinreb, 1964). Thus the seasonal cycles represented in Figure 8.5 span just over 1 year and therefore it is expected that one period of markedly lower $\delta^{18}O$ values indicating a wet season would be observed. However, no such periods are observed in the defective teeth and there is an apparent absence of a wet period in these teeth. It thus appears that the rainy/wet part of the cycle (i.e. winter) is completely or partly missing in defective teeth. The implication is that increased aridity or periods

of drought may have contributed to the manifestation of defects. Another explanation could be that defective enamel has a greater diagenetic potential. The occurrence of defective enamel bands and isotopic patterning across a tooth crown however, are not at all related indicating that this explanation is very unlikely.

The presence of several defects on a tooth crown (Chapter 6, section 6.3.2.6) suggests that stress events were episodic. This implies that the stress-causing conditions are interspersed with more favourable conditions (during tooth crown development). Stable isotope results presented here however, suggest that development of the entire tooth crown (with defects) occurred under conditions of increased aridity, due to the lack of a wet season. The possibility that altered chemistry in defective areas could produce the differences in $\delta^{18}O$ (between normal and defective teeth) is remote since the defects manifest in the enamel organic template. In addition, there are no indications of differences in the absorbance spectra of enamel apatite (Chapter 6, section 6.3.3).

The above results imply that defective teeth developed under adverse conditions. It is proposed that two climate scenarios existed, with different $\delta^{18}O$ values – one in which there were regular (or at least fairly regular) wet seasons, higher seasonal amplitude, and no enamel hypoplasia, and the other where the wet season was frequently lacking, seasonal amplitude was low and defects were prevalent. The latter scenario suggests increased occurrence of periods of drought. It has been suggested that a strongly seasonal rainfall regime existed at LBW 5 Myr ago (Hendey, 1983a), based on pollens (Scott, 1995) and the taphonomic context, which strongly suggests flood episodes (Hendey, 1981b). The inference that the stress agent was aridity, as well as the lack of food, is supported by the distribution of stressed animals. The grazing hippopotamus and reduncine, both of which are extremely water-dependant today (Apps, 1986), have the highest incidence and average Tooth Hypoplastic Area (THA) scores (Chapter 5). Some predicted browsers (*Giraffa* sp. and boselaphine) also have fairly high THA scores suggesting that available drinking water was limited. Grazers that are less dependent on water (e.g. *Damalacra* sp. and *C. praecox*), and possibly migratory, have the lowest scores. *S. hendeyi* has an unexpectedly high prevalence and THA score for a seasonal

mixed feeder (based on tooth morphology, microwear and mesowear analyses – see Chapter 7), which suggests that this animal was perhaps water-dependent.

Alternatively many ungulates (including giraffes) are known to chew on bones and/or soils (known as osteophagia and geophagia, respectively) in order to correct imbalances in the mineral content of food (Langman, 1978). Langman (1978) found a high frequency for this behaviour in wild giraffes and concludes that the minerals obtained in this manner are an important dietary supplement. This behaviour is not a consequence of a mineral deficiency but rather of an imbalance in the ratios of minerals ingested, especially just prior to and during the dry period. At LBW, the bones of animals that died upstream were most likely deposited at the river mouth (Hendey, 1981b) and were thus available for osteophagia in the lower reaches of the river. It has been suggested that some animals (such as the sivathere) favoured the estuary area as opposed to migrating further upstream (Hendey, 1981b, 1983, 1984).

A population-limiting factor in extant giraffes is low nutrition especially during dry months, mainly because their preferred food, the *Acacia*, looses its leaves at this time so food is scarce (Hall-Martin, 1976b). Extant giraffes are thus particularly stressed at the end of the dry season. Both *Giraffa* cf. *jumae* (probably a browser) and *S. hendeyi* (a mixed feeder) have similar high THA scores indicating that they were equally subjected to the unfavourable environmental conditions (i.e. the increased aridity) experienced at Langebaanweg. *Palaeotragus* on the other hand has an extremely low incidence of enamel hypoplasia (see Chapter 5), suggesting that either it had different tolerance levels to the increased aridity, or that it had a different behavioural strategy to avoid the increased aridity. Another possibility is that it was not contemporaneous with the other two giraffids. *Palaeotragus* is a presumed browser but favours closed canopy environments today. From the very low number of *Palaeotragus* teeth recovered from the Pelletal Phosphate Member at Langebaanweg it is seems likely that either this animal lived further upstream than the sivathere and long-necked giraffe (hence the low recovery of these fossils at the river mouth) or alternatively that it was not contemporaneous with the other two giraffids and thus not subjected to the adverse environmental conditions.

8.4.3 Local habitat and migration

The $^{87}Sr/^{86}Sr$ values for *S. hendeyi* and *C. praecox* are statistically different. The *S. hendeyi* values are most similar to that of coastal marine sands, whereas the rhinoceros values are most similar to those of inland terrestrial animals living on Table Mountain shale (Figure 8.7). These results suggest that these two animals were probably feeding in different areas, the sivathere near the coast (or at the river mouth) and the rhinoceros further inland. The high prevalence of enamel hypoplasia in the sivathere from LBW (compared to the rhinoceros), suggests that the coastal areas (inhabited by the sivathere) experienced more adverse environmental conditions than the inland areas (inhabited by the rhinoceros). The $^{87}Sr/^{86}Sr$ values across both the rhinoceros and sivathere tooth are also variable, indicating that migration during tooth development (i.e. juvenile years) probably occurred within each geological habitat.

These interpretations are however preliminary, as there are two main problems associated with the analysis. Firstly, only one tooth from each animal was sampled, and secondly large standard deviations are reported at each position (A-D) on the tooth crown (Figure 8.6). Geochemists routinely measure strontium ratios to five decimal places since variations in the fifth place are meaningful in geochronology. However, in biological organisms differences in the fifth decimal place may detect too much variation, and may therefore be less meaningful than variations in the third decimal (Sealy and Sillen, work in progress). These authors also suggest that in order to determine the validity of strontium variations between individuals, the background $^{87}Sr/^{86}Sr$ signature must be understood. The problem with this suggestion is that background $^{87}Sr/^{86}Sr$ available to biota is best determined by sampling plants, but this is not possible when dealing with fossils. Sediments may be sampled in order to assess the complexity of the strontium ratios (for instance, whether marine-derived strontium has been incorporated). In order to make a sound assessment of the local (geological) habitats and possible migration patterns of the Langebaanweg fauna, more extensive investigations consisting of many more samples (including local sediments) are thus required.

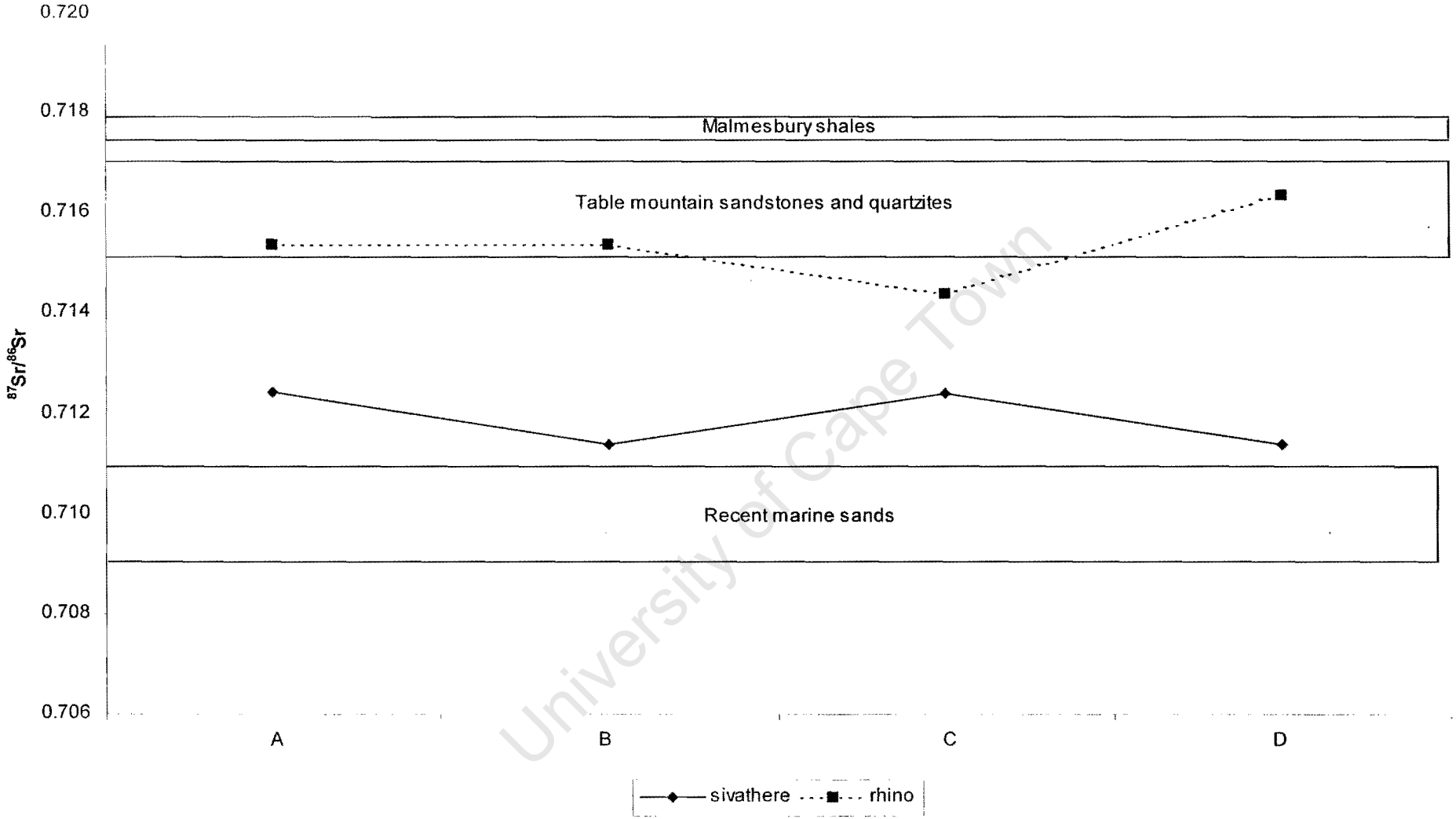

Figure 8.7. $^{87}Sr/^{86}Sr$ values across rhinoceros (*C. praecox*) and sivathere (*S. hendeyi*) enamel. Strontium ratios for the geological substrates of the western coast of South Africa were reported by Sealy et al. (1991).

8.5 CONCLUSIONS

Serial isotope data across individual tooth crowns suggest that (i) defects in the second molar of *S. hendeyi* are not related to weaning, (ii) that there is a correlation between the presence of linear enamel hypoplasia and a lack of a winter rainfall season, which implies increased aridity at Langebaanweg during the Early Pliocene, and (iii) that preliminary strontium results from two individuals (one sivathere and one rhinoceros) suggest that climatic variations in local habitats may explain the different incidences of defects reported in earlier chapters. A more extensive examination of these ratios is however required before conclusive results regarding local habitats and possible migration can be made.

Stable light isotope ratios suggest that the adverse climatic conditions (with increased aridity due to the lack of significant wet seasons) persisted from development and throughout adulthood, and placed several herbivores under severe systemic stress. This stress ultimately resulted in the manifestation of linear enamel hypoplasia. In addition, serial $\delta^{18}O$ values from giraffid second molars also demonstrate that high-resolution isotope analyses can provide insight into the weaning behaviour of extinct animals, which is otherwise unobtainable.

Chapter 9

SUMMARY OF RESEARCH FINDINGS

9.1 Introduction

The aims of the study were to evaluate the extent of pathologies in several ungulates from the Pelletal Phosphate Member (PPM) at Langebaanweg (LBW), and to use this information together with stable isotope analyses, to reassess the palaeoenvironment during deposition of this highly fossiliferous deposit. These two approaches, namely the presence of defects and stable isotopes, provide different perspectives on environmental conditions. Dental defects, such as enamel hypoplasia, which is present in many taxa at LBW, manifests during the initial enamel laying down phase of tooth development. The presence of these defects therefore provides information on the conditions that prevailed during development of a specific portion of a tooth crown. For cells to be disturbed to such an extent that a defect manifests, conditions must have been relatively severe and stressful (Goodman and Rose, 1990). Stable isotopes on the other hand, which are incorporated into the enamel apatite during tooth development, provide a more average or overall signature of the environmental conditions. Specifically they enable the prevailing vegetation (i.e. C_3 or C_4 dominated), climate regime (i.e. winter-wet/summer-dry or vice versa) and seasonality (amplitude of seasonal cycles and frequency) to be evaluated. Thus by analysing the defects and the isotopic signatures of the LBW fauna a fairly accurate reassessment of the environment on the west coast of South Africa during the Early Pliocene can be made. This chapter summarises the most significant findings of this research.

The overall good preservation of the LBW material and the lack of diagenesis found in the enamel apatite (Chapter 4, section 4.4.1), enabled subtle differences in stable isotope values to be used to their fullest potential. One constraint – the exact timing of deposition of the PPM – could not be overcome and created some difficulty with regards to interpretations presented in this thesis. Hendey (1981b, 1984) suggested that deposition of this deposit together with the underlying Quartzose Sand Member was less than 0.5 Myr. In addition, the PPM comprises two channel deposits, Bed 3aS and Bed 3aN. Most of the material studied in this thesis was

recovered from the later Bed 3aN, and therefore timing of deposition of this deposit is considerably less than 0.5 Myr. There is evidence from catastrophic mortality profiles (Klein, 1981, 1982) to suggest rapid accumulation of Bed 3aN deposits. Further refinement of the timing of the accumulation of the LBW deposits is essential in order to resolve the local fauna, climate and habitat on a smaller time-scale.

9.2 Developmental stress in the LBW fauna

Enamel hypoplasia is a developmental dental defect that manifests primarily as the result of systemic stress. Hendey (1981b) was the first to note the prevalence of enamel hypoplasia in the sivathere (*S. hendeyi*) from LBW. He assumed these animals were browsers and suggested that the observed defects were the result of nutritional stress, because of browser habitat decline during the Early Pliocene.

A thorough quantitative evaluation of the extent of pathologies in the LBW fauna demonstrated that several taxa have a high prevalence of enamel hypoplasia and that different taxa are not equally affected (Chapter 5, section 5.3.1.1). The hippopotamus (Gen & sp. not det.), sivathere (*S. hendeyi*) and reduncines (*Kobus* sp.) have high incidences of linear enamel hypoplasia (greater than 20%) compared to less than 10% in several other animals (the rhino *C. praecox*, the giraffe *Giraffa* cf. *jumae* and the boselaphine *Mesembriportax acrae*). These results indicate that conditions at Langebaanweg were not optimal for many animals. The presence of enamel hypoplasia in both the developing permanent teeth of sub-adults and in the continually erupting hippopotamus tusks of adults indicates that both age groups were affected. The early erupting deciduous teeth of *S. hendeyi*, however, lack defects (Chapter 6, section 6.3.2.2), demonstrating that young suckling animals (i.e. juveniles) were protected from the events causing systemic stress later in life.

The position of defects in *S. hendeyi* mandibular first molars (i.e. at the base of the crown) coincides closely with the time when birth and/or weaning occur in extant giraffes (*G. camelopardalis*). The defects in this tooth type suggest a relationship to either of these physiologically stressful events. High-resolution stable isotope analyses across mandibular second molars indicated that weaning in the sivathere occurs at a similar ontogenetic age to that in extant giraffes, and that the m2 cervical defects do not develop during the weaning period. The defects in all the

permanent teeth that develop after the first molar, therefore either relate to poor diet or to poor climate, since weaning can be ruled out. No patterning between dietary strategies (such as browsing or grazing) and defects was however found (Chapter 5, section 5.4), suggesting that diet (and thus nutritional stress) is not responsible for the observed defects as previously proposed. The occurrence of defects may rather relate to patterns of water-dependence. The hippopotamus for example, has the highest incidence of linear enamel hypoplasia (~30%). This animal is likely to have been water-dependent 5 Myr ago (as it is today), based on depleted $\delta^{18}O$ values (see Chapter 4). The sivathere has a marginally lower incidence of defects (~28%). The diet of this animal was investigated by means of hypsodonty index, mesowear and microwear analyses and was found to be most similar to that of an atypical browser or seasonal mixed feeder (Chapter 7, section 7.5). In addition, depleted $\delta^{18}O$ values from *S. hendeyi* (Chapter 4, Figure 4.7) suggest that it may have been water-dependent (or alternatively drank frequently). In summary, although patterning of defects amongst the different taxa is not clear, it seems most likely that the observed linear enamel hypoplasia relates to a general environmental deterioration, and not to diet or weaning behaviour.

Analyses of $\delta^{18}O$ signatures across normal and defective *S. hendeyi* tooth crowns indicate that environmental conditions during development of these teeth are not the same. The isotopic amplitude of the seasonal cycle in defective teeth is reduced compared to normal teeth. The wet season appears to be completely or partially missing. This suggests that defects manifested during periods of increased aridity or drought. The widespread presence of these defects, in all permanent tooth types, in almost all taxa, and in both adults and juveniles, suggests that these periods of reduced rainfall prevailed for extended periods of time. This relatively dry climate would have had an adverse effect on vegetation, especially grasses, which have short roots and cannot reach deep, underlying water sources. Some presumed grazers are however, not affected (e.g. *C. praecox*). A small pilot study of strontium isotopes from the rhinoceros (*C. praecox*) and the sivathere (*S. hendeyi*) (Chapter 8), suggest that these animals may have inhabited different geological areas. This difference in local habitat (with presumably varied vegetation and rainfall etc.) may have contributed to the difference in the prevalence of defects. Klein (1981, 1982)

has suggested that the rhinoceros fossil material may have been reworked from the underlying QSM deposit (based on mortality profiles), and therefore this animal may not have been contemporaneous with the sivathere. Other animals with low prevalence of defects (the boselaphine, *M. acrae* and the buffalo, *S. demissum*) were also suggested by Klein (1981, 1982) to have been reworked into the PPM deposit from the QSM.

The similarity between the observed enamel hypoplasia and those resulting from fluoride toxicosis was discussed and explored in Chapter 6. A distinct possibility is that fluoride concentrations were greater in water pools during times of reduced rainfall (when defects manifest). Despite there being a source of fluoride from surrounding phosphatic rock outcrops, Fourier Transform Infrared (FTIR) spectroscopy of defective and normal enamel apatite indicate similarities in the absorbance spectra but do not support the presence of excessive amounts of fluoride in the apatite (see Chapter 6). A very slight shift in the absorbance at 875 cm^{-1} is the only hint that higher fluoride concentrations may be present in the defective enamel apatite (Chapter 6, section 6.3.3). With little evidence for the presence of fluoride in the LBW defective enamel, fluoride toxicosis is unlikely to have caused the observed enamel hypoplasia.

The banded nature and inferred periodicity of the defects is puzzling. In defective teeth, $\delta^{18}O$ values at defects and in "normal" enamel areas (i.e. in between these defects) are similar. This may be because the correlation between the time of defect manifestation and isotope incorporation is not precise and would be offset by some amount. Stable isotopes are incorporated into the inorganic enamel matrix over a longer period of time compared to defects and hence indicate the average climate. Defects represent a more defined moment in time when ameloblasts laying down the (organic) enamel matrix are pushed over a threshold level and are irreparably damaged. Alternatively the "normal" appearing enamel on defective tooth crowns may not be normal enamel. Histological analyses, however does not support this argument. The episodic nature of defects may be the result of ameloblast activity reaching a maximum threshold level of tolerance at a certain cell-age, as the effects of adverse conditions accumulate over time. Further resolution of the exact

timings of enamel development and incorporation of stable isotopes is required in order to fully explain the episodic nature of linear defects.

9.3 The palaeoenvironment of Langebaanweg revisited

Stable carbon isotope results from tooth enamel carbonate of several taxa indicate unequivocally that LBW was C_3-dominated during the Early Pliocene. The lack of evidence for a C_3 to C_4 grassland shift in this part of South Africa is not in line with changes at similar latitudes in South America, which show this transgression (MacFadden et al., 1996). This finding suggests that something prevented the expansion of C_4 grasses to the west coast of South Africa. The presence of C_3 grasslands at LBW suggests that the current climate regime was winter-wet/summer-dry. In addition, the Benguella Upwelling System, which is responsible for the current climate regime on the west coast of South Africa, was established during the Late Miocene-Early Pliocene (Tankard and Rogers, 1978; Siesser, 1980; Siesser and Dingle, 1981). It is most likely that because a Mediterranean-type climate had been established by ~ 5 Myr, tropical C_4 grasses, which favour a summer-wet climate regime, could not expand into this area, despite these expansions occurring at similar latitudes elsewhere in the world. South African Quaternary sites further inland (at Makapansgat for example), which experience summer rainfall today, show clearly that C_4 grasses existed at ~ 3 Myr (Sponheimer et al., 1999a; Sponheimer et al., 2001).

A change in the amplitude of seasonal cycles was observed in $\delta^{18}O$ values across normal *S. hendeyi* m3s (Chapter 6 and 8). A favourable environment during which no defects develop and with normal seasonal cycles existed and was interspersed with times when conditions were unfavourable (i.e. when defects manifest) and which had reduced rainfall and droughts. These changing seasonal cycles may have been periodic, alternating between unfavourable and favourable conditions for many years. This finding supports the ideas initially proposed by Hendey in the 1980s that the local environments were deteriorating and that seasonality in the LBW area was becoming steadily less stable (Hendey, 1984).

9.4 Conclusion

Through the effects on the local fauna, this study provides valuable insight into the climate and vegetation changes that were taking place during the Early Pliocene in the south-western part of South Africa. This was a time of major global climatic change that had profound effects on faunal communities (Janis, 1988). Stable $\delta^{13}C$ values obtained from several browsing and grazing ungulates from Langebaanweg (LBW), indicate that the local area was C_3-dominated. The high prevalence of enamel defects in several taxa from LBW further indicates that at times conditions were unfavourable. High-resolution $\delta^{18}O$ signatures across normal and defective *S. hendeyi* mandibular third molars support this finding and suggest that at times during the deposition of the Pelletal Phosphate Member (PPM) at LBW, droughts or climates lacking a substantial wet season were common and interspersed with more favourable conditions. Vegetation change from C_3 vegetation consisting of trees and temperate grasses to C_3 vegetation consisting mainly of fynbos, as well as climate change (with periodic droughts), probably contributed to the demise of the LBW fauna. Apart from these environmental changes, fires and floods were also common (Klein, 1981, 1982; Hendey, 1984) (see Chapter 2).

The approach of combining isotopic palaeoecology with an evaluation of defects that manifest during tooth development has enabled a unique understanding of the environmental conditions that prevailed at the time when the PPM accumulated. This study provides significant new insight into our understanding of environmental change on the Southern African subcontinent during the Early Pliocene. $\delta^{18}O$ values obtained from enamel carbonate demonstrated that the weaning behaviour of extinct animals can be deduced from the fossil record. The rich faunal assemblage at LBW offers great potential for further investigations into the prehistoric biodiversity of the south-western Cape, South Africa.

Chapter 10

REFERENCES

Arambourg C. 1947. Contribution a l'etude geologique et paleontologique du basin du Lac Rodolphe et de la basse valee de L'Omo. Mission Scientifique de L'Omo, Museum d'Histoire Naturelle, Paris 1932-33: 2: 232-562.

Akersten, W. A., T. M. Foppe, and G. T. Jefferson. 1988. New source of dietary data for extinct herbivores. Quaternary Research 30: 92-97.

Alaluusua, S., P.-L. Lukinmaa, M. Koskimies, S. Pirinen, P. Holtta, M. Kallio, T. Holttinen, and L. Salmenpera. 1996. Developmental dental defects associated with long breast feeding. European Journal of Oral Science 104: 493-497.

Ambrose, S. H. and M. J. DeNiro. 1986. The isotopic ecology of east African mammals. Oecologia 69: 395-406.

Apps, P. (ed.). 1986. Smither's Mammals of Southern Africa: A field guide. Struik Publishers (Pty) Ltd., Cape Town. Pp. 151-241.

Ayliffe, L. K. and A. R. Chivas. 1990. Oxygen isotope composition of the bone phosphate of Australian kangaroos: Potential as a palaeoenvironmental recorder. Geochimica Cosmochimica Acta 54: 2603-2609.

Balasse, M., S. H. Ambrose, A. B. Smith, and T. D. Price. 2001. Investigating birth seasonality and mobility in prehistoric domestic sheep by analysis of changes in C, O, and Sr isotope ratios in tooth enamel. The Sixth Advanced Seminar on Paleodiets, University of California, Santa Cruz.

Balasse, M., A. B. Smith, and S. H. Ambrose. 2002. The seasonal mobility model for prehistoric herders in the south-western Cape of South Africa assessed by isotopic analysis of sheep tooth enamel. Journal of Archaeological Science 29: 917-932.

Bennet, S. C. 1989. Pathologies of the large Pterodactyloid pterosaurs *Ornithocheirus* and *Pteranodon*. Journal of Vertebrate Paleontology 9(3): 13A.

Bernor, R. L., T. M. Kaiser, L. Kordos, and S. Scott. 1999. Stratigraphic context, systematic position and paleoecology of *Hippotherium sumebense* Kretzoi, 1984 from MN 10 (Late Vallesian of the Pannonian Basin). Mitteilungen des Bayerischen Staatssammlung feur Palaeontologie Historische Geologie. 39: 115-149.

Blakey, M. L. and G. J. Armelagos. 1985. Deciduous enamel defects in prehistoric Americans from Dickson Mounds: Prenatal and postnatal stress. American Journal of Physical Anthropology 66: 371-380.

Blakey, M., T. E. Leslie, and J. P. Reidy. 1994. Frequency and chronological distribution of dental enamel hypoplasia in enslaved African Americans: A test of the weaning hypothesis. American Journal of Physical Anthropology 95: 371-383.

Bocherens, H., P. L. Koch, A. Mariotti, D. Geraads, and J-J. Jaeger. 1996. Isotopic biogeochemistry (^{13}C, ^{18}O) of mammalian enamel from African Pleistocene hominid sites. Palaios 11: 306-318.

Boyde, A., 1964. The structure and development of mammalian enamel. Ph.D. Thesis. Faculty of Medicine , University of London, London.

Boyde, A. 1972. Influence of normal and abnormal enamel structure on cavity margins. British Dental Journal 133: 421-427.

Boyde, A. 1976. Amelogenesis and the structure of enamel. Scientific Foundations of Dentistry 335-352.

Boyde, A. and L. Martin. 1982. Enamel microstructure determination in hominoid and cercopithecoid primates. Anatomy and Embryology 165: 193-212.

Boyde, A. and L. Martin. 1984. The microstructure of primate dental enamel; Pp. 341-366 *in* D. J. Chivers, B. A. Wood and A. Bilsborough (eds.), Food acquisition and processing in primates. Plenum, New York.

Bozarth, S. and J. Hofman. 1998. Phytolith analysis of bison teeth calculus and impacta from sites in Kansas and Oklahoma. Current research in the Pleistocene 15: 95-96.

Brink, J. and J. A. Lee-Thorp. 1992. The feeding niche of an extinct springbok, *Antidorcas bondi* (Alcelaphini, Bovidae), and its palaeoenvironmental meaning. South African Journal of Science 88: 227-229.

Bromage, T. and M. Dean. 1985. Re-evaluation of the age at death of Plio-Pleistocene fossil hominids. Nature 317: 981-983.

Brothwell, D. R. 1963. The paleopathology of Pleistocene and more recent mammals; Pp. 275-278 *in* D. Brothwell, and E. Higgs (eds.), Science in Archaeology: A comprehensive survey of progress and research. Thames and Hudson, London.

Brown, W. A. B., P. V. Christofferson, M. Massler, and M. B. Weiss. 1960. Postnatal tooth development in cattle. American Journal of Veterinary Research 21: 7-34.

Bryant, J. D., P. N. Froelich, W. J. Showers, and B. J. Genna. 1996a. Biologic and climatic signals in the oxygen isotopic composition of Eocene-Oligocene equid enamel phosphate. Palaeogeography, Palaeoclimatology, Palaeoecology 126: 75-89.

Bryant, J. D., B. Luz, and P. N. Froelich. 1994. Oxygen isotopic composition of fossil horse tooth phosphate as a record of continental paleoclimate. Palaeogeography, Palaeoclimatology, Palaeoecology 107: 303-316.

Bryant, J. D., P. L. Koch, P. N. Froelich, W. J. Showers, and B. J. Genna. 1996b. Oxygen isotope partitioning between phosphate and carbonate in mammalian apatite. Geochimica et Cosmochimica Acta 60(24): 5145-5148.

Bryant, J. D. and P. N. Froelich. 1995. A model of oxygen isotope fractionation in body water of large mammals. Geochemica et Cosmochimica Acta 59(21): 4523-4537.

Carlson, S. J. 1990. Vertebrate Dental Structures 1; Pp. 531-556 *in* J. G. Carter (ed.). Skeletal Biomineralisation: Patterns, Processes and Evolutionary Trends. Van Nostrand Reinhold, New York.

Cerling, T. E. 1993. Expansion of C_4 ecosystems as an indicator of global ecological change in the Late Miocene. Nature 361: 344-345.

Cerling, T. E. and J. M. Harris. 1999. Carbon isotope fractionation between diet and bioapatite in ungulate mammals and implications for ecological and paleoecological studies. Oecologia 120: 347-363.

Cerling, T. E., J. M. Harris, S. H. Ambrose, M. G. Leakey, and N. Solounias. 1997a. Dietary and environmental reconstruction with stable isotope analyses of herbivore tooth enamel from the Miocene locality of Fort Ternan, Kenya. Journal of Human Evolution 33: 635-650.

Cerling, T. E., J. M. Harris, and M. G. Leakey. 1999. Browsing and grazing in elephants: the isotope record of modern and fossil proboscideans. Oecologia 120: 364-374.

Cerling, T. E., J. M. Harris, B. J. MacFadden, M. G. Leakey, J. Quade, V. Eisenmann, and J. R. Ehleringer. 1997b. Global vegetation change through the Miocene/Pliocene boundary. Nature 389: 152-157.

Chappell, J. and N. J. Shackleton. 1986. Oxygen isotopes and sea level. Nature 324: 137-140.

Chinsamy, A. and M. A. Raath. 1992. Preparation of fossil bone for histological examination. Palaeontologica africana 29: 39-44.

Churcher, C. S. 1978. Giraffidae; Pp. 509-532 *in* V. J. Maglio and H. B. S. Cooke (eds.). Evolution of African mammals. Harvard University Press, Cambridge.

Coetzee, J. A. 1978. Climatic and biological changes in south-western Africa during the Late Cainozoic. Palaeoecology of Africa 10: 13-29.

Coetzee, J. A. and Rogers, J. 1982. Palynological and lithological evidence for the Miocene palaeoenvironment in the Saldanha region (South Africa). Palaeogeography, Palaeoclimatology, Palaeoecology 39: 71-85.

Condon, K. W. 1981. The correspondence of developmental enamel defects between mandibular canine and first premolar. American Journal of Physical Anthropology 54(2): 211.

Coppens, Y., V. J. Maglio, C. T. Madden, and M. Beden. 1978. Proboscidea; Pp. 336-367 *in* V. J. Maglio and H. B. S. Cooke (eds.). Evolution of African mammals. Harvard University Press, Cambridge.

Corruccini, R. S., J. S. Handler, and K. P. Jacob. 1985. Chronological distribution of enamel hypoplasias and weaning in a Carribean slave population. Human Biology 57(4): 699-711.

Coryndon, S. C. 1970. The extent of variation in fossil *Hippopotamus* from Africa. Symposium of the Zoological Society, Academic Press, London.

Coryndon, S. C. and Y. Coppens. 1973. Preliminary report on Hippopotamidae (Mammalia, Artiodactyla) from the Plio/Pleistocene of the Lower Omo Basin, Ethiopia. Fossil Vertebrates of Africa 3: 139-157.

Dawson, S. D. and M. D. Gottfried. In press. Paleopathology in a Miocene Kentriodontid (Cetacea, Odontoceti). Smithsonian Contributions to Paleobiology series.

Deacon, H. J. and J. Deacon. 1999. Human beginnings in South Africa: Uncovering the secrets of the Stone Age. David Phillip Publishers (Pty) Ltd., Cape Town, South Africa.

DeMonecal, P. B. 1995. Plio-Pleistocene African climate. Science 270: 53-59.

DePaolo, D. J. and B. L. Ingram. 1985. High-resolution stratigraphy with strontium isotopes. Science 227: 938-941.

Deutsch, D. and I. Gedalia. 1980. Chemically distinct stages in developing human fetal enamel. Archives of Oral Biology 25: 635-639.

Dingle, R. V. 1971. Tertiary sedimentary history of the continental shelf off southern Cape Province, South Africa. Transactions of the Geological Society of South Africa 74: 173-186.

Dingle, R. V. 1973. The geology of the continental shelf between Luderitz and Cape Town (Southwest Africa), with special reference to Tertiary strata. Journal of Geological Society, London 129: 337-363.

Dingle, D. W., A. R. Lord, and Q. B. Hendey. 1979. New sections in the Varswater Formation (Neogene) of Langebaan Road, south-western Cape, South Africa. Annals of the South African Museum 78(8): 81-92.

Dobney, K. and A. Ervynck. 1998. A protocol for recording linear enamel hypoplasia on archaeological pig teeth. International Journal of Osteoarchaeology 8: 263-273.

Dobney, K. and A. Ervynck. 2000. Interpreting developmental stress in archaeological pigs: the chronology of linear enamel hypoplasia. Journal of Archaeological Science 27: 597-607.

Dompierre, H. and C. S. Churcher. 1996. Premaxillary shape as an indicator of diet of seven extinct Late Cenozoic New World Camels. Journal of Vertebrate Paleontology 16: 141-148.

Ehleringer, J. R., T. E. Cerling, and B. R. Helliker. 1997. C_4 photosynthesis, atmosphere CO_2, and climate. Oecologia 112: 285-299.

Ehleringer, J. R., R. F. Sage, L. B. Flanagan, and R. W. Pearcy. 1991. Climate change and the evolution of C_4 photosynthesis. Trends in Ecology and Evolution 6: 95-99.

Ellis, R. P., J. C. Vogel, and A. Fuls. 1980. Photosynthetic pathways and the geological distribution of grasses in South West Africa/Namibia. South African Journal of Science 76: 307-314.

El-Najjar, M. Y., M. V. DeSanti, and L. Ozebek. 1978. Prevalence and possible etiology of dental enamel hypoplasia. American Journal of Physical Anthropology 48: 185-192.

Ensor, B. E. and J. D. Irish. 1995. Hypoplastic area method for analysing dental enamel hypoplasia. American Journal of Physical Anthropology 98: 507-517.

Epstein, S., P. Thompson, and C. J. Yapp. 1977. Oxygen and hydrogen isotopic ratio in plant cellulose. Science 198: 1209-1215.

Ericson, J. E. 1985. Strontium isotope characterisation in the study of prehistoric human ecology. Journal of Human Evolution 14: 503-514.

Ezzo, J. A., C. M. Johnson, and T. D. Price. 1997. Analytical perspectives on prehistoric migration: A case study from east-central Arizona. Journal of Archaeological Science 24: 447-466.

Federation Dentaire International. 1982. An epidemiological index of developmental defects of dental enamel (DDE Index). International Dental Journal 32: 159-167.

Feranec, R. S. and B. J. MacFadden. 2000. Evolution of the grazing niche in Pleistocene mammals from Florida: Evidence from stable isotopes. Palaeogeography, Palaeoclimatology, Palaeoecology 162: 155-169.

Fortelius, M. 1985. Ungulate cheek teeth: developmental, functional and evolutionary interrelations. Acta Zoologica Fennica 180: 1-75.

Fortelius, M. and N. Solounias. 2000. Functional characterization of ungulate molars using the abrasion-attrition wear gradient: A new method for reconstruction of paleodiets. American Museum Novitates 3301: 1-36.

Fox, H. 1939. Chronic arthritis in wild animals. Transactions of the Philosophical Society 31: 73-148.

Fricke, H. C. and J. R. O'Neil. 1996. Inter - and intra- tooth variation in the oxygen isotopic composition of mammalian tooth enamel phosphate: implications for palaeoclimatological and palaeobiological research. Palaeogeography, Palaeoclimatology, Palaeoecology 126: 91-99.

Friedli, H., H. Lotscher, H. Oeschger, U. Siegenthaler, and B. Stauffer. Ice core record of the $^{13}C/^{12}C$ ratio of atmospheric CO_2 in the past two centuries. Nature 324: 237-238.

Gantt, D. G., N. Xirotiris, B. Kurten, and J. K. Meletis. 1980. The Petralona dentition - hominid or cave bear. Journal of Human Evolution 9: 483-487.

Gentry, A. W. 1974. A new genus and species of Pliocene boselaphine (Bovidae, Mammalia) from South Africa. Annals of the South African Museum 65: 145-188.

Gentry, A. W. 1980. Fossil Bovidae (Mammalia) from Langebaanweg, South Africa. Annals of the South African Museum 79: 213-337.

Glimcher, M. J. 1959. Molecular biology of mineralised tissues with particular reference to bone. Review of Modern Physics 31: 359-393.

Gobetz, K. and S. Bozarth. 2001. Implications for Late Pleistocene mastodon diet from opal phytoliths in tooth calculus. Quaternary Research 55: 115-122.

Gosz, J., D. G. Brookins, and D. I. Moore. 1983. Using strontium isotope ratios to estimate inputs to ecosystems. BioScience 33: 23-30.

Goodman, A. H. 1991. Stress, adaptation, and enamel developmental defects; Pp. 280-286 *in* D. J. Ortner and A. C. Aufderheide (eds.). Human Paleopathology: Current synthesis and future options. Smithsonian Institute Press, Washington.

Goodman, A. H. and G. J. Armelagos. 1985. Factors affecting the distribution of enamel hypoplasias within the human permanent dentition. American Journal of Physical Anthropology 68: 479-493.

Goodman, A. H., G. J. Armelagos, and J. C. Rose. 1980. Enamel hypoplasias as indicators of stress in three prehistoric populations from Illinois. Human Biology 52(3): 515-528.

Goodman, A. H., D. L. Martin, and G. J. Armelagos. 1984. Indicators of stress from bone and teeth; Pp. 13-41 *in* Paleopathology at the origins of agriculture, Academic Press Inc.

Goodman, A. H. and J. C. Rose. 1990. The assessment of systemic physiological pertubations from dental enamel hypoplasias and associated histological sections. Yearbook of Physical Anthropology 33: 59-110.

Goodman, A. H. and J. C. Rose. 1991. Dental enamel hypoplasias as indicators of nutritional stress; Pp. 279-293 *in* M. A. Kelley and C. S. Larson (eds.). Advances in Dental Anthropology, Wiley-Liss, New York.

Gordan, K. D. 1982. A study of microwear on chimpanzee molars: Implications for dental microwear analysis. American Journal of Physical Anthropology 59: 195-215.

Grimsdell, J. W. 1973. Reproduction in the African buffalo, *Syncerus caffer,* in western Uganda. Journal of Reproduction and Fertility Supplement, 19: 303-318.

Grine, F. E., G. Fosse, D. W. Krause, and W. L. Jungers. 1986. Analysis of enamel ultrastructure in archaeology: the indentification of *Ovis aries* and *Capre hircus* dental remains. Journal of Archaeological Science 13: 579-595.

Grine, F. E. and Q. B. Hendey. 1981. Earliest primate remains from South Africa. South African Journal of Science 77(8): 374-376.

Grine, F. E. and R. F. Kay. 1988. Early hominid diets from quantitative image analysis of dental microwear. Nature 333: 765-768.

Hall-Martin, A. J. 1976a. Dentition and age determination of the giraffe *Giraffa camelopardalis*. Journal of Zoology 180: 263-289.

Hall-Martin, A. J., 1976b. Studies on the biology and productivity of the giraffe *Giraffa camelopardalis.* Ph.D. Thesis, Zoology, University of Pretoria, Pretoria. Pp. 245.

Hamilton, W. R. 1978. Fossil giraffids from the Miocene of Africa and a revision of the phylogeny of the Giraffoidea. Philosophical Transactions of the Royal Society of London 283(996): 166-229.

Harris, C., B. M. Oom, and R. E. Diamond. 1999. A preliminary investigation of the oxygen and hydrogen isotope hydrology of the greater Cape Town area and an assessment of the potential for using stable isotopes as tracers. Water South Africa 25(1): 15-23.

Harris, J. M. 1976a. Pleistocene Giraffidae (Mammalia; Artiodactyla) from East Rudolf, Kenya. Fossil Vertebrates of Africa 4: 283-332.

Harris, J. M. 1976b. Pliocene Giraffoidea (Mammalia, Artiodactyla) from the Cape Province. Annals of the South African Museum 69(12): 325-353.

Harris, J. M. and T. D. White. 1979. Evolution of the Plio-Pleistocene African Suidae. Transactions of the American Philosphical Society 69(2): 1-128.

Haughton, S. H. 1932. The fossil Equidae of South Africa. Annals of the South African Museum 28: 407-427.

Hayek, L. C., R. L. Bernor, N. Solounias, and P. Steigerwald. 1992. Preliminary studies of hipparionine horse diet as measured by tooth microwear. Annales Zoologica Fennici 28: 128-200.

Hayes, J. M. 1982. Fractionation *et al.*: An introduction to isotopic measurements and terminology. Spectra 8(4): 3-8.

Heckathorn, S.A., S. J. McNaughton and J.S. Coleman. 1999. C_4 Plants and Herbivory; Pp. 285-307 *in* Sage, R. F. and R. K. Monson (eds.). C_4 Plant Biology. Academic press, San Diego.

Hendey, Q. B. 1970. A review of the geology and palaeontology of the Plio-Pleistocene deposits at Langebaanweg, Cape Province. Annals of South African Museum 56(2): 75-117.

Hendey, Q. B. 1974. The Late Cenozoic Carnivora of the South-western Cape Province. Annals of the South African Museum 63: 1-369.

Hendey, Q. B. 1976. The Pliocene fossil occurrences in 'E' quarry, Langebaanweg, South Africa. Annals of the South African Museum 69(9): 215-247.

Hendey, Q. B. 1980. *Agriotherium* (Mammalia, Ursidae) from Langebaanweg, South Africa, and relationships of the genus. Annals of the South African Museum 80(1): 1-109.

Hendey, Q. B. 1981a. Geological successsion at Langebaanweg, Cape Province, and global events of the Late Tertiary. South African Journal of Science 77: 33-38.

Hendey, Q. B. 1981b. Palaeoecology of the Late Tertiary fossil occurrences in 'E' quarry, Langebaanweg, South Africa, and a reinterpretation of their geological context. Annals of the South African Museum 84: 1-104.

Hendey, Q. B. 1983a. Palaeoenvironmental implications of the Late Tertiary vertebrate fauna of the fynbos region; Pp. 100-116 *in* H. J. Deacon, Q. B. Hendey and J. J. N. Lambrechts (eds.). Fynbos Palaeoecology: A preliminary synthesis. South African National Science Programmes Report. 75.

Hendey, Q. B. 1983b. Palaeontology and palaeoecology of the fynbos region: An introduction; Pp. 87-99 *in* H. J. Deacon, Q. B. Hendey and J. J. N. Lambrechts (eds.). Fynbos Palaeoecology: A Preliminary Synthesis. South African National Scientific Programmes Report. 75.

Hendey, Q. B. 1984. Southern African Late Tertiary vertebrates; Pp. 81-106 *in* R. G. Klein (ed.) Southern African prehistory and paleoenvironments. A.A. Balkema, Rotterdam.

Hiller, C. R., Robinson, C.and Weatherell, J. A. 1975. Variations in the composition of developing rat incisor enamel. Calcified Tissue Research 18: 1-12.

Hillson, S. W. 1986. Teeth. Cambridge University Press, Cambridge. Pp. 376.

Hillson, S. W. 1992. Dental enamel growth, perikymata and hypoplasia in ancient tooth crowns. Journal of the Royal Society of Medicine 85: 460-466.

Hoffman, S., W. S. McEwan, and C. M. Drew. 1969. Scanning electron microscope studies of dental enamel. Journal of Dental Research 48: 242-250.

Hofmann, R. R. and D. R. M. Stewart. 1972. Grazer or browser: a classification based on stomach-structure and feeding habits of East African ruminants. Mammalia 36: 226-240.

Hooijer, D. A. 1976. The Late Pliocene rhinoceros from Langebaanweg, Cape Province. Annals of the South African Museum 59: 151-191.

Hooijer, D. A. and B. Patterson. 1972. Rhinoceros from the Pliocene of north-western Kenya. Bulletin of the Museum of Comparative Zoology (Harvard University) 144: 1-26.

Hopley, P. J. 2001. Pleseiosaur spinal pathology: the first fossil occurrence of Schmorl's nodes. Journal of Vertebrate Paleontology 21(2): 253-260.

Hoppe K. A., P. L. Koch, R. W. Carlson and S. D. Webb. 1999. Tracking mammoths and mastodons: Reconstruction of migratory behaviour using strontium isotope ratios. Geology 27: 5: 439-442.

Ingram B. L. and P. K. Weber. 1999. Salmon origin in California's Sacramento - San Joaquin river system as determined by otolith strontium isotopic composition. Geology 27: 9: 851-854.

Janis, C. M. 1982. Evolution of horns in ungulates: ecology and paleoecology. Biological Reviews 57: 261-318.

Janis, C. M. 1988. An estimation of tooth volume and hypsodonty indices in ungulate mammals, and the correlation of these factors with dietary preference; Pp. 367-387 *in* D. E. Russel, J-P. Sanatoro, and D. Sigogneau-Russel (eds.). Teeth Revisited: Proceedings of the VIIth International Symposium on Dental Morphology. Paris.

Janis, C. M. 1989. A climatic explanation for patterns of evolutionary diversity in ungulate mammals. Palaeontology 32(3): 463-481.

Janis, C. M. 1993. Tertiary mammal evolution in the context of changing climates, vegetation, and tectonic events. Annual Review of Ecological Systems 24: 467-500.

Janis, C. M., J. Damuth, and J. M. Theodor. 2000. Miocene ungulates and terrestrial primary productivity: where have all the browsers gone? Proceedings of the National Academy of Science 97(14): 7899-7904.

Janis, C. M. and D. Ehrdardt. 1988. Correlation of relative muzzle width and relative incisor width with dietary preference in ungulates. Zoological Journal of the Linnean Society 92: 267-284.

Jones, S. J. and A. Boyde. 1974. Coronal cementogenesis in the horse. Archives of Oral Biology 19: 605-614.

Kaiser, T. M., N. Solounias, M. Fortelius, R. L. Bernor, and F. Schrenk. 2000. Tooth mesowear analysis on *Hippotherium primigenium* from the Vallesian Dinotheriensande (Germany) - A blind test study. Carolina 58: 103-114.

Kay, M. I., R. A. Young, and A. S. Posner. 1964. Crystal structure of hydroxyapatite. Nature 204: 1050-1052.

Kennedy B. P., C. L. Folt, J. D. Blum and C. P. Chamberlain. 1997. Natural isotope markers in salmon. Nature 387: 786-787.

Kierdorf, H. and U. Kierdorf. 1997. Disturbances of the secretory stage of amelogenesis in fluorosed deer teeth: a scanning electron-microscopic study. Cell and Tissue Research 289: 125-135.

Kierdorf, H., U. Kierdorf, A. Richards, and F. Sedlacek. 2000. Disturbed enamel formation in wild boars (*Sus scrofa* L.) from fluoride-polluted areas in central Europe. The Anatomical Record 259: 12-24.

Kierdorf, U. and H. Kierdorf. 1989. A scanning electron microscope study on surface lesions in fluorosed enamel of roe deer (*Capreolus capreolus* L.). Veterinary Pathology 26: 209-215.

Kierdorf, U., H. Kierdorf, and O. Fejerskov. 1993. Fluoride-induced developmental changes in enamel and dentine of European roe deer (*Capreolus capreolus* L.) as a result of environmental pollution. Archives of Oral Biology 38(12): 1071-1081.

Kierdorf, U., H. Kierdorf, F. Sedlacek, and O. Fejerskov. 1996. Structural changes in fluorosed dental enamel of red deer (*Cervus elaphus* L.) from a region with severe environmental pollution by fluorides. Journal of Anatomy 188: 183-195.

Kingdon, J. 1982. East African Mammals: An Atlas of Evolution in Africa. Volume IIIB. Academic Press, London. Pp. 1-436

Klein, R. G. 1981. Ungulate mortality and sediment facies in the Late Tertiary Varswater Formation, Langebaanweg, South Africa. Annals of South African Museum 84(6): 233-254.

Klein, R. G. 1982. Patterns of ungulate mortality and ungulate mortality profiles from Langebaanweg (Early Pliocene) and Elandsfontein (Middle Pleistocene), south-western Cape Province, South Africa. Annals of the South African Museum 90(2): 49-94.

Klevezal, G. A. 1996. Recording structures of mammals. A.A. Balkema, Rotterdam. Pp. 274.

Koch, P. L. 1998. Isotopic reconstruction of past continental environments. Annual Review of Earth and Planetary Science 26: 573-613.

Koch, P. L., D. C. Fisher, and D. Dettman. 1989. Oxygen isotope variation in the tusks of extinct proboscideans: A measure of season of death and seasonality. Geology 17: 515-519.

Koch, P. L., J. Hesinger, C. Moss, R.W. Carlson, M. L. Fogel, and A. K. Behrensmeyer. 1995. Isotopic tracking of change in diet and habitat use in African elephants. Science 267: 1340-1343.

Kohn, M. J., M. J. Schoeninger, and J. W. Valley. 1996. Herbivore tooth oxygen isotope composition: Effects of diet and physiology. Geochimica et Cosmochimica Acta 60(20): 3889-3896.

Kollar, E. J. and A. G. S. Lumsden. 1979. Tooth morphogenesis: the role of the innervation during induction and pattern formation. Journal of Biology Buccale 7: 49-60.

Kozawa, S. 1984. Development and the evolution of mammalian enamel structure; Pp. 437-441 *in* R. W. Fearnhead and S. Suga (eds.). Tooth enamel IV. Elsevier, Amsterdam.

Langman, V. A. 1978. Giraffe pica behaviour and pathology as indicators of nutritional stress. Journal of Wildlife Management 42(1): 141-147.

Lee-Thorp, J. A., 1989. Stable Carbon Isotopes in Deep Time: The diets of fossil fauna and hominids. Ph.D Thesis, Department of Archaeology, University of Cape Town, Cape Town, South Africa.

Lee-Thorp, J., L. Manning, and M. Sponheimer. 1997. Problems and prospects for carbon isotope analysis of very small samples of fossil tooth enamel. Bulletin de la Societé Geologique de France 168(6): 767-773.

Lee-Thorp, J. A., J. C. Sealy, and N. J. van der Merwe. 1989. Stable carbon isotope ratio differences between bone collagen and bone apatite and their relationship to diet. Journal of Archaeological Science 16: 585-599.

Lee-Thorp, J. A. and N. J. van der Merwe. 1987. Carbon isotope analysis of fossil bone apatite. South African Journal of Science 83: 712-715.

Lee-Thorp, J. A. and N. J. van der Merwe. 1991. Aspects of the chemistry of modern and fossil biological apatites. Journal of Archaeological Science 18: 343-354.

Lee-Thorp, J. A., N. J. van der Merwe, and C. K. Brain. 1994. Diet of *Australopithecus robustus* at Swartkrans from stable carbon isotope analyses. Journal of Human Evolution 27: 361-372.

LeGeros, R. Z. 1981. Apatites in biological systems. Progress in Crystal Growth and Characterisation 4: 1-45.

LeGeros, R. Z. (ed.). 1991. Calcium Phosphates in Oral Biology and Medicine. Monographs in Oral Science 15.

Likins, R. C., H. G. McCann, A. S. Posner, and D. B. Scott. 1960. Comparative fixation of calcium and strontium by synthetic hydroxyapaptite. Journal of Biological Chemistry 235: 2152-2156.

Longinelli, A. 1984. Oxygen isotopes in mammal bone phosphate: A new tool for paleohydrological and paleoclimatological research? Geochimica Cosmochimica Acta 48: 385-390.

Loutit, T. S. and J. P. Kennet. 1979. Application of carbon isotope stratigraphy to Late Miocene shallow marine sediments, New Zealand. Science 204: 1196-1199.

Lukacs, J. R. 2001. Enamel hypoplasia in the deciduous teeth of early Miocene catarrhines: evidence of perinatal physiological stress. Journal of Human Evolution 40: 319-329.

Luyt, J., 2001. Revisiting the palaeoenvironments of the South African hominid-bearing Plio-Pleistocene sites: New isotopic evidence from Sterkfontein. M.Sc. Thesis, Archaeology, University of Cape Town, Cape Town, South Africa. Pp. 138.

Luyt, J., J. A. Lee-Thorp, and G. Avery. 2000. New light on Middle Pleistocene west coast environments from Elandsfontein, western Cape Province, South Africa. South African Journal of Science 96(7): 399-404.

Luz, B. and Y. Kolodny. 1985. Oxygen isotope variations in phosphate of biogenic apatites IV. Mammal teeth and bones. Earth and Planetary Science Letters 75: 29-36.

Luz, B. and Y. Kolodny. 1989. Oxygen isotope variation in bone phosphate. Applied Geochemistry 4: 317-323.

MacFadden, B. J. and T. E. Cerling. 1994. Fossil horses, carbon isotopes and global change. Trends in Ecology and Evolution 9: 481-485.

MacFadden, B. J. and T. E. Cerling. 1996. Mammalian herbivore communities, ancient feeding ecology, and carbon isotopes: A 10 million-year sequence from Neogene of Florida. Journal of Vertebrate Paleontology 16(1): 103-115.

MacFadden, B. J., T. E. Cerling, and J. Prado. 1996. Cenozoic terrestrial ecosystems evolution in Argentina: Evidence from carbon isotopes of fossil mammal teeth. Palaios 11: 319-327.

MacFadden, B. J. and B. J. Shockey. 1997. Ancient feeding ecology and niche differentiation of Pleistocene mammalian herbivores from Tarija, Bolivia: morphological and isotopic evidence. Paleobiology 23(1): 77-100.

MacFadden, B. J., N. Solounias, and T. E. Cerling. 1999. Ancient diets, ecology, and extinction of 5-million-year-old horses from Florida. Science 283: 824-827.

Marino, B. D. and M. B. McElroy. 1991. Isotopic composition of atmospheric CO_2 inferred from carbon in C_4 plant cellulose. Nature 349: 127-131.

Martin, R. D. 1981. Relative brain size and basal metabolic rate in terrestrial vertebrates. Nature 293: 57-60.

Martin, T. 1992. Scmelzmikrostruktur in den Inzisiven alt- und neuweltlicher hystricognather Nagetiere. Palaeovertebrata, Memoiré extraordinaire 1: 1-168.

McNaughton, S. J., J. L. Tarrants, M. M. MacNaughton, and R. H. Davis. 1985. Silica as a defense against herbivory and a growth promoter in African grasses. Ecology 66: 528-535.

Mead, A. J. 1999. Enamel hypoplasia in Miocene rhinoceroses (*Teleoceras*) from Nebraska: Evidence of severe physiological stress. Journal of Vertebrate Paleontology 19(2): 391-397.

Miles, A. E. W. and C. Grigson (eds.). 1990. Coyler's variations and diseases of the teeth of animals. Cambridge University Press, Cambridge. Chapters 16-20.

Milewski, A. V. and R. E. Diamond. 2000. Why are very large herbivores absent from Australia? A new theory of micronutrients. Journal of Biogeography 27: 957-978.

Moggi-Cecchi, J., E. Pacciani, and J. Pinto-Cisternas. 1994. Enamel hypoplasia and age at weaning in 19th century Florence, Italy. American Journal of Physical Anthropology 93: 299-306.

Moller, I. J. 1982. Fluorides and dental fluorosis. International Dental Journal 32(21): 135-147.

Morgan, M. E., J. D. Kingston, and B. D. Marino. 1994. Carbon isotope evidence for the emergence of C_4 plants in the Neogene from Pakistan and Kenya. Nature 367: 162-165.

Neiburger, E. J. 1990. Enamel hypoplasia: Poor indicators of dietary stress. American Journal of Physical Anthropology 82: 231-232.

Nelson, B. K., M. J. DeNiro, M. J. Schoeninger, D. J. DePaolo, and P. E. Hare. 1986. Effects of diagenesis on strontium, carbon, nitrogen and oxygen concentrations and isotopic composition of bone. Geochimica et Cosmochimica Acta 50: 1941-1949.

Niven, L. B. 2002. Enamel hypoplasia in bison: Paleoecological implications for modeling hunter-gatherer procurement and processing on the northwestern plains. Archaeozoologica 11: 101-112.

Okazaki, M. 1983. F^{-}-CO_3^{-2} interaction in IR spectra of fluoridated CO_3-apatites. Calcified Tissue International 35: 78-81.

Osborn, J. W. and A. R. TenCate (eds.). 1983. Advanced Dental Histology. Wright, PSG, London.

Owen-Smith N. and J. E. Danckwerts. 1997. Herbivory; Pp 397-420 *in* R. M. Cowling, D. M. Richardson and S. M. Pierce (eds.). Vegetation of Southern Africa. Cambridge University Press, Cambrdige,

Pagani, M., M. A. Arthur, and K. Freeman. 1999a. Miocene evolution of atmospheric carbon dioxide. Palaeoceanography 14(3): 273-292.

Pagani, M., K. H. Freeman, and M. A. Arthur. 1999b. Late Miocene atmospheric CO_2 concentrations and the expansion of C_4 grasses. Science 285: 876-879.

Park, R. and S. Epstein. 1960. Carbon isotope fractionation during photosynthesis. Geochimica et Cosmochimica Acta 21: 110-126.

Poole, C. 1967. Enamel structure in primitive mammals. Journal of Dental Research 46: 124.

Pough, F. H., J. B. Heiser, and W. N. McFarland (eds.). 1996. Vertebrate Life. Prentice-Hall International, Inc., New Jersey. Pp. 798.

Price, T. D., A. Bentley, J. Luning, D. Gronenborn, and J. Wahl. 2001. Prehistoric human migration in the *Linearbandkeramik* of central Europe. Antiquity 75: 593-603.

Price, T. D., C. M. Johnson, J. A. Ezzo, J. Ericson, and J. H. Burton. 1994. Residential mobility in the prehistoric southwest United States: A preliminary study using strontium isotope analysis. Journal of Archaeological Science 21: 315-330.

Quade, J., T. E. Cerling, P. Andrews, and B. Alpagut. 1995. Paleodietary reconstruction of Miocene faunas from Pasalar, Turkey using stable carbon and oxygen isotopes of fossil tooth enamel. Journal of Human Evolution 28: 373-384.

Quade, J., T. E. Cerling, J. C. Barry, M. E. Morgan, D. R. Pilbeam, A. R. Chivas, J. A. Lee-Thorp, and N. J. van der Merwe. 1992. A 16-Ma record of paleodiet using carbon and oxygen isotopes in fossil teeth from Pakistan. Chemical Geology 94: 183-192.

Quade, J., T. E. Cerling, and J. R. Bowman. 1989. Development of Asian monsoon revealed by marked ecological shift during the latest Miocene in northern Pakistan. Nature 342: 163-166.

Reason, R. C. 1991. Preliminary observations on growth and development in the okapi. International Zoology Yearbook 30: 216-219.

Regnier, P., A. C. Lasaga, and R. A. Berner. 1994. Mechanism of CO_3^{-2} substitution in carbonate-fluorapatite: Evidence from FTIR spectroscopy, ^{13}C NMR, and quantum mechanical calculations. American Mineralogist 79: 809-818.

Reid, D. J. and M. C. Dean. 2000. Brief Communication: The timing of linear hypoplasias on human anterior teeth. American Journal of Physical Anthropology 113: 135-139.

Rensberger, J. M. and W. von Koenigswald. 1980. Functional and phylogenetic interpretation of enamel microstructure in rhinoceroses. Paleobiology 6(4): 477-495.

Retzius, A. 1836. Mikroskopiska undersökninger öfver tändernas, särdeles tandbenets, struktur. Kongelige Vetenskap Akadamie Handelingen (Stockholm) 52-140.

Rey, C., V. Renugopalakrishnan, M. Shimizu, B. Collins, and M. J. Glimcher. 1991. A revolution-enhanced Fourier Transform Infrared spectroscopic study of the environment of the CO_3^{-2} ion in the mineral phase of enamel during its formation and maturation. Calcified Tissue International 49: 259-268.

Rich, P. V. 1980. Preliminary report on the fossil avian remains from Late Tertiary sediments at Langebaanweg (Cape Province), South Africa. South African Journal of Science 76: 166-170.

Rink, W. J. and H. P. Schwarcz. 1995. Tests for diagenesis in tooth enamel: ESR dating signals and carbonate contents. Journal of Archaeological Science 22: 251-255.

Rodney, J. D. 1983. The age related distribution of dental indicators of growth disturbance in ancient lower Nubia: an ethological model from the ethnographic record. Journal of human evolution 12: 535-543.

Rose, J. C. 1977. Defective enamel histology of prehistoric teeth from Illinois. American Journal of Physical Anthropology 46: 439-446.

Rothschild, B. M. and L. D. Martin. 1993. Paleopathology: Disease in the fossil record. CRC Press Ltd., Florida. Pp. 386.

Rothschild, B. M. and R. E. Molnar. 1988. Osteoarthritis in fossil marsupial populations of Australia. Annals of Carnegie Museum 57: 155-158.

Rothschild, B. M., X-M. Wang, and J. Shoshani. 1991. Proboscidean (sic) hijinks in the Pleistocene: are there changes indicative of venereally-acquired spondyloarthropathy? Journal of Vertebrate Paleontology 11(3): 53A.

Rothschild, B. M., X-M. Wang, and R. Cifelli. 1993. Spondyloarthropathy in Urisidae: A sexually transmitted disease? Research and Exploration 9(3): 382-384.

Sahni, A. 1984. The evolution of mammalian enamels: evidence from Multituberculata (Allotheria, extinct); primitive whales (Archaeocete, Cetacea) and early rodents; Pp. 457-461 *in* R. W. Fearnhead and S. Suga (eds.). Tooth enamel IV. Elsevier, Amsterdam.

Schour, I. and M. M. Hoffman. 1940. Studies in tooth development: The 16 micron calcification rhythm in the enamel and dentine from fish to man. Journal of Dental Research 18: 91-102.

Schour, I. and M. C. Smith. 1934. The histologic changes in the enamel and dentine of the rat incisor in acute and chronic experimental fluorosis. Techinical Bulletin, University of Arizona 52: 69-91.

Schulze, R. E. 1997. Climate; Pp 21-42 *in* R. M. Cowling, D. M. Richardson and S. M. Pierce (eds.). Vegetation of Southern Africa. Cambridge University Press, Cambrdige,

Scott, J. H. and N. B. B. Symons. 1977. Introduction to dental anatomy. Churchill Livingstone, Edinburgh. Pp. 464.

Scott, L. 1995. Pollen evidence for vegetational and climatic change in southern Africa during the Neogene and Quaternary; Pp. 65-76 *in* E. S. Vrba, G. H. Denton, T. C. Partridge and L. H.

Burckle (eds.). Paleoclimate and evolution with emphasis on human origins. Yale University Press, Yale.

Scott, L. 2002. Grassland development under glacial and interglacial conditions in southern Africa: review of pollen, phytolith and isotope evidence. Palaeogeography, palaeoclimatology, palaeoecology 177: 47-57.

Scott, L., H. M. Anderson, and J. M. Anderson. 1997. Vegetation history; Pp. 62-90 *in* R. M. Cowling, D. M. Richardson and S. M. Pierce (eds.). Vegetation of Southern Africa. Cambridge University Press, Cambridge.

Sealy, J. C. 1989. The use of chemical techniques for reconstructing prehistoric diets: a case study in the south-western Cape. South African Archaeological Society Goodwin Series 6: 69-76.

Sealy, J. C., N. J. van der Merwe, A. Sillen, F. J. Kruger, and H. W. Krueger. 1991. $^{87}Sr/^{86}Sr$ as a dietary indicator in modern and archaelogical bone. Journal of Archaeological Science 18: 399-416.

Shearer, T. R., D. L. Kolstad, and J. W. Suttie. 1978. Bovine dental fluorosis: Histological and physical characteristics. American Veterinary Medical Association 39(4): 597-602.

Shupe, M. F., A. E. Olson, H. B. Peterson, and J. B. Low. 1984. Fluoride toxicosis in wild ungulates. Journal of the American Veterinary Medical Association 185(11): 1295-1300.

Siesser, W. G. 1980. Late Miocene origin of the Benguela Upwelling System off northern Namibia. Science 208: 283-285.

Siesser, W. G. and R. V. Dingle. 1981. Tertiary sea-level movements around southern Africa. Journal of Geology 89: 83-96.

Sillen, A., G. 1990. Repsonse to N. Tuross, A. K. Behrensmeyer and E. D. Eanes. Journal of Archaeological Science 17: 5.

Sillen, A., G. Hall, and R. Armstrong. 1995. Strontium calcium ratios (Sr/Ca) and strontium isotopic ratios ($^{87}Sr/^{86}Sr$) of *Australopithecus robustus* and *Homo* sp. from Swartkrans. Journal of Human Evolution 28: 277-285.

Sillen, A., G. Hall, S. Richardson, and R. Armstrong. 1998. $^{87}Sr/^{86}Sr$ ratios in modern and fossil food-webs of the Sterkfontein Valley: Implications for early hominid habitat preference. Geochimica et Cosmochimica Acta 62(14): 2463-2473.

Sinclair, A. R. E., S. A. R. Mduma, and P. Arcesse. 2000. What determines phenology and synchrony of ungulate breeding in Serengeti? Ecology 81(8): 2100-2111.

Singer, R. and E. L. Bone. 1960. Modern giraffes and the fossil giraffids of Africa. Annals of the South African Museum 65: 375-548.

Skinner, M. F. 1986. An Enigmatic Hypoplastic Defect of the Deciduous Canine. American Journal of Physical Anthropology 69: 59-69.

Skinner, M.F. 1996. Developmental stress in immature hominines from Late Pleistocene Eurasia: Evidence from enamel hypoplasia. Journal of Archaeological Science 23: 833-852.

Skinner, M.F. and A. H. Goodman. 1992. Anthropological uses of developmental defects of enamel; Pp. 153-174 *in* S. R. Saunders (ed.). Skeletal Biology of Past Peoples, Wiley-Liss, Inc., New York.

Skinner, M. F. and J. T. W. Hung. 1986. Localised enamel hypoplasia of the primary canine. Journal of Dentistry for Children 53: 197-200.

Skinner, M. F. and J. T. W. Hung. 1989. Social and biological correlates of localised enamel hypoplasia of the human deciduous canine tooth. American Journal of Physical Anthropology 79: 159-175.

Solounias, N., M, Fortelius, and P. Freeman. 1994. Molar wear rates in ruminants: a new approach. Annales Zoologici Fennici 31: 219-227.

Solounias, N. and L-A. C. Hayek. 1993. New methods of tooth microwear and application to dietary determination of two extinct antelopes. Journal of Zoology 229: 421-445.

Solounias, N., W. S. McGraw, L. Hayek, and L. Werdelin. 2000. The paleodiet of Giraffidae; Chapter 6 *in* E. S. Vrba and G. B. Schaller (eds.), Antelopes, Deer and Relatives: Fossil record, behavioural ecology, systematics and conservation. Yale University, New York.

Solounias, N. and M. C. Moelleken. 1993a. Determination of dietary adaptation in an archaic antelope through tooth microwear and premaxillary analysis. Lethaia 26: 261-268.

Solounias, N. and M. C. Moelleken. 1993b. Determination of dietary adaptations of some extinct ruminants determined by premaxillary shape. Journal of Mammology 74(4): 1059-1071.

Solounias, N. and G. Semprebon, 2002. Advances in the recontruction of ungulate ecomorphology and application to early fossil equids. American Museum Novitates Histoire.

Solounias, N., M. Teaford, and A. Walker. 1988. Interpreting the diet of extinct ruminants: the case of a non-browsing giraffid. Paleobiology 14(3): 287-300.

Spinage, C. A. 1967. Ageing the Uganda defassa waterbuck *Kobus defassa* Ugandae. East African Wildlife Journal 5: 1-17.

Sponheimer, M. and J. A. Lee-Thorp. 1999a. Alteration of enamel carbonate environments during fossilisation. Journal of Archaeological Science 26: 143-150.

Sponheimer, M. and J. A. Lee-Thorp. 1999b. Oxygen Isotopes in Enamel Carbonate and their Ecological Significance. Journal of Archaeological Science 26: 723-728.

Sponheimer, M. and Lee-Thorp, J. A. 2001. The oxygen isotope composition of mammalian enamel carbonate from Morea estate, South Africa. Oecologia 126: 153-157.

Sponheimer, M., K. E. Reed, and J. A. Lee-Thorp. 1999. Combining isotopic and ecomorphological data to refine bovid paleodietary reconstruction: A case study from the Makapansgat Limeworks hominin locality. Journal of Human Evolution 36: 705-718.

Sponheimer, M., K. Reed, and J. A. Lee-Thorp. 2001. Isotopic palaeoecology of Makapansgat Limeworks Perissodactyla. South African Journal of Science 97: 327-329.

Stallibrass, S. 1982. The use of cement layers for the absolute ageing of mammalian teeth: A selective review of the literature, with suggestions for further studies and alternative applications; Pp. 109-126 *in* B. Wilson, C. Grigson and S. Payne (eds.). Ageing and sexing animal bones from archaeological sites. BAR British Series, England 109.

Stewart, R. E. and A. E. Poole. 1982. The orofacial structures and their association with congenital abnormalities. Pediatric Clinic North America 29:547-584.

Stock, W. D., F. van der Heyden and O. A. M. Lewis. 1992. Plant structure and function; Pp 226-240 *in* R. Cowling (ed.). The ecology of fynbos, nutrition, fire and diversity. Oxford University Press, Cape Town.

Suckling, G. W. 1989. Developmental defects of enamel –historical and present-day perspectives of their pathogenesis. Advances in Dental Research 3(2): 87-94.

Suckling, G. W. and D. J. Purdell-Lewis. 1982. The pattern of mineralisation of traumatically induced developmental defects of sheep enamel assessed by microhardness and microradiography. Journal of Dental Research 61(10): 1211-1216.

Suckling, G. and D. C. Thurley. 1984. Developmental defects of enamel: factors influencing their macroscopic appearance; Pp. 357-362 *in* R. W. Fearnhead and S. Suga (eds.). Tooth Enamel IV. Elsevier Science Publishers, New York.

Suga, S. 1982. Progressive mineralisation pattern of developing enamel during the maturation stage. Journal of Dental Research 61: 1532-1542.

Suga, S. 1989. Enamel hypomineralisation viewed from the pattern of progressive mineralisation of human and monkey developmental enamel. Advances of Dental Research 3: 188-198.

Tankard, A. J. 1975. Varswater Formation of the Langebaanweg-Saldanha area, Cape Province. Transactions of the Geological Society of South Africa 77: 265-283.

Tankard, A. J. and J. Rogers. 1978. Late Cenozoic palaeoenvrionments on the west coast of southern Africa. Journal of Biogeography 5: 319-337.

Teaford, M. F. 1988. Scanning electron microscope diagnosis of wear patterns versus artifacts on fossil teeth. Scanning Microscopy 2(2): 1167-1175.

Teaford, M. F. and J. G. Robinson. 1989. Seasonal or ecological differences in diet and molar microwear in *Cebus nigrivittatus*. American Journal of Physical Anthropology 80: 391-401.

Thackeray, J. F. and J. A. Lee-Thorp. 1992. Isotope analysis of equid teeth from Wonderwerk Cave, northern Cape Province, South Africa. Palaeogeography, Palaeoclimatology, Palaeoecology 99: 141-150.

Trombe, J. C., 1972. Contribution a l'étude de la decomposition et de la reactivité de certaines apatites hydroxylées carbonatées ou fluorêes alcalino terreuses. Thesis d'Etat, Universite Paul Sabitier, Toulouse.

Van Couvering, J. A. 1976. The terminal Miocene event. Marine Micropalaeontology 1: 263-286.

Van der Merwe, N. J. and E. Medina. 1991. The canopy effect, carbon isotope ratios and foodwebs in Amazonia. Journal of Archaeological Science 18: 249-256.

Van der Merwe, N. J. and J. F. Thackeray. 1997. Stable carbon isotope analysis of the Plio-Pleistocene ungulate teeth from Sterkfontein. South African Journal of Science 93: 194.

Vogel, J. C. 1978. Isotopic assessment of the dietary habits of ungulates. South African Journal of Science 74: 298-301.

Vogel, J. C., A. Fuls, and R. P. Ellis. 1978. The geographical distribution of Kranz grasses in southern Africa. South African Journal of Science 74: 209-214.

von Koenigswald, W. and H. U. Pfretzschner. 1987. Hunter-Schreger-Bander im Zahnschmelz von Saugtieren (Mammalia). Zoomorphology 106: 329-338.

von Koenigswald, W., J. M. Rensberger, and H. U. Pretzschner. 1987. Changes in the tooth enamel of Early Paleocene mammals allowing increased diet diversity. Nature 328: 150-152.

von Koenigswald, W. and P. M. Sander (eds.). 1997. Tooth enamel microstructure. Balkema, Rotterdam. Pp. 267-297.

Vrba, E. 1985. Ecological and adaptive changes associated with early hominid evolution; Pp. 63-71 *in* E. Delson (ed.). Ancestors: The hard evidence. Alan R. Liss, New York.

Vrba, E. 1982. Biostratigraphy and chronology, based particularly on Bovidae of Southern hominid-associated assemblages: Makapansgat, Sterkfontein, Taung, Kromdraai, Swartkrans, and Elandsfontein (Saldanha), Broken Hill (now Kabwe) and Cave of Hearths. Proceedings: Congres de Paléontologie Humaine 1er Congres. 707-752. Nice.

Vrba, E. S. and F. E. Grine. 1978. Australopithecine prism patterns. Science 202: 890-892.

Walker, A., H. N. Hoeck, and L. Perez. 1978. Microwear of mammalian teeth as indicators of diet. Science 201: 908-910.

Wang, Y. and T. E. Cerling. 1994. A model of fossil tooth and bone diagenesis: implications for paleodiet reconstruction from stable isotopes. Palaeogeography, Palaeoclimatology, Palaeoecology 107: 281-289.

Weinreb, M. M. 1964. Tooth development in sheep. American Journal of Veterinary Research 25(107): 891-908.

Wright, L. E. and H. P. Schwartz. 1999. Correspondence between stable carbon, oxygen, and nitrogen isotopes in human tooth enamel and dentine: Infant diets at Kaminaljuyu. Journal of Archaeological Science 26: 1159-1170.

Yakir, D. 1992. Variations in the natural abundances of oxygen-18 and deuterium in plant carbohydrates. Plant, Cell and Environment 15: 1005-1020.

Young, T. P. and L. A. Isbell. 1991. Sex differences in giraffe feeding ecology: energetic and social constraints. Ethology 87: 79-89.

Zachos, J., M. Pagani, L. Sloan, E. Thomas, and K. Billups. 2001. Trends, Rhythms, and Abberations in Global Climate 65 Ma to present. Science 292: 685-693.

Zazzo, A., H. Bocherens, M. Brunet, A. Beauvilain, D. Billiou, H. T. Mackaye, P. Vignaud, and A, Mariotti. 2000. Herbivore paleodiet and paleoenvironment changes in Chad during the Pliocene using stable isotope ratios of tooth enamel carbonate. Paleobiology 26(2): 294-309.

Chapter 11

APPENDICES

Appendix A. Sketch of an aerial view of the Varswater Formation ('E' quarry) showing the relative positions of the Quartzose Sand Member (QSM) and the Pelletal Phosphate Member (PPM). West wall and main river channel are PPM deposits. The bottom cut of the west wall is Bed 3aS and the top cut is Bed 3aN. East stream and far east area are QSM deposits.

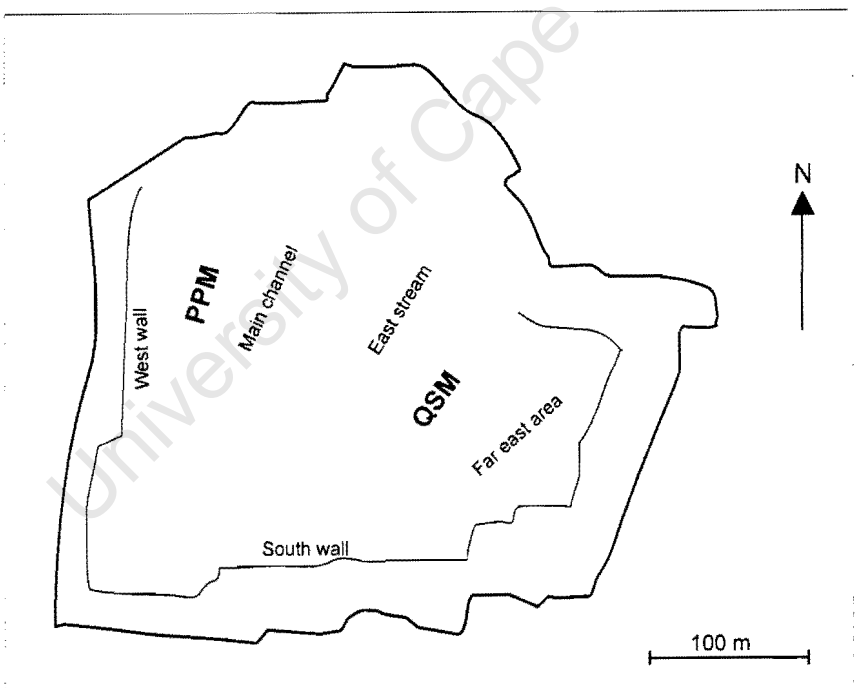

Appendix B. The Early Pliocene mammals of the Varswater Formation, Langebaanweg (Hendey, 1984). (See Hendey, 1981b for original species list and list for lower vertebrates).

	QSM	PPM 3aS	PPM 3aN
ORDER INSECTIVORA			
Family Chrysochloridae (golden moles)			
Chrysochloris sp.	x	x	x
Family Soricidae (shrews)			
Myosorex sp.	x		
Suncus sp.	x		
Soricidae gen. & sp. not det.	x	x	x
Family Macroscelididae (elephant shrews)			
Elephantulus sp.	x	x	x
ORDER CHIROPTERA			
Family Vespertilionidae			
Eptesicus sp.	x		
ORDER PRIMATES			
Family Cercopithecidae (monkeys etc.)			
Gen. & sp. indet.	x		
ORDER PHOLIDOTA			
Phataginus sp.	x		
ORDER TUBULIDENTATA (aardvarks)			
Gen. & sp. not det.	x		x
ORDER CARNIVORA			
Family Canidae (foxes, jakkals, etc.)			
Gen. & sp. not det.		x	?
Vulpes sp. (fox)		x	x
Family Ursidae (bears)			
Agriotherium africanum		x	x
Family Mustelidae (weasels, martins etc.)			
Plesiogulo monspessulanus	x	?	
Mellivora benfieldi (honey badger)		x	x
Enhydriodon africanus (otter)		x	x
Family Phocidae (seals)			
Homiphoca capensis	x	x	x
Family Viverridae (mongooses etc.)			
'Viverra' leakeyi (civet)	x		x
Viverrinae gen. & sp. not det. (civet)	x	x	x
Genetta sp. (genet)	x		
Herpestes spp. A, B (mongooses)	x	x	
Herpestinae spp. C, D, E (mongooses)	x		
Herpestinae not det.		x	x
Family Hyaenidae (hyaenas)			
'Adcrocuta' australis	x	?	?
Ictitherium preforfex		x	x
Hyaena abronia (striped hyaena)	x	x	x
Hyaenictitherium namaquense	x		
Euryboas sp. (hunting hyaena)	x	x	x
Hyaenidae sp. E		x	
Hyaenidae not det.		x	x
Family Felidae (cats)			
'Machairodus' sp. (sabre-tooth)	x		
Homotherium sp. (sabre-tooth)	x	x	?
Felis sp. (wildcat)	x		
Felis aff. *issiodorensis* (lynx)	x	x	x
Felis obscura		x	

(Contd.)

	QSM	PPM 3aS	PPM 3aN
Family Felidae (continued)			
Dinofelis diastemata (false sabre-tooth)	x	x	x
Felidae not det.		x	x
Carnivora not det.			
Gen. & sp. not det. (Canidae or Viverridae)	x		
Gen. & sp. not det. (?Procyonidae)	x		
Gen. & sp. not det. (?Lutrinae)	x		
ORDER PROBOSCIDEA (elephants, mastodons etc.)			
Family Gomphotheriidae			
Anancus sp.	x	x	
Family Elephantidae			
Mammuthus subplanifrons	x	?	x
ORDER HYRACOIDEA (hyraxes or dassies)			
Family Procaviidae			
Procavia cf. *antiqua*	x		?
ORDER PERISSODACTYLA			
Family Equidae (horses)			
Hipparion cf. *baardi*	x	x	x
Family Rhinocerotidae (rhinos)			
Ceratotherium praecox	x	x	
ORDER ARTIODACTYLA			
Family Tayassuidae (peccaries)			
Pecarichoerus (or *Barberahyus*) *africanus*		x	x
Family Suidae (pigs)			
Nyanzachoerus cf. *pattersoni* (or *kanamensis*)	x		
Nyanzachoerus cf. *jaegeri*		x	
Family Hippopotamidae (hippos)			
Gen. & sp. not det.		x	x
Family Giraffidae (giraffes, okapi, etc.)			
Sivatherium hendeyi	x	x	x
Palaeotragus cf. *germaini*			x
Giraffa sp.	x	x	x
Family Bovidae (buffaloes, antelopes etc.)			
Tragelaphus sp. A (nyala-like)	x	x	x
Tragelaphus sp. B (nyala-like)			x
Mesembriportax (or *Miotragoceros*) *acrae* (kudu-like relative of the niglai)	x	x	x
Simatherium demissum (buffalo)	x	x	x
Kobus subdolus (kob-like)		x	x
Kobus sp. B (kob-like)			x
Damalacra neanica (hartebeest-like)		x	x
Damalacra acalla (hartebeest-like)	x	x	x
Raphicerus paralius (steenbok)	x	x	x
Gazella sp. (gazelle)	x	x	x
Ovibovini gen. & at least 2 spp. not det.	x	x	x
ORDER LAGOMORPHA			
Family Leporidae (hares, rabbits)			
Pronolagus sp.	x	x	x
ORDER RODENTIA			
Family Bathyergidae (rodent moles)			
Bathyergus sp.	x	x	x
Cryptomys sp.	x		?
Family Hystricidae (porcupines)			
Gen. & sp. not det. A	x		
Gen. & sp. not det. B		x	x

(Contd.)

	QSM	PPM 3aS	PPM 3aN
ORDER RODENTIA (continued)			
Family Cricetidae (rats, mice, gerbils etc.)			
Mystromys sp. A.	x		
Mystromys cf. *darti*	x		
Mystromys cf. *hausleitneri*	x		
Gerbillus or *Desmodillus* sp.	x		
Dendromus sp.	x		
Steatomys or *Malacothrix* sp.	x		
Family Muridae (rats, mice)			
Aethomys spp. A and B	x		
Mus spp. A and B	x		
Rhabdomys sp.	x		
Euryotomys pelomyoides	x		
Family Muscardinidae (dormice)			
Graphiurus sp.	x		
Rodentia not det.	x	x	x
ORDER CETACEA (whales, dolphins)			
Gen. & spp. not det.	x	x	x

Appendix C. Excavations and dumps analysed in this study. (A) Table showing the excavations/dumps and river channel (Bed 3aN and Bed 3aS) deposits, together with the animals from each area. Giraffids include *Sivatherium (S), Giraffa (G)* and *Palaeotragus (P)*. Other animals include reduncines (*Kobus*), boselaphine (*Mesembriportax*), alcelaphines (*Damalacra*), bovines (*Simatherium*), equids (*Hipparion*), suids (*Nyanzachoerus*), rhinoceros (*Ceratotherium*) and hippopotamus (not det.). (B) A sketch showing the relationship between the Bed 3aN excavations and dumps that were studied. Wet and dry channels are indicated by curved arrows and represent the seasonal fluctuations of the main river channel during high and reduced rainfall periods. The current excavation at the West Coast Fossil Park, Langebaanweg is also shown.

A

Excavation/dump	PPM channel deposit	animals studied
1966/2, Bottom Cut West Wall	Bed 3aS	reduncines
		boselaphines
		alcelaphines
		rhinoceros
		bovines
		equids
		hippopotamus
		suids
1975/1, Top Cut West Wall	Bed 3aN	equids
1976/2, Indent West of Rock Platform	Bed 3aN	giraffids *(S, G)*
		equids
		hippopotamus
Dump 8	Bed 3aN	equids
		giraffids *(S, G)*
		alcelaphines
Dump 9	Bed 3aN	equids
Dump 10	Bed 3aN	boselaphines
		giraffids *(G, S, P)*
		hippopotamus
		equids
		alcelaphines
Area 2 1975 light grey sand	PPM	equids

B

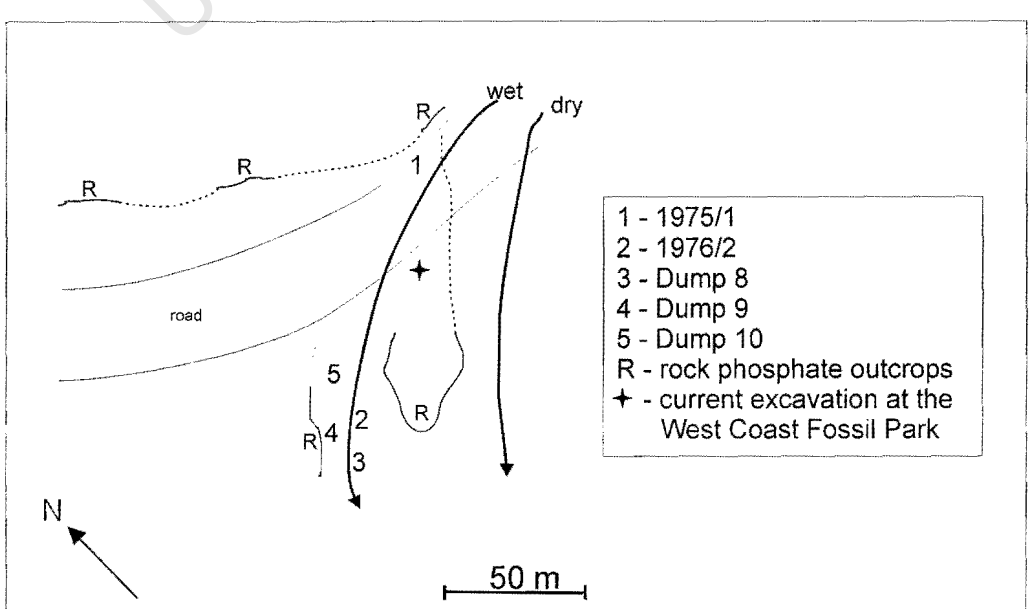

Appendix D. Expected and predicted diets of the ungulates from LBW compared to other African localities. (G) grazers, (B) browsers and (MF) mixed feeders.

	Modern	**LBW**	**Other fossil localities ****		
LBW fauna	**Extant diet** (Apps, 1986; Kingdon, 1982; Harris and White, 1979)	**Inferred diet * (~ 5 Myr)** (Hendey, 1984)	**North Africa (Chad)** (Zazzo et al., 2000)	**South Africa (Makapansgat and Sterkfontein)** (Sponheimer et al. ,1999, 2001, submitted; Luyt, 2001)	**Other African localities**
Order Artiodactyla					
Family Giraffidae					
Giraffa sp.	B	B	B (5-6 Myr)	B (3 Myr)	
Palaeotragus sp.		B			B (Fort Ternan, Kenya) (13.9-14 Myr) (Cerling et al., 1997a)
Sivatherium sp.		B	G (3-3.5 Myr) (Zazzo, pers comm., 2000)	B (3 Myr)	G (1.8 Myr) (Olduvai, Tanzania) (Van der Merwe, pers comm., 2000)
Family Bovidae					
Boselaphini (*Mesembrioportax* sp.)		B			
Reduncini (*Kobus* sp.)	G	B	MF to G (3-3.5 Myr); G (4-5 Myr); MF to G (5-6 Myr)	G (3 Myr)	
Bovini (*Simatherium* sp.)		G	MF to G (3-3.5 Myr); MF to G (5-6 Myr)	MF (3 Myr)	
Alcelaphini (*Damalacra* sp.)	G	G	G (3-3.5 Myr)	G (2.6 Myr)	
Family Hippopotamidae	G		G (4-5 Myr); MF (5-6 Myr)		
Family Suidae (*Nyanzachoerus* sp.)	G, B		G (4-5 Myr); MF (5-6 Myr)		
Order Perrissodactyla					
Family Equidae (*Hipparion* sp.)	G	G	G (3-3.5 Myr); G (5-6 Myr)	G (3 Myr) G (2.6 Myr)	
Family Rhinocerotidae (*Ceratotherium* sp.)	G	G	G (3-3.5 Myr); MF to G (4-5 Myr)	MF (3 Myr)	

* inferred from tooth morphology and the diets of modern analogues ; ** based on stable isotopes from tooth enamel and premaxilla shape.

Appendix E. Corrected individual and mean $\delta^{13}C$ and $\delta^{18}O$ values for modern and fossil species. All values are in parts per mil (‰) relative to PDB standard. (PPM = Pelletal Phosphate Member). (UCT accession numbers refer to material from the Archaeometry Department, University of Cape Town, South Africa).

Accession number	Animal	Source	$\delta^{13}C$	$\delta^{18}O$
	Modern Animals	**From South Africa**		
UCT 7421R	*Giraffa camelopardalis*	summer rainfall area	-13.0	1.17
UCT 7285R	*Connochaetes taurinus*	summer rainfall area	-1.8	-0.96
UCT 7557	*Raphicerus campestris*	winter rainfall area	-13.0	-5.90
UCT 7556	*Raphicerus melanotis*	winter rainfall area	-12.1	-3.93
UCT 7555	*Damaliscus dorcas*	winter rainfall area	-8.0	-1.84
UCT 7554	*Damaliscus dorcas*	winter rainfall area	-10.9	-2.47
UCT 5276	*Damaliscus dorcas*	winter rainfall area	-11.6	-3.66
	Fossil animals			
	Order Artiodactyla			
	Family Giraffidae		-11.5 ± 1.1	-2.8 ± 1.4
PQL 43928	*Sivatherium hendeyi*	Bed 3aN, PPM	-12.0	-3.0
PQL 43931	*Sivatherium hendeyi*	Bed 3aN, PPM	-13.5	-5.9
PQL 43932	*Sivatherium hendeyi*	Bed 3aN, PPM	-13.6	-3.9
PQL 64186B	*Sivatherium hendeyi*	Bed 3aN, PPM	-10.5	-1.2
PQL 64186Y	*Sivatherium hendeyi*	Bed 3aN, PPM	-10.4	-2.0
PQL 45091A	*Sivatherium hendeyi*	Bed 3aN, PPM	-10.7	-2.8
PQL 45744	*Sivatherium hendeyi*	Bed 3aN, PPM	-10.5	-2.8
PQL 44047	*Sivatherium hendeyi*	Bed 3aN, PPM	-10.7	-0.6
PQL 44045	*Sivatherium hendeyi*	Bed 3aN, PPM	-10.3	-3.6
PQL 44043	*Sivatherium hendeyi*	Bed 3aN, PPM	-11.1	-3.3
PQL 50325	*Sivatherium hendeyi*	Bed 3aN, PPM	-9.9	-1.8
PQL 43927	*Sivatherium hendeyi*	Bed 3aN, PPM	-11.1	-0.3
PQL 44044	*Sivatherium hendeyi*	Bed 3aN, PPM	-11.9	-3.0
PQL 44046	*Sivatherium hendeyi*	Bed 3aN, PPM	-11.6	-3.4
PQL 44050	*Sivatherium hendeyi*	Bed 3aN, PPM	-13.5	-3.4
PQL 44051	*Sivatherium hendeyi*	Bed 3aN, PPM	-12.7	-5.3
PQL 45091B	*Sivatherium hendeyi*	Bed 3aN, PPM	-10.8	-2.3
PQL 50320F	Giraffid	Bed 3aN, PPM	-11.1	-3.5
PQL 44048	Giraffid	Bed 3aN, PPM	-12.3	-1.1
PQL 44049	Giraffid	Bed 3aN, PPM	-11.1	-3.8
PQL 43934	Giraffid	Bed 3aN, PPM	-13.2	-2.3
PQL 50320A	Giraffid	Bed 3aN, PPM	-12.1	-4.0
PQL 50320D	Giraffid	Bed 3aN, PPM	-12.5	-1.1
PQL 50320E	Giraffid	Bed 3aN, PPM	-10.4	-2.9
PQL 50320C	Giraffid	Bed 3aN, PPM	-11.3	-3.8
	Family Hippopotamidae		-12.0 ± 1.5	-5.9 ± 1.0
PQL 50287A	Gen. and sp. not determined	Bed 3aN, PPM	-10.9	-3.8.
PQL 52743A	Gen. and sp. not determined	Bed 3aN, PPM	-13.3	-7.4
PQL 50288B	Gen. and sp. not determined	Bed 3aN, PPM	-11.6	-4.7
PQL 43926	Gen. and sp. not determined	Bed 3aN, PPM	-12.7	-5.4
PQL 43925	Gen. and sp. not determined	Bed 3aN, PPM	-14.9	-6.5
PQL 60533B	Gen. and sp. not determined	Bed 3aN, PPM	-12.0	-7.5
PQL 44038	Gen. and sp. not determined	Bed 3aN, PPM	-11.8	-6.4
PQL 44039	Gen. and sp. not determined	Bed 3aN, PPM	-9.4	-6.2
PQL 44040	Gen. and sp. not determined	Bed 3aN, PPM	-12.1	-5.1
PQL 44041	Gen. and sp. not determined	Bed 3aN, PPM	-11.5	-4.9

(Contd.)

Accession number	Animal	Source	$\delta^{13}C$	$\delta^{18}O$
PQL 44042	Gen. and sp. not determined	Bed 3aN, PPM	-13.6	-6.1
PQL 50288C	Gen. and sp. not determined	Bed 3aN, PPM	-10.0	-5.7
PQL 50288D	Gen. and sp. not determined	Bed 3aN, PPM	-13.8	-6.4
PQL 49135	Gen. and sp. not determined	Bed 3aN, PPM	-11.7	-7.0
PQL 49609	Gen. and sp. not determined	Bed 3aN, PPM	-10.3	-5.7
	Family Suidae		-11.8 ± 1.0	-3.1 ± 0.8
PQL 42671	*Nyanzachoerus* cf. *jaegeri*	Bed 3aS, PPM	-12.2	-2.9
PQL 3924	*Nyanzachoerus* cf. *jaegeri*	Bed 3aS, PPM	-10.3	-4.2
PQL 43930	*Nyanzachoerus* cf. *jaegeri*	Bed 3aS, PPM	-12.5	-3.0
PQL 41650	*Nyanzachoerus* cf. *jaegeri*	Bed 3aS, PPM	-12.0	-2.2
	Family Bovidae		-10.8 ± 0.9	-3.2 ± 1.5
PQL 40361	*Kobus* sp.	Bed 3aS, PPM	-10.7	-4.3
PQL 30574	*Kobus* sp.	Bed 3aS, PPM	-10.7	-1.4
PQL 63650B	*Damalacra* sp.	Bed 3aN, PPM	-11.4	-4.4
PQL 63661C	*Damalacra* sp.	Bed 3aN, PPM	-12.3	-4.6
PQL 63654B	*Damalacra* sp.	Bed 3aN, PPM	-9.3	-2.3
PQL 63654A	*Damalacra* sp.	Bed 3aN, PPM	-10.5	-1.5
PQL 63661A	*Damalacra* sp.	Bed 3aN, PPM	-10.3	-4.2
PQL 63661B	*Damalacra* sp.	Bed 3aN, PPM	-10.3	-1.3
PQL 10167	*Damalacra* sp.	Bed 3aS, PPM	-11.5	-4.4
	Order Perissodactyla			
	Family Rhinocerotidae		-11.1 ± 0.8	-4.4 ± 1.2
PQL 2519J	*Ceratotherium praecox*	Bed 3aS, PPM	-11.1	-5.2
PQL 11133A	*Ceratotherium praecox*	Bed 3aS, PPM	-10.1	-2.6
PQL 11152A	*Ceratotherium praecox*	Bed 3aS, PPM	-10.5	-5.7
PQL 10989A	*Ceratotherium praecox*	Bed 3aS, PPM	-11.7	-4.5
PQL 11148A	*Ceratotherium praecox*	Bed 3aS, PPM	-11.9	-4.2
	Family Equidae		-11.3 ± 0.9	-3.6 ± 1.9
PQL 52910	*Hipparion* cf. *baardi*	Bed 3aN, PPM	-11.7	-5.6
PQL 43922	*Hipparion* cf. *baardi*	Bed 3aN, PPM	-12.9	-5.6
PQL 10954	*Hipparion* cf. *baardi*	PPM	-11.0	-4.6
PQL 50237	*Hipparion* cf. *baardi*	Bed 3aN, PPM	-11.2	-2.2
PQL 44037	*Hipparion* cf. *baardi*	Bed 3aS, PPM	-10.7	-1.3
PQL 40924	*Hipparion* cf. *baardi*	PPM	-10.4	-2.3

Appendix F. Corrected $\delta^{13}C$ and $\delta^{18}O$ values taken from across *S. hendeyi* mandibular third molars. The lowercase letter after each accession number indicates the sample position ('a' is at base of the tooth).

Accession number	$\delta^{13}C$	$\delta^{18}O$
PQL 43944 a	-9.773	0.156
PQL 43944 b	-9.732	0.087
PQL 43944 c	-10.295	-1.040
PQL 43944 d	-11.020	-1.729
PQL 43944 e	-10.860	-1.365
PQL 43944 f	-10.992	-1.530
PQL 43944 g	-11.139	-1.171
PQL 43944 h	-11.018	-0.965
PQL 43944 i	-11.182	-1.275
PQL 43944 j	-11.046	-0.820
PQL 43944 k	-10.806	-0.685
PQL 43944 l	-10.797	-0.666
PQL 43944 m	-10.970	-1.881
PQL 43944 n	-10.758	-0.273
PQL 43944 o	-11.321	0.011
PQL 62733/16 a	-10.486	-0.670
PQL 62733/16 b	-10.479	-0.312
PQL 62733/16 c	-10.752	-0.632
PQL 62733/16 d	-10.897	-1.233
PQL 62733/16 e	-10.960	-1.890
PQL 62733/16 f	-10.858	-2.939
PQL 62733/16 g	-10.392	-1.370
PQL 62733/16 j	-10.034	-0.829
PQL 62733/16 k	-9.931	-0.862
PQL 62733/16 l	-10.184	-0.821
PQL 62733/57 a	-11.152	0.831
PQL 62733/57 b	-11.015	-0.800
PQL 62733/57 c	-11.115	-1.423
PQL 62733/57 d	-10.944	-1.091
PQL 62733/57 e	-10.940	-0.369
PQL 62733/57 f	-10.321	-0.192
PQL 62733/57 g	-10.369	-0.086
PQL 62733/57 h	-10.252	1.167
PQL 62733/57 i	-10.508	0.503
PQL 62733/57 j	-10.724	0.007
PQL 62733/57 k	-10.723	-
PQL 62733/57 l	-10.496	0.250
PQL 62733/57 m	-10.849	-0.856
PQL 62733/57 n	-10.682	-0.947
PQL 62733/57 o	-10.708	-1.054
PQL 62733/57 p	-10.619	-0.571
PQL 62733/57 q	-10.470	0.553

Appendix G. Skeletal elements that were examined. (Rhinoceros = *C. praecox*, Hippopotamus = Gen and Sp. not determined, Sivathere = *S. hendeyi* and Equid = *Hipparion* cf. *baardi*.

Complete specimens

	astralagus	calcaneum	clavicle	digit bones	femur	fibula	humerus	metapodial	patella	pelvis	phalanges	radius	rib	scapula	sternum	tibia	ulna	vertebrae
Rhinoceros	0	0	0	0	0	0	0	1	0	0	0	2	0	0	0	0	0	0
Hippopotamus	4	4	0	6	4	0	0	12	0	1	15	0	0	0	0	0	0	2
Sivathere	2	1	0	26	1	1	0	18	0	0	8	1	0	0	0	2	1	0
Equid	2	0	0	2	0	0	0	0	0	0	8	0	0	0	0	0	0	0

Partial specimens

	astralagus	calcaneum	clavicle	digit bones	femur	fibula	humerus	metapodial	patella	pelvis	phalanges	radius	rib	scapula	sternum	tibia	ulna	vertebrae
Rhinoceros	0	0	0	0	4	0	0	0	0	0	0	11	0	0	0	7	0	0
Hippopotamus	1	1	0	1	0	0	0	12	0	1	0	1	0	1	0	1	1	1
Sivathere	0	1	0	3	0	0	3	30	0	0	1	0	0	1	0	2	0	0
Equid	0	1	0	3	1	0	0	5	0	0	5	4	0	0	0	0	0	0

Appendix H. Linear enamel hypoplasia in each tooth type for each animal indicating the number of teeth with linear defects, without defects and the total number of teeth analysed. Deciduous teeth are in parentheses.

		With LEH	Without defects	Total number
Bovidae				
Reduncini	Molars	5	23	28
(*Kobus* sp.)	Premolars	4	6 (1)	11
	Incisors	0	3	3
	Canines	0	0	0
	Unknown	0	1	1
	TOTAL	**9**	**34**	**43**
Bovini	Molars	6	49	55
(*S. demissum*)	Premolars	6	55 (13)	74
	Incisors	0	0	0
	Canines	0	0	0
	Unknown	0	0	0
	TOTAL	**12**	**117**	**129**
Boselaphini	Molars	2	69	71
(*M. acrae*)	Premolars	3 (1)	78 (30)	112
	Incisors	0	0	0
	Canines	0	0	0
	Unknown	0	0	0
	TOTAL	**6**	**177**	**183**
Alcelaphini	Molars	12	128	140
(*Damalacra* sp.)	Premolars	4	44 (6)	54
	Incisors	0	3 (3)	6
	Canines	0	0	0
	Unknown	0	0	0
	TOTAL	**16**	**184**	**200**
Indeterminate	Molars	6	22	28
	Premolars	0 (1)	4	5
	Incisors	1	37 (15)	51
	Canines	0	0	0
	Unknown	0	0	0
	TOTAL	**8**	**78**	**84**
Giraffidae				
(Palaeotragus)	Molars	0	0	0
	Premolars	0	24 (5)	29
	Incisors	0	0	0
	Canines	0	0	0
	Unknown	0	0	0
	TOTAL	**0**	**29**	**29**

(Contd.)

		With LEH	Without defects	Total number
(*S. hendeyi*)	Molars	135	316 (5)	456
	Premolars	87	287 (159)	533
	Incisors	193	440	633
	Canines	20	66 (51)	137
	Unknown	0	0	0
	TOTAL	**433**	**1321**	**1759**
Rhinocerotidae	Molars	3	24 (4)	31
(*C. praecox*)	Premolars	0	14 (5)	19
	Incisors	0	0	0
	Canines	0	0	0
	Unknown	0	0	0
	TOTAL	**3**	**47**	**50**
Hippopotamidae	Molars	23	59 (1)	83
(Gen. & sp. not det.)	Premolars	15 (2)	27 (32)	76
	Incisors	6 (1)	16 (4)	27
	Canines	21	20 (0)	41
	Unknown	3 (1)	6	10
	TOTAL	**72**	**165**	**237**

Appendix I. *Giraffa camelopardalis* teeth examined. Teeth are present in both left and right jaws unless otherwise stated.

Accession number	Age	Description
ZM 39558	Juvenile	mandibles: di1, di2. di3, dc, dp2, dp3, d4 maxillae: dP2, dP3, dP4
ZM 39204	Juvenile	mandibles, di1,di2, di3, dp2, dp3, dp4, m1 (unerupted) maxillae: dP2, dP3, dP4, M1 (unerupted)
ZM 39795	Sub-adult	mandibles: i1, i2, i3, c, dp2, dp3, dp4 maxillae: dP2, dP3, dP4
ZM 35365	Sub-adult	mandibles: dp2, dp3, dp4, m1, m2, m3 maxillae: dP2, dP3, dP4, M1, M2 (right only)
ZM 36851	Sub-adult	mandible, di1, di2, di3, dc, dp2, dp3, dp4, m1, m2, m3 (still erupting) maxillae: dP2, dP3, dP4, M1, M2, M3 (still erupting)
ZM 33540	Sub-adult	mandibles: dp2, dp3, dp4, m1, m2 (embedded, still erupting) maxillae: dP2, dP3, dP4, M2 (embedded, still erupting)
ZM 35364	Adult	mandibles: p2, p3, p4, m1, m2, m3 maxillae: P2, P3, P4, M1, M2, M3
ZM 39692	Adult	mandibles: p2, p3, p4, m1, m2, m3 maxillae: P2, P3, P4, M1, M2, M3
ZM 35363	Adult	mandibles: none maxillae: P2 (right only), P3, P4, M1, M2, M3
ZM 36655	Adult	mandibles: none maxillae: P2, P3, P4, M1, M2, M3 (right only)
ZM 36654	Adult	mandibles: i1-3 (isolated), p2, p3, p4, m1, m2, m3 maxillae: P2, P3, P4, M1, M2, M3
ZM 37058	Adult	mandibles: p2, p3, p4, m1, m2, m3 maxillae: P2, P3, P4, M1, M2, M3
ZM 17176	Adult	mandibles: p2, p3, p4, m1, m2, m3 maxillae: P2, P3, P4, M1, M2, M3

Appendix J. Numbers of *S. hendeyi* mandibular teeth affected with each defect type. Numbers in parentheses are possibly defective. 'n' refers to the total number of teeth examined.

Tooth type	n	Numbers of teeth			Numbers of defects			
		Defective	Linear enamel hypoplasia (LEH)	Non-linear enamel hypoplasia	Single pit	Area missing enamel	Multiple pits (not LEH)	Short groove (not LEH)
di	5	0	0	0	0	0	0	0
dc	51	15	0	14	5	8	4	0
dp2	59	17	0	17	10	9	0	0
dp3	48	3	0	3	2	2	0	0
dp4	52	6	0	6	2	5	0	1
Incisor	633	326	193 (18)	190	46	22	146 (4)	9 (6)
Canine	86	50	20 (1)	38	16	3	28	0 (1)
p2	151	61	31 (3)	43	13	4	32 (1)	8 (1)
p3	134	66	30	46	5	2	21	0
p4	89	58	27	40	6	3	40	5 (2)
m1	120	51	32 (23)	33	6	4	12	15 (5)
m2	115	62	35 (13)	43	11	3	24	15
m1 or m2	81	46	21 (11)	36	9	9	12	18 (1)
m3	135	101	47 (8)	79	27	15	65	7

Appendix K. Results from Student's t-test comparing the widths of grooves to the widths of bands of pits. (No canines have grooves).

Tooth type	*p* value	t-statistic	degrees of freedom
Incisors	$p < 0.0001$	5.237	336
p2	$p = 0.145$	-1.475	64
p3	$p = 0.06$	-1.919	56
p4	$p < 0.05$	-2.044	66
m1	$p < 0.0001$	-8.917	54
m2	$p < 0.001$	-3.554	66
m3	$p < 0.0001$	5.905	112

Appendix L. Associated mandibular first (m1) and second (m2) molars used for sorting isolated teeth. Anteroposterior (AP) and buccolingual (BL) measurements and dental index (DI) are given. The accession numbers for each mandible fragment are given. Dashes indicate teeth that were broken so that no measurement could be taken. AP and BL measurements are in millimetres and DI is a percentage and is described in section 7.2.2.2.

	m1			M2		
Accession numbers	**AP**	**BL**	**DI**	**AP**	**BL**	**DI**
PQL 62736	48.63	34.58	71.1	50.29	35.15	68.9
PQL 45008	50.71	35.53	69.7	49.03	-	-
PQL 45122	44.55	32.70	73.4	50.71	35.33	69.7
PQL 45128	50.75	35.61	70.2	55.04	38.54	70.0
PQL 45289	-	33.65	-	50.91	35.77	70.3
PQL 45000	42.47	34.65	81.59	47.25	34.15	72.3

Appendix M. Specimens used to calculate the hypsodonty index of *S. hendeyi*.

Accession number	**Crown height (mm)**	**Width (mm)**	**Hypsodonty index**
PQL 62733/63, unworn	43.50	29.72	1.46
PQL 62732/33, unworn	46.89	30.33	1.55
PQL 62733/11	39.18	32.10	1.22
PQL 62733/20	40.63	30.28	1.34
PQL 62733/43	44.78	35.42	1.26
PQL 62732/12	42.10	35.08	1.20
PQL 62732/26	47.88	36.03	1.33
PQL 62732/28	47.52	31.28	1.52
PQL 62732/42	45.70	36.52	1.25
PQL 62732/45	45.26	35.87	1.26
PQL 62732/49	40.04	32.83	1.22

Appendix N. Raw mesowear data of *S. hendeyi* m2's. Cusp shape is described as round (R), sharp (S) and blunt (B). Occlusal relief is defined as distance from the valley to tip of the crown over crown height.

Lower m2					Upper M2				
Accession number	Cusp shape	Crown height (mm)	Distance from valley to tip (mm)	Occlusal relief (mm)	Accession number	Cusp shape	Crown height (mm)	Distance from valley to tip (mm)	Occlusal relief (mm)
PQL 43967	R	41.29	7.44	0.180	PQL 44658	S	38.27	8.78	0.229
PQL 43976	S	46.61	10.41	0.223	PQL 44659	S	41.28	9.15	0.222
PQL 43997	R	38.87	7.31	0.188	PQL 44661	R	35.00	9.78	0.279
PQL 44001	R	34.57	7.32	0.212	PQL 44663	R	35.59	8.60	0.242
PQL 44004	R	35.80	8.93	0.249	PQL 44668	S	33.84	8.83	0.261
PQL 44008	R	28.38	8.00	0.282	PQL 44665	R	41.61	9.22	0.222
PQL 44024	R	37.02	8.53	0.230	PQL 44660	S	33.82	7.71	0.228
PQL 43994	S	42.79	8.07	0.189	PQL 44664	R	41.18	8.87	0.215
PQL 43978	R	32.72	8.19	0.250	PQL 44674	R	42.98	7.00	0.163
PQL 43889	S	42.09	9.02	0.214	PQL 44671	S	43.97	9.69	0.220
PQL 44895	R	35.82	9.11	0.254	PQL 44672	R	25.25	8.62	0.341
PQL 44956	R	40.01	8.73	0.218	PQL 44673	R	40.35	7.53	0.187
PQL 44943	R	33.04	6.92	0.209	PQL 44670	R	45.08	7.63	0.169
PQL 44957	R	41.38	7.12	0.172	PQL 44751	R	42.49	7.04	0.166
PQL 44921	R	37.93	9.11	0.240	PQL 44755	R	33.29	8.99	0.270
PQL 44917	R	36.85	8.61	0.234	PQL 44758	R	33.72	9.65	0.286
PQL 44968	R	48.75	8.73	0.179	PQL 44743	S	39.33	10.65	0.271
PQL 44978	S	40.60	9.02	0.222	PQL 44745	R	44.88	8.63	0.192
PQL 44970	R	36.68	8.48	0.231	PQL 44759	R	39.63	8.22	0.207
PQL 44967	S	41.02	7.99	0.195	PQL 44760	R	38.06	9.69	0.255
PQL 44966	R	41.86	7.22	0.172	PQL 44740	R	28.88	6.27	0.217
PQL 44985	R	39.82	9.37	0.235	PQL 44761	S	43.91	8.66	0.197
PQL 45167	S	31.39	7.67	0.244	PQL 44739	S	38.89	9.03	0.232
PQL 44032	R	46.65	9.21	0.197	PQL 44734	R	36.00	4.91	0.136
PQL 44021	R	39.32	10.98	0.279	PQL 44736	S	44.44	8.80	0.198
PQL 43995	R	43.21	9.50	0.220	PQL 44937	S	42.54	8.35	0.196
PQL 43959	R	33.51	8.29	0.247	PQL 44729	S	42.42	7.83	0.185
PQL 44028	R	36.14	7.59	0.210	PQL 44731	R	41.23	10.07	0.244
PQL 43992	S	40.39	11.08	0.274	PQL 44723	R	35.40	7.24	0.205
PQL 44035	R	37.52	6.48	0.173	PQL 44752	R	34.07	6.54	0.192

Appendix O. Microwear data for *S. hendeyi*. Counts for pits and scratches (scr) in two counting areas per tooth are given as well as an assessment of large pits (0=small pits, 1=large pits), scratch texture (1= fine, 2 = coarse, 3= mixed), cross scratches and gouges(0=absent, 1=present).

Accession number	pits	pits	average pits	large pits	scr	scr	average scr	scr texture	cross scr	gouges
PQL 62737/25	33	13	23	1	2	0	1	1	0	1
PQL 62737/49	23	18	20.5	1	5	4	4.5	3	0	0
PQL 43964	15	25	20	1	7	3	5	2	0	0
PQL 62737/19	34	14	24	1	7	4	5.5	1	0	0
PQL 62737/2	15	4	9.5	1	6	5	5.5	3	0	0
PQL 44011	35	12	23.5	0	3	8	5.5	3	0	0
PQL 62737/24	44	37	40.5	0	6	7	6.5	2	0	0
PQL 44950	13	19	16	1	5	8	6.5	3	0	0
PQL 62737/5	12	15	13.5	0	5	8	6.5	2	0	0
PQL 44003	24	11	17.5	0	5	8	6.5	2	0	1
PQL 43995	47	60	53.5	0	5	8	6.5	3	0	0
PQL 44034	28	34	31	0	7	6	6.5	1	0	0
PQL 62737/28	12	9	10.5	0	5	8	6.5	3	0	0
PQL 44972	17	20	18.5	0	9	5	7	1	0	1
PQL 62737/22	26	30	28	0	5	11	8	1	0	1
PQL 62737/45	43	53	48	0	7	10	8.5	3	0	0
PQL 62737/15	35	63	49	0	3	14	8.5	3	0	0
PQL 44952	45	49	47	0	6	12	9	3	0	0
PQL 44020	34	41	37.5	1	13	5	9	1	0	0
PQL 62737/11	35	23	29	0	10	8	9	2	0	0
PQL 44008	8	35	21.5	1	9	9	9	1	0	0
PQL 44012	8	14	11	1	12	7	9.5	1	0	1
PQL 62737/12	72	69	70.5	0	7	12	9.5	2	0	1
PQL 44945	33	37	35	1	9	10	9.5	1	0	0
PQL 43976	38	54	46	1	12	8	10	2	0	1
PQL 62737/50	6	23	14.5	1	11	10	10.5	1	0	0
PQL 44948	36	32	34	0	9	12	10.5	3	0	0
PQL 44021	21	12	16.5	0	12	10	11	3	0	0
PQL 62737/36	26	38	32	0	12	10	11	3	0	0
PQL 43966	34	53	43.5	0	14	9	11.5	1	1	0
PQL 44976	4	6	5	1	10	14	12	2	0	0
PQL 62737/23	2	8	5	0	10	15	12.5	1	0	0
PQL 62737/27	35	15	25	1	13	12	12.5	1	0	0
PQL 62737/34	42	8	25	0	15	10	12.5	1	0	0
PQL 44004	2	23	12.5	1	16	10	13	3	1	0
PQL 62737/26	29	19	24	1	6	20	13	3	0	1
PQL 62737/39	0	6	3	1	14	13	13.5	3	0	0
PQL 43994	42	23	32.5	1	12	15	13.5	3	0	0
PQL 62738/38	2	15	8.5	1	14	14	14	2	1	0
PQL 62737/36	72	50	61	1	12	17	14.5	1	0	0
PQL 44970	1	8	4.5	1	13	17	15	1	1	0
PQL 62737/4	28	29	28.5	0	17	13	15	3	0	0
PQL 44024	24	20	22	0	20	11	15.5	3	0	0
PQL 44971	47	37	42	0	20	11	15.5	2	0	0

(Contd.)

Accession number	pits	pits	average pits	large pits	scr	scr	average scr	scr texture	cross scr	gouges
PQL 44941	21	39	30	0	13	19	16	1	1	0
PQL 62737/32	9	21	15	1	12	20	16	3	0	1
PQL 62737/43	33	10	21.5	0	17	15	16	1	0	0
PQL 62737/44	32	41	36.5	0	13	19	16	3	0	0
PQL 44977	32	44	38	0	19	14	16.5	3	0	0
PQL 43999	60	74	67	0	25	15	20	3	0	0
PQL 44959	11	17	14	0	28	13	20.5	2	0	0
PQL 62737/16	34	33	33.5	0	23	21	22	3	0	0
PQL 44956	17	18	17.5	0	27	21	24	1	0	1

Appendix P. Solounias' microwear data for *S. hendeyi* casts. Abbreviations as in Appendix O.

Accession numbers	pits	pits	average pits	large pits	scr	scr	average scr	scr texture	cross scr	gouges
PQL 62737/34	19	24	21.5	1	4	4	4	1	0	1
PQL 62737/43	20	28	24	1	4	4	4	1	1	1
PQL 62737/28	5	7	6	0	4	6	5	1	0	0
PQL 44959	7	6	6.5	1	8	3	5.5	1	1	1
PQL 62737/5	40	37	38.5	0	4	8	6	1	0	0
PQL 44945	13	15	14	0	6	7	6.5	1	0	1
PQL 62737/11	5	11	8	1	9	6	7.5	1	0	0
PQL 62737/15	9	14	11.5	1	8	8	8	1	1	1
PQL 44948	15	13	14	1	7	9	8	3	1	0
PQL 44008	5	15	10	1	4	14	9	3	0	1
PQL 62737/24	25	20	22.5	1	8	10	9	3	1	1
PQL 43994	6	6	6	1	16	4	10	1	1	1
PQL 62737/22	20	2	11	0	12	8	10	1	1	0
PQL 43976	4	9	6.5	0	7	14	10.5	1	0	1
PQL 43995	10	7	8.5	1	13	8	10.5	3	1	1
PQL 62737/43	24	19	21.5	0	10	11	10.5	1	0	1
PQL 62737/50	7	8	7.5	0	10	12	11	3	0	1
PQL 62737/44	20	20	20	1	13	9	11	3	1	0
PQL 62737/32	50	40	45	0	12	10	11	1	1	0
PQL 44034	32	34	33	0	12	14	13	3	0	0
PQL 62737/2	66	80	73	0	8	19	13.5	2	0	1
PQL 62737/25	20	25	22.5	0	18	10	14	2	1	0
PQL 62737/49	30	35	32.5	0	12	17	14.5	2	0	1
PQL 43999	9	14	11.5	1	17	14	15.5	1	1	1
PQL 44950	36	4	20	0	12	19	15.5	1	1	1
PQL 44977	28	14	21	0	23	8	15.5	1	0	1
PQL 62737/26	19	26	22.5	1	17	14	15.5	1	1	0
PQL 44021	6	8	7	1	14	18	16	1	1	1
PQL 44952	30	42	36	1	17	15	16	3	1	0
PQL 44971	9	5	7	0	14	19	16.5	2	1	0
PQL 62737/4	8	19	13.5	1	9	24	16.5	3	0	0
PQL 62737/23	23	18	20.5	1	16	19	17.5	3	1	1
PQL 44011	46	11	28.5	0	18	17	17.5	3	1	1
PQL 44012	42	26	34	0	16	20	18	1	1	0
PQL 43966/212	22	24	23	0	17	22	19.5	1	1	1
PQL 44020	28	16	22	0	22	18	20	2	1	0
PQL 62737/38	28	24	26	0	23	18	20.5	1	1	0
PQL 44003	14	45	29.5	1	18	23	20.5	2	1	0
PQL 44972	70	60	65	1	21	20	20.5	3	1	1
PQL 62737/12	18	34	26	1	14	28	21			1
PQL 62737/16	8	7	7.5	1	21	23	22	1	1	0
PQL 44941	6	22	14	0	19	25	22	1	1	0
PQL 44024	24	15	19.5	0	26	19	22.5	1	1	0
PQL 62737/36	18	27	22.5	1	24	21	22.5	3	1	1

(Contd.)

Accession numbers	pits	pits	average pits	large pits	scr	scr	average scr	scr texture	cross scr	gouges
PQL 62737/27	20	12	16	1	22	24	23	3	1	0
PQL 43964	30	15	22.5	0	24	26	25	3	1	0
PQL 62437/18	20	19	19.5	1	27	24	25.5	3	0	1
PQL 44970	28	18	23	0	24	27	25.5	1	1	0
PQL 44956	10	26	18	0	35	18	26.5	1	1	0
PQL 44976	8	18	13	0	29	25	27	3	1	0
PQL 62737/39	15	8	11.5	0	30	25	27.5	1	0	0
PQL 44004	4	3	3.5	1	39	37	38	1	1	0

Appendix Q. $\delta^{18}O$ and $\delta^{13}C$ values for *S. hendeyi* and *G. camelopardalis* mandibular second molars. Lower case letters after each accession number represents each enamel sample taken from the tooth crown ('a' is at the base of the crown). Distance from the base of the crown is given in millimetres for each sample.

S. hendeyi samples

Accession number	distance (mm)	$\delta^{18}O$	$\delta^{13}C$
PQL 43988 a	2.84	-0.181	-10.998
PQL 43988 b	4.75	-1.232	-11.150
PQL 43988 c	7.86	-1.410	-11.184
PQL 43988 d	11.39	-1.781	-11.297
PQL 43988 e	14.06	1.075	-11.279
PQL 43988 f	17.02	0.071	-11.428
PQL 43988 g	19.45	1.115	-11.432
PQL 43988 h	22.04	1.143	-11.424
PQL 43988 i	24.41	0.257	-11.468
PQL 43988 j	26.5	0.193	-11.624
PQL 43988 k	28.37	0.219	-11.505
PQL 43988 l	30.67	0.883	-11.580
PQL 43988 m	32.83	0.297	-11.604
PQL 43988 n	34.96	1.078	-11.732
PQL 43988 o	37.99	1.938	-12.001
PQL 43988 p	39.9	2.565	-12.280
PQL 43988 q	42.12	3.928	-12.606
PQL 44046 a	3.17	1.150	-10.772
PQL 44046 b	4.98	-0.182	-11.300
PQL 44046 c	7.52	0.291	-11.320
PQL 44046 d	10.19	-0.283	-11.332
PQL 44046 e	12.22	-1.039	-11.577
PQL 44046 f	15.07	-0.756	-11.488
PQL 44046 g	16.94	-1.429	-11.059
PQL 44046 h	18.65	-0.491	-10.453
PQL 44046 i	20.95	-0.989	-11.030
PQL 44046 j	23.16	-0.730	-10.775
PQL 44046 k	25.14	-0.525	-10.760
PQL 44046 l	27.41	0.342	-10.735
PQL 44046 m	29.75	0.521	-10.825
PQL 44046 n	31.8	0.094	-10.948
PQL 44045 o	34.32	-0.456	-11.163
PQL 44046 p	36.83	0.637	-11.082
PQL 43982 a	2.23	-0.326	-9.606
PQL 43982 b	4.42	-0.756	-9.574
PQL 43982 c	7.14	-1.064	-9.830
PQL 43982 d	9.89	-0.285	-9.921
PQL 43982 e	13.11	-0.453	-9.612
PQL 43982 f	14.76	-1.617	-10.496
PQL 43982 g	17.23	-1.600	-10.318
PQL 43982 h	19.62	-1.829	-10.254
PQL 43982 i	22.31	-1.678	-10.414
PQL 43982 j	24.35	-1.002	-10.330

(Contd.)

Accession number	distance (mm)	$\delta^{18}O$	$\delta^{13}C$
PQL 43982 k	26.72	-2.042	-10.254
PQL 43982 l	28.7	-1.583	-10.098
PQL 43982 m	30.84	-1.849	-10.202
PQL 43982 n	32.79	-1.290	-10.279
PQL 43982 o	34.92	-0.831	-10.277
PQL 43982 p	36.97	1.210	-11.130
PQL 62738/22 a	1.8	-0.646	-10.384
PQL 62738/22 b	4.27	-1.721	-10.377
PQL 62738/22 c	6.43	-1.001	-10.627
PQL 62738/22 d	8.56	-1.868	-10.465
PQL 62738/22 e	11	-1.781	-10.166
PQL 62738/22 f	13.25	-2.336	-9.917
PQL 62738/22 g	15.63	-2.011	-9.920
PQL 62738/22 h	18.43	-1.913	-9.849
PQL 62738/22 i	20.67	-1.104	-9.912
PQL 62738/22 j	23	-1.560	-9.890
PQL 62738/22 k	25.28	-1.576	-9.938
PQL 62738/22 l	27.96	-1.708	-10.041
PQL 62738/22 m	30.23	-1.359	-10.193
PQL 62738/22 n	32.2	-1.208	-10.335
PQL 62738/22 o	34.47	-1.468	-10.564
PQL 62738/22 p	37.07	0.032	-11.006
PQL 43985 a	1.99	0.459	-11.420
PQL 43985 b	3.93	1.910	-11.483
PQL 43985 c	7.45	1.223	-11.717
PQL 43985 d	10.14	0.889	-11.755
PQL 43985 e	13.12	0.945	-12.041
PQL 43985 f	16.35	1.251	-12.458
PQL 43985 g	19.09	1.748	-12.793
PQL 43985 h	22.32	1.787	-12.929
PQL 43985 i	25.03	2.190	-13.086
PQL 43985 j	27.19	2.521	-13.242
PQL 43985 k	29.69	2.057	-13.002
PQL 43985 l	32.33	1.433	-13.151
PQL 43985 m	35.11	2.124	-12.883
PQL 43985 n	38.33	1.339	-12.677
PQL 43985 o	40.31	1.075	-9.915
PQL 43985 p	42.50	1.041	-9.100

G. camelopardalis samples

UCT 8174 a	2.2	1.318	-12.957
UCT 8174 b	4.24	0.420	-13.072
UCT 8174 c	6.28	0.578	-13.693
UCT 8174 d	8.06	0.492	-13.101
UCT 8174 e	9.9	0.185	-13.827
UCT 8174 f	12.3	0.897	-11.021
UCT 8174 g	14.43	0.416	-14.320
UCT 8174 h	16.46	-0.319	-13.396
UCT 8174 i	17.92	2.870	-14.342

Appendix R. $\delta^{18}O$ and $\delta^{13}C$ values for *S. hendeyi* mandibular third molars with defects. Headings as in Appendix Q.

Accession number	distance (mm)	$\delta^{18}O$	$\delta^{13}C$
PQL 62733/62 a	4.6	-0.911	-9.514
PQL 62733/62 b	9.66	-1.103	-10.021
PQL 62733/62 c	13.35	-0.761	-10.229
PQL 62733/62 d	16.69	-0.730	-10.121
PQL 62733/62 e	20.08	-0.785	-10.446
PQL 62733/62 f	23.21	-0.175	-9.967
PQL 62733/62 g	25.66	-0.641	-9.704
PQL 62733/62 h	28.58	-0.958	-9.753
PQL 62733/62 i	31.85	-0.442	-9.561
PQL 62733/62 j	34.52	-1.022	-9.649
PQL 62733/62 k	38.14	-0.723	-10.168
PQL 62733/62 l	41.61	-0.504	-11.792
PQL 62733/61 a	2.38	-0.870	-10.994
PQL 62733/61 b	5.86	-1.586	-11.150
PQL 62733/61 c	8.57	0.202	-11.532
PQL 62733/61 d	11.49	-0.839	-11.339
PQL 62733/61 e	14.96	-0.111	-11.375
PQL 62733/61 f	17.94	-0.732	-11.094
PQL 62733/61 g	19.98	-0.949	-11.261
PQL 62733/61 h	23.1	-0.889	-10.624
PQL 62733/61 i	25.68	-0.405	-10.816
PQL 62733/61 j	29.04	-0.533	-10.536
PQL 62733/61 k	32	0.011	-10.522
PQL 62733/13 a	4.78	-1.618	-10.885
PQL 62733/13 b	7.82	-0.688	-10.959
PQL 62733/13 c	11.43	-2.054	-10.941
PQL 62733/13 a	13.96	-1.703	-10.705
PQL 62733/13 e	17.68	-1.164	-10.468
PQL 62733/13 f	20.8	-0.892	-10.512
PQL 62733/13 g	25.03	0.137	-10.103
PQL 62733/13 h	29.21	-0.805	-10.160
PQL 62733/13 i	33.07	0.499	-10.249